DESIGN, SYNTHESIS AND BIOLOGICAL STUDIES OF NOVEL MOLECULES DERIVED FROM MORITA-BAYLIS-HILLMAN (MBH) ACETATES AND TACRINE DERIVATIVES AS ACETYLCHOLINESTERASE INHIBITORS

A THESIS

submitted by

Koti Reddy Eeda

for the award of the degree

of

DOCTOR OF PHILOSOPHY

Under the guidance of

Dr Shaik Anwar

DEPARTMENT OF SCIENCE AND HUMANITIES,
VIGNAN`S FOUNDATION FOR SCIENCE, TECHNOLOGY AND RESEARCH UNIVERSITY, VADLAMUDI
GUNTUR – 522213, ANDHRA PRADESH, INDIA

NOV 2017

Dedicated

My beloved Wife & Daughter

DECLARATION

I certify that

a. The work contained in the thesis is original and has been done by myself under the general supervision of my supervisor.
b. I have followed the guidelines provided by the Institute in writing the thesis.
c. I have conformed to the norms and guidelines given in the Ethical Code of Conduct of the Institute.
d. Whenever I have used materials (data, theoretical analysis, and text) from other sources, I have given due credit to them by citing them in the text of the thesis and giving their details in the references.
e. Whenever I have quoted written materials from other sources, I have put them under quotation marks and given due credit to the sources by citing them and giving required details in the references.
f. The thesis has been subjected to plagiarism check using a professional software and found to be within the limits specified by the University.
g. The work has not been submitted to any other Institute for any degree or diploma.

(KOTI REDDY EEDA)

CERTIFICATE

This is to certify that the thesis entitled **DESIGN, SYNTHESIS AND BIOLOGICAL STUDIES OF NOVEL MOLECULES DERIVED FROM MBH ACETATES AND TACRINE DERIVATIVES AS ACETYLCHOLINESTERASE INHIBITORS** submitted by **KOTI REDDY EEDA**to the Vignan's Foundation for Science, Technology and Research University, Vadlamudi. Guntur for the award of the degree of **Doctor of Philosophy** is a bonafide record of the research work done by him under my supervision. The contents of this thesis, in full or in parts, have not been submitted to any other Institute or University for the award of any degree or diploma.

Dr. Shaik Anwar
Associate Professor,
Dept. of Science and Humanities
VFSTR University, Andhra Pradesh, India

Place: Guntur
Date: 18Nov 2017

ACKNOWLEDGEMENTS

I would like to acknowledge my deep sense of gratitude to my supervisor ***Dr. Shaik Anwar*** Department of Science and Humanities, Vignan's Foundation for Science, Technology and Research University, Vadlamudi, Guntur, for his constant valuable guidance and encouragement. He gladly accepted all the pains in going through my work again and again, and giving me opportunity to learn essential research skills. His ability to quickly understand the depth of the problem and suggesting a clear solution has always surprised me. This thesis would not have been possible without his insightful and critical suggestions, his active participation in constructing right models and a very supportive attitude. I will always remain grateful to him for giving direction to my life.

I wish to express my sincere thanks to***Dr. Sajith A. M,*** Research Scientist, Syngene International Ltd, A Biocon Company, Bangalore for his valuable suggestions and constant encouragement from time to time. His valuable advice and help have been a source of inspiration to carry out my research successfully.

I am indebted to the present Director ***Dr. L. Rathaiah,*** **vice chancellor,** for having given me an opportunity to carry out the work and allowing me to submit in the form of thesis.

I wish to express my sincere thanks to ***Dr. N. srinivasu***, Head of the department for providing the necessary facilities foe carrying out the research work. I would like to thank the Doctoral committee panel, ***Dr. D. Nagaraju, Dr.M.sreenivasslu***and other staff of **VFSTER** University for their cooperation and timely help during the course of my work.

I take this opportunity to thank***Dr.Sadasivan, Professor in Bio-informatics***, Kannur University, Kannurfor providing all facilities to the biological studies of my research work. I am also very thankful to ***Prof. Omkumar R. V, Professor in Biotechnology***, Rajiv Gandhi Centre for Biotechnology (RGCB), Trivandrum, Kerala for extending help in Biological studies.

My grateful thanks to ***Ms. RemyaChandran, Deelip K. V and Montosh Kumar*** for helping extending a helping hand and discussions in biological studies whenever required during my research. I appreciate the co-operation and assistance by dearest friend ***Dr. Kiran Kumar*** throughout my research career.

It gives me immense pleasure to thank the encouragement and wholehearted motivation I received from my supervisors ***Dr. Rajesh Sankernayanan, Dr. Rajiv Kapoor,*** **Dr.Sheetal*and Dr. Prashant*.**

I appreciate the co-operation and assistance by my lab mates ***Shanti Kumar, Veerababu, Firoz, Nagendra Prasad and Nagaraju*** for providing a friendly atmosphere in the lab throughout my research career. I am greatful thanks to ***Amar Hosamani*** for proving facilities to single X-ray crystal analysis

My sincere thanks to faculty members and staff of R&D cell of VFSTR University, Vadlamudi, Guntur for their kind help and encouragement in carrying out the research work.

I owe more than myself to my beloved parents ***Sri EedaMaheswara Reddy &Sambrajaym***, brother ***Srikanth*** and my wife***Srisravanthi***who always dreamt that I reach golden heights. I also acknowledge all my other family members, cousins, friends, classmates and well-wishers for their constant support.

KOTI REDDY EEDA

ABSTRACT

DESIGN, SYNTHESIS AND BIOLOGICAL STUDIES OF NOVEL MOLECULES DERIVED FROM MBH ACETATES AND TACRINE DERIVATIVES AS ACETYLCHOLINESTERASE INHIBITORS

Alzheimer's disease (AD), a progressive neurodegenerative disorder among elderly people is characterized by loss of memory, progressive deficits in cognitive functions and behavioural abnormalities. It is estimated that more than 36 million people are presently suffering from AD and it still continues to be one of the leading causes of death due to neurological diseases in developed countries.Over the past decades, despite several efforts from various researchers across the globe, its pathogenesis still remains unclear. Several factors including accumulation of β-amyloid, hyperphosphorylation of tau protein, oxidative stress and deficit of acetylcholine (ACh) seem to play a major roles in the progression of the disease. Current clinical therapy is mainly based on cholinergic hypothesis, which suggests that decline of ACh levels leads to memory loss. Hence sustaining or recovering the cholinergic function is supposed to be clinically beneficial.

Acetyl Cholinesterase inhibitors (AChEIs) temporarily restore native levels of the neurotransmitter acetylcholine (Ach) and prevents the loss of cholinergic transmission in brain areas. However, cholinergic deficit is one of the hallmarks of Alzheimer`s disease (AD). Alzheimer`s disease, is associated with selective loss of cholinergic neurons and reduce the levels of acetylcholine neurotransmitter and it is characterised by progressive loss of memory, attention and depression. According to the Alzheimer`s Association, AD is the one of the top 10 causes of death in world. In recent decades, researchers focused on increasing cholinergic neurotransmission by inhibiting the enzyme acetylcholinesterase (AChE) as one of the main stream option for AD. Currently, the drugs launched in market for cholinergic approach for AD such as tacrine, donepezil, rivastigmine and galantamine increase neurotransmission at cholinergic synapses in the brain and improving cognition.The total work carried out in the present research programme is being presented in six chapters.

Chapter 1: This chapter describes a general introduction of Alzheimer`s Disease, symtoms, causes and treatment for Alzheimer`s Disease.

Chapter 2: The second chapter describes the literature review of Tarine derivatives and novel heterocyclic molecules as Acetylcholinessterase inhibitors.

Chapter 3: This chapter describes the synthesis of dihydroazopyrimidines from MBH Acetates and it`s biological studies as Acetylcholinesteraseinhibiors.

Chapter 4: This chapter describes the design, synthesis of novel tacrine-2-amide derivatives as Acetylcholinesterase inhibitors and studies on cytotoxicity and hepatotoxicity.

Chapter 5: This chapter describes the synthesis of Imidazopyridine[4,5-c]uinoline-6-esters and Imidazopyridine[4,5-d]azepin-2-one derivatives from MBH Acetates and biological studies as Acetylcholinesterase inhibitors.

KEYWORDS: Acetylcholinesterase, AzepinoneTacrine, Docking studies, Imidazopyrine, MBH Acetate, Pyrimidine and Quinolines.

CONTENTS

LIST OF TABLES

LIST OF FIGURES

LIST OF SYMBOLS AND ABBREVIATIONS

°C	Degree centigrade
hr	Hour
s	Second
Aββ-amyloid	
ACh	Acetylcholine
AChE	Acetykcholinesterase
AChT	Acetylthiocholine
AD	Alzheimer`s Disease
ADME	Absorption, Distribution, Metabolism and Excretion
ALT	Alanine aminotransferase
BACE	Beta-secretase
BuChE	Buttylcholinesterase Enzyme
CAS	Catalytic Active Site
CDKs	Cyclin-Dependent Kinases
ChEI	Cholinesterase Inhibitor
CNS	Central Nervous System
DIPEA	Di Isopopyl ethyl amine
DTNB	5,5-Dithiobis-2-nitrobenzoic acid
EDCI	1-Ethyl-3-(3-dimethylaminopropyl)carbodiimide
HATU	1-[Bis(dimethylamino)methylene]-1*H*-1,2,3-triazolo[4,5-*b*]pyridinium 3-oxid hexafluorophosphate
HBA	Hydrogen Bond Acceptors
HBD	Hydrogen Bond Donors
HOA	Human Oral Absorption
HOBT	Hydroxybenzotriazole
FDA	Food and Drug Administration
GSKs	Glycogen-Synthase Kinases

LogP	Partition coefficient
LTP	Long Term Potentiation
MBHAs	Morita-Baylis-Hillman Acetates
MDCK	Mandin-Darby Canine Kidney
mMDH	Mitochondrial Malate Dehydrogenase
MTDLs	Multi-Target Drug Ligands
MW	Molecular Weight
NMDA	N-methyl D-asprate
PAS	Peripheral Active Site
PDB	Protein Databank
PSA	Polar Surface Area
ROS	Reactive Oxygen Species
RMSD	Roor-Mean-Square-Deviation
RT	Room temperature
SASA	Solvent accessible surface area
T_3P	Propylphosphonic anhydride
V	Volume

CHAPTER 1

INTRODUCTION

1.1 Alzheimer`s Disease and History

Alzheimer's disease (AD) is the most common cause of dementia [Alzheimer's disease International, 2010].The word dementia describes a set of symptoms that can include memory loss and difficulties with thinking, problem-solving, learning capacity or language. These symptoms occur when the brain is damaged by certain diseases, including Alzheimer's disease. AD was first described in 1906 by German physician Alois Alzheimer [Alzheimer A, 1906]. On November 1901, Alois Alzheimer met his patient, Auguste D., for the first time. At the time, the first conversation he realizes that the 51 year old woman shows symptoms unlike anyone he had ever seen before. When Alzheimer asked her questions, her replies didn`t match. She also often stopped mid as if she had forgotten what she was going to say. Her memory increasingly failed her, she was confused and anxious. On April 1906, Auguste died and Alzheimer received her brain for historical analysis. On November 1906 Alzheimer first reported his fidings at a meeting of psychiatrists and proposed that he had discovers a new disease. First names “Alzheimer`s disease” by Emil Kraepelin [Möller HJ. et. al 1998] a German psychiatrist who worked with Dr. Alois Alzheimer. According to WHO survey in 2016, 36 million people are suffering from AD and being expected to increase 114 million by 2050.

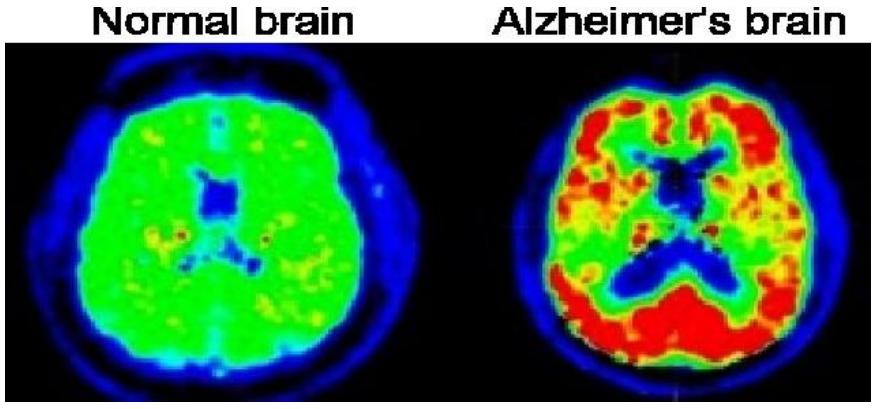

Figure 1.1: Normal brain vs Alzheimer`s brain

1.2 Symptoms

For most people with Alzheimer's, the earliest symptoms are memory lapses. In particular, they may have difficulty recalling recent events and learning new information. There are three main stages of the disease, each with its own challenges and symptoms. By identifying the current stage of the disease, physicians can predict what symptoms can be expected in the future and possible [Forstl et al, 1999].

1.2.1: Early-stage Alzheimer's disease:

This mild stage, which usually lasts 2 to 4 years, is often when the disease is first diagnosed [Raschetti R, et. Al, 2007]. In this stage, family and friends may begin to realize that there has been a decline in the patient's cognitive ability. Common symptoms at this stage include

- Difficulty retaining new information
- Difficulty with problem solving or decision making. Patients may start to have trouble managing finances or other instrumental activities of daily living.
- Personality changes. The person may begin to withdraw socially or show lack of motivation.
- Difficulty expressing thoughts
- Misplacing belongings or getting lost.

1.2.2: Moderate Alzheimer's disease

Lasting 4 to 10 years, this is longest stage of the disease [National Institute for Health and Clinical Excellence]. Patients often experience increased difficulty with memory and may need help with activities of daily living. Symptoms frequently reported during this stage include

- Increasingly poor judgment and confusion. The patient may begin to confuse family members, lose orientation to time and place, and may begin wandering, making it unsafe for them to be left alone.
- Difficulty completing complex tasks, including many of the instrumental activities of daily living, such as managing finances, grocery shopping, planning, and organization.
- Greater memory loss. Patients may begin to forget details of their personal history.

- Significant personality changes. The person may become withdrawn from social interactions and develop unusually high suspicions of caregivers.

1.2.3: Severe Alzheimer's disease

In this final stage of the disease, cognitive capacity continues to decline and physical ability is severely impacted. This stage can last between 1 and 3 years. Due to the family's decreasing ability to care for the patient, this stage often results in nursing home or other long term care facility placement. Common symptoms appearing in this stage include.

- Loss of ability to communicate. The patient may still speak short phrases, but are unable to carry on a coherent conversation.
- Reliance on others for personal care, such as eating, bathing, dressing, and toileting. Many patients become incontinent.
- Inability to function physically. The person may be unable to walk or sit independently. Muscles may become rigid and swallowing can eventually be impaired.

1.3: Treatment of Alzheimer`s disease

There is currently no cure for AD, however there are multiple drugs that have been proven to slow disease progression and treat symptoms [Alzheimer's Association 2010]. When initiating treatment for AD patients, physicians divide the symptoms into "cognitive" and "behavioral and psychiatric" categories. This enables treatment that is specific to the symptoms being experienced. Cognitive symptoms affect memory, language, judgment, and thought processes. Behavioral symptoms alter a patient's actions and emotions.

1.3.1: Treatment for Cognitive Symptoms

Treatment of cognitive symptoms involves altering the effect of some important chemical messengers in the brain. These chemical messengers help to transmit signals around the brain. When there is a shortage of them, the signals are not transmitted as effectively.These symptoms occur because the early damage in Alzheimer's is usually to a part of the brain called the hippocampus, which has a central role in day-to-day memory [Williams College Neuroscience, 1998].The Food and Drug Administration (FDA) has approved two types of medication for this purpose. The first type is called a

cholinesterase inhibitor, which hinders the enzyme responsible for the breakdown of acetylcholine in the brain. Acetylcholine is an important neurotransmitter involved in learning and memory [Riedel G, et. al, 2003]. Normal aging causes a slight decrease in acetylcholine concentration, causing periodic forgetfulness. In addition to cholinesterase inhibitors, a medication called memantine has also been approved for the treatment of AD. Memantine regulates the activity of glutamate in the brain. Glutamate is an excitatory neurotransmitter involved in learning and memory. Overstimulation of nerves by glutamate may be the cause of the neuron degeneration seen in AD, called excitotoxicity [Reisberg, Barry et al]. Glutamate binds to N-methyl-D-aspartate (NMDA) receptors on the surface of brain cells. Memantine functions by blocking the NMDA receptors and therefore protecting the nerves from excessive glutamate stimulation [Saltiel, et al, 2010]. Memantine is indicated in the treatment of moderate to severe AD and can temporarily delay worsening of cognitive symptoms.

1.3.2: Treatment for Behavioral and Psychiatric Symptoms

In addition to cognitive and functional decline, AD can cause severe behavioral and psychiatric symptoms. These symptoms include anxiety, sleeplessness, agitation, hallucinations, and delusions [Alzheimer's disease Education & Referral, 2008]. Possible treatment methods involve non-drug interventions and medications to treat the symptoms being presented. Altering the environment to eliminate obstacles and increase security is an effective non-drug approach. Another possibility is investigating any potential interactions between the patient's medications that could cause adverse effects to behavior or psychiatric health. If these interventions do not improve the symptoms, medication may be required. There are multiple medications that could be chosen depending on the symptoms. For example, if the patient is experiencing depression, an antidepressant such as Prozac or Zoloft can be prescribed. Antipsychotics and anxiolytics may be taken to reduce hallucinations and anxiety, respectively.

There are two types of FDA approved drugs to treat the Alzheimer's Disease

1. The first type are called cholinesterase inhibitors, these inhibitors prevent the breakdown of acetylcholine which is a chemical messenger important for learning memory.
2. Second one is N-methyl D-asprate (NMDA) receptors which regulate the activity of glutamate, a different chemical messenger involved in memory and learning.

1.4 Cholinergic hypothesis

A classical theory regarding the biological mechanism of Alzheimer's is based on the cholinergic hypothesis [Jantzi M, 2010]. It is the oldest, most frequently targeted pathway for the treatment of Alzheimer"s disease. The brain relays information to other parts of the body through a system of nerve cells, known as neurons. These neurons are typically composed of three parts: the dendrite, the axon and the terminal. The dendrite interacts with the terminal of the preceding neuron at the synapse. When a part of the body needs to be activated, a signal is sent down the system of nerve cells. The pre-synaptic neuron relays the signal to the post-synaptic neuron chemically by releasing neuro-transmitters (molecules that bind to receptor sites on the post-synaptic cell) that tell the post-synaptic neuron to continue sending the signal. Neuro-transmitters are then broken down by enzymes to ensure that the neuron is not over-stimulated (which could lead to cell damage). The signal is transmitted in this fashion until it reaches the part of the body that requires stimulation. A number of neuro-transmitters have distinct roles in different regions of the brain. In normal brain signaling, acetylcholine (ACh) is a neuro-transmitter related to preserving and accessing memory, as well as function. ACh is broken down by cholinesterase enzymes (ChE): acetylcholinesterase and butylcholinesterase, so that post-synaptic receptors are not over-stimulated and so that ACh does not accumulate in the synapse.

The cholinergic hypothesis postulates that Alzheimer's is caused by a reduction in an individua's ability to synthesize ACh, leading to gradual neuro-degeneration [Francis PT, et. Al, 1999]. The observed cognitive deficits in Alzheimer's patients with decreased ACh receptor binding led researchers to hypothesize that increasing the availability of ACh in the brain could assuage the cognitive decline associated with Alzheimer's. Administration of a cholinesterase inhibitor (ChEI) decreases the activity of ChE in the synapse, thus leaving more ACh available for signal propagation. Inhibition of ChE explains many of the adverse effects of the ChEIs, as Ach is also an important neuro-transmitter in the digestive tract, the cardiovascular system, and the neuro-muscular junction. As a result, ChEIs may cause nausea, diarrhea, bradycardia, and muscle cramps [APA Practice Guidelines, 2007]. Aside from the cholinergic hypothesis, investigators have proposed other potential mechanisms for the development of dementia, including the buildup of amyloid plaques in the brain due to genetic risk factors (though attempts at removal of

these plaques has not yet led to improved patient outcomes [Holmes C, et. al, 2008] the presence of tau tangles (the abnormal aggregation of tau proteins typically used to stabilize cell structure), which decrease the ability of nerve cells to receive nutrients; and, age-related breakdown of myelin (insulating material that preserves the potency of the electric potential traveling down the axon of a neuron) in the brain [Bartzokis G et al, 2007].

1.4.1 Acetylcholine

Acetylcholine (Ach), is a small, organic molecule that is a derivative of choline and acetic acid and it is the neurotransmitter produced by neurons referred to ascholinergicneurons.Acetylcholine is one of the most important neurotransmitter and it act as messenger to the brain. These messengers help to transmit signals around the brain. When there is a shortage of these messengers, the signals are not transmitted as effectively to the brain causes memory loss and difficulty in thinking, etc. Ach is the most plentiful neurotransmitter, which may be found in both the peripheral nervous system (PNS) and central nervous systems (CNS). In the central nervous system, acetylcholine serves as an important transmitter at nerve-to-nerve synapses in the brain. Acetylcholine used to be the primary neurotransmitter to be discovered. This neurotransmitter was found by Henry Hallett Dale in the year 1914 and its existence was confirmed by Otto Loewi. It is helpful to think of neurotransmitters as messengers of the brain. These chemicals, which originate within the body, assist in delivering messages from one neuron to another neuron in milliseconds. Basically, neurons that use acetylcholine to send the messages are recognized as cholinergic neurons.

1.4.2. Chemistry of Acetylcholine

Acetylcholine is an ester of acetic acid and choline, with the chemical formula $CH_3COOCH_2CH_2N^+(CH_3)_3$ and chemical structure shown in Figure 1.2. Acetylcholine was first identified in 1914, by Henry Hallett Dale for its actions on heart tissue. It was confirmed as a neurotransmitter by Otto Loewi, who initially gave it the name vagusstoff because it was released from the vagus nerve. Both received the 1936 Nobel Prize in physiology or medicine for their work.

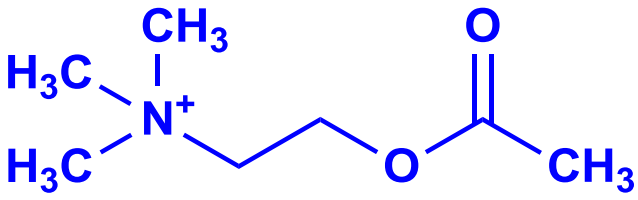

Figure 1.2: Molecular structure of Acetylcholine

Acetylcholine is synthesized in certain neurons by the enzyme choline acetyltransferase from the compounds choline and acetyl-CoA. Organic mercurial compounds have a high affinity for sulfhydryl groups, which causes dysfunction of the enzyme choline acetyl transferase. This inhibition may lead to acetylcholine deficiency, and can have consequences on motor function. Normally, the enzyme acetylcholinesterase converts acetylcholine into the inactive metabolites choline and acetate (Scheme 1.1). This enzyme is abundant in the synaptic cleft, and its role in rapidly clearing free acetylcholine from the synapse is essential for proper muscle function. It is a fast enzyme that can rapidly hydrolyze acetylcholine-10,000 molecules of acetylcholine can be hydrolysed in one second by one molecule of this enzyme.

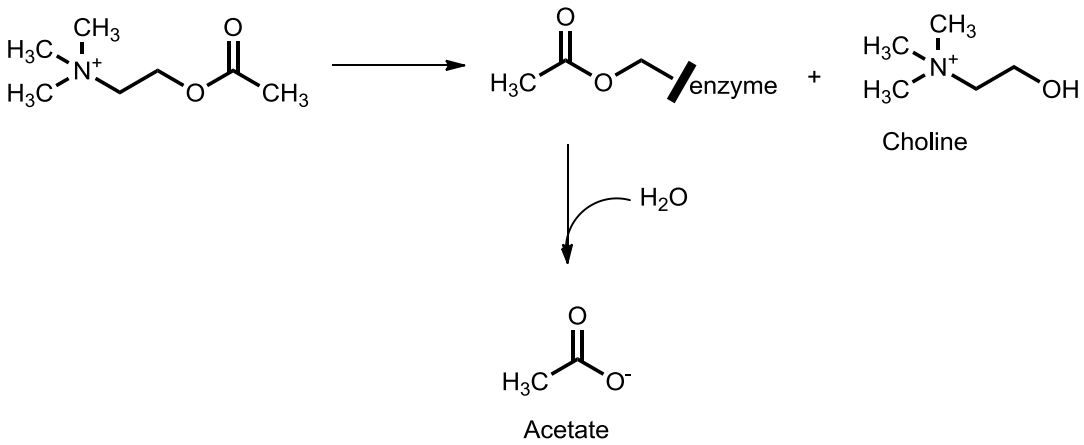

Scheme 1.1: Mechanism of Acetylcholine enzyme

1.4.3 Therapeutic treatments for Acetylcholine

Since AChE inhibitors still continues to be effective drugs for improving the symptoms of AD, several approaches were focussed on modifying a known AChE inhibitor. The FDA approved drugs were tacrine (THA, Cognex), donepezil (Aricept), rivastigmine (Exelon) and galantamine (Reminyl) in market for cholinergic approach for AD is known to work

by increase the neurotransmission at cholinergic synapses in the brain and improving cognition (Figure 1.3).

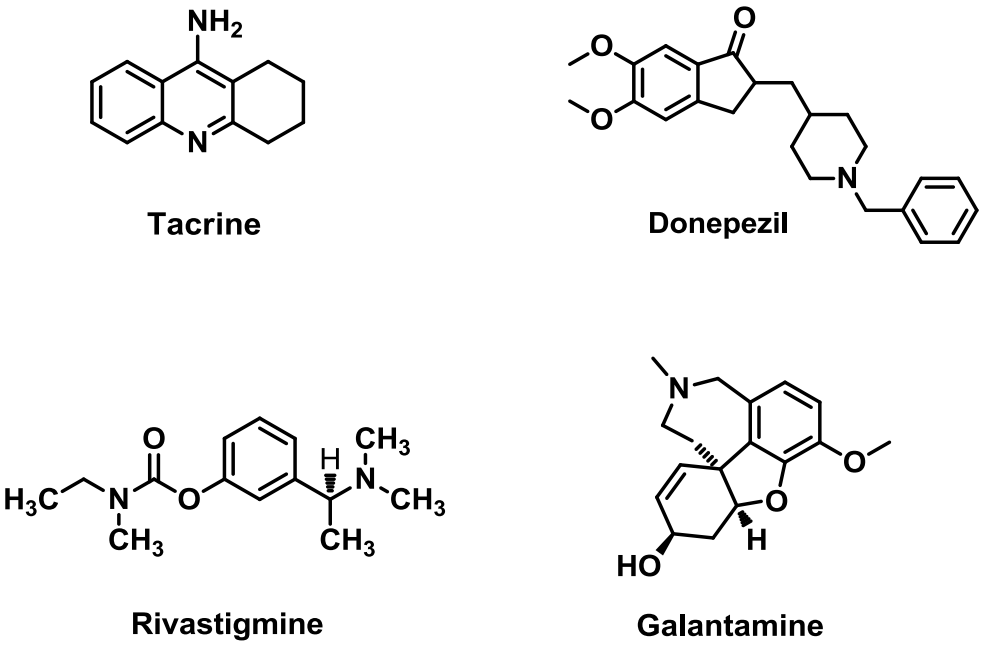

Figure 1.4.3.1: AChE inhibitors clinically used for the treatment of AD.

Tacrine (brand name Cognex)

Tacrine, the first drug approved cholinesterase inhibitor by the FDA for the treatment of AD, is a non-competitive irreversible acetylcholinesterase and is prescribed for mild to moderate dementia. The first synthesis of tacrine was reported in 1945 by Albert and Gledhill [Albert, A et al, 1945]. Working in Australia, these researchers were attempting to discover antibacterial agents to be used on the battle fields of World War II. Soon after the publication of the 1945 paper, penicillin became more economical, leading to the demise of the acridines as antibiotics. However, tacrine was first described as an anticholinesterase in 1953 [Shaw, F. H, 1953]. Since that time, much research has been conducted to elucidate the mechanism by which tacrine inhibits acetylcholinesterase. This section focuses on the historical aspects of the discovery and development of tacrine for clinical applications. In 1961, Heilbronn [Heilbronn, E, 1961] showed that tacrine is a reversible inhibitor of both AChE and another biologically important cholinesterase, butyrylcholinesterase (BChE). The field of tacrine research met with some controversy

due to the work of Summers and co-workers [Summers, W. K. et al, 1986] whose preliminary report claimed that tacrine may be used as a palliative treatment for AD-related dementia. Summers had previously used tacrine for the treatment of overdose coma and delirium [Summers, W. K et al, 1980]. In the controversial AD study, seventeen patients with moderate to severe AD began the non-blinded Phase I. In this phase, subjects who received tacrine exhibited a marked decrease in dementia symptoms. Phase II was a controlled, double-blind, crossover study of 14 subjects. Again, subjects who received tacrine exhibited a marked decrease in dementia symptoms. However, the group to which the placebo was administered showed no significant symptomatic change versus the control group to which no drug was administered. The reported Phase III results were based on 12 subjects. In this phase, tacrine was administered over an average of nearly 13 months. In that time, subjects exhibited symptomatic improvement and a lack of tacrine-related side effects. Soon after the Summers study was published, the editors of the New England Journal of Medicine began to receive letters critical of the simplicity of the Summers study, but no arguments that the study was so flawed as to be unpublishable [Relman, A. S, 1991]. In 1992 – 1994, several studies published in the course of a multicenter study demonstrated the effectiveness and relative safety of tacrine as an AD treatment [Davis, K. L et al, 1992]. Interestingly, the FDA halted clinical trials of tacrine on October 23, 1987 because of liver toxicity exhibited by eight of the first 41 patients who received the drug [Watkins, P. B et al, 1994]. Eventually, the multicenter study was allowed to progress, and it was concluded that tacrine in high doses (i.e., 160 mg/day) could induce a significant improvement on tests designed to measure the progression of dementia. Tacrine received FDA approval for AD related dementia in 1993.

One of the studies that emanated from the large multicenter study focused on the hepatotoxic effects of tacrine [Shutske, G. M. et al, 1989 & Shutske, G. M. et al, 1988] In that study, 2446 suspected AD patients who were at least years old were given tacrine and monitored for the elevation of serum alanine aminotransferase (ALT) levels. This elevation of ALT levels is symptomatic of hepatotoxicity. While nearly half of the patients experienced ALT levels greater than the upper limit of normal, discontinuation of the treatment allowed the ALT levels to return to normal. Furthermore, 88% of those patients who discontinued the tacrine treatment were able to resume long-term treatment with tacrine after ALT levels returned to normal. It is important to note that no deaths

directly attributable to the tacrine treatment occurred over the course of the long-term study. As a possible amelioration of the liver toxicity effect, Shutske and coworkers examined a series of 9-amino-1,2,3,4-tetrahydroacridin-1-ols (Figure 1.4) compounds which were physiological metabolites of tacrine but did not possess the high lipophilicity (and the resulting tissue accumulation effects) that plagued the drug. The results showed that velnacrinewas an order of magnitude less effective than tacrine for inhibition of mouse AChE (IC_{50} = 4.8 μM and 0.31 μM, respectively) but exhibited a similar pharmacological profile. However, oral toxicity of velnacrinein mice was much improved versus that of tacrine (LD_{50} = 136 mg/kg and 39.8 mg/kg, respectively). Interest in velnacrine waned after the FDA approval of tacrine, and this metabolite has not enjoyed clinical use.

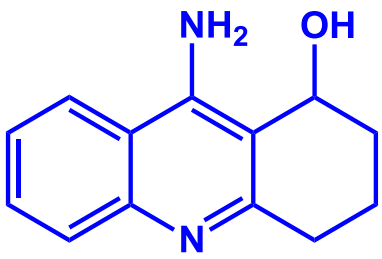

Figure 1.4: 9-Amino-1,2,3,4-tetrahydroacridin-1-ol, Velnacrine

Donepezil hydrochloride (Brand name Aricept)

This medication has been approved to treat all stages of AD by preventing the breakdown of acetylcholine in the brain. Donepezil is a highly selective and reversible antagonist for acetylcholinesterase (AChE). The pharmacology profile and long half-life allow for a once daily dosage. A study published in the 1998 Archives of Internal Medicine examined the effects of this treatment on 468 participants. The patients had mild to moderate AD according to results from the MMSE and Clinical dementia Ratings [Lippincott, Williams et al, 2010]. The study excluded patients with any coexisting medical conditions that might interfere with the trial. The participants were divided into three groups. One group received two placebo tablets. Another group received one placebo tablet and one 5-mg donepezil tablet. The final group received two 5-mg donepezil tablets. Among the groups receiving the drug, 32% of the 5-mg treatment group and 38% of the 10-mg treatment group showed clinical improvement on various psychiatric and mental scales. Donepezil is the only cholinesterase inhibitor approved to

treat severe AD. Overall, research has shown that this drug is effective at slowing cognitive decline.

Galantamine hydrobromide (Brand name Razadyne)

Galantamine is indicated in the treatment of mild to moderate AD by blocking the hydrolysis and increasing the concentration of acetylcholine. Unlike donepezil, galantamine must be administered twice daily due to a short half-life of only seven hours [Hansen, Richard A. et al, 2008]. A research study conducted by Loy and Schneider investigated the effect of galantamine on cognitive symptoms at three and six month intervals [Loy C and Schneider L, 2006]. Patients taking doses of 18-32 mg/day showed significant improvements at both time intervals. The effects were greater after six months of treatment and were effective at improving the cognitive examination scores of the participants. A meta-analysis of AD treatment studies by Hansen and a group of researchers found that galantamine is able to slow the decline of cognitive function with adverse effects occurring in a small percentage of participants [Lanctot, Krista L. 2009].

Rivastigmine tartrate (Brand Name Exelon)

This medication is prescribed less frequently than other cholinesterase inhibitors for the treatment of mild to moderate AD. A study conducted by the Department of Psychiatry at the Sunnybrook Health Sciences Center in Toronto examined the effectiveness of rivastigmine at various dosages and time periods. A lower dose of 1-4 mg/day and a higher dose of 6-12 mg/day were tested at 12, 18, and 26 week intervals. The group taking the highest dosage showed the greatest improvement in cognitive examination scores and activities of daily living over all time intervals. The lower dosage showed improvement only after the 26 week duration and did not alter the activities of daily living ability. Side effects were experienced in a small percentage of participants taking the higher dosage when compared to the placebo. Overall, this drug has been proven to be effective in treating the cognitive symptoms of AD when taking 6-12 mg daily over a long period of time [Kemp JA, 2002].

1.5. NMDA receptors

The N-methyl-D-aspartate receptor (also known as the **NMDA receptor** or NMDAR), is a glutamate receptor and ion channel protein found in nerve cells. It is activated when glutamate and glycine (or D-serine) bind to it, and when activated it allows positively charged ions to flow through the cell membrane. They are critical for the development of

the central nervous system (CNS), generation of rhythms for breathing and locomotion, and the processes underlying learning, memory, and neuroplasticity. Consequently, abnormal expression levels and altered NMDAR function have been implicated in numerous neurological disorders and pathological conditions. NMDAR hypofunction can result in cognitive defects, whereas overstimulation causes excitotoxicity and subsequent neurodegeneration. Therefore, NMDARs are important therapeutic targets for many CNS disorders [Jansen M et al, 2003; Chazot PL, 2004] including stroke, hypoxia, ischemia, head trauma, Huntington's, Parkinson's, and Alzheimer's diseases, epilepsy, neuropathic pain, alcoholism, schizophrenia, and mood disorders.

1.5.1 Memantine (Brand Name Namenda)

Memantine is a NMDA receptor antagonist approved for the treatment of moderate to severe AD24. According to a study published in the 2003 New England Journal of Medicine, memantine-induced regulation of NMDA receptors resulted in a decrease in deterioration and alleviation of AD symptoms [Reisberg, Barry et al, 2003]. Of the 345 participants initially screened, 181 completed the 28-week double-blind trial. The participants were fifty years of age or above with a diagnosis of moderate to severe AD. Each also had CT and MRI scans within the previous 12 months. Twenty-nine percent of the memantine group and ten percent of the placebo group showed a positive response to the medication. There were adverse effects in nearly all of the participants, although most were unrelated to the medication. The most common side effect was agitation. Although this trial showed results in fewer participants, this was to be expected compared to studies of cholinesterase inhibitors. Those trials were conducted on patients with mild to moderate AD, making them more likely to show improvement following treatment. Overall, the data obtained indicates that memantine can effectively reduce deterioration in patients with advanced AD.

CHAPTER - 2

LITERATURE REVIEWAND SCOPE OF WORK

2.1 Introduction

To combat the multifactorial nature of the Alzheimer's disease (AD), design of new safer therapeutics is an important research endeavour. One approach towards this end is the multi-target synthesis of hybrid drugs based on the typical structural and biochemical properties of AChE. Gauging the importance of design of new multifunctional hybrids against AD could be accentuated by the data obtained after a quick overview to the Scopus database under the key words "Synthesis & Cholinesterase" from 2005-2016 as is depicted in figure 2.1. Structural analysis of AChE by X-ray crystallography has revealed that the enzyme possesses two binding sites: the catalytic active site (CAS) and the peripheral anionic site (PAS) connected by a gorge that is about 20 A^{o} long [Sussman, J L, 1991]. Various studies have found that AChE is responsible for several non-catalytic actions like proggregation activity of Aβ protein likely through the interaction with the PAS amino acid residues. Therefore, the molecules that can interact specifically with PAS or CAS residues are important in AChE inhibition and can help in prevention of Aβ aggregation facilitated by AChE [Castro, A, 2001; Muñoz-Ruiz, P, 2005; Najafi, Z, 2016; Camps, P, 2010]. A popular strategy being employed over the past several years is multi-target drug ligands (MTDLs) by which a known AChE inhibitor is linked with another moiety to create bi or multifunctional hybrid capable of binding to the PAS and or exerting any beneficial properties in the treatment of AD[Ismaili L, 2002]. The AChE moiety of the hybrid favors the interaction of molecule with CAS and the other part of the hybrid interacts with PAS to increase potency, disrupt metal chelation, Aβ aggregation, and scavenge ROS.

In a normal brain, AChE plays a vital role in hydrolyzing 90% of ACh terminating its action while BuChE plays a secondary role. It has been revealed that the level of AChE decreases in patients whereas BuChE increases in some specific regions of brain [Perry, E K, 1978]. In recent years inhibition of BuChE has shown some significant results suggesting that the selective or nonselective inhibition of BuChE may elicit neuroprotective and disease modifying effects [Greig, N H, 2005]. In this regard,

indolinone[Akrami, H, 2014] based scaffolds, coumarin-3-carboxamides bearing N-benzylpiperidine moiety,[Asadipour, A, 2013], 5-oxo-4,5-dihydropyrano[3,2-*c*]chromen derivatives,[Khoobi, M, 2015] coumarin-3-carboxamides bearing tryptamine moiety, [Ghanei-Nasab, S, 2016], benzylidenechroman-4-ones [Pourshojaei, Y, 2015] bearing cyclic amine side chain, 7-hydroxycoumarin derivatives, [Alipour, M, et al, 2014] and tacrine analogues [Mahdavi, M, 2016] have exhibited efficient anti-ChE activity.

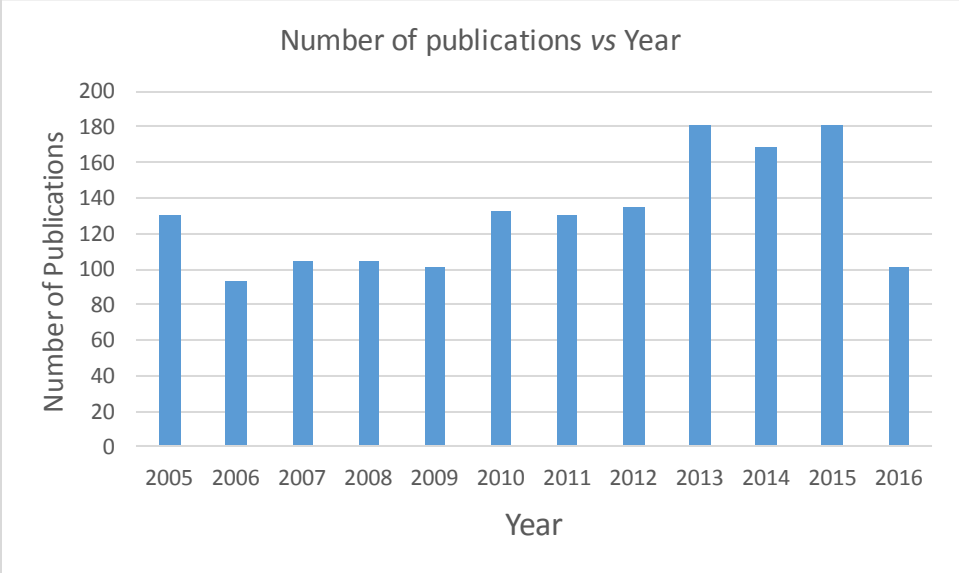

Figure 2.1: Number of publications *vs* year

2.2: Tacrine based Scaffolds as AChE and BuChE inhibitor

Compounds which can selectively or non-selectively inhibit ChE's may be helpful in managing the AD symptoms based on "cholinergic theory" which asserts that the decrease of acetylcholine level in certain regions of brain and loss of cholinergic transmission are important aspects to be mitigated by treatment with such molecules. Tacrine is a classical pharmacophore which inhibits both AChE and BuChE at micro-molar scale.

2.2.1: Tetracyclic Tacrine scaffolds

Khoobi et al, 2015, synthesized tetracyclic-tacrine analogues (Scheme 2.1) by replacing benzene ring of tacrine with aryl-dihydropyrano[3,2-c]pyrazoles via one-pot multi component reaction, followed by friedlander reaction. Most of the synthesized compounds showed potent and selective AChE activity in µM range. The most potent compound IC_{50}= 0.19 µM bearing 3,4-dimethoxyphenyl rings showed significant

neuronal protection against oxidative stress at low concentrations in *in-vitro* assay equal to querectin as reference compound. *In silico* studies of the above mentioned compound revealed that *R*-enantiomer occupies catalytic anionic site (CAS) through its dimethoxyphenyl moiety forming H-bond favorably with Phe330 residue and π-π stacking with His-440, while *S*-enantiomer established H-bonding through pyrazole ring with Ser286 and dimethoxyphenyl ring aligned towards Trp279 of the peripheral anionic site (PAS) through π-π stacking.

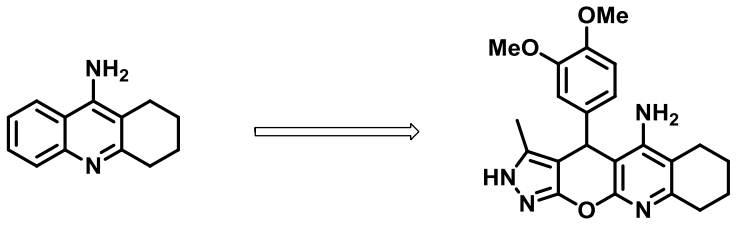

IC_{50}: AChE: 0.19 uM
BuChE: 100 uM

Scheme 2.1: Tetracyclicne tacrine analogs.

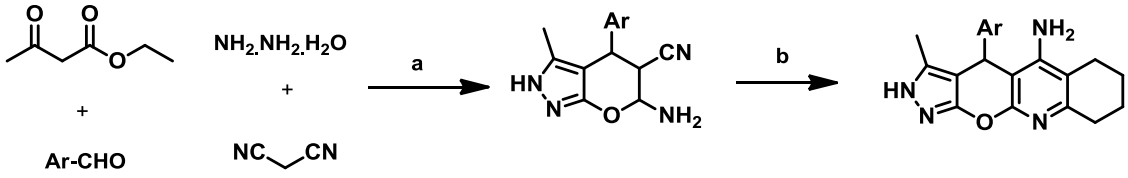

Scheme 2.2: Synthetic scheme for tetracyclictacrine analogs. (a) Ultrasonic irradiation, (*S*)-proline H_2O/EtOH, rt, 10-35 min (b) Cylohexanone, $ClCH_2CH_2Cl$, $AlCl_3$.

2.2.2: Tacrine-Lophine hybrids

da Costa, J S, et al, 2013 reported tacrine–lophine hybrids or (tacrine-2,4,5-triphenyl-1*H*imidazole) (Scheme 2.3) as AChE and BuChE inhibitors. Change in substitution X and linker length influenced the activity and selectivity, linker length of eight was found optimal for the activity. *In vitro* experiments showed the congener with linker length of 8 and X = Cl as the most active hybrid, 18.5 fold selective towards AChE IC_{50} = 5.87 nM. Replacement of X with 4- CN, 4-NO_2 afforded selective anti-BuChE compounds. Introduction of X = 3-Cl led the compound inactive toward both ChEs. Introduction of 6-methylene rendered the compounds inactive towards AChE and selective BuChE with IC_{50} values of 12.44 nM – 58.00 nM. Introduction of heptyl chain, substitution of 4-CN

provided selective BuChE inhibitors with no activity towards AChE. Compounds with 4-F, 4-OMe, and 4-NO_2 showed activity towards both AChE and BuChE, whereas the compound with X = 3-Cl was inactive towards both ChE's. It can be concluded that all phenyl rings on the imidazole ring are not co-planar and the dihedral angles between the rings can be increased by the substituents at the *meta*- position. The loss of AChE activity of derivatives possessing *meta*-substituted aryls may be attributed towards the weak π-π interactions between the lophine moiety and enzyme active sites as displayed by docking studies. In contrary, presence of *para*-substituted aryls with small dihedral angle favors π-π interaction between the ligand and the receptor.

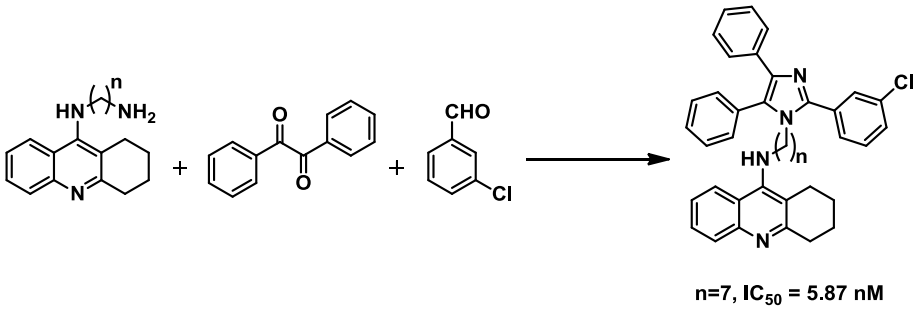

Scheme 2.3: Tacrine-Lophine hybrids. Conditions and reagents: NH_4OAc, $InCl_3$ (0.15 eq), EtOH, 78 °C, 96 h.

2.2.3: Tacrine –Melatonin hybrids

Melatonin is a well- known antioxidant agent, radical scavenger, pineal hormone whose level decreases in AD. Tacrine unlike its non-selective anticholinesterase activity doesn't contribute to anti-oxidant activity. Fernade et al. reported tacrine-melatonin hybrids[Fernández-Bachiller, 2009& Leong. S, W, 2016] (Scheme 2.4) as fascinating multifunctional agents with cholinergic, antioxidant and neuroprotective properties. Synthesized compoundselicited good cholinesterase inhibitory activity in nano-molar range. SAR of the synthesized compounds showed that the linker length of 5 and 6 between NH and the amide exhibited better cholinesterase inhibitory activity. Introduction of Cl into 8-position or F atom into 7-position decreased the cholinesterase inhibitory activity. Substitution of Cl at 6-position or dichloro at 6,8-positions of tacrine moiety demonstrated more potent inhibitory activity and remarkable selectivity (200-1000 fold) towards AChE. Replacement of amide with thioamide decreased inhibitory activity in comparison to their analogues. It has been proved that compounds which specifically binds to the CAS of enzyme have not been reported to be involved in inhibiting amyloid aggregation like tacrine [Bencharit, S, et al 2003]. The

tacrinemelatonin hybrids also elicited higher anti-oxidative property than trolox, vitamin E analog, and melatonin, equivalent to the endogenous anti-oxidant catalase against mitochondrial and amyloid induced oxidative stress.

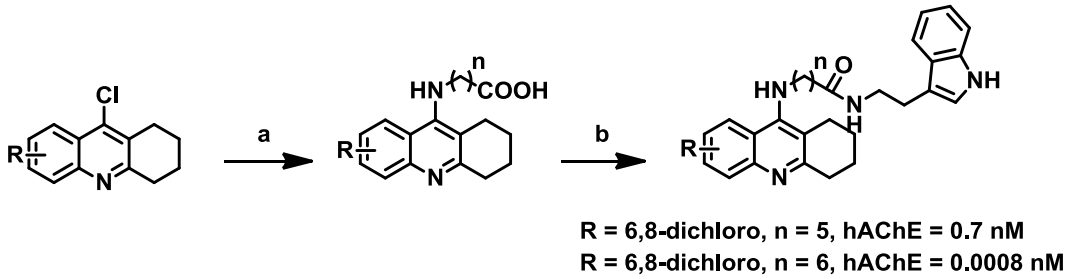

Scheme 2.4: Tacrine-Melatonin hybrids. Reagents and conditions: Conditions and reagents: (a) $NH_2(CH_2)$nCOOH, *n*-pentanol, NaOH (b) $NH_2(CH_2)_2$ indole, BOP, Et_3N

2.2.4: Tacrine- 8-hydroxyquinoline hybrids

The multifaceted nature of the AD asserts the need for the development of molecules with more than one complementary biological effect. There is a growing body of evidence which supports the role of oxidative stress in progression of AD[Lin. M, T, et al 2006 &Barnham. K, J, et al, 2004]. Endogenous anti-oxidative stress protection system progressively weakens during aging and further decline is observed in AD. Metal ions have been found to play a critical role in the precedence of pathogenic hallmark amyloid plaques, and tangle formation [Perry, G, et al 2008]. Spectroscopic studies have demonstrated increased levels of metal ions like Zn and Cu in amyloid plaques as well as their role in the production of reactive oxygen species (ROS) leading to oxidative stress [Dong, J, et al, 2003]. Many natural phenolic compounds like caffeine acid [Touaibia, M, et al, 2011], ferulic acid and related substructures like huperzine-A,[Gemma, S, et al, 2006], tacrine-caffenic acid[Chao, X, et al, 2012]; tacrine-lipoic acid, lapocrine (a hybrid consisting of tacrine and lipoic; potent anti-oxidative activity) has shown significant pharmacological activity ranging from AChE inhibition, AChE-induced Aβ aggregation, and protection against ROS[Rosini. M, et al, 2005]. Many anti-oxidant agents, ROS scavengers and metal chelators have been either developed or proposed and several chelating agents like 5-iodo-6-chloro-8-hydroxyquinoline, desferrioxamine, D-penicillamine, cloquinol are under clinical trials [McLachlan. D, C, et al, 1991 &Squitti, R, et al, 2002]. 8-Hydroxyl derivatives without iodine substitution have shown fascinating results towards amyloid fibril formation mobilization and clearance without

diiodide toxicity. Fernandez-Bachiller described tacrine–quinolone (Scheme 2.5) derivatives[Fernández-Bachiller, et al, 2010] as potent multifunctional agents (Scheme 2.6). Synthesized compoundsdisplayed potent cholinesterase inhibitory activity in sub micro molar to nano molar range. Compoundwith unsubstituted quinoline moiety with methylene length of **7** exhibited the highest AChE inhibitory activity (IC_{50} = 20 nM). Substitution in the quinoline ring decreased cholinesterase inhibitory activity. Tacrine has negligible radical scavenging potential and does not decrease beta amyloid fibril formation, tacrine-hydroxyquinoline scaffolds displayed potent peroxy absorbing capacity and good propidium displacement affinity. Compound with unsubstituted tacrine ring and linker length of 7 displayed 33-fold higher peroxy absorbance ability than Vitamin-E. Compounds at 0.3 µM, elicited a propidium displacement of22, 19, and 27 % respectively which provides an insight that these molecules can inhibit the AChE-induced fibril formation. Imbalance of bio-metals in AD plays an imperative role in protein aggregation. Cu_2^+ has higher affinity towards amyloid plaques than Fe_2^+. Hybridelicited remarkable Cu_2^+ scavenging ability under UV-spectrometry evaluation assay on addition of $CuSO_4$.

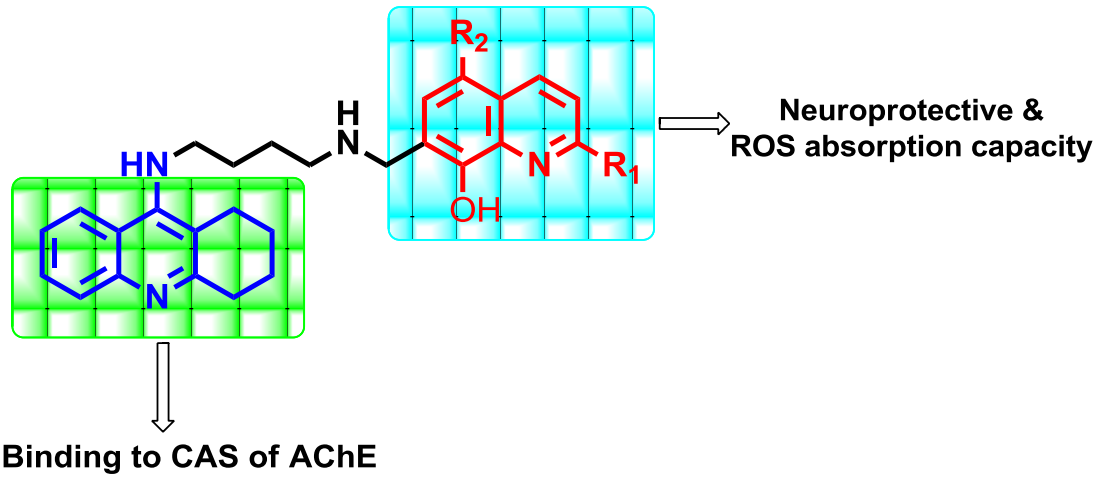

Scheme 2.5: Tacrine-Quinoline hybrids

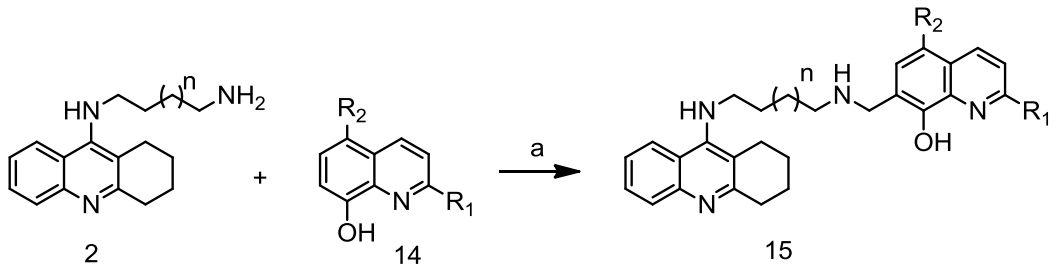

15a, R_1 = H, R_2 = H, n= 4, IC_{50}, AChE = 20 nM
15b, R_1 = H, R_2 = H, n= 2, IC_{50}, AChE = 25 nM
15c, R_1 = CH_3, R_2 = H, n= 3, IC_{50}, AChE = 75 nM
15d, R_1 = H, R_2 = Cl, n= 4, IC_{50}, AChE = 85 nM

Scheme 2.6: Tacrine-Quinolone hybrids **15**. Conditions and reagents: (a) $(CH_2O)n$, EtOH, reflux.

2.2.5: Tacrine-chromene hybrids

Coumarins are naturally occurring compounds ubiquitous in plants, elicit multiple biological activities like antifungal, anti-HIV [Ong, E B B, et al, 2011], anticoagulants [Lowenthal, J, et al, 1969], anti-inflammatory, anti-oxidant,[Fylaktakidou. K, C, et al, 2004] cytotoxic[Kostova, I, et al, 2005] etc. Studies have also demonstrated that coumarin congeners inhibit ChE and amyloid aggregation. Recent studies have shown that flavonoids[Shimmyo, Y, et al, 2008] which are abundant in fruits and vegetables can decrease amyloid production through inhibiting beta-secretase (BACE-1) (an enzyme which instigates the cleavage of amyloid precursor protein).[Spencer. J, P, et al, 2010]. In view of the multifactorial nature of AD. The new tacrine−4-oxo-4H-chromene hybrids [Fernández-Bachiller, et al, 2012](Scheme 2.7) inhibit human acetyl- and butyrylcholinesterase (h-AChE and hBuChE), being more potent than the parent inhibitor, tacrine. They are also potent inhibitors of human BACE-1, better than the parent flavonoid, apigenin. They show interesting antioxidant properties and could be able to penetrate into the CNS according to the *in vitro* PAMPA-BBB assay. Among the hybrids investigated, 6-hydroxy-4-oxo- N-{10-[(1,2,3,4-tetrahydroacridin-9-yl)amino]decyl}-4 H-chromene-2-carboxamide shows potent combined inhibition of human BACE-1 and ChEs, as well as good antioxidant and CNS-permeable properties.

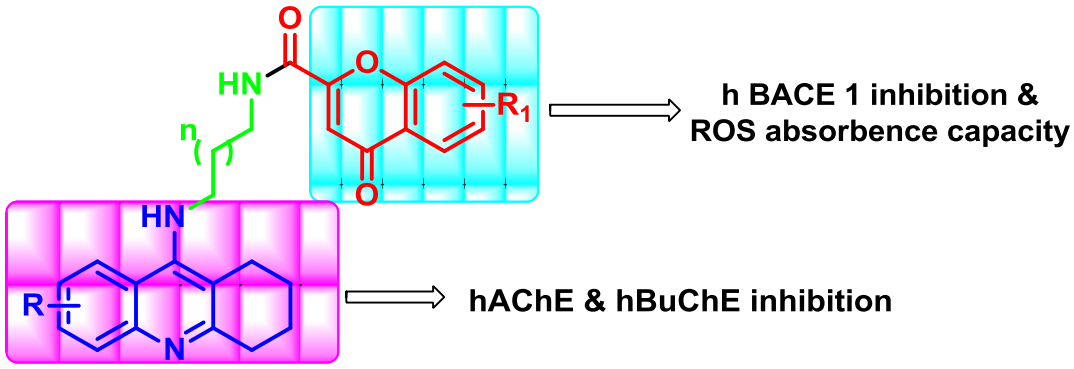

Scheme 2.7: Tacrine-Chromene hybrids

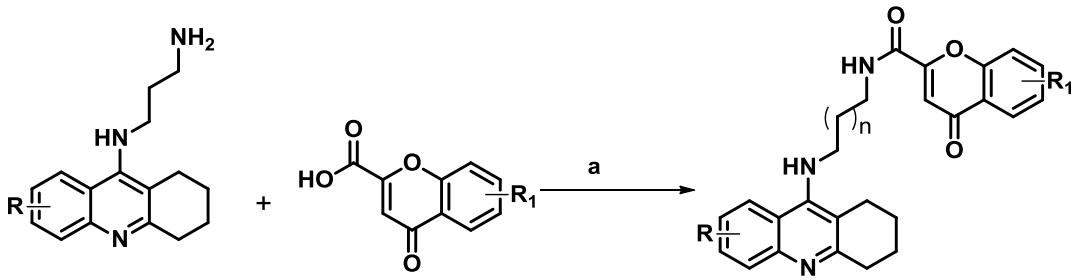

R = H, R_1 = 6-OCH_3, n = 8, hAChE = 35 nM, hBuChE = 0.324 nM
R = Cl, R_1 = 6-OCH_3, n = 8, hAChE = 5 nM, hBuChE = 0.425 nM
R = H, R_1 = 6-OH, n = 8, hAChE = 75 nM, hBuChE = 1.0 nM
R = Cl, R_1 = 5-OH, n = 8, 7-OCH_3, hAChE = 38 nM, hBuChE = 0.175 nM
R = Cl, R_1 = 6,7-diOH, n = 8, hAChE = 17.5 nM, hBuChE = 28 nM

Scheme 2.8: Synthesis of Tacrine-Chromene derivatives, (a) BOP, TEA, CH_2Cl_2

2.2.6: Tacrine homodimers (Bis-7-Tacrine)

In 2002, reported tacrine homodimers tethered by carbon linker lengths 6-8 as shown in Scheme 2.9. Among the synthesized compounds, one compound (Scheme 2.10) displayed the highest AChE inhibitory activity 3000 times higher than tacrine (IC_{50} = 0.07 nM, AChE). Unsubstituted tacrine ring with a linker length of 7 was 221 fold more selective towards AChE with (IC_{50} = 0.2 nM). Compound tethered by a linker length of 8 exhibited the highest AChE (IC_{50} = 0.3 nM). Shrinking the size of the cycloalkyl to cyclopentyl decreased both potency and selectivity. Introduction of halogen at position 6 led to an increase in potency and selectivity which is in concurrence with the previously reported communication[Recanatini. M, et al, 2000]. The analogues with an aza group in the tacrine elicited moderate inhibitory effect. In conclusion, the size of the ligand proved an overwhelming factor in determining the favorable interaction with the active pockets of the enzyme.

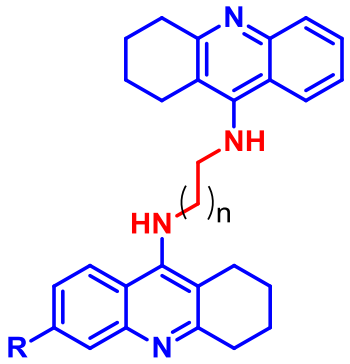

R = H, n = 7, hAChE, IC_{50} = 0.2 nM
R = Cl, n = 7, hAChE, IC_{50} = 0.02 nM
R = Cl, n = 8, hAChE, IC_{50} = 0.3 nM

Scheme 2.9: Bis-7-tacrine hybrids

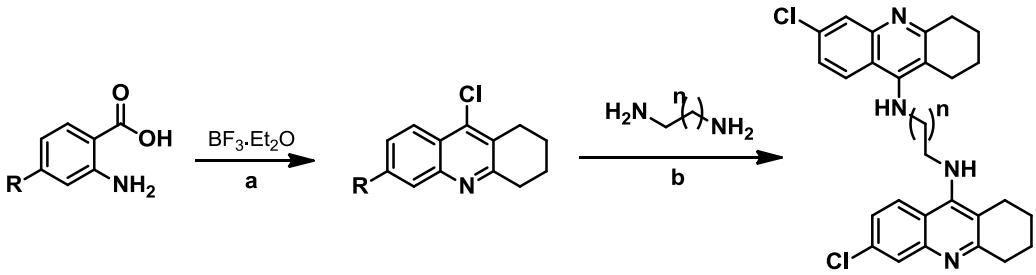

Scheme 2.10: Synthetic scheme for Bis-7-tacrine; (a) Cyclohexanone, BF_3,Et_2O, toluene, 110^o C, 4h; (b) PhOH, NaI, 180^{o}C, 2h

2.2.7: Tacrine scaffolds with NO donor group

Nitric oxide (NO) is an intracellular relaxing-factor derived from endothelium besides maintaining vascular tone, mediates several other vital immunological, vascular, cerebral circulation and neuronal actions in a cell. NO facilitates long term potentiation (LTP), modulates activities like cerebral blood flow and memory. Several studies have reported that the production of NO decreases in neurodegenerative disorders like Alzheimer and Parkinson which has been endorsed due to the decrease in level of cofactor tetrahydrobiopterin BH4 - important for the synthesis of NO synthetase (NOS) [Alp. N, J, et al, 2004]. Compounds that can manipulate NO production may be beneficial in the enhancement of cognitive function in AD. Since in AD, oxidative stress significantly contributes to its pathogenicity, nitroxides are stable free radicals and can penetrate through cell membrane, may prevent free radical formation; mimic extracellular and intracellular suproxide Dismutase (SOD) by oxidizing metal ions. Reduced forms of the nitroxides, hydroxynitroxides have also been found to facilitate anti-oxidative activity [Kuiper. M, A, et al, 1994]. In 2008, synthesized NO-donor tacrine based scaffolds with

varying linker length between two NH groups and NH and NO_2 groups as cholinesterase inhibitors with vasorelaxation and hepatoprotective effects in in-vitro assays. All the compounds elicited potent AChE inhibitory effects in nano molar range 5.2093. Compounds (Scheme 2.11) showed the most potent AChE inhibitory 7- fold higher than tacrine with IC_{50} values.

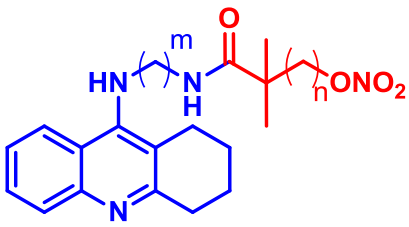

m =3, n=3, AChE = 6.4 nM, BuChE, IC_{50} = 5.4 nM
m =3, n=6, AChE = 6.3 nM, BuChE, IC_{50} = 21.7 nM
m =4, n=3, AChE = 5.6 nM, BuChE, IC_{50} = 9.9 nM

Scheme 2.11: Tacrine with NO hybrids

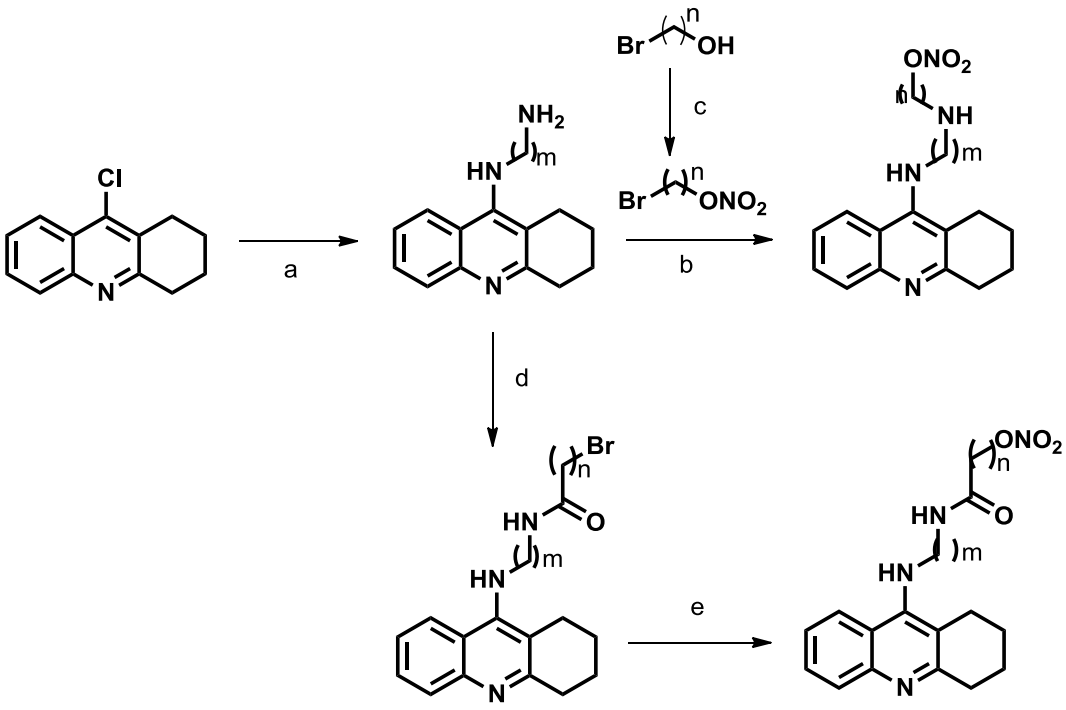

Scheme 2.12: Synthetic scheme for Tacrine-NO hybrids; (a) n-pentanol, $NH_2(CH_2)mNH_2$, reflux, 18h, (b) 100% HNO_3, CH_2Cl_2, -5°C, (c) K_2CO_3, CH_2Cl_2, 12h, (d) $Br(CH_2)nCOCl$, CH_2Cl_2, -5°C, 30 min, (e) CH_3CN, $AgNO_3$, reflux, 8h.

2.2.8: Tacrine-lipoic acid hybrids

Lipoic acid is an antioxidant agent[Packer. L, et al, 1995&Biewenga. G P, et al, 1997] displayed neuroprotective effect against hydrogen peroxide and Aβ induced cytotoxicity [Zhang. L, et al, 2001], [Gemma. S, et al, 2006] linked tacrine with lipoic acid tethered by spacers of varying lengths as cholinesterase inhibitors with anti-oxidative and feeble anti-Aβ aggregation activity with reference to anti-amyloid propidium (Scheme 2.13). Change in linker length between two nitrogen atoms led to the significant change in activity. Introduction of chlorine atom into tacrine ring resulted in 1676-fold increase in cholinesterase inhibitory activity than prototype tacrine. Insertion of lipoic acid moiety at position 3 of tacrine resulted in drastic decrease in cholinesterase activity.

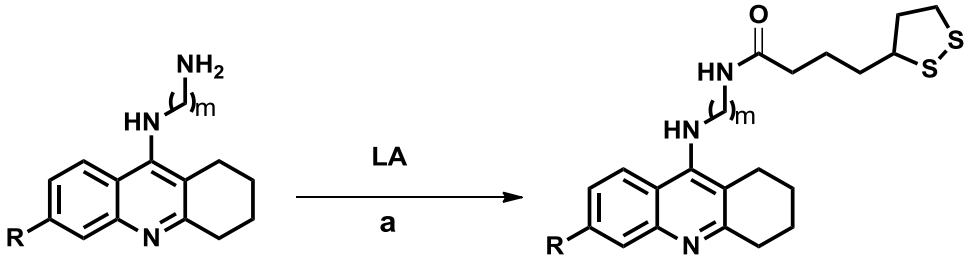

R = H, n = 3, AChE = 6.96 nM, BuChE = 12.0 nM
R = Cl, n = 3, AChE = 0.253 nM, BuChE = 10.8 nM

Scheme 2.13: Synthesis of Tacrine-Lipoic acid hybrid; (a) EDCI.HCl, HOBT, TEA, DMF, 2h, RT

2.2.9: Tacrine-ferulic acid scaffolds

Fang. L et al.2008, reported synthesis of tacrine-ferulic acid hybrids linked by alkyldiamine citing ferulic acid's role towards hepatoprotective effect in addition to anti-oxidative stress (Scheme 2.14). *In vitro* assay of the synthesized compounds showed better activity towards AChE inhibition than tacrine and comparable activity towards BuChE, compounds displayed the highest AChE inhibitory activity IC_{50} = 3.2 and 3.5 nM, respectively.

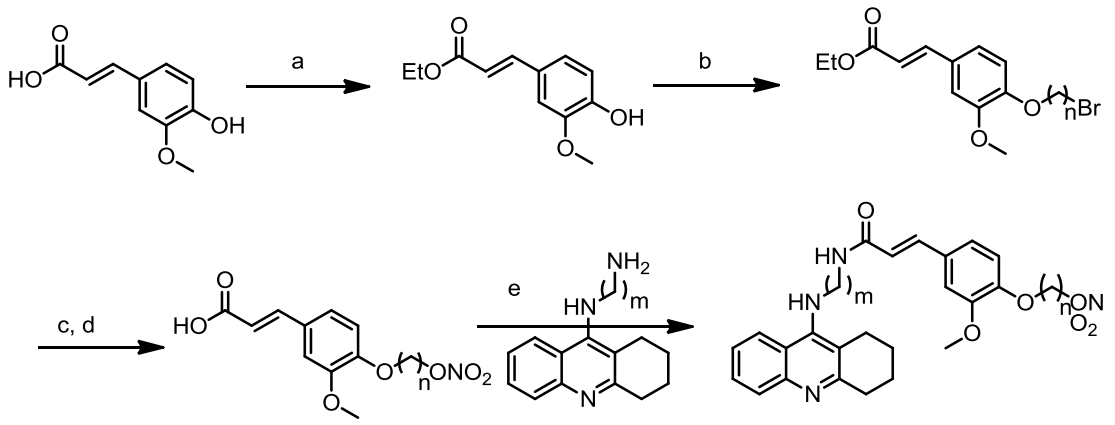

m =3, n =4, AChE, IC_{50} =3.6 nM, BuChE, IC_{50} =6.2 nM
m =6, n =2, AChE, IC_{50} =8.3 nM, BuChE, IC_{50} =5.2 nM
m =6, n =3, AChE, IC_{50} =4.4 nM, BuChE, IC_{50} =5.6 nM
m =6, n =4, AChE, IC_{50} =3.7 nM, BuChE, IC_{50} =1.4 nM
m =6, n =6, AChE, IC_{50} =4.8 nM, BuChE, IC_{50} =2.0 nM
m =8, n =2, AChE, IC_{50} =5.5 nM, BuChE, IC_{50} =1.6 nM
m =3, n =4, AChE, IC_{50} =3.6 nM, BuChE, IC_{50} =6.2 nM

Scheme 2.14: Synthetic scheme for Tacrine -Ferulic acid hybrid: (a) EtOH, H_2SO_4, relux, 2h, (b) $Br(CH_2)nBr$, DMF, K_2CO_3, 65^o C, 6h, (c) $AgNO_3$, CH_3CN, 60^o C, 6h, (d) $LiOH.H_2O$, THF/H_2O, MeOH, 4h, room temperature, (e) DCC, DMAP, CH_2Cl_2, room temp, 24h.

2.2.10: Tacrine-carbazole hybrid scaffolds

Carbazoles are widely found in nature in many plant species and fungi, possess a vast range of biological activities including radical scavenging ability [Tachibana, Y, et al, 2001]. Tacrine-carbazole hybrids[Thiratmatrakul et al, 2014] were synthesized and evaluated towards cholinesterase inhibitory and radical scavenging ability (Scheme 2.15). All the compounds displayed good and selective AChE inhibitory activity with IC50 in the range 0.48 - 1 µM. The linker length displayed an important effect on activity. Compound bearing linker length of 5 exhibited highest AChE inhibitory activity with IC_{50} = 0.48 µM.

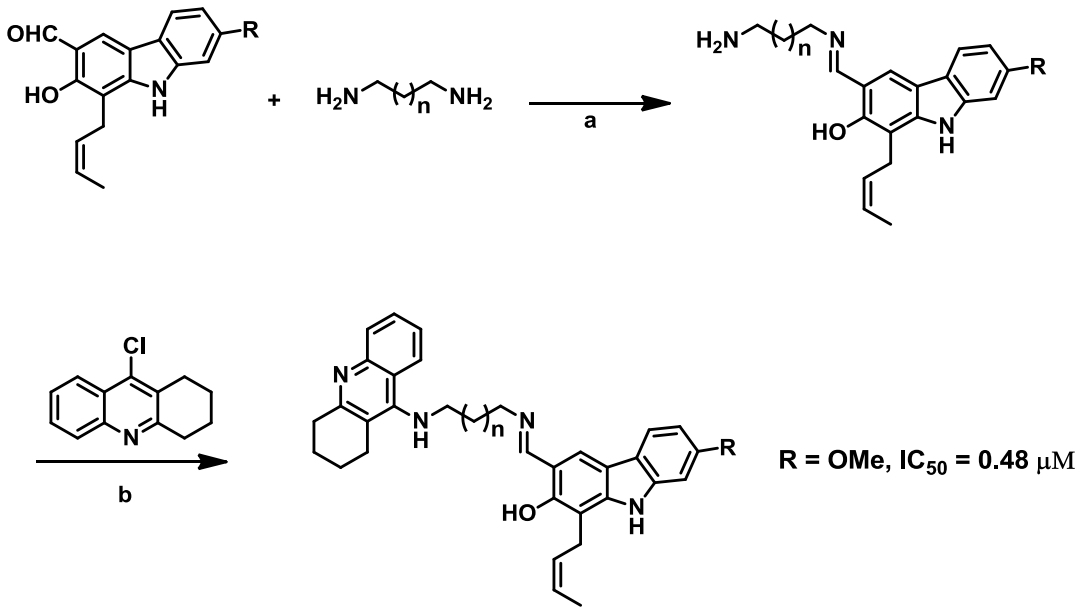

Scheme 2.15: Synthetic scheme for Tacrine-Carbazole hybrid: (a) Methanol, reflux, 24 h (b) n-pentane, reflux, 24 h.

2.2.11 heterobivalent tacrine derivatives

Wen Luo, et al,2011, reports the synthesis of new heterobivalent tacrine derivatives and evaluated as potential multi-functional anti-Alzheimer agents for their inhibitory activity on cholinesterases, antioxidant activity and self-induced β-amyloid (Aβ) aggregation. All these synthesized compounds had potent inhibition activity on acetylcholinesterase (AChE) and butyrylcholinesterase (BuChE) at nanomolar range (4.55 nM to 300 nM). A LineweavereBurk plot and molecular modeling study showed that these compounds targeted both the catalytic active site (CAS) and the peripheral anionic site (PAS) of AChE. The compounds showed a very good potent towards AChE activity of 4.55 nM, 4.67 nM, 6.14 nM, 7.98 nM and 4.70 nM (scheme 2.16). In addition, compound exhibited higher self-induced Aβ aggregation inhibitory activity than curcumin, which could become a multifunctional agent for further development for the treatment of AD.

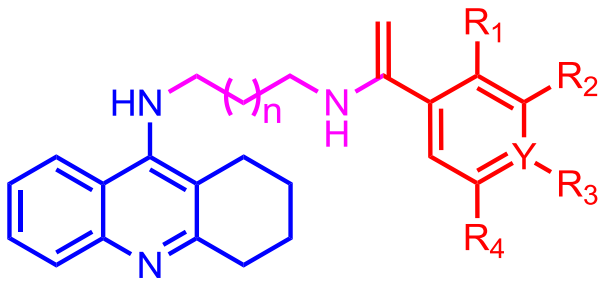

AChE, IC_{50} = 4.5 nM, n=8, Y=C, R_1=R_4=H, R_2=OMe, R_3=OH
AChE, IC_{50} = 4.67 nM, n=8, Y=C, R_1=H, R_2=R_4=OMe, R_3=OH
AChE, IC_{50} = 6.14 nM, n=8, Y=C, R_1=R_2=R_4=H, R_3=OH
AChE, IC_{50} = 7.98 nM, n=8, Y=C, R_1=H, R_2+R_3=OCH_2O, R_4=OMe
AChE, IC_{50} = 4.70 nM, n=8, Y=N, R_1=R_2=R_3=R_4=H

Scheme 2.16: Heterobivalent tacrine derivatives

2.3: Novel heterocyclic molecules as Acetylcholinesterase inhibitors

2.3.1 Anti-cholinesterase activity of Coumarin derivatives

A Shafiee 2014, designed a series of 7-hydroxycoumarin derivatives connected by an amidic linker to the different amines and synthesized as cholinesterase inhibitors. Most compounds showed remarkable inhibitory activity against acetylcholinesterase (AChE) and butyrylcholinesterase (BuChE). Among them, *N*-(1-benzylpiperidin-4-yl)acetamide derivativewith IC_{50} value of 1.6 μM was the most potent compound against AChE. The selectivity index of compound for anti-AChE activity was about 26 times. Moreover, the compoundsignificantly protected PC12 neurons against H_2O_2-induced cell death at low concentrations. The docking study of compoundwith AChE enzyme showed that both CAS and PAS are occupied by the ligand.

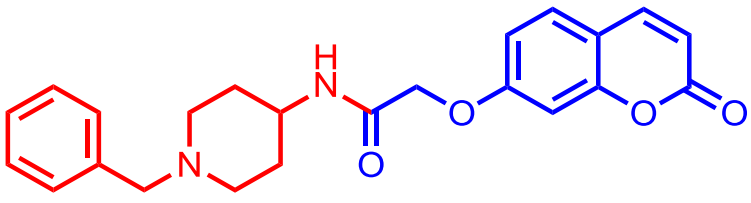

AChE, IC_{50} = 1.6 μM
BuChE, IC_{50} = 42 μM

Scheme 2.17: 7-hydroxy coumarin derivatives

Basha S J, et al, 2016 developed a series of fused tricyclic coumarin derivatives bearing iminopyran ring connected to various amide moieties as potential multifunctional anti-Alzheimer agents for their cholinesterase inhibitory and radical scavenging activities. *In-vitro* studies revealed that most of these compounds exhibited high inhibitory activity on acetylcholinesterase (AChE), with IC_{50} values ranging from 0.003 to 0.357 µM. Specifically, the most potent AChE inhibitor (IC_{50} 0.003 ± 0.0007 mM) has an excellent antioxidant profile as determined by the ABTS method (IC_{50} 7.98 ± 0.77 mM). Accordingly, the molecular modeling study demonstrated that all molecules with substituted benzyl amide moiety possessed an optimal docking pose with interactions at catalytic active site (CAS) and peripheral anionic site (PAS) of AChE simultaneously and thereby they might prevent aggregation of Aβ induced by AChE.

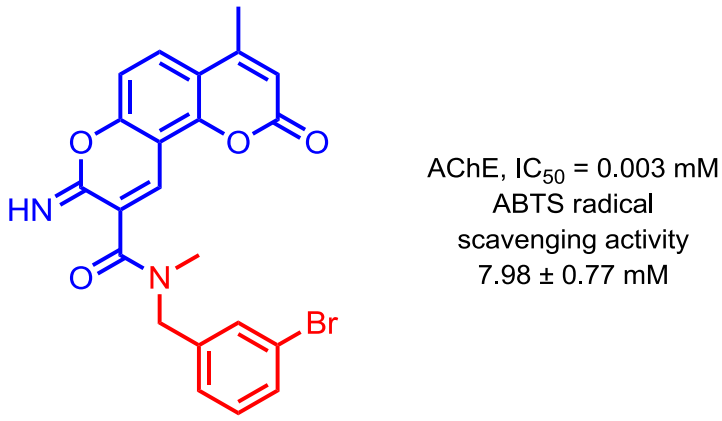

Scheme 2.18: Tricyclic coumarin derivatives

2.3.2 triazine-triazolopyrimidine hybrids as multitarget anti-Alzheimer agents

Jameel E et al, 2017, designed a series of triazine-triazolopyrimidine hybrids, synthesized and characterized against acetylcholinesterase inhibitors. In total, seventeen compounds were synthesized in which the di-substituted triazine-triazolopyrimidine derivativesshowed better acetylcholinesterase (AChE) inhibitory activity than the corresponding trisubstituted triazine-triazolopyrimidine derivatives. Out of the disubstituted triazinetriazolo pyrimidine based compounds,showed encouraging inhibitory activity on AChE with IC_{50} values 0.065 and 0.092 µM, respectively. Interestingly, di-substituted triazine-triazolopyrimidine derivativesalso demonstrated good inhibition selectivity towards AChE over BuChE by ~28 folds.

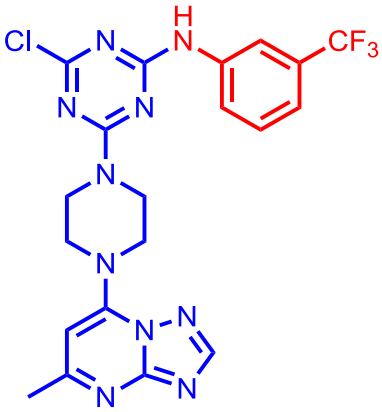

AChE, IC_{50} = 0.065 μM
BuChE, IC_{50} = 1.88 μM

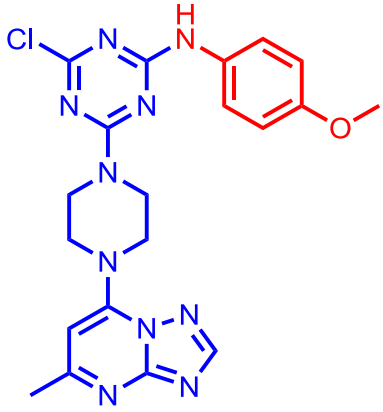

AChE, IC_{50} = 0.092 μM
BuChE, IC_{50} = 1.52 μM

Scheme 2.19: Triazine-triazolopyrimidine derivatives

The same team reported[Kumar. J, et al, 2016]a series of new cyanopyridine–triazine hybrids were designed, synthesized and screened as multitargeted anti-Alzheimer's agents. These molecules were designed while using computational techniques and were synthesized via a feasible concurrent synthetic route. Inhibition potencies of synthetic compounds against cholinesterases, oxidative stress, cytotoxicity, and neuroprotection against Aβ1–42-induced toxicity of the synthesized compounds were evaluated. Compounds showed promising inhibitory activity on acetylcholinesterase (AChE) with IC_{50} values 0.059 and 0.080 μM, along with good inhibition selectivity against AChE over butyrylcholinesterase (BuChE).

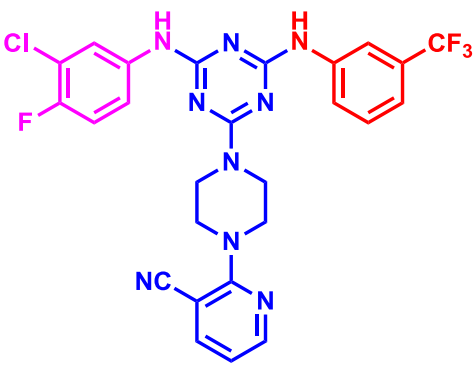

4d
AChE, IC_{50} = 0.059 μM
BuChE, IC_{50} = 3.603 μM

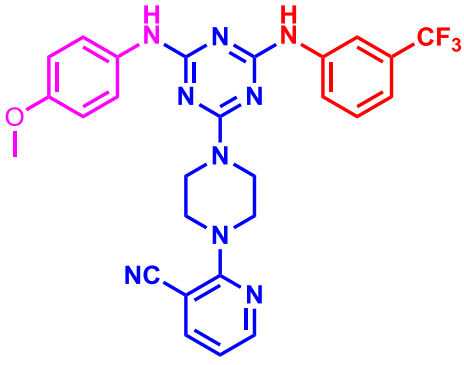

4h
AChE, IC_{50} = 0.080 μM
BuChE, IC_{50} = 2.015 μM

Scheme 2.20: cyanopyridine–triazine hybrids

2.3.3 Anti-cholinesterase activity of Flavanoid derivatives

Luo W et al 2016, the synthesis of 4-aminoethyl flavonoid derivatives and evaluated as acetylcholinesterase inhibitors and anti-oxidation activity against Alzheimer`s disease. Molecular modeling study showed that these compounds interacted at both catalytic active site and peripheral anionic site of AChE. Compoundsignificantly protected PC12 neurons against H_2O_2-induced cell death at low concentrations.

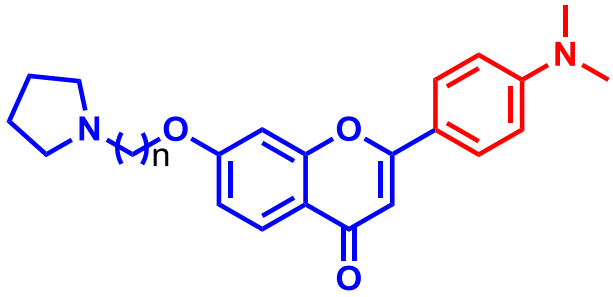

n = 8

AChE, IC_{50} = 1.99 μM

BuChE, IC_{50} = 2.60 μM

Scheme 2.21: Flavanoid derivatives as acetylcholinesterase inhibitors

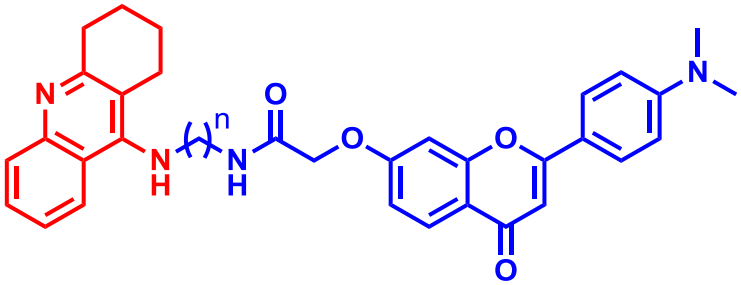

n = 6

AChE, IC_{50} = 0.059 μM

BuChE, IC_{50} = 0.046 μM

Scheme 2.22: Tacrine - Flavanoid hybrids as acetylcholinesterase inhibitors

2.3.4: 2-arylethenylquinoline derivatives as Acetylcholinesterase inhibitors

Wang. X-Q, et al, 2015, reported the biological evaluation of 2-arylethenylquinoline derivatives as Acetylcholinesterase inhibitors for the treatment of Alzheimer's disease. *In-vitro* studies showed that the compound (scheme 2.23) is potent inhibitory activity for cholinesterase with IC_{50} values of 0.2 μM and 64.1 μM against butyrylcholinesterase (BuChE) and acetylcholinesterase (AChE), respectively. Besides,was also capable of

disassembling the self-induced Aβ1-42 aggregation fibrils with a ratio of 59.8% at 20 μM concentration, and had a good metal chelating activity.

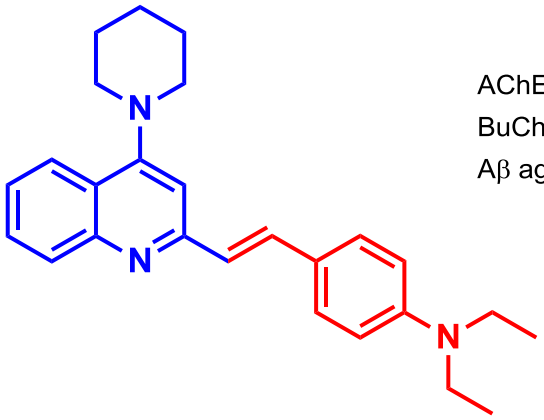

AChE, IC_{50} = 64.1 μM
BuChE, IC_{50} = 0.2 μM
Aβ aggregation, IC_{50} = 9.7 μM

Scheme 2.23: 2-arylethenylquinoline derivatives as Acetylcholinesterase inhibitors

2.3.5 Triazolopyrimidine-quinoline hybrids as Acetylcholinesterase inhibitors

Kumar J, et al, 2016, reported the synthesis of triazolopyrimidine-quinoline and cyanopyridine-quinoline hybrids and evaluated as acetylcholinesterase inhibitors (AChEIs). Three triazolopyrimidine based compounds showed nanomolar activity towards acetylcholinesterase. Among them the compound, strongly inhibited AChE with IC_{50} value of 42 nM. Furthermore compound was identified as most promising compound with 12 fold selectivity against butyrylcholinesterase (BuChE).

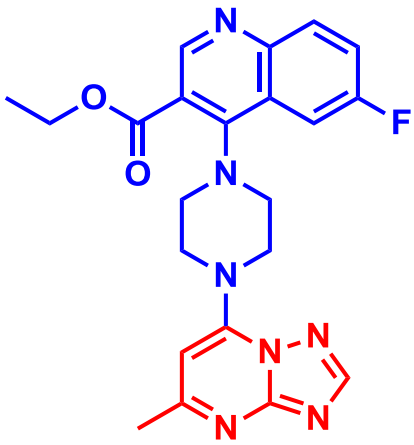

AChE, $1C_{50}$ = 42 nM
BuChE, IC_{50} = 510 nM
Aβ disaggregation = 73%
ORAC (trolex) = 2.43

Scheme 2.24: Triazolopyrimidine-quinoline derivatives as Acetylcholinesterase inhibitors

CHAPTER 3

FUNCTIONALISED DIHYDRAZO PYRIMIDINE DERIVATIVES FROM MBH ACETATES: SYNTHESIS AND STUDIES AGAINST ACETYLCHOLINESTERASE AS ITS INHIBITORS

3.1 Introduction

Diversely functionalised heterocyclic rings exist in nature and in many biologically relevant compounds, such as nucleic acids, antibiotics and hormones. A wide range of pharmacological properties shown by heterocyclic units inspired synthetic organic and medicinal chemists to pursue the synthesis of novel molecules and study their biological properties. Among them,benzimidazoles, imidazoles, triazoles and tetrazoles have exhibited biological properties such as anticancer and antimicrobial, and serve as antitubercular agents, benzodiazepine receptor agonists, calcium channel blockers and are also present as core structures in several currently marketed drugs.[Margiotta, N., et al 2007; Veron, J. B., et al 2008; Enguehard-Gueiffier, C., et al, 2007; Harrison, T. S., et al, 2005; Hanson, S. M., et al, 2008]. The various biological properties of imidazole and fused imidazole derivatives, such as antibacterial, antifungal, analgesic, antitubercular, anticancer, anti-HIV, antiarthritic and antitumor, have been extensively investigated [Masaki M., et al, 1996; Desai K. G., et al, 2006; Kazimierczuk Z., et al, 2005] Imidazo[4,5-b]pyrimidines, which are structurally related to benzimidazoles have shown diverse biological activities such as cytotoxic activities depending on the substituents of the heterocyclic ring [Sajith A. M., et al, 2015]. Several anxiolytic drugs such as fasiplon, taniplon, and divaplon holding imidazopyrimidine fragments are currently used as drugs in market[Tully W. R., et al, 1991; Clements-Jewery S., et al, 1988]. (Fig. 3.1).

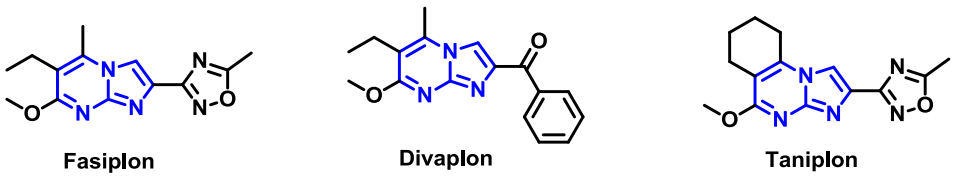

Figure 3.1: Imidazopyrimidine containing drugs

The main concept for the synthesis of novel dihydroimidazo pyrimidine ester derivatives originated from biological importance of dihydropyrimidines and imidazole derivatives. They exhibit pharmacological properties like anticancer activity, antiplatelet activity, HIV-1 integrase inhibitors [Puttaraju, K. B., et al 2013; Di Braccio, M.,et al, 2013] and anti-Alzheimer's disease [Zhi, H., et al, 2008; Rivkin, A., et al, 2010; Messer W. S., et al, 2000].

Moreover, these pyrimidines and imidazole/ benzimidazole derivatives are reported to have AChE inhibitory properties [Kypta, R. M., et al, 2005; Valasani, K. R., et al, 2013; Alpan, A. S., et al, 2013; Yoon, Y. K.,et al, 2013]. Also the structure activity studies proved that pyrimidine moieties plays an important role in the inhibition of AChE and the benzimidazole scaffold is the ring isoster of indanone moiety of donepezil, one of the most potent AChE inhibitor. Hence it was assumed that combining the two inhibitory moieties may further enhance the inhibitory potency towards AChE. More over expansion of aromatic plane may improve stacking and hydrophobic interaction with the enzyme as these interactions plays a crucial role in the binding of inhibitors to AChE. Acetylcholinesterase inhibitors (AChEIs) temporarily restore native levels of the neurotransmitter acetylcholine (Ach) and prevents the loss of cholinergic transmission in brain areas. In recent decades, researchers focused on the increase of cholinergic neurotransmission by inhibiting the enzyme AChE as one of the main stream option for AD. Currently, the drugs launched in market for cholinergic approach for AD such as tacrine, donepezil, rivastigmine and galantamine increase neurotransmission at cholinergic synapses in the brain and improving cognition.

3.2 MBH Acetates

The carbon-carbon bond formation and the functional group transformations are the most fundamental reactions for the construction of a molecular framework and hence represent a forefront of research in organic chemistry [Carey, F., et al, 1990; March, J., et al, 1992; Trost, B., et al, 1991; Hassner, A., et al, 1998]. Several carbon-carbon bond-forming reactions have been discovered and their applications in organic chemistry have also been well-documented in the literature. The most important ones include the aldol reaction [Mahrwald, R., et al, 1999; Heathcock, C. H., et al, 1984], Reformatsky reaction [Furstner, A., et al, 1989], Claisen rearrangements,[Ziegler, F. E., et al, 1988] Friedel-Crafts reaction [Olah, G. A., et al, 1990] Grignard reaction [Walborsky, H. M., et al, 1990] Diels-Alder reaction [Oppolzer, W., et al, 1984; Helmchen, G., et al, 1986], Wittig

reaction [Maryanoff, B. E., et al, 1989], Heck reaction [Meijere, A., et al, 1994], Suzuki coupling [Miyaura, N., et al, 1995],Grubb's ring closing metathesis [Grubbs, R. H., et al, 1991; Furstner, A., et al, 2000] and so forth. The very recent developments in organic chemistry have clearly established that the atom economy, selective (regio-, and stereo-) transformations and catalytic processes have become primary and the most essential requirements for the development of any efficient synthetic reaction [Trost, B. M., et al, 1991]. During the past years, synthetic organic chemistry has seen enormous growth, not only in terms of development of new methodologies for the construction of carbon-carbon bonds and functional group transformations but also in terms of development of new reagents, catalysts, strategies, transformations, and technologies often involving the concepts of atom economy and selectivity. Though the arsenal of synthetic organic chemistry is now very rich in the sense that there are methods available to synthesize any molecule which was once thought to be difficult to prepare, the continuing sophistication in and ever changing scenario of synthetic organic chemistry requires and even demands the continuous evolution of synthetic methods that meet the requirements of atom economy and very high levels of selectivity. Very recently, the Baylis-Hillman reaction [Baylis, A. B,, et al, 1972; Drewes, S. E., et al, 1988],yet another important reaction, has been added to the list of these useful carbon-carbon bond-forming reactions (Figure 3.1). Since the Baylis-Hillman reaction possesses the two most important requirements, atom economy and generation of functional groups, it qualifies to be in the list of efficient synthetic reactions.

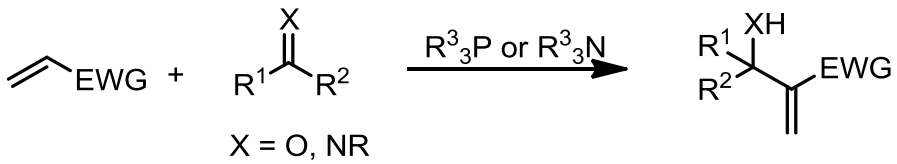

Scheme 3.1: General reaction of MBH reaction.

3.2.1: MBH Nitroallylic Acetates and it`s synthesis

Earlier, Baylis and Hillman reported the synthesis of α-hydroxyethyl nitroethylenes from MBH reaction [Morita K., et al, 1968]. Later, Namboothiri and Chen made further investigation on this reaction and emphasized the use of electrophilic ethyl glyoxylate [Deb, I., et al, 2006; Deb, I., et al, 2009; Kuan, H., et al, 2010]. The MBH reaction of nitroalkenes has been utilised for the synthesis of several heterocycles and carbocycles

[Gopi, E., et al, 2014; Yeh, F. H., et al, 2012; Cao C. L., et al, 2009]. The Morita–Baylis–Hillman (MBH) reaction has an attractive strategy for the synthesis of multifunctional heterocyclic molecules in recent years. The MBH reaction is a key step in the synthesis of bioactive and designed molecules. Further acetylation on hydroxyl group of these conjugated nitroalkene afforded MBH acetates as excellent Michael acceptors containing four potential electrophilic sites (α, β, γ, δ) (scheme 3.2). All four electrophilic sites are highly reactive and used as efficient synthons to synthesise the diversified molecules. The MBH adducts, can act as dielectrophilic reagents to undergo cascade reactions with various bifunctional nucleophiles.

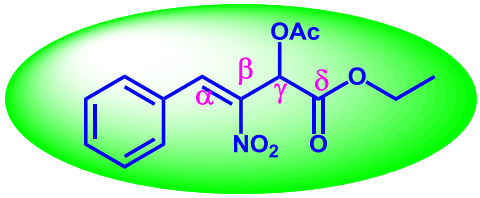

Figure 3.2: Structure of MBH Acetate derived from nitro alkenes

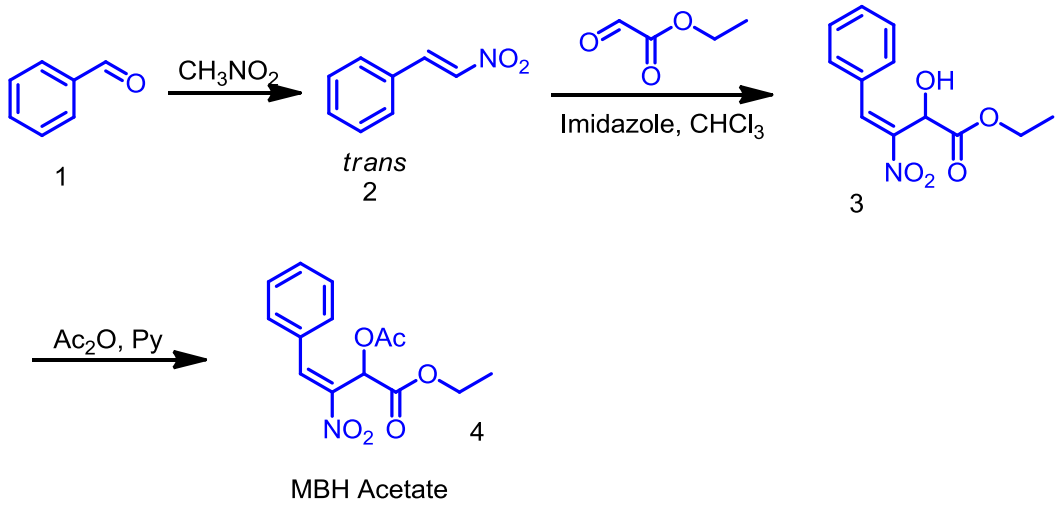

Scheme 3.2: Synthetic scheme of nitro allylic MBH Acetate

3.2.2: Biological active heterocyclic compounds from MBH Acetates

Recently Namboothiri and Chen demonstrated that the potential electrophilic site at α-position and further Michael addition at β-position in the synthesis of fused furans **6**[Anwar, S., et al, 2013; Kumar, T., et al, 2013; Mane, V., et al, 2015], imidazopyridines**5** and 2-substituted imidazoles [Gopi, E., et al, 2015]. Li Lue

demonstrated the formation of γ – α and γ – β cyclic products using 2-mercapto benzimidazoles for the synthesis of benzimidazo[2,1-b]-1,3-thiazine**9** and thiazolo[3,2-a]benzimidazole **10** respectively [Zhang, J. Q., et al, 2014]. Nair, reported the synthesis of fused pyrans**11** using MBH acetates with cyclopentanedione as α – γ cyclic product [Nair, D. K., et al, 2012]. Recently, Shao reported the cascade reaction of MBH acetates with N-substituted hydrazine for the synthesis of pyrazoles, in which the reaction was initiated by a S_N2 reaction at the electrophilic γ-position followed by Michael addition at a-position [Shao, N., et al, 2014]. Zou demonstrated the reactivity of all four subsequent potential electrophilic sites (α, β, γ, δ) of MBHAs to form imidazo[1,2-a] pyridines**8** (α – α), indolizines (α – β), pyrroles **7**(α – γ) and benzo[b] [1,6]oxazocin-2-ones**12** (α – δ) [Zhu, H., et al, 2013].

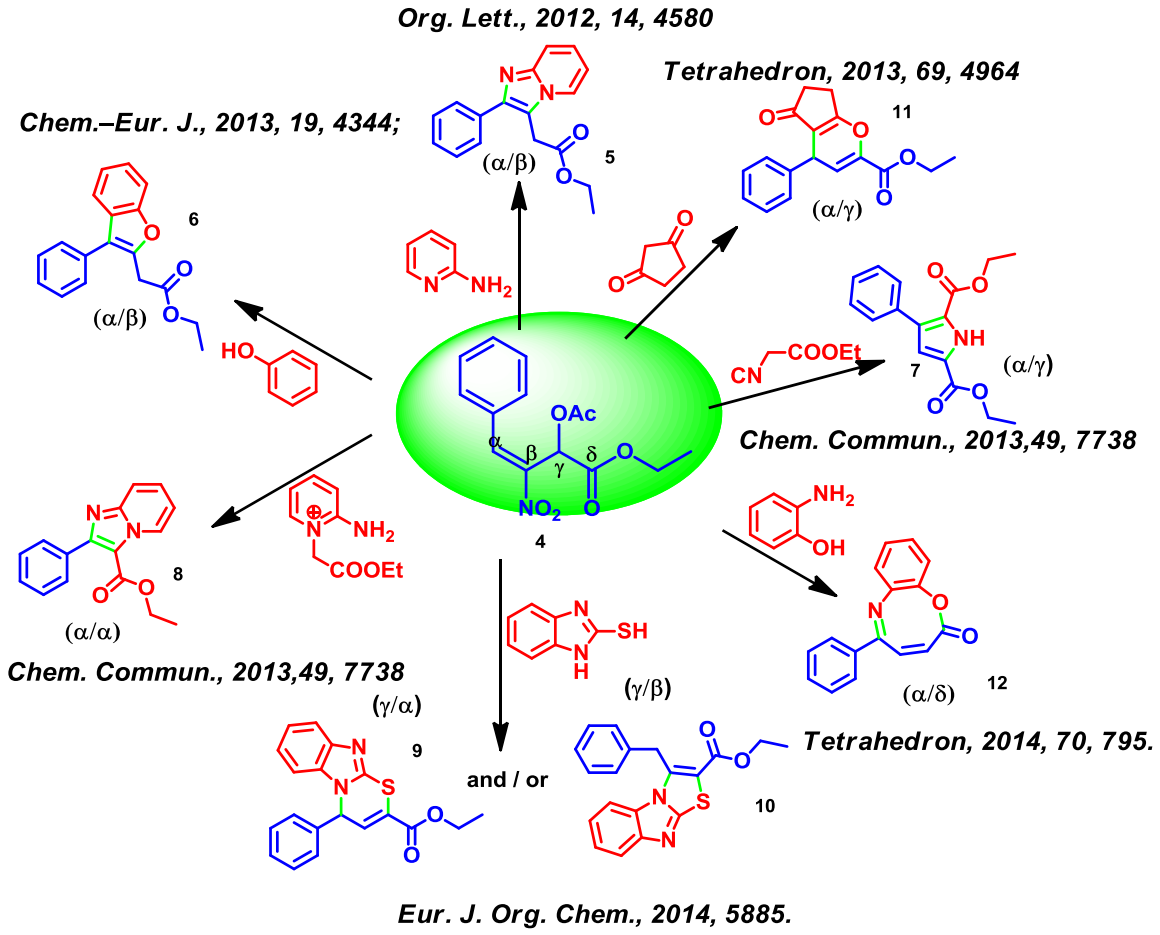

Scheme 3.3: Cascade reactions of MBH acetates with different binucleophiles

Therefore, the desirable protocols that would generate various heterocyclic compounds for the synthesis of natural and bio-active compounds is of great demand. Recently,

cascade reactions gained tremendous potential in the area of organic synthesis to maximise the results. We envisioned that synthesis of dihydro[1,5]azo[1,2-a] pyrimidine 2-ester derivatives could be possible by reaction of nitrostyrene derived MBH acetates and aminoazole derivatives (Scheme 3.4).

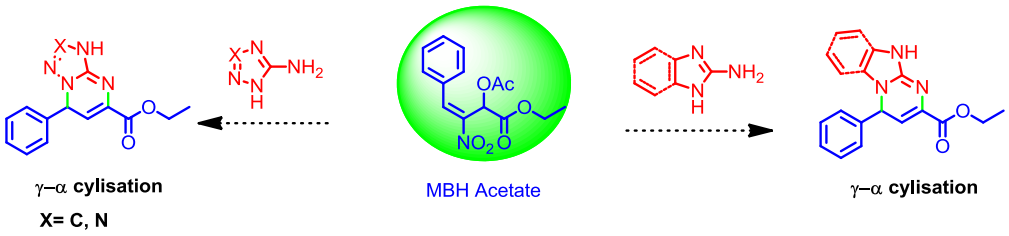

Scheme 3.4: Strategy towards construction of dihydroazo pyrimidine derivatives

3.3 Results and discussion

3.3.1 Synthetic studies

Our initial efforts were focused on optimising the reaction parameters with respect to base, solvent and temperature. Accordingly, the reaction was studied with MBH acetate of nitro alkene **4** and 2-amino benzimidazole **13** as a model substrate. The reaction was performed in THF at room temperature without base. Unfortunately no product formation was observed by LCMS even after heating at 70 ^{o}C (Table 3.1, entry 1 and 2). While adding organic bases like triethylamine and DIPEA, we observed the formation of 4-phenyl-1,4-dihydrobenzo[4,5]imidazo[1,2-a]pyrimidine-2-carboxylic ester **14** in low yields (Table 1, entries 3 and 4). Our subsequent efforts were focused on use of bases such as pyridine, 2,6-lutidine, DABCO, DBU which delivered **14** in 40–50% yield (Table 1, entry 5–8) and inorganic bases like K_2CO_3, Cs_2CO_3 gave compound **14** in moderate to good yields (Table 3.1, entry 9 and 10). Among all the bases screened, Cs_2CO_3 was found to give a superior yield (80%) in THF over 12 h at RT. Among the solvent screens (CH_2Cl_2, $CHCl_3$, MeOH, EtOH, CH_3CN, and 1,4-dioxane) (Table 3.1, entry 11–16), CH_3CN and 1,4-dioxane shows the formation of compound 3 in good yield (81%). Finally we optimised the condition is Cs_2CO_3 (2.0 eq.) in acetonitrile/1,4-dioxane as a solvent of choice to yield compound **14** (82%) at RT.

Table 3.1: Screening of reaction conditions

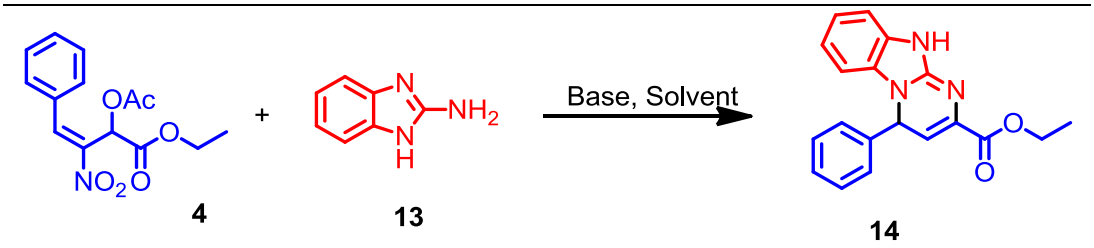

S.No	Base	Solvent	Temp	Yield[b] (%)
1	--	THF	RT	0
2	--	THF	70°C	0
3	Et_3N	THF	RT	20
4	DIPEA	THF	RT	22
5	Pyridine	THF	RT	40
6	2,6-Lutidine	THF	RT	40
7	DABCO	THF	RT	44
8	DBU	THF	RT	49
9	K_2CO_3	THF	RT	60
10	Cs_2CO_3	THF	RT	80
11	Cs_2CO_3	CH_2Cl_2	RT	45
12	Cs_2CO_3	$CHCl_3$	RT	48
13	Cs_2CO_3	MeOH	RT	60
14	Cs_2CO_3	EtOH	RT	68
15	Cs_2CO_3	CH_3CN	RT	82
16	Cs_2CO_3	1,4-dioxane	RT	81

Having these optimised conditions in hand, we explored the scope of **13** with different MBH acetates **4**. All the reactions were completed in 12 h at room temperature to give the desired product in moderate to good yields. The yields were good with MBH acetates possessing electron donating groups (**14**b, **14**c, **14**h and **14**l) to afford the corresponding products in excellent yields (73–82%). On other hand, MBH acetates bearing hindered aryl groups at ortho position (**14**d, **14**e, **14**i) delivered moderate yields (60–70%). The yields were good in case of MBH acetates having strong electron withdrawing groups (**14**k) and pyridine substrates (**14**f, **14**g). We next carried the scope of this optimised conditions with 2-aminoimidazoles for the synthesis of 5-phenyl-5,8-dihydroimidazo[1,2-

a]pyrimidine-7-carboxilic ester derivatives (**14**m–**14**r). It was observed that, compared to 2-aminobenzimidazole, 2-aminoimidazole required 15 h to obtain the desired product in moderate yields (45–66%) (scheme 3.5).

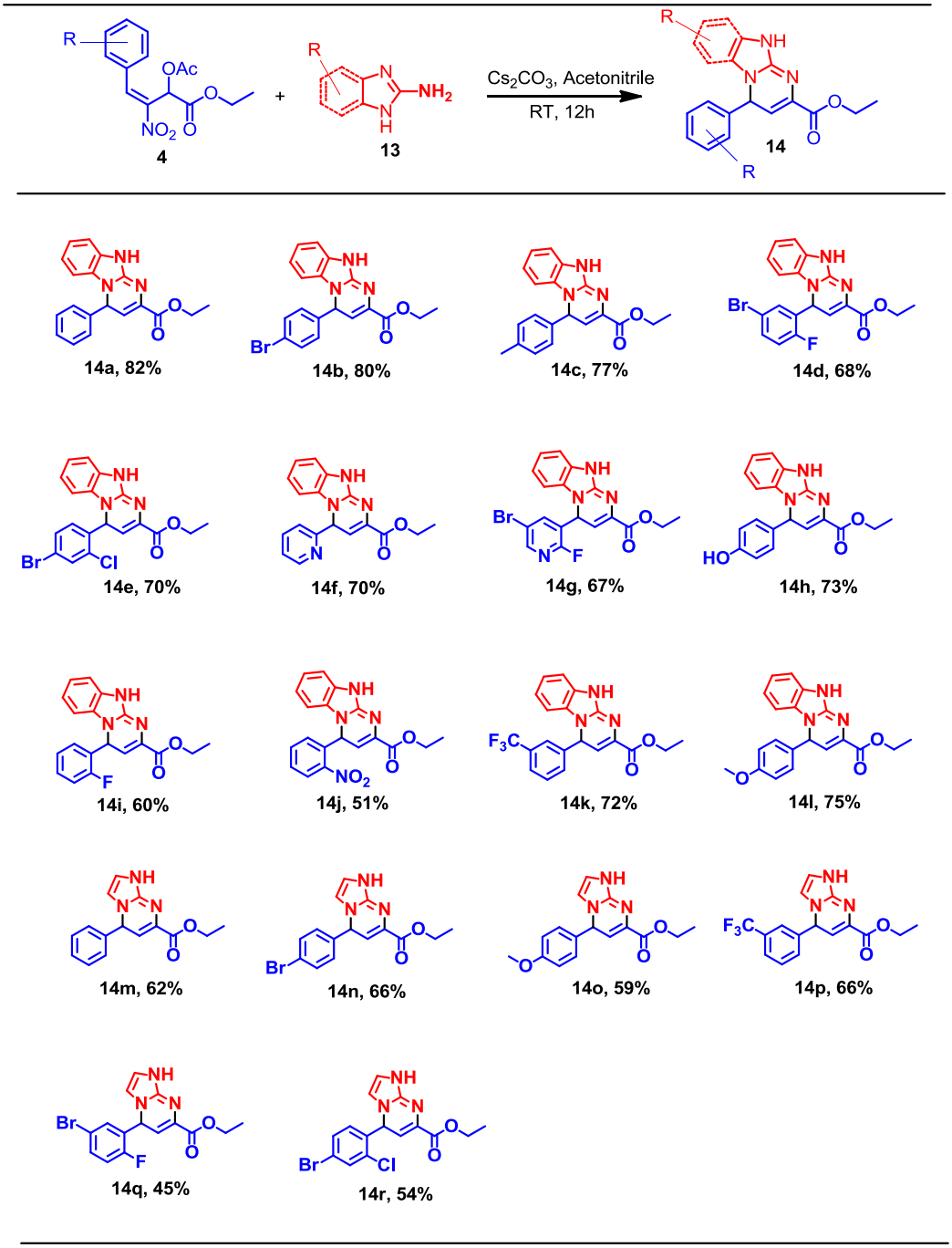

Scheme 3.5: Substrate Scope of MBHAs towards reaction with 2-aminobenzimidazoles and 2-aminoimidazoles

Our studies were extended to use of 3-amino-1,2,4-triazoles for the synthesis of 7-phenyl-4,7-dihydro-[1,2,4]triazolo[1,5-a] pyrimidine-5-carboxylicesters with MBHAs using the optimised conditions. In case of 3-amino 1,2,4-triazoles, we observed two regio isomers in the ratio of 7:3 by LCMS and NMR. To improve the regioselectivity, different solvents (MeOH, THF, CH_3CN, 1,4-dioxane and DMF) were tried. To our delight, DMF provided the excellent regioselectivity (9:1) at 60 ^oC by using Cs_2CO_3 as a base (Scheme 3.6). The yields are good in case of MBHAs possessing substituents at meta- and para- position (**15**b–**15**f) compared to MBHAs having substitutions at ortho- positions (**15**g and **15**h).

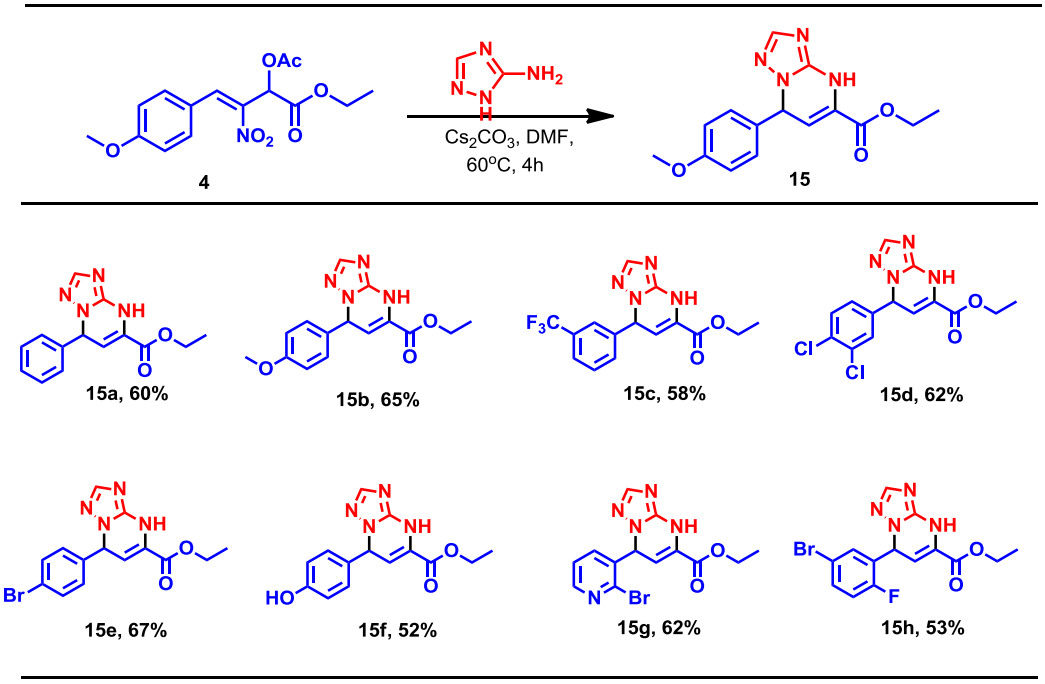

Scheme 3.6: Synthesis of dihydro triazopyrimidine derivatives

After the successful demonstration of the reactivity of different MBHAs with 3-amino-1,2,4-triazole, we focused our attention for the synthesis of 7-phenyl-4,7-dihydrotetrazolo[1,5-a]pyrimidine-5-carboxylic esters (16a & 16b) by reacting 5-amino tetrazoles with different MBHAs and are summarised in Scheme-5. The above conditions were, not suitable for reacting MBHAs with guanidine hydrochloride. Thus, there is no reaction was observed even after 12h reflux when guanidine hydrochloride was treated with MBH acetates.

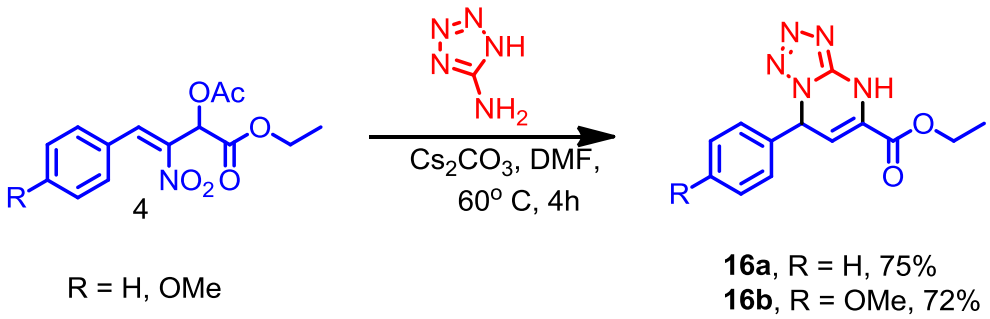

Scheme 3.7: Synthesis of dihydro tetrazolopyrimidine derivatives

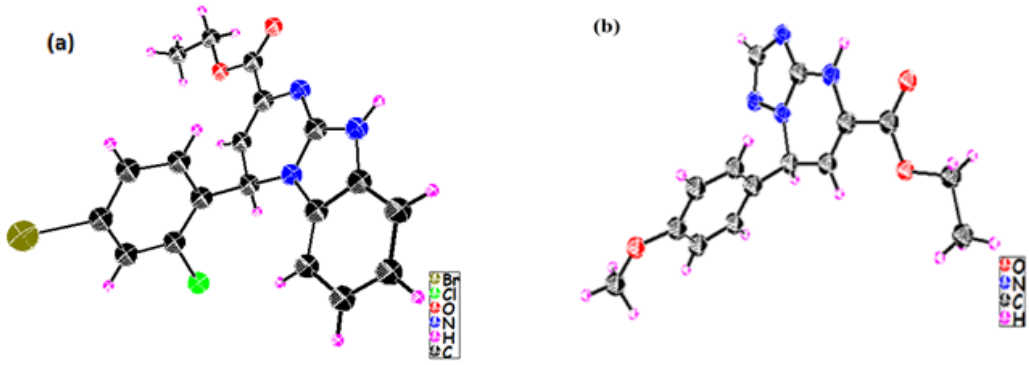

Figure 3.3: ORTEP diagram of (a) compound 14e and (b) compound 15b.

A possible mechanism for the synthesis is described in Scheme 3.8. The primary amine of 2-amino benzimidazole attacks the γ-electrophilic site of MBH acetate through S_N2 reaction to afford intermediate I. Intramolecular Michael addition occurs atα-electrophilic site of MBH acetate to generate intermediate II via 6-endo trig process. The intermediate II results in formation of III by loss of hydrogen atom, which on tautomerisation gives IV. The excess base facilitates the elimination of HNO_2 to give dihydro-benzo[4,5]imidazo[1,2-a]pyrimidine-2-carboxylic ester as **14**. Thus the reaction is completed by formal γ-α cyclisation on MBH acetate. Reaction of N-methyl 2-amino-benzimidazole with MBH acetate shows very low conversion for the desired product with nearly 10% product formation. Reaction with N-benzyl and N-Boc derivative of amino-benzimidazole resulted in recovery of the starting material, with no trace of product formation even at 70 ^oC. This can be easily anticipated due to steric hindrance by the nucleophilic nitrogen to attack at the electrophilic SP3 carbon atom of MBH acetate.

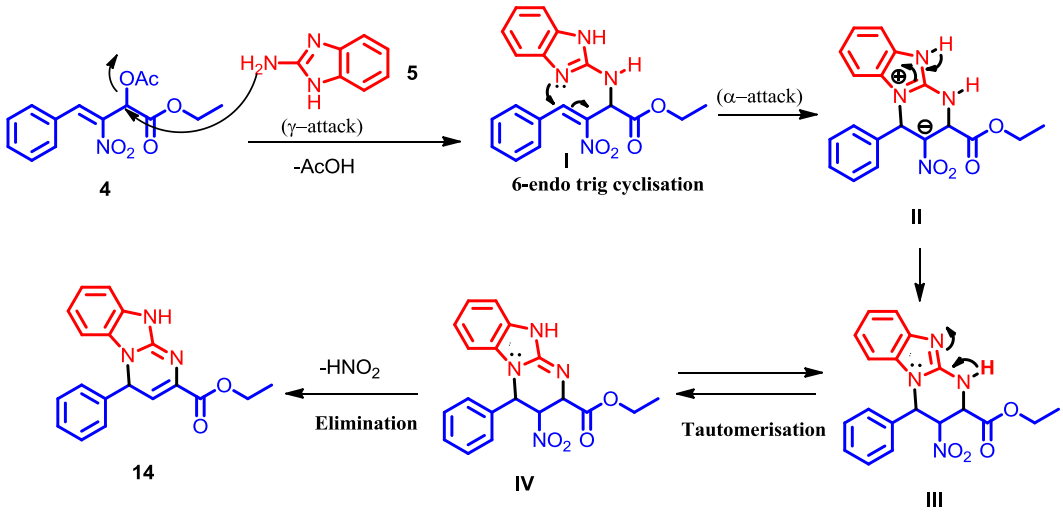

Scheme 3.8: Proposed mechanism.

3.3.2 Acetylcholine activity studies

The in vitro inhibitory effect of newly synthesized ligands were assessed by Ellman's method using AMPLITE™ AChE assay kit (AAT Bioquest, Inc., Sunnyvale, CA). In order to check the inhibitory activity of the compounds towards the AChE an initial screening has been carried out with a ligand concentration of 208 nM. Enzyme and ligands were incubated for 15 minutes and checked the enzyme activity towards the substrate. A control experiment has also been carried out without ligand. Finally the optical density was plotted against time (velocity time graph) (Fig. 3.4) and deduced the percentage of inhibition of the compounds (Table 3.2). Since all the compounds were displayed strong inhibitory activity, the half maximal inhibitory activity (IC_{50}) value for all compounds were deduced. Enzyme inhibition studies revealed that the newly synthesized compounds exhibit inhibitory activity against AChE in nM range. All of these compounds displayed enhanced inhibitory profile than tacrine and reported IC_{50} of galantamine (two known AD drugs). The maximum and minimum IC_{50} values obtained are 91.8 and 42.52 nM respectively. The compound **14a** exhibited an IC_{50} value 70.78 nM. It was also noticed that the phenyl group baring any substitutions are found to have lower IC_{50} value except **14**c. The presence of methyl group in the phenyl ring of the compound **14**c has drastically increased the IC_{50} value to 91.8 nM. With the substitution of polar groups such as –OH (**14**h) and $–NO_2$ (**14**j), the AChE inhibitory effects was better as compared with 14a. Introduction of halogens in phenyl moiety exerted prominent AChE inhibition (IC_{50} values in the range of 42–53 nM) of the compounds such as **14**b, **14**d, **14**e and **14**i. It was already reported that the substitution of halogen is

an important method in drug design since it can increase the binding affinity of the compounds through halogen bonding and alters the physico chemical properties. Substitution of an additional halogen in the phenyl ring of the compounds **14**d and **14**e make it more effective against AChE with IC_{50} values 46.86 and 42.52 nM respectively (Figure 3.5). Whereas the substitution of phenyl ring with pyridine ring (**14**g) has markedly decreased the inhibitory effect towards AChE. The IC_{50} values of all compounds are shown in Table 3.2.

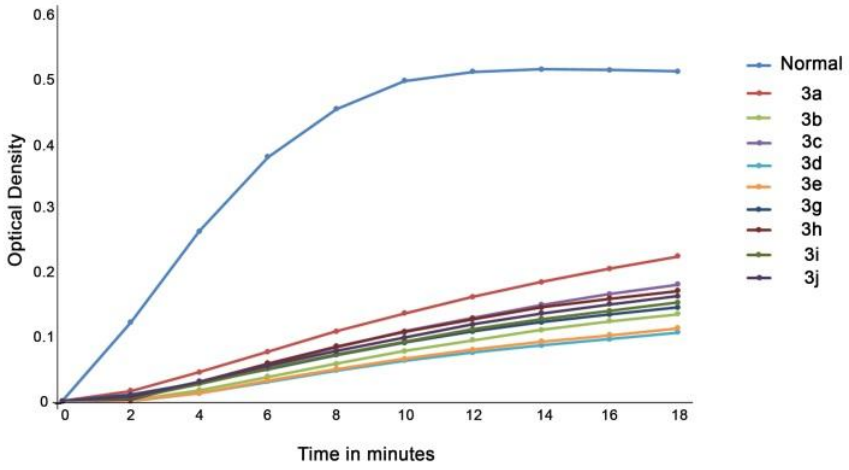

Figure 3.4: Velocity time graph obtained for native enzyme and in presence of compounds (208 nM)

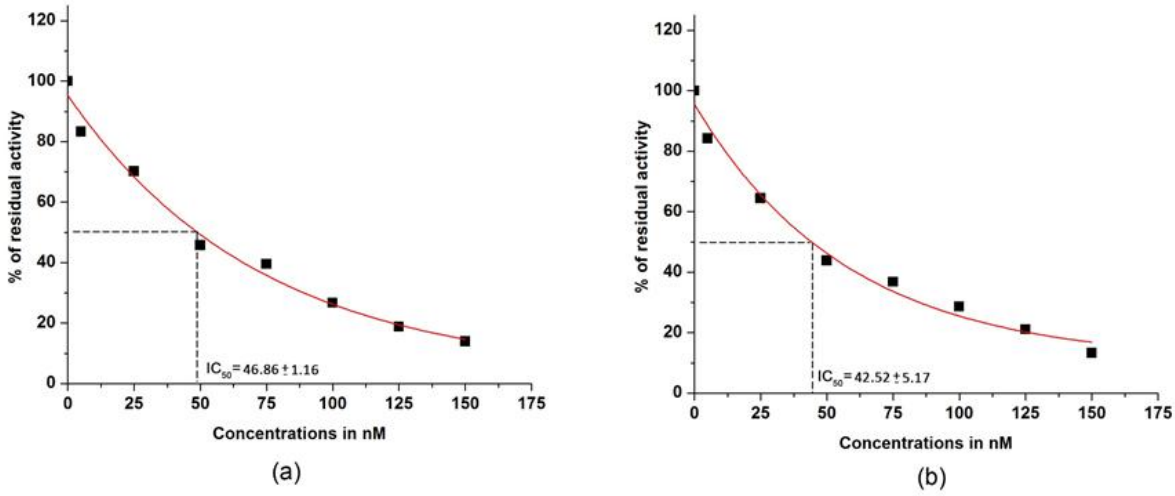

Figure 3.5: Relative residual activity of AChE plotted against the different concentrations of the most potent compounds **14d (a)** and 14**e (b).**

Table 3.2: The *in vitro* AChE inhibitory profile of compounds **14a-14j**

Compound	% of Inhibition at 208 nM	hAChE IC_{50} (nM)+ SD
14a	53	70.78 ± 10.01
14b	70	52.64 ± 1.07
14c	62	91.8 ± 3.6
14d	**76**	**46.86 ± 1.16**
14e	**74**	**42.52 ± 5.17**
14g	69	71.48 ± 5.04
14h	61	67.32 ± 4.94
14i	67	52.58 ± 15.65
14j	65	68.4 ± 7.94
Tacrine	66	551.58 ±19.17
Galanthamine		360 ±10[1]

3.3.3: *In-silico* studies

The newly synthesized compounds were evaluated for their drug like behavior through *in silico* predictions. The ADME profiles of the compounds are given in Table 3.3. Some of the important parameters [molecular weight (MW) and volume (V), CNS activity, partition coefficient (LogP), number of hydrogen bond donors and acceptors (HBD and HBA), polar surface area (PSA), number of rotatable groups (rotor), number of N and O (N and O), BBB permeability (LogBB), permeability across Mandin-Darby canine kidney, (MDCK) and intestinal epithelial cells (Caco-2), Solvent accessible surface area (SASA) and % of human oral absorption (% HOA)] that are crucial for CNS activity were identified and displayed in Table 3.3 along with the reference values[Pajouhesh, H., et al, 2005; Alavijeh, M. S., et al, 2005; Ghose, A. K., et al, 2012; Clark, D. E., et al, 1999; Lenz, G. R., et al, 1999].

Table 3.3: ADME profile of the compounds predicted by QikProp program

Compound	MW (≤ 450 Da)	HBD (≤ 3)	HBA (≤ 7)	LogP (≤ 5)	CNS (≥0)	Rotor (≤ 7)	N and O (≤7)
14a	319	1	3	4.35	0	2	5
14b	398	1	3	4.92	0	2	5
14c	333	1	3	4.66	0	2	5
14d	416	1	3	5.01	0	2	5
14e	433	1	3	5.32	0	2	5
14g	417	1	4	4.41	0	2	6
14h	335	2	4	3.58	-2	3	6
14i	337	1	3	4.53	0	2	5
14j	348	1	5	3.51	-2	3	7

Compound	BBB (-1.2 -1.2)	SASA (320-735 Å^2)	Volume (≤1250 Å^3)	PSA (60 –70 Å^2)	Caco (≥ 500 nm/s)	MDCK (≥ 500 nm/s)	% HOA
14a	-0.51	605	1052	64	1171	587	100
14b	-0.35	634	1105	64	1171	1554	100
14c	-0.54	637	1112	64	1171	587	100
14d	-0.27	641	1118	64	1170	2391	100
14e	-0.22	649	1141	63	1174	3126	100
14g	-0.51	634	1106	76	675	1362	100
14h	-1.12	618	1077	86	355	161	94
14i	-0.43	612	1065	64	1169	899	100
14j	-1.16	620	1090	96	319	144	92

Using these physicochemical properties it is possible to differentiate the CNS drugs from a group of molecules. It was found that the values for MW, volume, N and O, rotor, HBD and HBA were in the preferred range for all the compounds. The lipophilicity (derived from Log P) of molecules are in the allowed limits except **14d** and 14**e**. It was already reported that CNS acting agents may have slightly higher LogP value. PSA is always linked to with BBB penetration and normally for CNS active molecules the PSA values will be low compared to other therapeutics. For majority of the compounds, the PSA value is optimal except **14g**, **14h** and **14j**. The upper limit of PSA for the BBB permeability was reported as 90 Å^2, and hence the two compounds such as **14g** and **14h** can also be taken into consideration[Deli, M. A., et al, 2005]. The SASA of all compounds are seems to be in the range of CNS acting agents. The polar groups

containing compounds such as **14h** and **14j** has very poor BBB, MDCK cell permeability, Caco cell permeability and CNS activity. MDCK and Caco cell lines are used as *in vitro* models to study the BBB permeability[Reichel, A., et al, 2003]. The online BBB prediction tool also gave the similar results. It showed all compounds except **14h** and **14j** have the ability to cross BBB.

3.3.4: Docking studies

The conclusion made from the enzyme kinetics studies was further explored with the help of molecular docking followed by binding energy calculations. The close analysis of the AChE-ligand complexes revealed a common binding pattern for all the newly synthesized ligands. They binds at the bottom of the active site, spanning along the acyl binding pocket and makes contacts with peripheral anionic site residues also. In all complexes, the aromatic residues such as F297, F295, F338, Y337, Y341 and H447 are oriented perpendicular to the dihydrobenzimidazo pyrimidine ring and arrests the rotational and translational movement of the ligands in the active site. Apart from these, hydroxyl group of Y337 and Y124 are acting as an anchor to hold the compounds at its current positions through a series of hydrogen bonds with keto group and ring nitrogens. A classical π-π stacking interaction was also observed between the phenyl ring of the compounds and the indole ring of W86. Furthermore, π-π stacking between dihydrobenzimidazo pyrimidine ring system and H447 an F338 was also observed. Docking studies also showed that the compounds **14d** and **14e** were more potent inhibitors than other compounds with binding energies -87.03 and -92.26 Kcal/mol respectively. These compounds forms additional hydrogen bonds with keto group and Y341. They also exhibit halogen bonds with the polar atoms of the following residues such as Y119, G120, G121, S125 and Y133. Apart from that a series of van der Waals interactions and hydrophobic interactions are also found to stabilize the interactions. The residue such as Y72, V73, W86, Y124, Y133, F295, F297, Y337, F338, Y341 and I451 seems to be involved in the hydrophobic interactions. Whereas in case of tacrine, the interactions are mainly favoured by stacking formed against Y337 and W86. A hydrogen bond with N atom and main chain carbonyl oxygen of H447 is also seen. It also forms a series of hydrophobic interactions like the compounds **14d/14e.** But it lacks halogen bonding and other hydrogen bonding interactions as seen in case of **14d** and **14e.** These interactions may be partly contributing to the highest inhibitory potency of the compounds over tacrine. The binding mode of the

top scored ligands (**14d** and **14e**) was displayed in Figure 3.6. The binding energies of all the compounds are mentioned in Table 3.4.

Table 3.4: The Binding energetics of the compounds at the active site of hAChE

Compound	Glide score	Binding energy	Interacting residues
14a	-8.24	-74.38	F338,H447,Y337 and W86
14b	-8.62	-75.55	F338,H447, Y337, Y124 and W86
14c	-8.09	-72.60	F338,H447,Y124,Y337 and W86
14d	-9.15	-87.03	F338,H447, Y341,Y124,Y337 andW86
14e	-9.79	-92.26	F338,H447,Y341,Y337, Y124 and W86
14g	-8.70	-85.55	F338,Y124,Y337 and W86
14h	-9.11	-75.07	F338,Y124,Y133, G121 and W86
14i	-8.90	-76.65	F338,H447,Y124,Y337 and W86
14j	-9.04	-74.13	F338,H447,Y124,Y337 andW86
Galanthamine	-9.69	-81.51	F338,S203,E202 and Y337

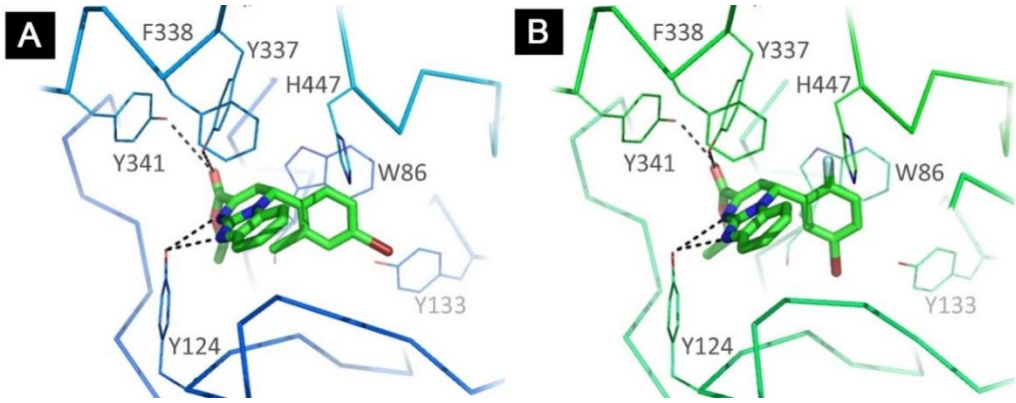

Figure 3.6: Binding pattern of compounds **14e** (A) and compound **14d** (B) at the active site of hAChE. The protein residues are shown in lines and the compounds are shown in stick. The hydrogen bonds are indicated by dotted lines.

In general, the effective AChE inhibition of the compounds are achieved by interaction with the residues in the peripheral anionic site (Y72, Y124 and Y341), anionic site (W86

and Y337), acyl binding site (F295 and F297) and active site (H447). Also the orientation of these compounds in the ligand binding site is in such a manner that it completely mask the entry of the substrate in to the active site. Also it can hinder H447 and make it unavailable for the catalytic activities. Stability of the compounds (**14d** and **14e**) at their bound positions was investigated through 20 ns MD simulation. During the simulation, the intermediate structures were saved and superimposed to the native structure with respect to the ligand position. The RMSD indicates that none of the complex deviates much from their respective binding positions. The maximum deviation observed for ligand was 1.4 Å and the minimum was 0.6 Å. The studies indicate that the ligands are stable in their binding position. The RMSD of two top scored compounds **14**d and **14**e were displayed in Figure 3.7.

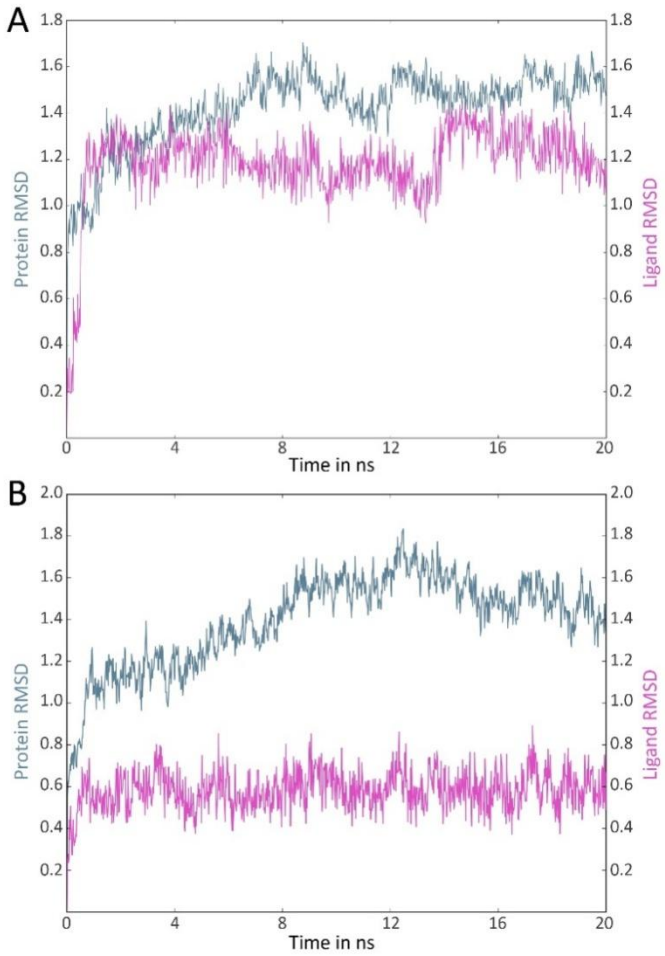

Figure 3.7: The RMSD graph of Cα (blue in colour), ligand displacement (pink in colour) of compound **14**d (A) & compound **14**e (B)

3.4 Conclusions

In summary, we have carried out a regioselective (γ-α) attack of bifunctional nucleophiles to MBH acetates. Various bifunctional nucleophiles such as 2-aminobenzimidaole, 2-aminoimidazole and 3-amino 1,2,4 triazole on reaction with MBH acetate gave moderate to excellent yields (45–82%) of dihydroazo pyrimidine derivatives. Interestingly, of all the potential elctrophilic sites (α, β, γ, δ) the first Michael addition occurs at γ position of MBH acetates in a S_N2 followed by another nucleophilic attack at α position with a *6-endo trig* cyclisation to give rise to functionalised dihydroazo pyrimidine derivatives. The in vitro enzyme inhibition studies of these derivatives indicate that they exhibits much higher potency than the known drugs such as tacrine and galantamine. The above results describes the importance of MBHAs in the synthesis of dihydroazo pyrimidine derivatives and their possible utilization against AD treatment as AChE inhibitors.

3.5 Experimental Section

3.5.1 Chemistry

Experimental procedure for synthesis of compound (14a-14l): To a solution of 2-aminobenzimidazole (0.15 mmol) in CH_3CN (1.0 mL) was added MBH Acetate of nitro alkene (0.18 mmol) and Cs_2CO_3 (0.3 mmol) at RT. The reaction mixture was stirred for 12h at RT. After completion of reaction (monitored by LCMS), the reaction mixture was quenched with water (5 mL). The reaction mixture was extracted with ethyl acetate (3x 30 mL). The combined organic layers were dried over anhydrous sodium sulphate, filtered and concentrated to give the crude product. To this crude product was added methanol (4 mL) and stirred for 30 min at RT. A white precipitate was obtained which was filtered to give the desired product (60% - 82%).

Ethyl 4-phenyl-4,10-dihydrobenzo[4,5]imidazo[1,2-a]pyrimidine-2-carboxylate (14a):

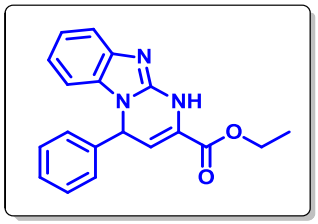

White solid; yield 46 mg, 82%; MP: 145-147 ^{o}C

^{1}H NMR (400 MHz, Chloroform-*d*): δ 7.55 (dd, *J* = 7.9, 3.0 Hz, 1H), 7.39 - 7.28 (m, 5H), 7.17-7.13(m, 1H), 6.97-6.93(m, 1H), 6.79-6.77 (m, 1H), 6.19 (d, *J* = 4.0 Hz, 1H), 5.99 (d, *J* = 4.0 Hz, 1H), 4.38-4.30 (dq, *J*= 7.2 Hz, 4.8Hz, 2.0Hz, 2H), 1.35 (t, *J* = 7.4 Hz, 3H).

^{13}C NMR (75 MHz, Chloroform-*d*) **δ** 162.39, 144.42, 143.65, 137.79, 133.55, 129.53, 129.07, 128.19, 126.39, 122.96, 122.39, 122.19, 118.64, 109.97, 62.75, 59.28, 14.10. **LCMS:***m/z* calculated for $C_{19}H_{17}N_3O_2$: 319.13; Observed mass: 320.2 (M+1)

Anal. Calculated for $C_{19}H_{17}N_3O_2$: C, 71.46; H, 5.37; N, 13.16. Found: C, 71.44; H, 5.35; N, 13.18.

Ethyl-4-(4-bromophenyl)-4,10-dihydrobenzo[4,5]imidazo[1,2-a]pyrimidine-2-carboxylate (14b):

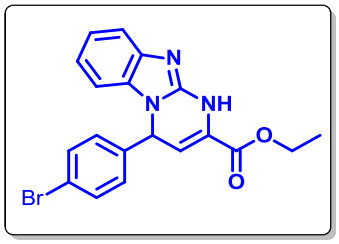

Pale brown solid; yield 57 mg, 80%; MP: 151-153 ^{o}C

^{1}H NMR (400 MHz, Chloroform-*d*): δ 7.57 (d, *J* = 8.0 Hz, 1H), 7.51 (d, *J* = 1.8 Hz, 1H), 7.50 (d, *J* = 1.9 Hz, 1H), 7.21 – 7.14 (m, 3H), 6.99-6.95 (m, 1H), 6.75 (d, *J* = 8.0 Hz, 1H), 6.17 (d, *J* = 4.0 Hz, 1H). 5.92 (d, *J* = 4.0 Hz, 1H), 4.35 (qq, *J* = 7.3, 3.7 Hz, 2H), 1.34 (t, *J* = 7.1 Hz, 3H).

^{13}C NMR (75 MHz, Chloroform-*d*) δ 161.71, 146.59, 142.04, 138.62, 132.44, 132.04, 131.51, 128.11, 126.17, 122.70, 122.52, 120.67, 117.21, 109.41, 105.84, 62.36, 57.40, 14.07.

LCMS:*m/z* calculated for $C_{19}H_{16}BrN_3O_2$: 397.04; Observed mass: 398.2, 400.2 (M+1, M+3);

Anal. Calculated for $C_{19}H_{16}BrN_3O_2$: C, 57.30; H, 4.05; N, 10.55;. Found: C, 57.31; H, 4.07; N, 10.54.

Ethyl-4-(p-tolyl)-4,10-dihydrobenzo[4,5]imidazo[1,2-a]pyrimidine-2-carboxylate (14c):

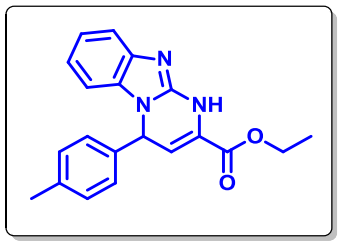

White solid; yield 46 mg, 77%; MP: 143-145 ^{o}C

^{1}H NMR (400 MHz, DMSO-*d6*) δ (ppm) 7.93 (d, *J* = 6.56 Hz, 2H), 7.84–7.81 (m, 2H), 7.61-7.56 (m, 2H), 7.34-7.29 (m, 2H), 6.57 (d, *J* = 4.0 Hz, 1H), 6.16 (d, *J* = 4.0 Hz, 1H), 4.17 (q, *J* = 6.8 Hz, 2H), 2.11 (s, 3H), 1.23 (t, *J* = 6.8 Hz, 3H).

^{13}C NMR δ (ppm) 161.94, 148.24, 144.41, 143.67, 133.13, 127.23, 126.11, 124.90, 123.99, 123.49, 122.88, 119.06, 63.05, 58.43, 23.08, 14.08.

LCMS:*m/z* calculated for $C_{20}H_{19}N_3O_2$: 333.15; Observed mass: 334.2 (M+1).

Anal. Calculated for $C_{20}H_{19}N_3O_2$: C, 72.05; H, 5.74; N, 12.60; Found: C, 72.07; H, 5.75; N, 12.64

Ethyl-4-(5-bromo-2-fluorophenyl)-4,10-dihydrobenzo[4,5]imidazo[1,2-a]pyrimidine-2-carboxylate (14d):

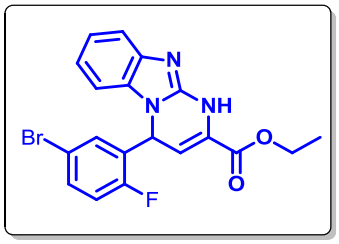

Yellow solid; yield 46 mg, 68%; MP: 150-152 ^{o}C

^{1}H NMR (300 MHz, DMSO-*d6*): δ 10.15 (bs, 1H), 7.79 (s, 1H), 7.54 (dd, J – 8.2, 2.2 Hz, 1H), 7.37 (d, J = 7.7 Hz, 1H), 7.08-7.03 (m, 2H), 6.90 (t, J = 7.6 Hz, 1H), 6.73-6.70 (m, 2H), 5.83 (d, *J* = 3.9 Hz, 1H), 4.25 (q, *J* = 7.0 Hz, 2H), 1.28 (t, *J* = 7.0 Hz, 3H).

^{13}C NMR (101 MHz, DMSO) δ 166.89, 161.63, 153.30, 150.78, 142.39, 131.47, 131.41, 130.59, 127.97, 125.85, 125.56, 123.80, 123.76, 121.28, 121.24, 118.20, 106.17, 62.18, 59.24, 14.31.

LCMS:*m/z* calculated for $C_{19}H_{15}BrFN_3O_2$: 415.03; Observed mass: 416.2, 418.2 (M+1, M+3); Anal. Calculated for $C_{19}H_{15}BrFN_3O_2$: C, 54.82; H, 3.63; N, 10.10; Found: C, 54.83; H, 3.65; N, 10.12.

Ethyl-4-(4-bromo-2-chlorophenyl)-4,10-dihydrobenzo[4,5]imidazo[1,2-a]pyrimidine-2-carboxylate (14e):

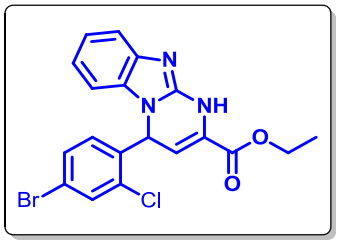

White solid; yield 54 mg, 70%; MP: 153-155 ^{o}C

^{1}H NMR (400 MHz, Chloroform-*d*): δ 7.65 (d, *J* = 1.6 Hz, 1H), 7.55 (d, *J* = 8.0 Hz, 1H), 7.31 (dd, *J* = 8.4, 1.6 Hz, 1H), 7.20 (t, 7.2 Hz, 1H), 7.02 (t, *J* = 8.0 Hz, 1H), 6.85 (d, *J* =

8.0 Hz, 1H), 6.77 (d, *J* = 8.0 Hz, 1H), 6.67 (d, *J* = 4.0 Hz, 1H), 6.01 (d, *J* = 4.0 Hz, 1H), 4.36 (qq, *J* = 7.2 Hz, 2H), 1.37 (t, *J* = 7.2 Hz, 3H).

^{13}C NMR (75 MHz, Chloroform-*d*) δ 161.47, 135.37, 132.69, 131.32, 129.56, 126.72, 122.93, 122.81, 121.13, 117.19, 109.15, 103.84, 62.52, 50.80, 14.07.

LCMS:*m/z* calculated for $C_{19}H_{15}BrClN_3O_2$: 431.00; Observed mass: 431.2, 433.2 (M+1, M+3)

Anal. Calculated for $C_{19}H_{15}BrClN_3O_2$: C, 52.74; H, 3.49; N, 9.71; Found: C, 52.76; H, 3.50; N, 9.73.

Ethyl-4-(pyridin-2-yl)-4,10-dihydrobenzo[4,5]imidazo[1,2-a]pyrimidine-2-carboxylate (14f):

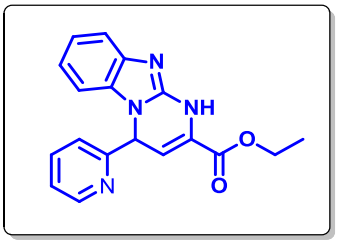

White solid; yield 40 mg, 70%; MP: 155-156 ^{o}C

^{1}H NMR (300 MHz, DMSO-*d6*): δ 7.73-7.61 (m, 4H), 7.48 (d, *J* = 7.8 Hz, 1H), 7.10-7.06 (m, 2H), 6.85-6.81 (m, 1H), 6.46 (d, *J* = 3.9 Hz, 1H), 5.86 (d, *J* = 3.9 Hz, 1H), 4.25 (qq, *J* = 7.2, 3.6 Hz, 2H), 1.25 (t, *J* = 7.1 Hz, 3H).

^{13}C NMR (101 MHz, DMSO-*d6*) δ 166.88, 161.51, 153.29, 150.95, 150.65, 140.81, 139.03, 136.16, 131.40, 128.88, 125.86, 124.63, 121.25, 121.30 118.20, 103.72, 62.26, 59.34, 14.33.

LCMS:*m/z* calculated for $C_{18}H_{16}N_4O_2$: 320.13; Observed mass: 321.2 (M+1).

Anal. Calculated for $C_{18}H_{16}N_4O_2$: C, 67.49; H, 5.03; N, 17.49; Found: C, 67.51; H, 5.03; N, 17.48.

Ethyl-4-(5-bromo-2-fluoropyridin-3-yl)-4,10-dihydrobenzo[4,5]imidazo[1,2-a]pyrimidine-2-carboxylate (14g):

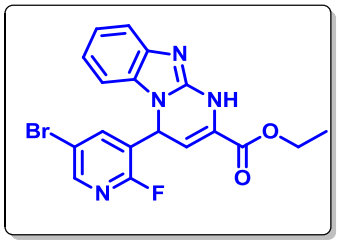

Brown solid; yield 50 mg, 67%; MP: 162-164 ^{o}C

^{1}H NMR (300 MHz, Chloroform-*d*): 8.35 (s, 1H), 7.81 (s, 1H), 7.62-7.55 (m, 2H), 7.35-7.25 (m, 2H), 6.67 (d, J= 3.9 Hz, 1H), 6.02 (d, J= 3.9 Hz, 1H), 4.36 (q, J= 7.2 Hz, 2H), 1.36 (t, J= 7.2 Hz, 3H).).

^{13}C NMR (75 MHz, Chloroform-*d*) δ 162.32, 143.99, 143.68, 140.10, 133.40, 127.46, 127.22, 126.80, 126.16, 123.40, 123.10, 122.48, 118.79, 109.70, 62.82, 53.92, 14.11.

LCMS: *m/z* calculated for $C_{18}H_{14}BrFN_4O_2$: 416.03; Observed mass: 417.2, 419.2 (M+1, M+3)

Anal. Calculated for $C_{18}H_{14}BrFN_4O_2$: C, 51.82; H, 3.38; N, 13.43; Found: C, 51.83; H, 3.40; N, 13.46.

Ethyl-4-(3-hydroxyphenyl)-4,10-dihydrobenzo[4,5]imidazo[1,2-a]pyrimidine-2-carboxylate (14h):

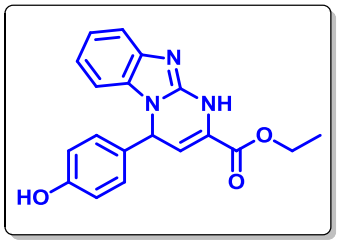

Colour less gummy nature; yield 44 mg, 73%; MP: 134-137 ^{o}C

^{1}H NMR (400 MHz, Chloroform-*d*): δ 7.88 – 7.86 (m, 1H), 7.78 (dd, J = 8.8, 2.4 Hz, 2H), 7.69-7.66 (m, 2H), 7.18 (dd, J = 8.8, 2.4 Hz, 1H), 7.15 (d, J = 2.4 Hz, 1H), 6.73 (d, J

= 4.0 Hz, 1H), 6.39 (d, J = 4.0 Hz, 1H), 5.88 (bs, 1H), 4.18 (q, J = 7.2 Hz, 2H), 1.31 (t, J = 7.2 Hz, 3H).

^{13}C NMR (101 MHz, $CDCl_3$) δ 161.48, 151.75, 150.36, 139.70, 133.37, 131.35, 131.05, 129.22, 127.78, 126.54, 126.03, 122.34, 120.94, 119.11, 104.86, 62.52, 59.58, 14.12.

LCMS: *m/z* calculated for $C_{19}H_{17}N_3O_3$: 335.13; Observed mass: 336.2 (M+1)

Anal. Calculated for $C_{19}H_{17}N_3O_3$: C, 68.05; H, 5.11; N, 12.53; Found: C, 68.07; H, 5.13; N, 12.55.

Ethyl-4-(2-fluorophenyl)-4,10-dihydrobenzo[4,5]imidazo[1,2-a]pyrimidine-2-carboxylate (14i):

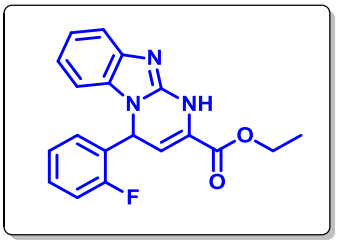

Pale yellow solid; yield 36 mg, 60%; MP: 141-143 ^{o}C

^{1}H NMR (400 MHz, Chloroform-*d*): δ 8.74 (dd, *J* = 7.2, 2.4 Hz, 1H), 8.27 (s, 1H), 7.90 (m, 1H), 7.82 -7.79 (m, 2H), 7.56 – 7.49 (m, 1H), 7.48 – 7.43 (m, 2H), 7.38 (d, *J* = 4.0 Hz, 1H), 6.55 (d, *J* = 4.0 Hz, 1H), 4.54 (q, *J* = 7.2 Hz, 2H), 1.48 (t, *J* = 7.2 Hz, 3H).

^{13}C NMR (75 MHz, $CDCl_3$) δ 162.47, 160.06, 144.40, 143.60, 133.54, 129.81, 128.50, 127.76, 122.92, 122.33, 121.74, 118.58, 114.83, 110.04, 62.72, 58.73, 14.11.

LCMS:*m/z* calculated for $C_{19}H_{16}FN_3O_2$: 337.12; Observed mass: 338.2 (M+1)

Anal. Calculated for $C_{19}H_{16}FN_3O_2$: C, 67.65; H, 4.78; N, 12.46; Found: C, 67.65; H, 4.76; N, 12.45.

Ethyl-4-(2-nitrophenyl)-1,4-dihydrobenzo[4,5]imidazo[1,2-a]pyrimidine-2-carboxylate (14j):

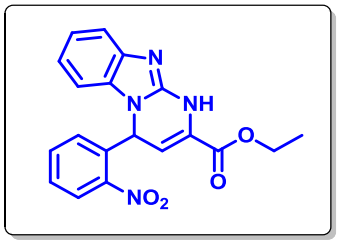

White solid; yield 33 mg, 51%; MP: 150-153 ^{o}C

^{1}H NMR (400 MHz, Chloroform-*d*): δ 8.13 (dd, *J* = 7.2 Hz, 2.0 Hz, 1H), 7.57-7.48 (m, 3H), 7.18 (dt, *J* = 7.2 Hz, 1H), 7.03 (dd, *J* = 7.2 Hz, 2.0 Hz, 1H), 6.99-6.97 (m, 1H), 6.95 (d, *J* = 4.0 Hz, 1H), 6.64 (d, *J* = 8.0 Hz, 1H), 6.27 (d, *J* = 4.0 Hz, 1H), 4.38 (dq, *J* = 7.2Hz, 2H), 1.37 (t, *J* = 7.2 Hz, 3H).

^{13}C NMR (75 MHz, $CDCl_3$) δ 161.78, 156.28, 148.83, 140.06, 134.69, 129.78, 129.16, 127.69, 127.24, 124.47, 121.53, 119.41, 114.12, 111.95, 61.94, 58.09, 14.24.

LCMS:*m/z* calculated for $C_{19}H_{16}N_4O_4$: 364.12; Observed mass: 365.2 (M+1)

Anal. Calculated for $C_{19}H_{16}N_4O_4$: C, 62.63; H, 4.43; N, 15.38; Found: C, 62.65; H, 4.44; N, 15.40.

Ethyl-4-(3-(trifluoromethyl)phenyl)-1,4-dihydrobenzo[4,5]imidazo[1,2-a]pyrimidine-2-carboxylate (14k):

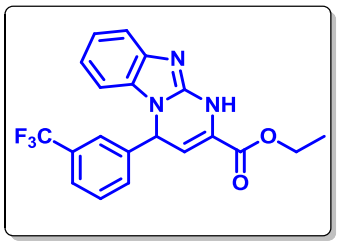

White powder; yield 50 mg, 72%; MP: 140-142 ^{o}C

^{1}H NMR (300 MHz, Chloroform-*d*): δ 7.61-7.50 (m, 4H), 7.32 (m, 2H), 7.14 (m, 2H), 6.29 (d, *J* = 3.9 Hz, 1H), 5.90 (d, *J* = 3.9 Hz, 1H), 4.36 (q, *J* = 7.2 Hz, 2H), 1.34 (t, *J* = 7.2 Hz, 3H).

^{13}C NMR (101 MHz, $CDCl_3$) δ 166.04, 161.61, 151.97, 150.24, 148.71, 138.70, 132.69, 132.22, 131.51, 128.85, 128.47, 127.53, 125.99, 123.03, 122.31, 120.90, 119.22, 105.49, 62.37, 60.03, 14.13.

LCMS:*m/z* calculated for $C_{20}H_{16}F_3N_3O_2$: 387.12; Observed mass: 388.2 (M+1)

Anal. Calculated for $C_{20}H_{16}F_3N_3O_2$: C, 62.01; H, 4.16; N, 10.85; Found: C, 62.03; H, 4.17; N, 10.87.

Ethyl-4-(4-methoxyphenyl)-1,4-dihydrobenzo[4,5]imidazo[1,2-a]pyrimidine-2-carboxylate (14l):

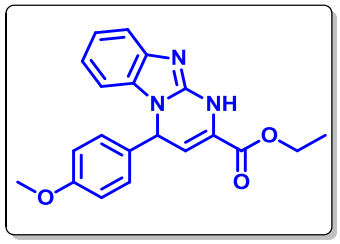

White solid; yield 47 mg, 75%; MP: 146-147 ^{o}C

^{1}H NMR (400 MHz, Chloroform-*d*): δ 9.68 (bs, 1H), 7.61-7.56 (m, 2H), 7.35-7.31 (m, 1H), 7.26 (d, *J* = 8.4 Hz, 2H), 7.16-7.12 (m, 1H), 6.91 (d, *J* = 8.4 Hz, 2H), 6.17 (d, *J* = 4.0 Hz, 1H), 5.93 (d, *J* = 4.0 Hz, 1H), 4.41-4.29 (m, 2H), 3.80 (s, 3H), 1.35 (t, *J* = 7.2 Hz, 3H).

^{13}C NMR (101 MHz, $CDCl_3$) δ 161.82, 160.01, 150.06, 148.62, 132.03, 131.57, 128.54, 127.18, 125.97, 122.29, 120.88, 119.27, 114.40, 106.45, 62.19, 60.05, 55.33, 14.14.

LCMS:*m/z* calculated for $C_{20}H_{19}N_3O_3$: 349.14; Observed mass: 350.2 (M+1)

Anal. Calculated for $C_{20}H_{19}N_3O_3$: C, 68.75; H, 5.48; N, 12.03; Found: C, 68.77; H, 5.49; N, 12.05.

Ethyl-5-phenyl-5,8-dihydroimidazo[1,2-a]pyrimidine-7-carboxylate (14m):

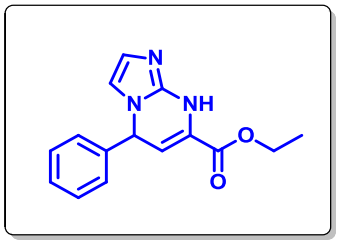

Colourless solid; yield 30 mg, 62%; MP: 162-164 ^{o}C

^{1}H NMR (400 MHz, Chloroform-*d*): δ 7.43-7.25 (m, 5H), 7.15 (dd, *J* = 3.9 Hz, 8.4 Hz, 1H), 6.53 (d, *J* = 3.6 Hz, 1H), 6.21 (dd, *J* = 3.9 Hz, 8.4 Hz, 1H), 5.92 (dd, *J* = 3.9 Hz, 8.4 Hz, 1H), 4.36 (dq, *J* = 7.2 Hz, 3.6 Hz, 2H), 1.35 (t, *J* = 7.2 Hz, 3H).

^{13}C NMR (75 MHz, $CDCl_3$) δ 161.78, 148.83, 140.06, 134.69, 129.78, 129.16, 127.69, 127.24, 124.47, 121.53, 119.41, 111.95, 61.94, 58.09, 14.24.

LCMS:*m/z* calculated for $C_{15}H_{15}N_3O_2$: 269.12; Observed mass: 270.2 (M+1)

Anal. Calculated for $C_{15}H_{15}N_3O_2$: C, 66.90; H, 5.61; N, 15.60; Found: C, 66.92; H, 5.60; N, 15.62.

Ethyl-5-(4-bromophenyl)-5,8-dihydroimidazo[1,2-a]pyrimidine-7-carboxylate (14n):

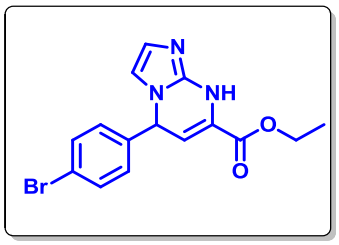

Pale brown solid; yield 41 mg, 66%; MP: 169-172 ^{o}C

^{1}H NMR (400 MHz, Chloroform-*d*): δ 10.25 (bs, 1H), 7.46 (d, *J* = 8.0 Hz, 2H), 7.38 (d, *J* = 1.6 Hz, 2H), 7.16-7.11 (m, 1H), 6.54 (d, *J* = 3.6 Hz, 1H), 6.16 (d, *J* = 4.0 Hz, 1H), 5.85 (d, *J* = 4.0 Hz, 1H), 4.36 (dq, *J* = 7.2 Hz, 3.6 Hz, 2H), 1.36 (t, *J* = 7.2 Hz, 3H).

^{13}C NMR (101 MHz, DMSO) δ 161.67, 150.63, 149.25, 140.47, 132.20, 129.49, 127.73, 121.94, 114.08, 106.46, 62.15, 59.11, 14.34.

LCMS: *m/z* calculated for $C_{15}H_{14}BrN_3O_2$: 347.03; Observed mass: 348.2, 350.2 (M+1, M+3)

Anal. Calculated for $C_{15}H_{14}BrN_3O_2$: C, 51.74; H, 4.05; N, 12.07; Found: C, 51.76; H, 4.07; N, 12.08.

Ethyl-5-(4-methoxyphenyl)-5,8-dihydroimidazo[1,2-a]pyrimidine-7-carboxylate (14o):

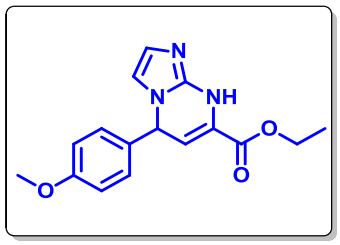

White solid; yield 31 mg, 59%; MP: 162-164 ^{o}C

^{1}H NMR (400 MHz, Chloroform-*d*): δ 9.59 (bs, 1H), 7.27-7.24 (m, 2H), 7.12 (d, *J* = 3.2 Hz, 2H), 6.90 (d, *J* = 8.4 Hz, 1H), 6.53 (d, *J* = 3.6 Hz, 1H), 6.15 (d, *J* = 3.6 Hz, 1H), 5.29 (d, *J* = 3.6 Hz, 1H), 4.33 (q, *J* = 7.2 Hz, 2H), 3.80 (s, 3H), 1.35 (t, *J* = 7.2 Hz, 3H).

^{13}C NMR: (75 MHz, Chloroform-*d*) δ 161.58, 150.20, 148.70, 138.71, 132.33, 128.84, 128.57, 127.57, 123.01, 105.39, 62.12, 61.58, 54.35, 14.16.

LCMS: *m/z* calculated for $C_{16}H_{17}N_3O_3$: 299.13; Observed mass: 300.2 (M+1)

Anal. Calculated for $C_{16}H_{17}N_3O_3$: C, 64.20; H, 5.72; N, 14.04; Found: C, 64.22; H, 5.74; N, 14.06.

Ethyl-5-(3-(trifluoromethyl)-phenyl)-5,8-dihydroimidazo[1,2-a]pyrimidine-7-carboxylate (14p):

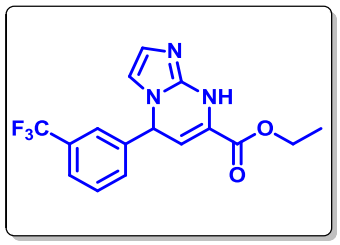

White solid, yield 40 mg, 66%; MP: 155-157 ^{o}C

^{1}H NMR (400 MHz, Chloroform-*d*): δ 7.72-7.61 (m, 2H), 7.57-7.46 (m, 2H), 7.04 (d, *J* = 4.0 Hz, 1H), 6,51 (d, *J* = 4.0 Hz, 1H), 6.27 (d, *J* = 3.8 Hz, 1H), 5.90 (d, *J* = 4.0 Hz, 1H), 4.38 (dq, *J* = 7.2 Hz, 3.6 Hz, 2H), 1.36 (t, *J* = 7.2 Hz, 3H).

^{13}C NMR (126 MHz, DMSO) δ 161.62, 150.80, 149.35, 142.41, 131.49, 130.63, 129.69, 127.91, 125.62, 123.79, 113.91, 106.18, 62.19, 59.20, 14.33.

LCMS:*m/z* calculated for $C_{16}H_{14}F_3N_3O_2$: 337.10; Observed mass: 338.2 (M+1)

Anal. Calculated for $C_{16}H_{14}F_3N_3O_2$: C, 56.97; H, 4.18; N, 12.46; Found: C, 56.96; H, 4.19; N, 12.48.

Ethyl-5-(5-bromo-2-fluorophenyl)-5,8-dihydroimidazo[1,2-a]pyrimidine-7-carboxylate (14q):

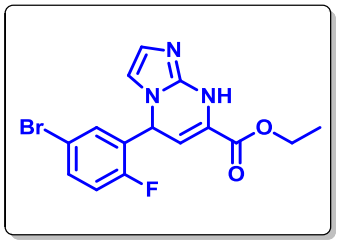

Pale brown solid; yield 30 mg, 45%; MP: 170-172 ^{o}C

^{1}H NMR (300 MHz, Chloroform-*d*): δ 10.02 (bs, 1H), 7.52 (dd, *J* = 7.0 Hz, 1.8 Hz, 1H), 7.27-7.16 (m, 2H), 7.10 (d, *J* = 3.6 Hz, 1H), 6.53 (d, *J* = 3.6 Hz, 1H), 6.16 (d, *J* = 3.9 Hz, 1H), 5.87 (d, *J* = 3.9 Hz, 1H), 4.35 (dq, *J* = 7.2 Hz, 3.6 Hz, 2H), 1.35 (t, *J* = 7.2 Hz, 3H).

^{13}C NMR (126 MHz, DMSO) δ 161.59, 150.80, 149.25, 141.91, 131.86, 131.60, 131.45, 129.36, 128.01, 127.67, 113.64, 105.78, 62.20, 58.61, 14.34.

LCMS:*m/z* calculated for $C_{15}H_{13}BrFN_3O_2$: 365.02; Observed mass: 366.2, 368.2 (M+1, M+3)

Anal. Calculated for $C_{15}H_{13}BrFN_3O_2$: C, 49.20; H, 3.58; N, 11.48; Found: C, 49.22; H, 3.59; N, 11.50.

Ethyl-5-(4-bromo-2-chlorophenyl)-5,8-dihydroimidazo[1,2-a]pyrimidine-7-carboxylate (14r):

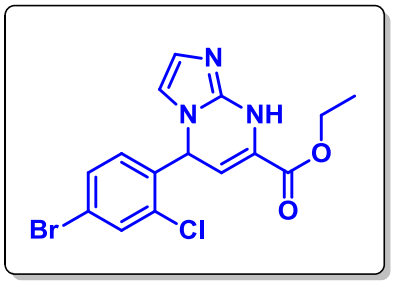

White solid; Yield 34 mg, 54%; MP: 171-173 ^{o}C

^{1}H NMR (500 MHz, DMSO) δ 10.22 (s, 1H), 7.69 (s, 1H), 7.64 (d, *J* = 8.3 Hz, 1H), 7.52 (d, *J* = 2.0 Hz, 1H), 7.18 – 7.16 (m, 1H), 6.81 (s, 1H), 6.35 (d, *J* = 3.9 Hz, 1H), 5.83 (d, *J* = 3.9 Hz, 1H), 4.25 – 4.20 (m, 2H), 1.31 – 1.24 (m, 3H)

^{13}C NMR (126 MHz, DMSO) δ 161.59, 150.80, 149.25, 141.91, 131.86, 131.60, 131.45, 129.36, 128.01, 127.67, 113.64, 105.78, 62.20, 58.61, 14.34

LCMS:*m/z* calculated for $C_{15}H_{13}BrClN_3O_2$: 381.00; Observed mass: 382.2, 384.2 (M+1, M+3).

Anal. Calculated for $C_{15}H_{13}BrClN_3O_2$: C, 47.08; H, 3.42; N, 10.98; Found: C, 47.09; H, 3.44; N, 1.00.

Experimental procedure for synthesis of compound (15a-15h):

To a solution of 3-amino 1, 2, 4-triazole (0.30 mmol) in DMF (2.0 mL) was mixed with MBH Acetate of nitro alkene (0.36 mmol) and cesium carbonate (0.6 mmol) and the reaction mixture was heated to 60^{o}C for 4h. After completion of reaction (monitored by LCMS), the reaction mixture was quenched with water (30 mL). The reaction mixture was extracted with ethyl acetate (3x 30 mL). The combined organic layers were dried over anhydrous sodium sulphate, filtered and concentrated over vacuum to give the crude product. To this crude product was added methanol (4 mL) and stirred for 30 min at RT. A white precipitate was obtained which was filtered gave the product (55% - 70%). The mother liquid contains a small amount of product along with small amount of other region isomer by LCMS.

Ethyl-7-phenyl-4,7-dihydro-[1,2,4]triazolo[1,5-a]pyrimidine-5-carboxylate-(15a):

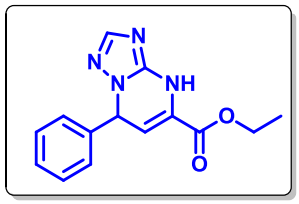

White solid; yield 60 mg, 60%; MP: 182-184 ^{o}C

^{1}H NMR (400 MHz, Chloroform-*d*): δ (ppm) 10.23 (bs, 1H), 7.78 (s, 1H), 7.42-7.28 (m, 5H), 6.22 (d, *J* = 4.0 Hz, 1H), 5.94 (d, *J* = 4.0 Hz, 1.6 Hz, 1H), 4.38 (dq, *J* = 7.2 Hz, 3.6 Hz, 2H), 1.36 (t, *J* = 7.2 Hz, 3H).

^{13}C NMR (75 MHz, Chloroform-*d*) δ (ppm) 161.82, 150.06, 148.99, 139.91, 129.02, 128.79, 127.42, 127.12, 106.10, 62.13, 60.63, 14.17.

LCMS:*m/z* calculated for $C_{14}H_{14}N_4O_2$: 270.11; Observed mass: 271.2 (M+1).

Anal. Calculated for $C_{14}H_{14}N_4O_2$: C, 62.21; H, 5.22; N, 20.73; Found: C, 62.22; H, 5.24; N, 20.75.

Ethyl-7-(4-methoxyphenyl)-4,7-dihydro-[1,2,4]triazolo[1,5-a]pyrimidine-5-carboxylate (15b):

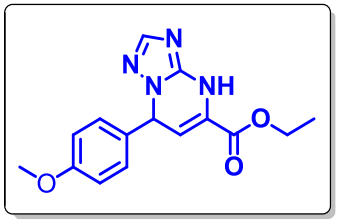

White solid; yield 70 mg, 65%; MP: 180-182 ^{o}C

^{1}H NMR (300 MHz, Chloroform-*d*): δ 9.86 (bs, 1H), 7.74 (s, 1H), 7.24 (dd, *J* = 9.0 Hz, 2.7 Hz, 2H), 6.92 (d, *J* = 9.0 Hz, 2H), 6.16 (d, *J* = 3.9 Hz, 1H), 5.93 (d, *J* = 3.9 Hz, 1H), 4.36 (dq, *J* = 7.2 Hz, 3.6 Hz, 2H), 3.81 (s, 3H), 1.36 (t, *J* = 7.2 Hz, 3H).

^{13}C NMR (75 MHz, Chloroform-*d*) δ 161.82, 159.98, 149.93, 148.64, 132.05, 128.54, 127.24, 114.38, 106.35, 62.15, 60.05, 55.33, 14.16. LCMS: *m/z* calculated for $C_{15}H_{16}N_4O_3$: 300.12; Observed mass: 301.2 (M+1)

Anal. Calculated for $C_{15}H_{16}N_4O_3$: C, 59.99; H, 5.37; N, 18.66; Found: C, 59.98; H, 5.39; N, 18.68.

Ethyl-7-(3-(trifluoromethyl)phenyl)-4,7-dihydro-[1,2,4]triazolo[1,5-a]pyrimidine-5-carboxylate (15c):

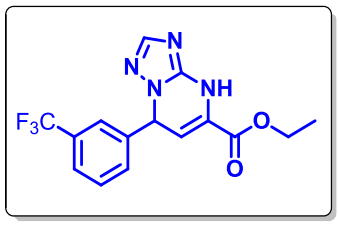

White solid; yield 70 mg, 58%; MP: 174-176 ^{o}C

^{1}H NMR (300 MHz, Chloroform-*d*): δ 10.45 (bs, 1H), 7.80 (s, 1H), 7.64-7.48 (m, 4H), 6.30 (d, *J* = 3.9 Hz, 1H), 5.91 (d, *J* = 3.9 Hz, 1H), 4.40 (dq, *J* = 7.2 Hz, 3.6 Hz, 2H), 1.37 (t, *J* = 7.2 Hz, 3H).

^{13}C NMR (126 MHz, $CDCl_3$) δ 161.53, 150.37, 148.82, 140.73, 131.62, 130.63, 129.63, 127.79, 125.76, 123.89, 105.05, 62.41, 60.25, 14.13.

LCMS:*m/z* calculated for $C_{15}H_{13}F_3N_4O_2$: 338.12; Observed mass: 339.2 (M+1)

Anal. Calculated for $C_{15}H_{13}F_3N_4O_2$: C, 53.26; H, 3.87; N, 16.56; Found: C, 53.28; H, 3.89; N, 16.58.

Ethyl-7-(3,4-dichlorophenyl)-4,7-dihydro-[1,2,4]triazolo[1,5-a]pyrimidine-5-carboxylate (15d):

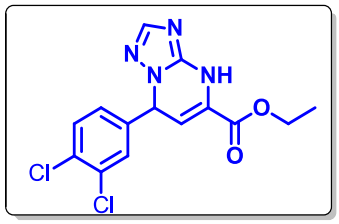

White solid; yield 75 mg, 62%; MP: 185-187 ^{o}C;

^{1}H NMR (300 MHz, Chloroform-*d*): δ 9.80 (bs, 1H), 7.77 (s, 1H), 7.46 (dd, *J* = 8.2 Hz, 1H), 7.28-7.26 (m, 1H), 7.18 (d, *J* = 8.4 Hz, 1H), 6.18 (d, *J* = 3.9 Hz, 1H), 5.87 (d, *J* = 3.9 Hz, 1H), 4.38 (dq, *J* = 7.2 Hz, 3.6 Hz, 2H), 1.37 (t, *J* = 7.2 Hz, 3H).

^{13}C NMR (126 MHz, DMSO) δ 161.51, 150.68, 140.81, 139.08, 136.15, 128.84, 124.65, 103.72, 62.27, 59.33, 14.34.

LCMS:*m/z* calculated for $C_{14}H_{12}Cl_2N_4O_2$: 338.03; Observed mass: 339.2 (M+1)

Anal. Calculated for $C_{14}H_{12}Cl_2N_4O_2$: C, 49.58; H, 3.57; N, 16.52; Found: C, 49.60; H, 3.58; N, 16.54.

Ethyl-7-(4-bromophenyl)-4,7-dihydro-[1,2,4]triazolo[1,5-a]pyrimidine-5-carboxylate (15e):

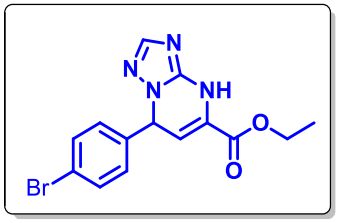

White solid; yield 83 mg, 67%; MP: 191-193 ^{o}C

^{1}H NMR (300 MHz, Chloroform-*d*): δ 9.65 (bs, 1H), 7.75 (s, 1H), 7.53 (d, *J* = 8.4 Hz, 2H), 7.19 (dd, *J* = 8.4 Hz, 1.8 Hz, 2H), 6.18 (d, *J* = 3.9 Hz, 1H), 5.90 (d, *J* = 3.9 Hz, 1H), 4.36 (dq, *J* = 7.2 Hz, 3.0 Hz, 2H), 1.36 (t, *J* = 7.2 Hz, 3H).

^{13}C NMR (300 MHz, Chloroform-*d*): 161.58, 150.12, 148.70, 138.71, 132.20, 128.84, 128.57, 127.57, 123.01, 105.39, 62.33, 60.02, 14.14:

LCMS: *m/z* calculated for $C_{14}H_{13}BrN_4O_2$: 348.02; Observed mass: 349.2, 351.2 (M+1, M+3)

Anal. Calculated for $C_{14}H_{13}BrN_4O_2$: C, 48.16; H, 3.75; N, 16.05; Found: C, 48.18; H, 3.76; N, 16.07.

Ethyl-7-(4-hydroxyphenyl)-4,7-dihydro-[1,2,4]triazolo[1,5-a]pyrimidine-5-carboxylate (15f):

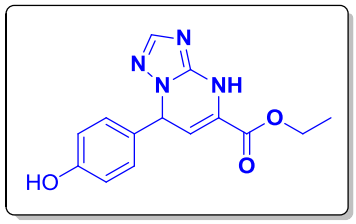

White solid; yield 53 mg, 52%; MP: 173-175 ^{o}C

^{1}H NMR (400 MHz, DMSO) δ 10.02 (s, 1H), 7.62 (s, 1H), 7.17 – 7.11 (m, 2H), 6.95 – 6.88 (m, 2H), 6.22 (d, *J* = 4.0 Hz, 1H), 5.79 (d, *J* = 4.0 Hz, 1H), 4.30 – 4.19 (m, 2H), 1.26 (t, *J* = 7.1 Hz, 3H).

^{13}C NMR (75 MHz, Chloroform-*d*) δ 161.98, 159.93, 149.82, 148.54 132.05, 128.64, 126.35, 114.15, 107.24, 62.38, 60.17, 14.04.

LCMS:*m/z* calculated for $C_{14}H_{14}N_4O_3$: 286.11; Observed mass: 287.2 (M+1)

Anal. Calculated for $C_{14}H_{14}N_4O_3$: C, 58.73; H, 4.93; N, 19.57; Found: C, 58.75; H, 4.95; N, 19.59.

Ethyl-7-(2-bromopyridin-3-yl)-4,7-dihydro-[1,2,4]triazolo[1,5-a]pyrimidine-5-carboxylate (15g):

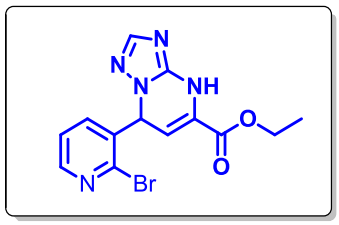

Brown solid; yield 77 mg, 62%; MP: 197-200 ^{o}C

^{1}H NMR (400 MHz, Chloroform-*d*): δ 9.88 (bs, 1H), 8.36 (s, 1H), 7.83 (m, 1H), 7.28-7.16 (m, 2H), 6.67 (d, *J* = 4.0 Hz, 1H), 6.01 (d, *J* = 4.0 Hz, 1H), 4.37 (q, *J* = 7.2 Hz, 2H), 1.38 (t, *J* = 7.2 Hz, 3H).

^{13}C NMR (101 MHz, DMSO) δ 160.50 (m), 150.81, 150.21, 149.16, 141.20, 136.84, 135.49, 128.86, 124.66, 103.72, 62.27, 59.33, 14.34;

LCMS:*m/z* calculated for $C_{13}H_{12}BrN_5O_2$: 349.02; Observed mass: 350.2, 352.2 (M+1, M+3)

Anal. Calculated for $C_{13}H_{12}BrN_5O_2$: C, 44.59; H, 3.45; N, 20.00; Found: C, 44.58; H, 3.46; N, 20.02.

Ethyl-7-(5-bromo-2-fluorophenyl)-4,7-dihydro-[1,2,4]triazolo[1,5-a]pyrimidine-5-carboxylate (15h):

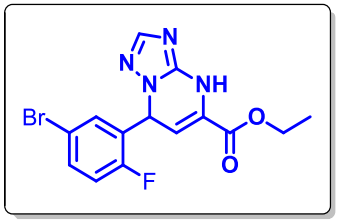

Pale brown solid; yield 35 mg, 53%; MP: 192-194 ^oC

^{1}H NMR (300 MHz, DMSO-*d6*): δ 10.18 (bs, 1H), 7.70-7.60 (m, 3H), 7.48 (d, *J* = 7.2 Hz, 1H), 6.45 (d, *J* = 3.9 Hz, 1H), 5.86 (d, *J* = 3.9 Hz, 1H), 4.24 (q, *J* = 7.2 Hz, 2H), 1.26 (t, *J* = 7.2 Hz, 3H).

^{13}C NMR (75MHz, DMSO-*d6*) δ 164.40, 152.93, 145.45, 140.82, 128.59, 128.41, 126.42, 125.18, 123.64, 65.93, 60.17, 13.14.

LCMS: *m/z* calculated for $C_{14}H_{12}BrFN_4O_2$: 366.01; Observed mass: 367.1, 369.1 (M+1, M+3);

Anal. Calculated for $C_{14}H_{12}BrFN_4O_2$: C, 45.80; H, 3.29; N, 15.26; Found: C, 45.82; H, 3.30; N, 15.28.

Experimental procedure for synthesis of compound (16a & 16b):

To a solution of 5-amino tetrazole (0.075 mmol) in DMF (1.0 mL) was mixed with MBH Acetate of nitro alkene (0.09 mmol) and cesium carbonate (0.15 mmol) and the reaction mixture was heated to 60^{o}C for 4h. After completion of reaction (monitored by LCMS), the reaction mixture was quenched with water (10 mL). The reaction mixture was extracted with ethyl acetate (3x 10 mL). The combined organic layers were dried over anhydrous sodium sulphate, filtered and concentrated over vacuum to give the crude product. To this crude product was added methanol (2 mL) and stirred for 30 min at RT. A white precipitate was obtained which was filtered gave the product (70% - 75%). The mother liquid contains a small amount of product along with small amount of other region isomer by LCMS.

Ethyl-7-phenyl-4,7-dihydrotetrazolo[1,5-a]pyrimidine-5-carboxylate (16a):

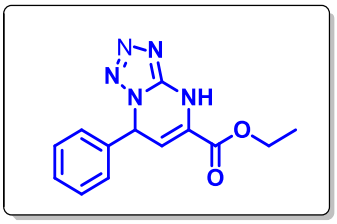

Yield 18 mg, 75%; MP: 201-204 ^{o}C

^{1}H NMR (300 MHz, Chloroform-*d*): δ 7.62-7.55 (m, 3H), 7.35-7.25 (m, 2H), 6.67 (d, *J* = 3.9 Hz, 1H), 6.02 (d, *J* = 3.9 Hz, 1H), 4.36 (q, *J* = 7.2 Hz, 2H), 1.36 (t, *J* = 7.2 Hz, 3H).

LCMS:*m/z* calculated for $C_{13}H_{13}N_5O_2$: 271.11; Observed mass: 272.2 (M+1).

Ethyl-7-(4-methoxyphenyl)-4,7-dihydrotetrazolo[1,5-a]pyrimidine-5-carboxylate (16b):

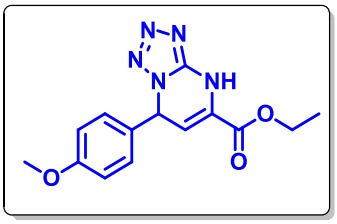

Yield 19 mg, 72%; MP: 200-202 ^{o}C

^{1}H NMR (300 MHz, DMSO-*d6*): δ 10.01 (s, 1H), 7.14 (d, *J* = 8.7 Hz, 2H), 6.92 (d, *J* = 8.7 Hz, 2H), 6.21 (d, *J* = 3.9 Hz, 1H), 5.78 (dd, *J* = 3.9 Hz, 1.5 Hz, 1H), 4.25 (dq, *J* = 7.2 Hz, 2H), 3.72 (s, 3H), 1.26 (t, *J* = 7.2 Hz, 3H).

LCMS:*m/z* calculated for $C_{14}H_{15}N_5O_3$: 301.12; Observed mass: 302.2 (M+1).

3.5.2 Enzyme Inhibition studies:

The *in vitro* inhibitory effect of newly synthesized ligands were assessed by Ellman's methodusing AMPLITE™ AChE assay kit (AAT Bioquest, Inc., Sunnyvale, CA). The assay system consists of AChE from electric eel (EC 3.1.1.7), 5,5-dithiobis-(2-nitrobenzoic acid) (DTNB, known as Ellman's reagent) and acetylcholine. The assay procedure is as follows, an aliquots (total volume 100 µL) was prepared by mixing 5.7 nM AChE (prepared in 0.1 % of BSA containing distilled water) with acetylcholine (500 µM) and DTNB in a reaction buffer of pH 7.4. As a result of enzyme substrate interaction, the yellow colour formation was monitored and measured at 405 nm using a

spectrophotometer at a time interval 2 minutes each for 20 minutes. Later the optical density was plotted against time. The same experiment (in triplicate) was repeated by incubating (15 minutes) the enzyme with different ligands. The relative activities of all ligands were expressed and compared with that of native enzyme activity. Finally the half maximal inhibitory concentration (IC_{50}) was determined for each ligands and compared with a known inhibitor tacrine.

3.5.3 Molecular modelling studies:

The physico chemical properties, atomic level of interactions and binding stability of newly synthesized compounds were predicted using different molecular modelling experiments. Initially the ligands (drawn using Chemsketch program) were prepared by correcting the bond lengths and bond angles followed by energy minimization using LigPrep module with OPLS-3 force field. Different tautomers of ligands were also generated and used for different studies. By using the module QikProp 4.7, the physico chemical, ADME (Absorption, Distribution, Metabolism and Excretion), lipinski rule of five, *in silico* BBB penetrability and CNS activity of newly synthesized ligands were predicted. The BBB permeability of the ligands were reasserted using a bayesian statistical model implemented in an online tool 'B3PP 09' (http://b3pp.lasige.di.fc.ul.pt). As a part of investigating the atomic level of interaction of newly synthesized ligands with human AChE a molecular modeling studies was carried out. Crystal structure of hAChE complex with galanthamine (4EY6) was downloaded from protein databank (PDB) and prepared by deleting all the crystallographic water molecules and adding hydrogen. The protonation states and partial charges were assigned for the charged residues during preparation. Finally the prepared structure was optimized and minimized. Later the ligand binding site was mapped by taking galanthamine as an axis point. Further the docking studies were performed between the prepared ligands and protein using extra precision (XP) mode of glide. The binding free energies of the ligand enzyme complex were also deduced using Prime MM-GBSA method.

The correlation between experimental IC_{50} values and theoretical binding energies were identified and highly active complex were selected for molecular dynamics (MD) simulation studies to predict the stability of the complex. The enzyme ligand complexes were prepared for MD simulation by soaking the complex in to an orthorhombic solvent box (volume 508093 $Å^3$) containing 13100 TIP3P water molecles. The whole system was

neutralized by adding 7 Na+ ions. Total simulation time lasts around 20 ns. The intermediate structures were saved at every 10 ps and superimposed to the native structure and deduced the RMS deviation. Finally a graph was plotted with RMS deviation against time.

CHAPTER 4

NOVEL TACRINE DERIVATIVES EXHIBITING IMPROVED ACETYLCHOLINESTERASE INHIBITION: DESIGN, SYNTHESIS AND BIOLOGICAL EVALUTION

4.1 Introduction

Alzheimer's disease (AD), a progressive neurodegenerative disorder among elderly people is characterized by loss of memory, progressive deficits in cognitive functions and behavioural abnormalities[Suh, Y. H., et al, 2002; Selkoe, D., et al, 2001; Tumiatti, V., et al, 2010, Piazzi, L., et al 2003]. It is estimated that more than 36 million people are presently suffering from AD and it still continues to be one of the leading causes of death due to neurological diseases in developed countries [Alzheimer's Disease International, 2011; Prince, M. et al, 2013; Tang, H.,et al, 2012].Over the past decades, despite several efforts from various researchers across the globe, its pathogenesis still remains unclear. Several factors including accumulation of β-amyloid, hyperphosphorylation of tau protein, oxidative stress and deficit of acetylcholine (ACh) seem to play major roles in the progression of the disease[Dominic, M., et al, 2004; Tumiatti, V., et al, 2010; Scarpini, E., et al, 2003; Nunomura, A., et al, 2006]. Current clinical therapy is mainly based on cholinergic hypothesis, which suggests that decline of ACh levels leads to memory loss. Hence sustaining or recovering the cholinergic function is supposed to be clinically beneficial [Alzheimer's Association. 2015; Tacrine, Donepezil, Rivastigmine,; Galantamine; Schneider, L. S., et al, 2014].

Tacrine is the first drug approved as cholinesterase inhibitor by FDA for the treatment of AD, but it has been withdrawn from the market due to its side effects such as hepatotoxicity[Minarini, A., et al, 2013; de Aquino, R. A., et al, 2013;Giacobini, E., et al, 1998; Dominguez, J. L., et al, 2015]. Many tacrine derivatives/hybridshave been designed and synthesized in order to remove the adverse side effects while retaining the AChE inhibitory property. Development of new derivatives based on tacrine is being actively pursued. As a part of efforts to develop novel AChE inhibitors[Reddy,E. K., et al, 2016; Remya, C., et al, 2012; Remya, C., et al, 2013; Remya, C., et al, 2012] a series of tacrine derivatives have been designed, synthesized and their potential on AChE inhibition are

being explored. Conventionally most of the tacrine derivatives were made by substitution on the amine moiety of tacrine. On the contrary,our research focus was to explore the substitutions on aromatic and cyclohexyl ring of tacrine with various functionalities.

4.2. Results and discussion

4.2.1. Synthetic studies

The key intermediate **19**was synthesisedas the condensation of cyclohexanone-4-carboxylic ester **18** and 2-amino benzonitrile **17** in presence of lewis acid ($BF_3.Et_2O$) to yield the product **19** in 80% yield as shown in Scheme 4.1. The compounds **19a** and **19 b** was treated with methyl amine and hydrazine hydrazide gave compounds **20a, 20b, 20c** and **20d.** The compound **19b** was trated with corresponding boronic acidsmediated Suzuki-Miyaura cross-coupling reaction resulted in the compounds **19c** and **19d**. Finally hydrolysis of compounds **19a-19d** using lithium hydroxide resulted **21a-21d.** Further coupling of compounds **21a-21d** with various amines using T_3P as the coupling agent yielded the final compounds **22a** – **22j** in good yields. The compounds **23a** and **23b** were synthesised from the compounds **21a & 21b** with 1-methyl pyrazole-5-amine with HATU as coupling reagent.

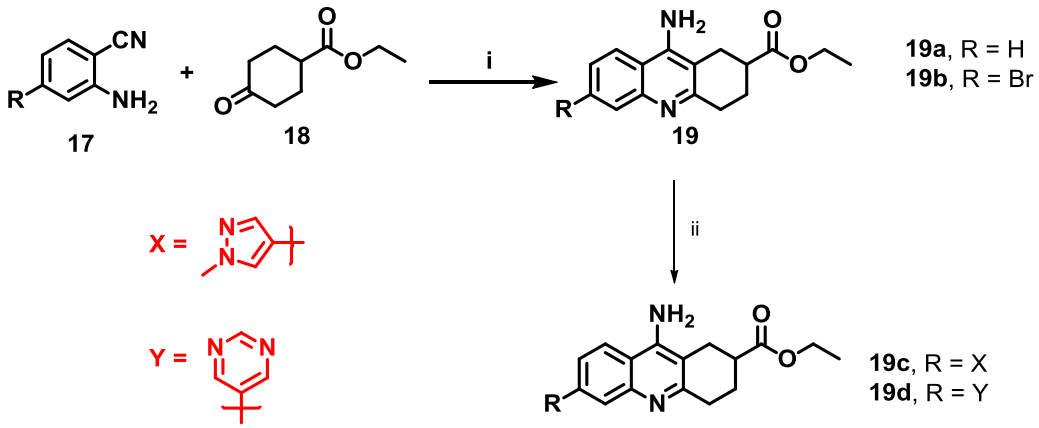

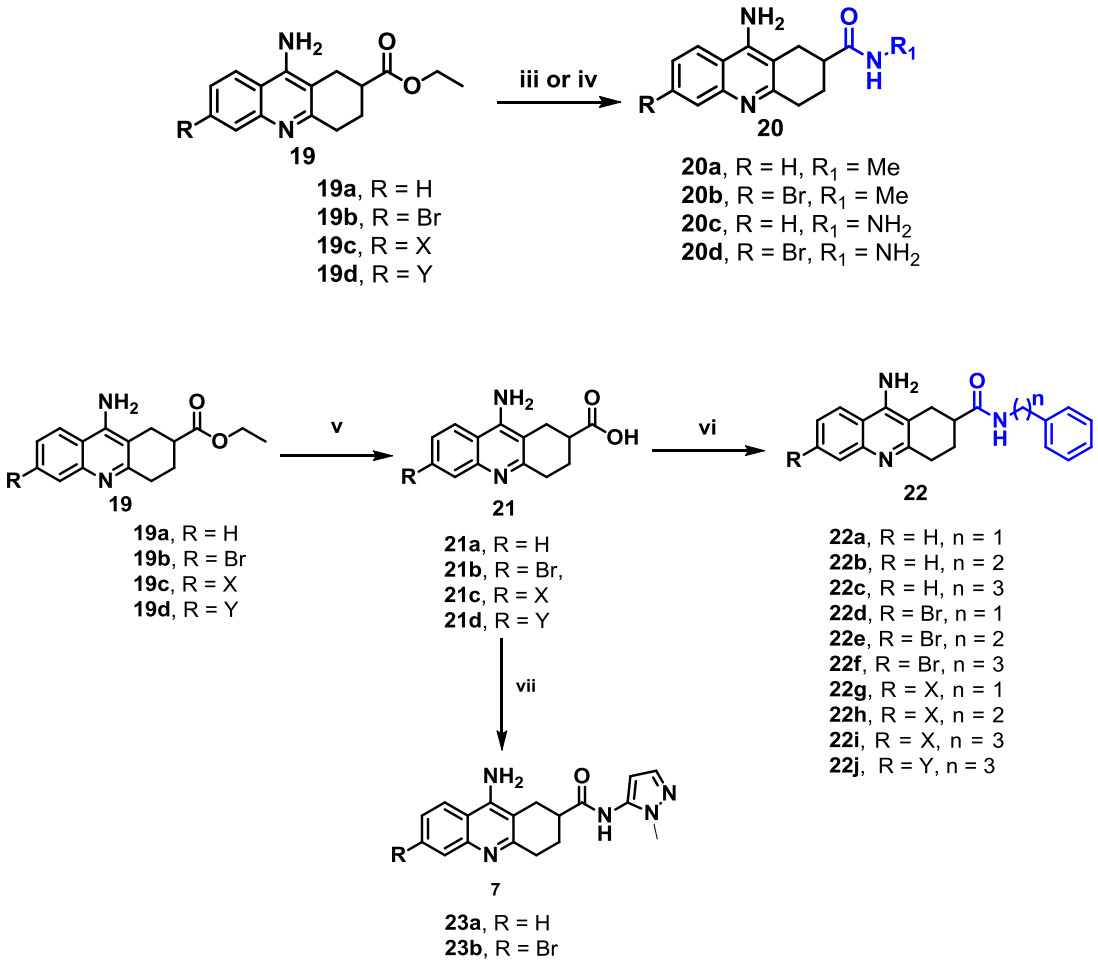

Scheme 4.1: Synthesis of compounds **22a-22j** and **23a-23b**; Reagents and conditions: i) $BF_3.Et_2O$, Toluene, 100^oC, 4h; ii) boronic ester, Na_2CO_3, $Pd(PPh_3)_4$, 1,4-dioxane: H_2O (9:1), 110_C, 2 h. iii) aq. CH_3NH_2, 70 ^oC, 2h; iii) $NH_2NH_2.H_2O$, 70 ^oC, 2h; iv) $LiOH.H_2O$, 1h; v) T_3P, Et_3N, DMF, 60 ^oC, 4h; vi) HATU, DIPEA, DMF, 12h, RT.

4.2.2. In vitro inhibition studies on AChE

In search for more effective AChE inhibitors, the synthesized novel tacrine derivatives were screened for AChE inhibitory potency by Ellman's method [Ellman, G. L., et al, 1961]. The pharmacophoric features of tacrine were retained as such while designing in order to make optimal interaction with target. The common pharmacophores predicted for all compounds are shown in Figure 4.1. The tacrine derivatives at a concentration of 200 nM was used for the initial enzyme inhibition studies. Percentage of enzyme activity in presence of different tacrine derivatives were calculated with respect to enzyme activity in the absence of inhibitor (Table 4.1). Further the potency of each derivative was determined by calculating half maximal inhibitory concentration (IC_{50}). IC_{50} values of

each compounds were not exactly correlating with the percentage of activity obtained in the initial screening. These compounds exhibit high AChE inhibitory potency with IC_{50} values in the nanomolar range (Table 4.1). All of these compounds except **22g** and **22h** showed an enhanced inhibitory profile compared to tacrine.

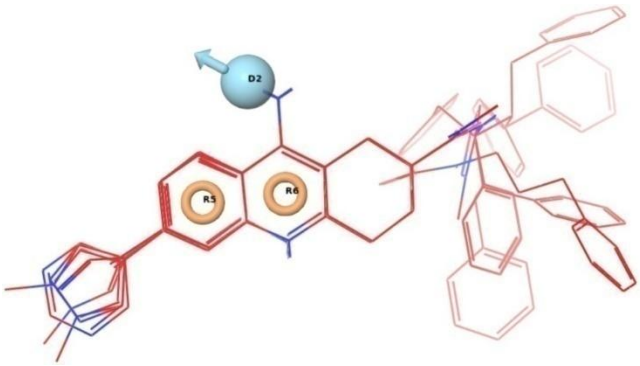

Figure 4.1: Three featured pharmacophores such as the two aromatic rings (R5 and R6) and a hyrogen bond donor (D2) predicted for tacrine along with its derivatives

Table 4.1: The *in vitro*AChE inhibitory profile of novel tacrine derivatives

Name	% of Activity at 200 nM	IC_{50}(nM) against AChE	IC_{50} (µM) against BuChE
20b	18.18	28.59±3.59	47.29 ± 5.98
20c	**9.09**	**12.97±0.47**	**2.99 ± 0.40**
22a	27.27	37.16±4.23	10.77 ± 0.68
22b	27.27	16.84±2.12	4.05 ± 0.66
22c	**18.18**	**5.17±0.24**	**3.68 ± 0.46**
22d	9.09	33.74±1.96	10.24 ± 1.74
22e	9.09	24.1±3.43	7.17 ± 0.68
22f	**13.63**	**7.14±0.78**	**5.11 ± 0.81**
22g	36.36	191.11±10.69	2.26 ± 0.15
22h	54.54	188.70±27.72	10.57 ± 1.44
22i	9.09	57.64±9.94	2.77 ± 0.32
22j	27.27	40.78±5.43	18.02 ± 0.53
23b	22.72	17.72±1.51	20.93 ± 1.07
Tacrine	30.98	94.69±4.88	0.014 ± 1.07

Even though the compounds were designed with AChE as the target, inhibitory properties of the compounds against Butyrylcholinesterase (BChE) were also tested by the same method. Moreover, AChE and BChE share more than 50% sequence identityand many of the known AChE inhibitors do inhibit BChE also. The IC50 values of the compounds against BChE were in the micromolar while that against AChE were in the nanomolar range. Hence, the compounds were less potent inhibitors as far as BChE isconcerned (Table 4.1). The IC50 value of tacrine against BChE is 14.26 ± 1.07 nM, indicating the selectivity of tacrine towards BChE over AChE as reported in the literature.

Over a series of derivatives tested, substitutions on cyclohexyl portion with amide moiety having propyl unit and benzene ring (n = 3) (**22c**) showed exceptionally improved inhibitory potency (IC_{50} = 5.17±0.24nM) than tacrine, which is almost 18 - 20 times more potent than tacrine. The similar extent of inhibition was observed for compound **22f** with a bromine substitution at 6th position (IC_{50} = 7.14±0.78nM). Amide analogues with ethyl (n = 2) and methyl units (n = 1) were found to be less potent when compared to propyl unit. Similarly, the derivatization by substitution of Br with a heterocyclic ring (pyrazole) with propyl unit attached to the cyclohexane ring (n = 3) (**22i**, IC_{50} = 57.64 ± 9.94 nM) also showed improved inhibitory profile than **22g** (IC_{50} = 191.11 ± 10.69 nM) and **22h** (IC_{50} = 188 ± 27.72 nM), which had methyl (n=1) and ethyl (n=2) units. Moreover the inhibitory potency of these compounds (**22g** and **22h**) were 2 fold lower when compared to tacrine. The derivative, which was obtained by the replacement of pyrazole moiety by pyrimidine with propyl unit on the cyclohexane substituent (**22j**, IC_{50} = 40.78 ± 5.43nM), showed slightly better inhibitory profile than **22i**. Another derivative (**22b**), that was having amide unit connected to a pyrazole moiety at cyclohexyl portion also efficiently inhibited AChE activity (IC_{50} = 17.72 ± 1.51nM). Amide substitution with shorter chain length (**20c**) gave almost similar inhibitory potency (IC_{50} = 12.97±0.47nM) as that of **22c** and **22f**. But **20b** showed less potency (IC_{50} = 28.59 ± 3.59nM) compared to **22c** and **22f**. The activities of AChE in the presence of **22c**, **22f** and **20c** are shown in the figure 4.2.

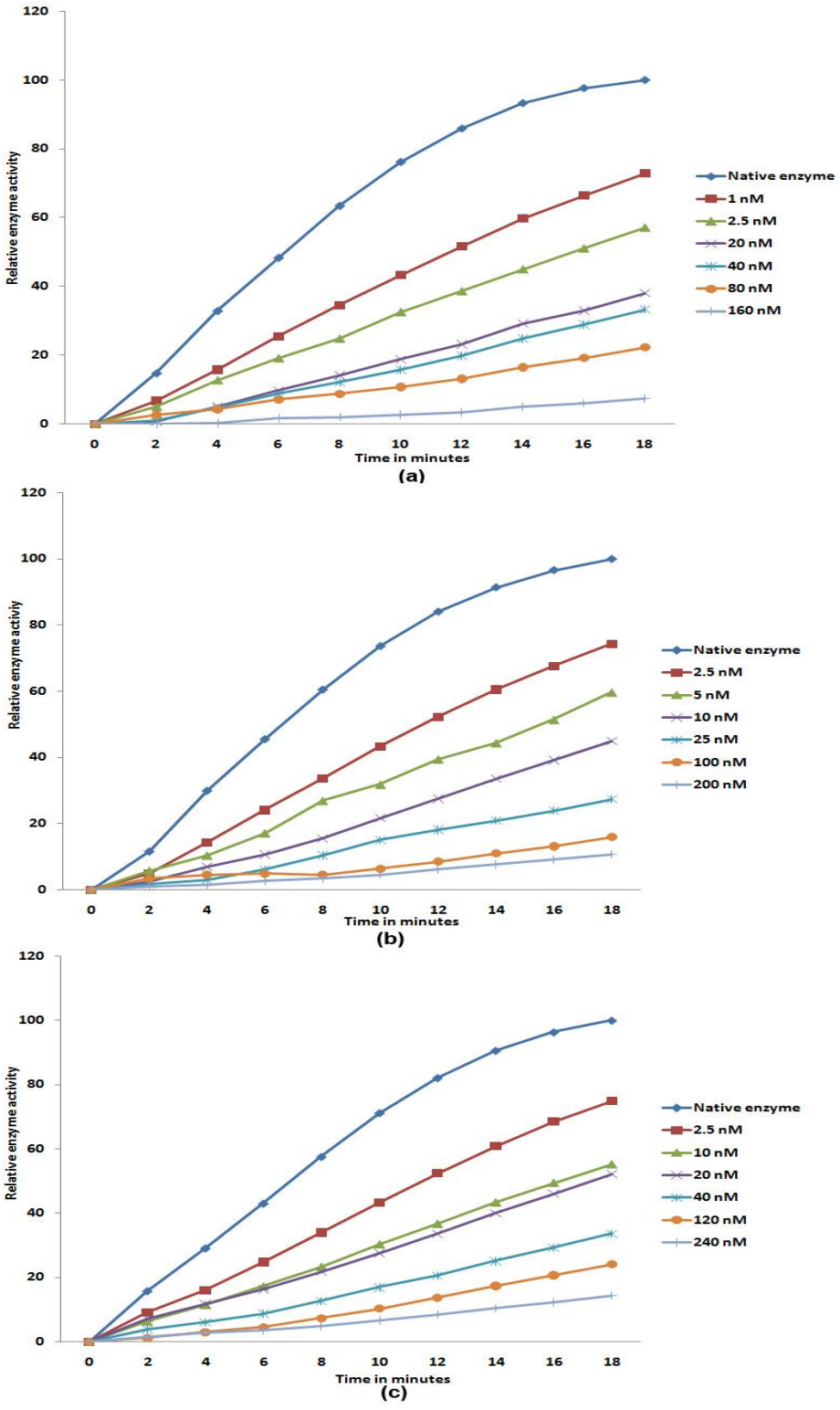

Figure 4.2: Concentration dependent inhibition of AChE activity in the presence of **22c** (a), **22f** (b) and **23c** (c). The relative enzyme activity is calculated as a percentage of maximal activity obtained for native enzyme reaction

4.2.3. In Silico predictions

The drug like behavior of the tacrine derivatives were assessed by *in silico* predictions. Some of the parameters predicted such as molecular weight (MW), partition coefficient (LogP), number of hydrogen bond donors and acceptors (HBD and HBA), polar surface area (PSA), number of rotatable groups (rotor) and solvent accessible surface area (SASA) are given in Table 4.2 along with the reference values[Pajouhesh, H., et al, 2005; Ghose, A. K., et al, 2012]. All derivatives met the criteria for the general drug like nature based on the Lipinski's rule of five [Lipinski CA, et al, 2001].Generally, the CNS acting drugs have lower range of values for the parameters when compared to drugs acting on other parts of the body. The parameters for derivatives such as **20b**, **22a**, **22b**, **22d**, **22e** and **22f** are in the preferred range. The HBD and PSA values of **20c** were slightly higher. The SASA of **22g, 22h, 22i** and **22j** were also found not to be in the preferred range of CNS acting drugs. The PSA and HBA values are also found to be slightly higher for **22j**.

Table 4.2: ADME profile of the compounds predicted by QikProp program.

Name	MW (≤450 Da)	HBD (≤ 3)	HBA (≤ 7)	LogP (≤ 5)	PSA (≤ 90Å^2)	SASA (≤735 Å^2)	Rotor (≤ 7)
20b	334	2.5	4.5	2.06	72	544	2
20c	256	4.5	5	1.89	101	497	3
22a	331	2.5	4.5	3.26	70	635	4
22b	345	2.5	4.5	3.62	71	671	5
22c	359	2.5	4.5	3.98	71	705	6
22d	410	2.5	4.5	3.82	70	663	4
22e	424	2.5	4.5	4.18	7	699	5
22f	438	2.5	4.5	4.55	71	733	6
22g	412	2.5	6	3.97	88	762	4
22h	426	2.5	6	4.32	88	798	5
22i	440	2.5	6	4.69	89	832	6
23b	400	2.5	5.5	3.38	86	629	3
22j	438	2.5	7.5	3.74	97	812	7
Tacrine	198	1.5	2	2.58	35	429	1

4.2.4. Molecular Docking studies

In silico docking studies were also conducted in order to understand the mode of interaction of tacrine derivatives on AChE. As the crystal structure of tacrine with hAChE was not available, all the docking studies were carried out using human AChE complexes (hAChE) with huprine W (a compound structurally similar to tacrine). Initially, tacrine was docked to hAChE, and the mode of binding was analyzed. Tacrine forms a sacking interaction with Y337 and W86 (sandwich model). The docking score obtained was -12.49 kcal/mol. The mode of binding was similar to that found in the crystal structure of Torpedo californica AChE (TcAChE) complexes with tacrine (PDB ID: 1ACJ). Superposition of tacrine docked on hAChE, tacrine complexes with TcAChE and huprine W with hAChE is shown in figure 4.3. Further utilizing the same docking parameters, all the derivatives of tacrine were docked to hAChE and their binding poses were compared (Figure 4.4). Tacrine moiety of all derivatives except **22g, 22h, 22i** and **22j** forms a sandwich between Y337 and W84 through stacking interactions. A potential hydrogen bond between the aromatic nitrogen and the main chain carbonyl of the active site residue H447 also formed with all these derivatives. H447 is one of the crucial residue, involved in the acetylcholine hydrolysis. The substrate binding to the active site is thought to be blocked by tacrine and its derivatives by interacting with H447. All derivatives except **22a** and **22d** adopts a 'V' shaped conformation by interacting with active site, acyl binding site and peripheral anionic site (PAS) residues. The binding of **20b** and **20c** is confined mainly in the bottom of the active site gorge and the binding is very similar with huprine W (Figure 4.5). The figure shows that the three membered ring system and the side chains of **20b** and **20c** are superimposable to the respective positions in huprine W. The amide chains of **22b, 22c, 22e, 22f** and **23b** are oriented in a similar fashion as seen in the case of **20b** and **20c** (pocket A). They bind at the bottom of the active site, spanning along the acyl binding pocket and makes contacts with peripheral anionic site residues also (Figure4.6 a). Whereas the amide side chains of derivatives such as **22a** and **22d** occupied in a small hydrophopic pocket (pocket B) surrounded by V73, Y72, P88, L130, Y133 and Y119 (Figure 4.6 b). The observed difference in binding might be due to the difference in length of the substituted groups. The shorter amide chains might not be fitting along the PAS (pocket A) due to the steric clash with the residues such as Y337, Y124, F338 and F297. Similarly, ethyl or propyl amide chains are restricted in the pocket B due to the residues such as P88, Q71, V73 and S125. Otherwise the residues have to

undergo substantial rearrangement in order to accommodate the ligands. Apparently, it is known that the conformational adaptations of the binding site residues according to the ligand binding is extremely difficult to predict. Bromine atom of the derivatives is nested in a hydrophobic cavity surrounded by W439, P446, Y449 and M443 as like chlorine atom positioned in the case of huprine W. The interaction diagrams for the most potent compounds such as **22c, 22f** and **20c** are given in **figure 4.7**. Additional stabilization of **22c** and **22f** is also observed in the form of hydrogen bond between amide nitrogen and hydroxyl group of Y124. In the case of **20c**, Y337 act as key residue playing major role in the binding. It form hydrogen bonds with the two nitrogen atoms in the hydrazide moiety of the cyclohexyl ring and locking the inhibitor in the active site. A slightly different binding pose was observed for **22g, 22h, 22i** and **22j**. Apart from that a number of van der Waals and hydrophobic interactions are also found to stabilize the binding. The residue such as Y72, V73, W86, Y124, Y133, F295, F297, Y337, F338, Y341 and I451 were involved in the hydrophobic interactions.

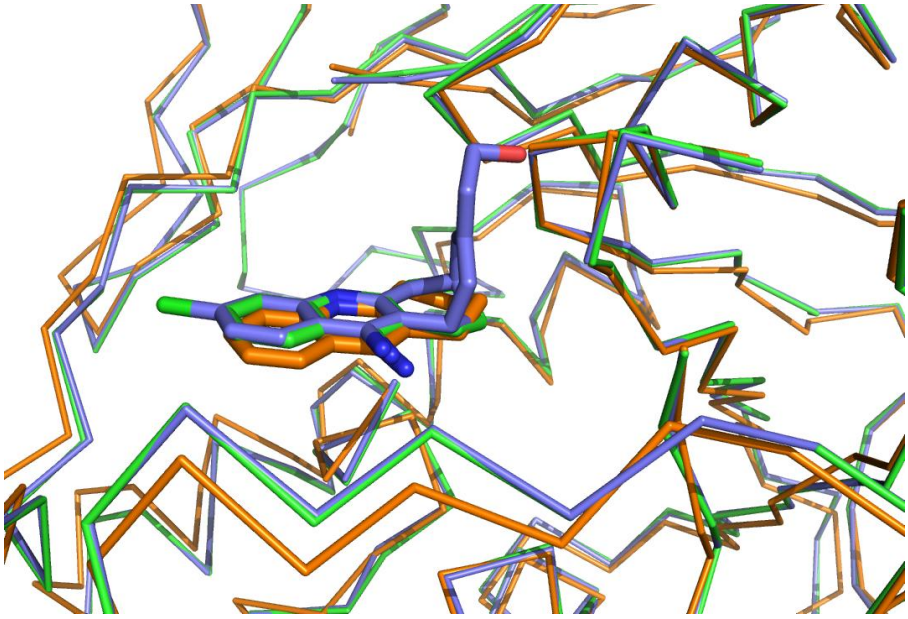

Figure 4.3: Superposition of tacrine docked to hAChE (Green), crystal structures of tacrine complex with TcAChE (Orange) and huprine (Blue) complex with hAChE

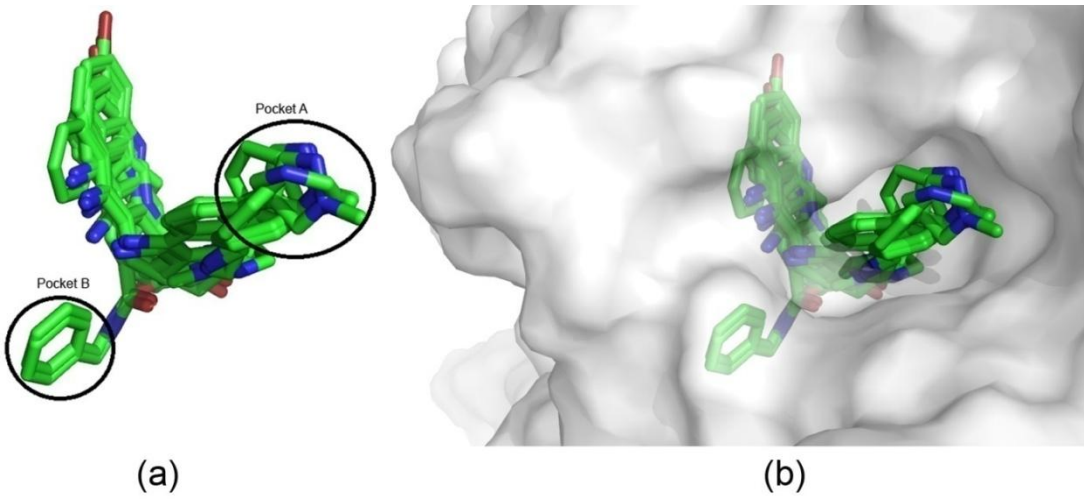

Figure 4.4: Binding mode of all ligands (a) and the same in the presence of protein surface (b)

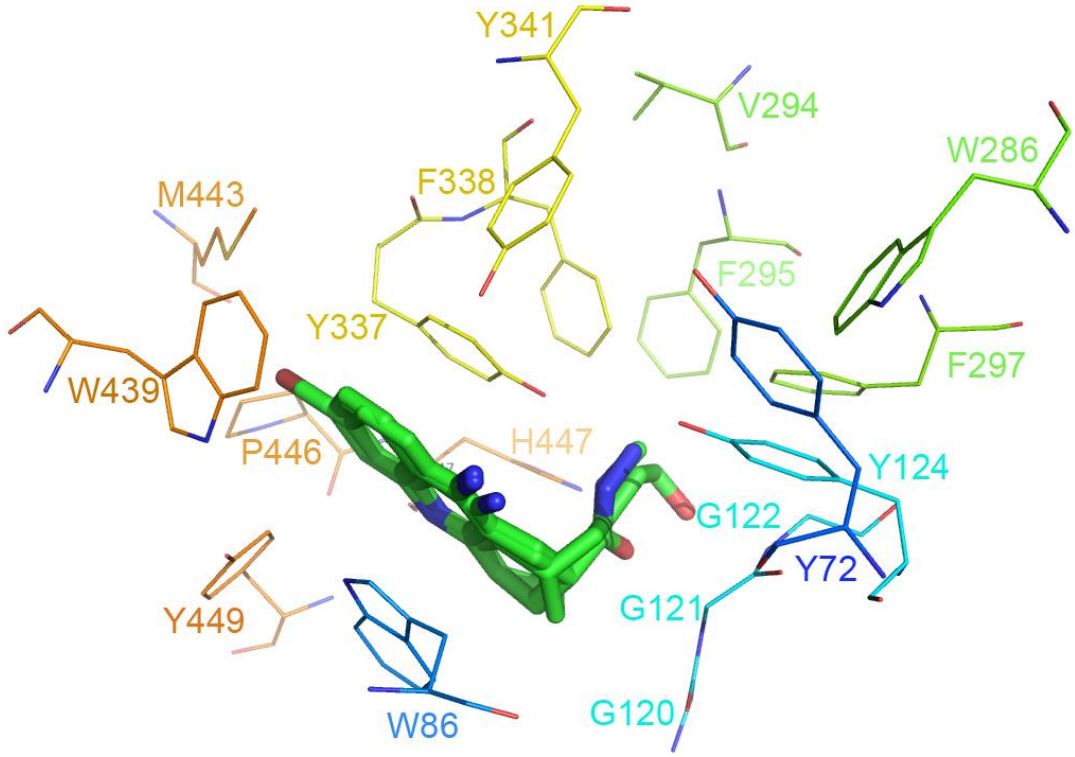

Figure 4.5: Overlay of the docked pose of **20b** and **20c** with huprine W in the active site of hAChE.

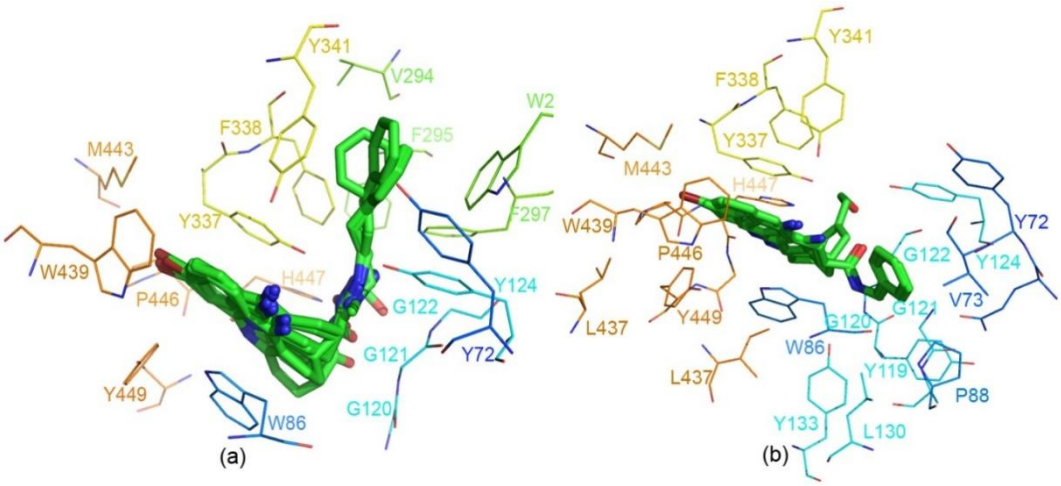

Figure 4.6: The binding mode of **22b, 22c, 22f** and **23b** (a) and **22a** and **22d** (b) in the active site of hAChE

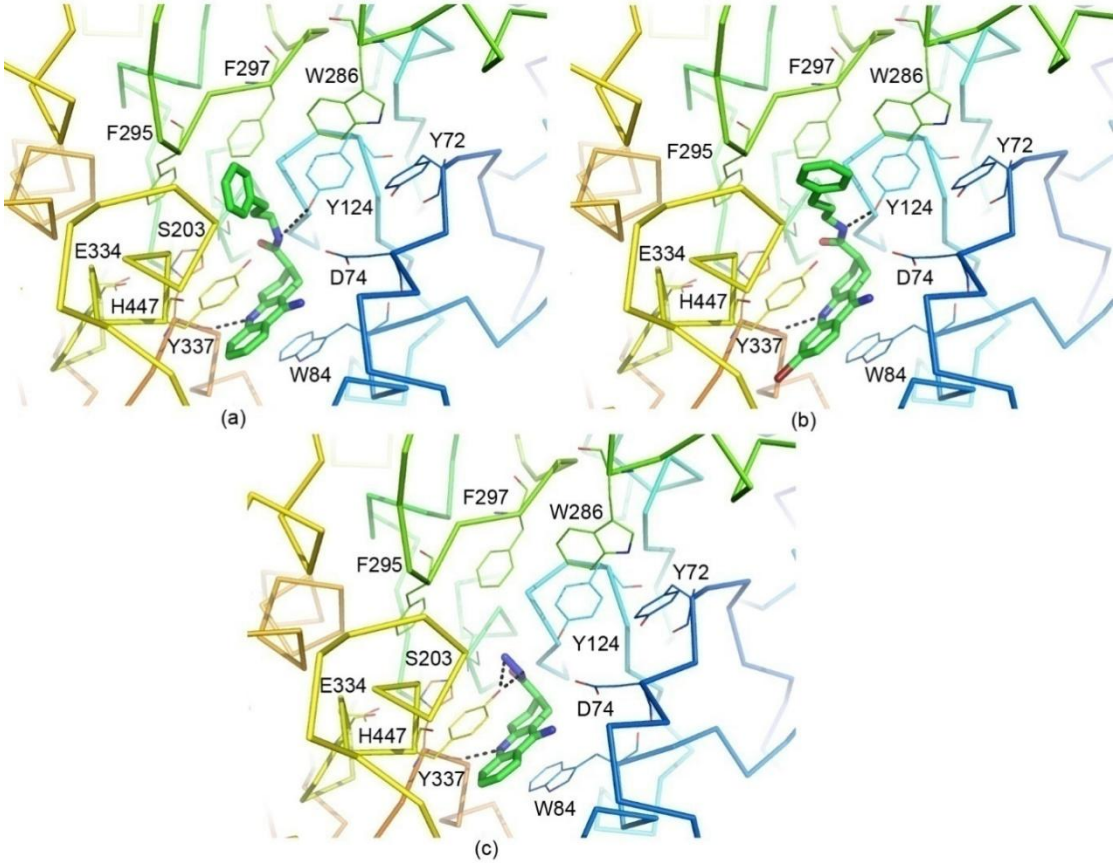

Figure 4.7: Interaction diagram of **22c**(a), **22f**(b) and **20c**(c). The hydrogen bonds are shown in dotted lines.

4.2.5. Cytotoxicity studies

In order to test the cytotoxicity of the newly synthesized compounds, HEK-293 cell line was used. In the concentration range tested, only **20c** was not cytotoxic in any of the concentrations. The compounds **22b, 22d, 22e, 22f, 22h** and **22j** are cytotoxic when the concentration was above 50 µM. **20b, 22d** and **23b** were safer upto 100 µM concentration (>80% cell viability is considered as non-toxic) (Figure 4.8).

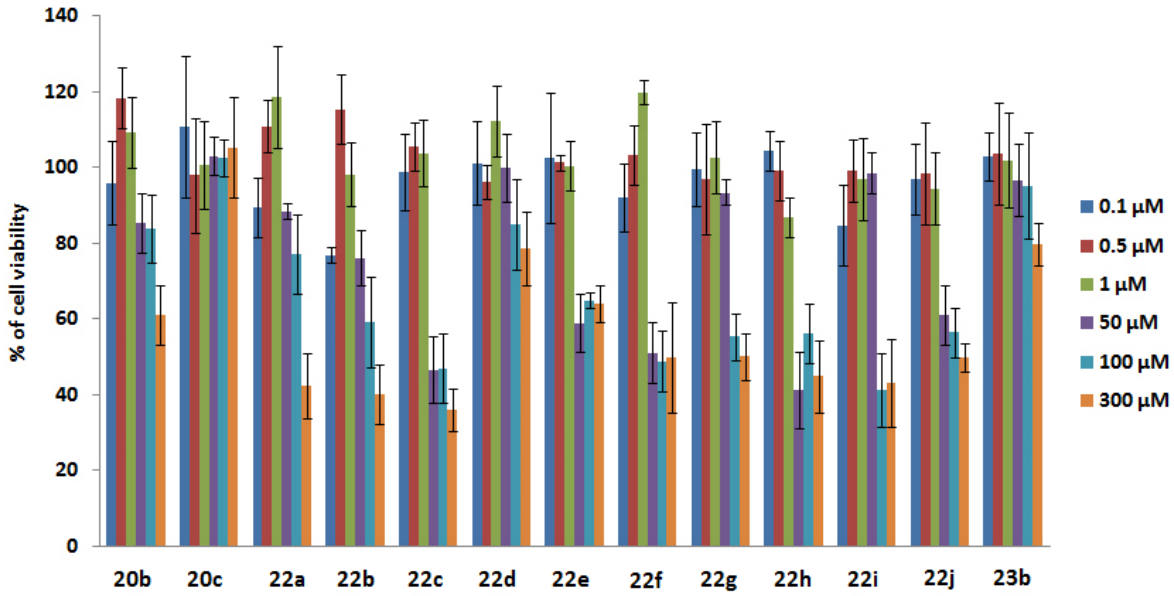

Figure 4.8: Viability of HEK-293 cells in presence of tacrine derivatives after 24hr treatment

4.2.6. Hepatotoxic studies

Since hepatotoxicity was the major reason for the withdrawal of tacrine from the clinic, the cytotoxicity of the highly potent tacrine derivatives were also tested on HepG2 cell line. HepG2 is one of the *in vitro* systems used to test the hepatoxicity of the compounds. As shown in the graph (Figure 4.9), tacrine was safe upto 50 µM and the cell viability started decreasing at 100 µM. At 300uM, significant reduction was observed in the cell viability. Among the tested tacrine derivatives, **22c, 22f, 22b, 22e** and **20b** were found to be more toxic than tacrine and showed significant reduction in cell viability started at 50 µM itself. But **20c** caused significantly less hepatotoxicity than tacrine and was safe even at 300 µM. The cells survived even after the treatment for 48 and 72 hours (Figure 4.10). Hence only **20c** possessed a good safety profile and proved to be non-toxic.

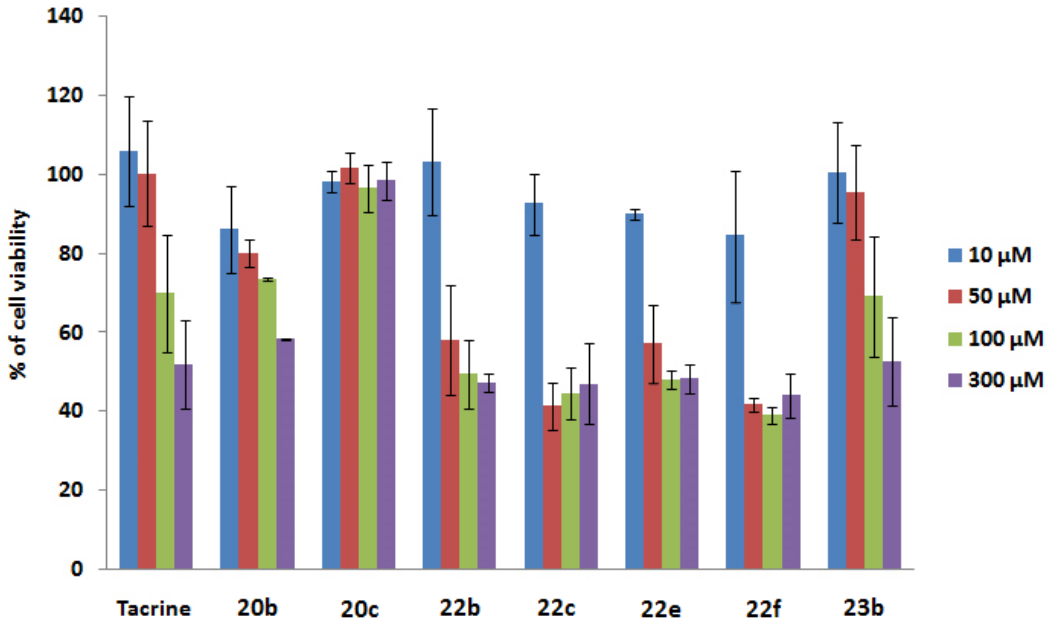

Figure 4.9: Cell viability of highly potent tacrine derivatives on HepG2 cell lines after 24hrs of treatment

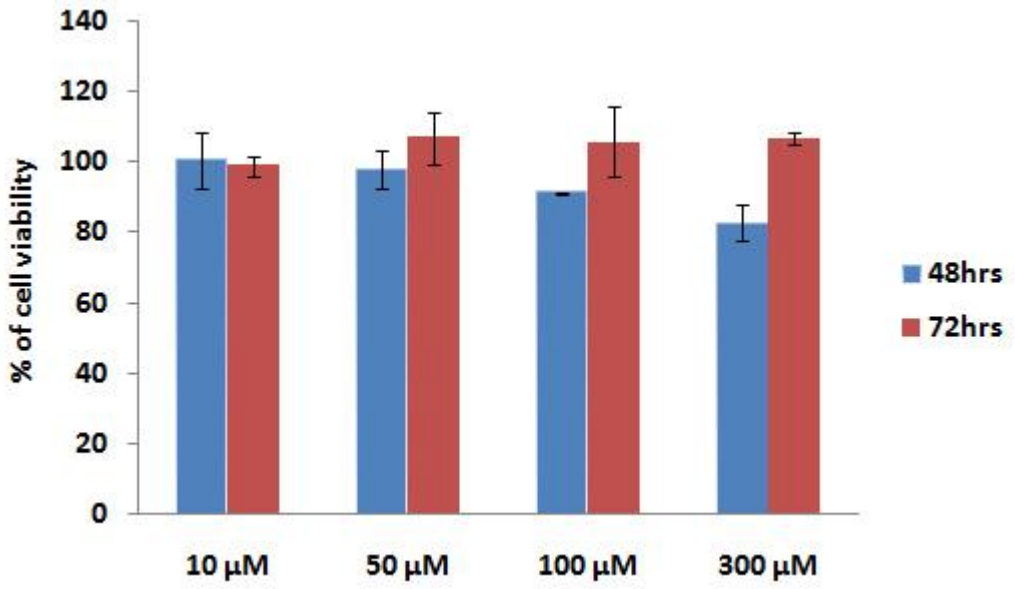

Figure 4.10: Cell viability of **20c** in HepG2 cell line after 48 and 72hrs of treatment

Since **20c** turned out to be a potential lead molecule, the binding affinity of **20c** on human butyrylcholinesterase (hBChE) was also assessed by means of molecular docking studies. Because BChE and AChE shares more than 50% of identity and many of the AChE inhibitors inhibit BChE also. Protein coordinates were taken from the crystal structure of hBChE in complexes with tacrine. The docking scores obtained for **20c** against hAChE

and hBChE were -13.23 kcal/mol and -6.56 kcal/mol respectively. This indicates that **20c** binds to hBChE with much lower potency than hAChE. The superposition of **20c** over hAChE and hBChE is given in the figure 4.11. Tacrine hydrazide adopts a different conformation in BChE when compared with that in hAChE. It oriented towards the 'pocket B' by interacting with G115. In the case of hBChE, A328 replaces Y337, the residue involved in the stacking and hydrogen bonding with hydrazide moiety of **20c**. The additional stabilization by aromatic stacking was also not observed in the case of binding with BChE. This might be partly explaining the selective binding of **20c** to hAChE.

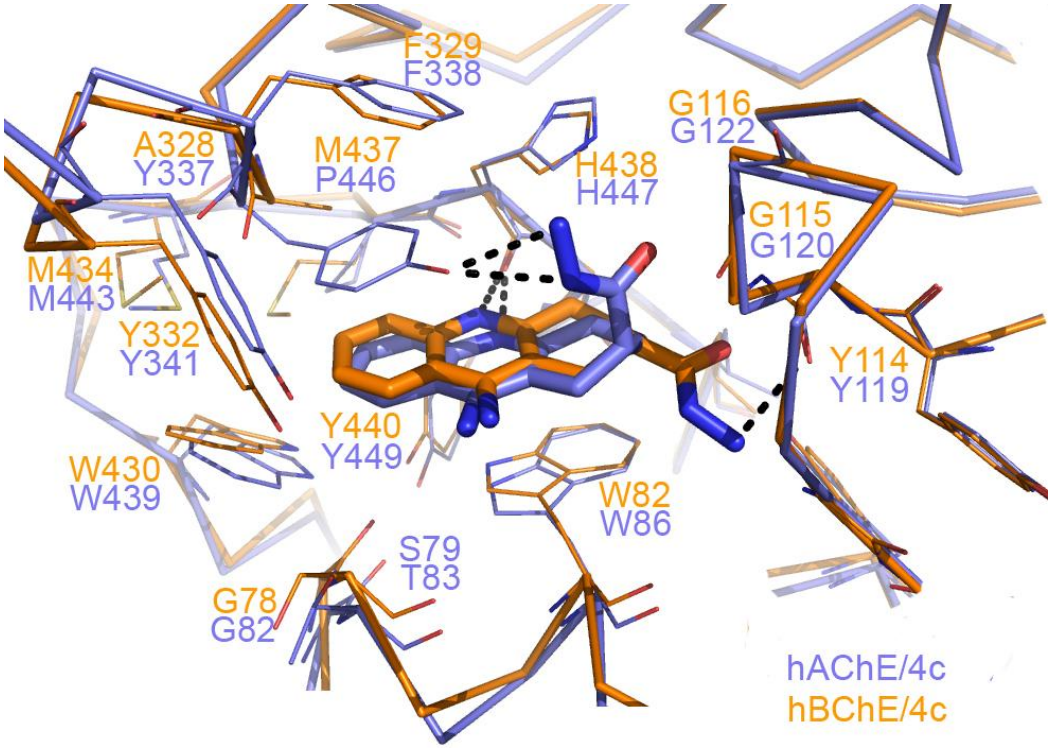

Figure 4.11: Superposition of **20c** in the active site of hAChE (Blue) and hBChE (orange)

4.3. Conclusions

A novel series of tacrine-2-amides were designed, synthesised and were studied for their *in vitro* inhibitory effect on AChE. Cytotoxic effects of these derivatives in HEK-293 and HepG2 cell lines were also studied. Over a series of tacrine derivatives tested, most of the compounds were potent inhibitors of AChE and the compounds **22c, 22f** and **20c** exhibited superior inhibition. **20c** is the most promising compound as it exhibited least toxicity. In the case of hepatotoxicity, it is less toxic than tacrine. Based on the studies,

the derivative **20c** could be considered as the potential lead compound for the development of drugs against AD. *In silico* ADME studies show that the lipophilicity of **20c** may be improved in order to obtain optimal permeation.

4.4. Experimental Section

4.4.1. Enzyme Inhibition Assays

AMPLITE™ AChE assay kit (AAT Bioquest, Inc., Sunnyvale, CA) was used to identify the in vitro inhibitory effect of the newly synthesized tacrine derivatives. The assay system works on the basis of Ellman's method (1). AChE from electric eel (EC 3.1.1.7), assay buffer (pH 7.4), 5,5-dithiobis-(2-nitrobenzoic acid (DTNB, known as Ellman's reagent) and the substrate acetylthiocholine (AChT) were there in the assay kit. 100 µL reaction mixture was prepared by mixing the enzyme (25 µL), 500 µM AChT solution in ddH2O and 500 µM DTNB in assay buffer. The enzyme activity was determined by measuring the increase in the absorbance as a result of enzyme substrate reaction at 405 nm for 2 minutes interval at 37^{o}C. The tacrine derivatives are dissolved in DMSO and were preincubated at room temperature with the enzyme for 20 mins, followed by the addition of the AChT and DTNB. The optical density in presence and absence of tacrine derivatives was plotted against time. The relative activities of all derivatives were calculated with respect to the native enzyme activity. Finally, the half maximal inhibitory concentration (IC_{50}) was determined for each derivatives by taking different inhibitor concentrations.

4.4.2. Ligand preparation and ADME property prediction

All tacrine derivatives were drawn using ChemSketch program. Bond length and angles of the derivatives were optimized by LigPrep module with OPLS-3 force field. LigPrep generates energy minimized 3D molecular structures. The prepared ligands were further used for docking and ADME studies. ADME predictions can be used in lead identification/optimization studies in order to understand the desired properties of a given compound. ADME studies were carried out using QikProp module. QikProp predicts a set of chemical descriptors that are relevant to the drug likeliness of the compounds.

4.4.3. Molecular docking studies

Docking simulation studies were carried out to understand the atomic level interaction of tacrine derivatives with AChE. Crystal structure of hAChE in complex with huprine (PDB ID: 4BDT) was taken from protein databank (PDB) and prepared using protein preparation wizard of Schrodinger program. Initially, all the crystallographic water molecules were deleted and hydrogens were added. The protonation states and partial charges were assigned for the charged residues during preparation. Finally, the structure was minimized by applying OPLS-3 force field. A grid was generated based on the binding position of huprine on AChE. The scaling factor of protein van der Waals radii for the receptor grid generation was set as 1 Å. The minimized ligands were docked to the grid volume. The extra precision (XP) method implemented in glide module was utilized for the docking process. Similarly, the BuChE complexes with tacrine (PDB ID: 4BDS) was also prepared and used for the docking studies.

4.4.4. Determination of the cytotoxicity of the derivatives

Cytotoxicity of the tacrine derivatives were tested in human embryonic kidney cells (HEK-293) by 3-(4,5-dimethylthiazol-2-yl)-2,5-diphenyltetrazolium bromide (MTT) assay method. HEK-293 cells were cultured in Dulbecco's modified Eagle's medium (DMEM) supplemented with 10% fetal bovine serum, 10,000 units/mL penicillin, 10 mg/mL streptomycin and 25 µg/mL amphotericin B. HEK-293 cells (~15 x 10^3 cells) were seeded in 96 well plate. After 24 hrs, the medium was removed and replaced with varying concentrations of tacrine derivatives for another 24 hrs. All compounds are dissolved in DMSO and diluted with fresh medium. The final DMSO concentration was 1.5%. After 24 hrs of the compound addition, MTT assay was carried out by treating the cells with 5 mg/mL MTT solution in PBS. After 3 hours of MTT treatment, the formazan crystals formed were dissolved in 100 µL DMSO. The absorbance was measured at 540 nm using enSpire Perkin Elmer multimode plate reader. Cell viability was expressed as the percentage of viable cells compared with untreated DMSO control cells.

4.4.5. Determination of Hepatotoxicity

In order to test the hepatotoxicity of the compounds, HepG2 cell lines were used. Cells were cultured as explained before. Cells were seeded at a density of 2×10^4 cells per well in 96 well plate for 24 hrs. Then the cells were treated with tacrine and its derivatives (with highest potency against AChE) in different concentrations with fresh medium for another 24 hrs. The MTT assay was carried out in the similar way and the percentage of cell viability was calculated. In addition, the cell viability in presence of 20c with different concentration was also checked for 48 and 72 hrs.

4.4.6. Chemistry

Ethyl 9-amino-1,2,3,4-tetrahydroacridine-2-carboxylate (19a*):* An oven dried RB flask was charged with 2-aminobenzonitrille **17a** (3g, 25.4 mmol) in anhydrous toluene (30 mL). $BF_3.Et_2O$ (3.2 ml, 30.48 mmol) was added slowly at room temperature. The reaction contents were cooled to 0^o C followed by the drop wise addition of ethyl 4-oxocyclohexanecarboxylate **18** (8.0 ml, 50.8 mmol). The reaction contents was then refluxed to 100^o C for 4 hours. After completion of the reaction as indicated by TLC the reaction mixture was quenched with aq. NaOH solution to adjust the pH to around 12 and diluted the reaction mixture with ethyl acetate. The organic layers were then separated, dried over anhydrous sodium sulphate, filtered and concentrated to obtain the crude material which was recrystallized from dichloromethane to yield the product **19a** (5.0 gm, 72%) as pale yellow solid. TLC: MDC: MeOH (9:1).

^{1}H NMR (300 MHz, DMSO-*d6*): δ 8.14 (d, 1H, *J* = 8.37 Hz), 7.61 (d, 1H, *J* = 8.31 Hz), 7.48 (t, 1H, *J* = 6.9 Hz), 7.27 (t, 1H, *J* = 6.93 Hz), 6.43 (s, 2H), 4.18-4.08 (m, 2H), 2.87-2.82 (m, 4H), 2.72-2.62 (m, 1H), 2.26-2.12 (m, 1H), 1.88-1.82 (m, 1H), 1.23 (t, 3H, *J* = 7.11 Hz).

LCMS: *m/z* calculated for $C_{16}H_{18}N_2O_2$: 270.33; Observed mass: 271.2 (M+1)

Anal. Calculated for $C_{16}H_{18}N_2O_2$: C, 71.09; H, 6.71; N, 10.36. Found: C, 72.01; H, 6.67; N, 10.76

Ethyl 9-amino-6-bromo-1,2,3,4-tetrahydroacridine-2-carboxylate (19b):

White solid; Yield 9.0 g, 84 % [Starting material 6.0 g]

^{1}H NMR (400 MHz, DMSO-*d6*): δ 8.13 (d, 1H, *J* = 8.96 Hz), 7.79 (s, 1H), 7.40 (dd, 1H, *J* = 8.92, 8.92 Hz), 6.61 (s, 2H), 4.19-4.07 (m, 2H), 2.94-2.85 (m, 4H), 2.68-2.61 (m, 1H), 2.15-2.11 (m, 1H), 1.89-1.80 (m, 1H), 1.24 (t, 3H, *J* = 7.12 Hz).

LCMS: *m/z* calculated for $C_{16}H_{17}BrN_2O_2$: 349.22; Observed mass: 351.7 (M+2)

Anal. Calculated for$C_{16}H_{17}BrN_2O_2$: C, 55.03; H, 4.91; N, 8.02; Found: C, 55.58; H, 5.24; N, 8.64.

Ethyl-9-amino-6-(1-methyl-1H-pyrazol-4-yl)-1,2,3,4-tetrahydroacridine-2-carboxylate (19c): To a solution of **19b** (1.0 g, 2.87 mmol) in 1,4-dioxane (10 ml) and water (1 ml) was added 1-methyl pyrazole 4-boronic ester (0.9 g, 4.31mmol) and Na_2CO_3 (0.6 g, 5.74 mmol). The reaction mixture was degassed for 10 min and added $Pd(PPh_3)_4$ (0.33 g, 0.287 mmol). The reaction mixture was heated to 110 ^{o}c for 2h in seal tube. The reaction mixture was filtered through celite and the filtrate was diluted with water (100 ml) and extracted with ethyl acetate (3 x 100 ml). The organic layers separated was dried over anhydrous Na_2SO_4 and concentrated under vacuum. The residue obtained was recrystallized in dichloromethane to afford compound 19**c** (0.52 g, 52%).

White solid

^{1}H NMR (400 MHz, DMSO-*d6*): δ 8.26 (s, 1H), 8.16 (d, J = 8.0 Hz, 1H), 7.99 (s, 1H), 7.82 (s, 1H), 7..63 (s, 1H), 7.55 (d, J = 8.0 Hz, 1H), 6.57 (bs, 2H), 4.15 (m, 2H), 3.89 (s, 3H), 2.88 (m, 4H), 2.69 (m, 1H), 2.16 (m, 1H), 1.90 (m, 1H), 1.26 (t, J = 7.12, 3H).

LCMS: *m/z* calculated for $C_{20}H_{22}N_4O_2$: 350.17; Observed mass: 351.2 (M+1)

Anal. Calculated for$C_{20}H_{22}N_4O_2$: C, 68.55; H, 6.33; N, 15.99; Found: C, 68.76; H, 6.24; N, 16.12

9-amino-N-methyl-1,2,3,4-tetrahydroacridine-2-carboxamide (20a): To a solution of compound **19a** (100 mg, 0.37 mmol) in methanol (4 ml) was added aq. ammonia (1 ml) and the reaction mixture was heated to 60^{o}Cfor 2h. The reaction mixture was concentrated to dryness and recrystallized from dichloromethane gave compound **20a**.

White solid; Yield 70 mg, 84%.

^{1}H NMR (400 MHz, DMSO-*d6*): δ 8.15-8.12 (m, 1H), 7.94 (d, J = 4.4 Hz, 1H), 7.81 (m, 1H), 7.42 (d, J = 8.8 Hz, 1H), 6.68 (bs, 3H), 2.88 (s, 3H), 2.76-2.68 (m, 3H), 2.15-2.12 (m, 1H), 2.01-1.98 (m, 1H), 1.91-1.81 (m, 2H).

LCMS: *m/z* calculated for $C_{15}H_{17}N_3O$: 225.14; Observed mass: 226.2 (M+1)

Anal. Calculated for $C_{15}H_{17}N_3O$: C, 70.56; H, 6.71; N, 16.46; Found: C, 70.12; H, 6.37; N, 16.38.

9-amino-1,2,3,4-tetrahydroacridine-2-carbohydrazide (20c): To a solution of compound **19a** (100 mg, 0.37 mmol) in methanol (4 ml) was added hydrazine hydrate (1 ml) and the reaction mixture was refluxed for 3h at 70^{0} C. The reaction mixture was concentrated and recrystallized from dichloromethane gave compound **20c**.

Brown solid; Yield 80 mg, 85%

^{1}H NMR (400 MHz, MeOD): δ 8.28-8.20 (m, 1H), 7.82-7.80 (m, 1H), 7.74-7.71 (m, 1H), 7.69-7.58 (m, 1H), 3.09-3.03 (m, 2H), 2.91-2.80 (m, 3H), 2.26-2.22 (m, 1H), 2.06-2.03 (m, 1H).

LCMS: *m/z* calculated for $C_{14}H_{16}N_4O$: 256.13; Observed mass: 257.2 (M+1).

Anal. Calculated for $C_{14}H_{16}N_4O$: C, 65.61; H, 6.29; N, 21.86; Found: C, 65.48; H, 6.34; N, 21.76.

9-amino-6-bromo-1,2,3,4-tetrahydroacridine-2-carbohydrazide (20d): Synthesised following the same protocol as **20c**.

White solid; Yield 70 mg, 73 %.

^{1}H NMR (400 MHz, DMSO-*d6*): δ 8.15 (s, 1H), 8.11 (d, J = 8.8 Hz, 1H), 7.79 (d, J = 2.0 Hz, 1H), 7.40-7.37 (m, 1H), 6.56 (s, 2H), 4.24 (bs, 2H), 2.91-2.77 (m, 2H), 2.72-2.67 (m, 2H), 1.96 (m, 1H), 1.83 (m, 1H).

LCMS: *m/z* calculated for $C_{14}H_{15}BrN_4O$: 334.04; Observed mass: 336.2 (M+2).

Anal. Calculated for$C_{14}H_{15}BrN_4O$: C, 50.16; H, 4.51; N, 16.71; Found: C, 50.27; H, 4.76; N, 16.68.

9-amino-1,2,3,4-tetrahydroacridine-2-carboxylic acid (21a): To a solution of **19a** (1.0 g, 3.70 mmol) in THF:H_2O: MeOH (4:1:1) was added lithium hydroxide monohydrade (0.31g, 7.40 mmol) and stirred for 3h at RT. The reaction mixture was diluted with water (100 ml) and ethyl acetate (100 ml). The aq. layer was separated and neutralized with conc. HCl, pH = 4.0. A white precipitate formed was filtered and dried over vacuum gave **21a**.

White solid; yield 0.8 g, 90%.

^{1}H NMR (400 MHz, DMSO-*d6*): δ 13.78 (s, 1H), 12.65 (s, 1H), 8.98 (s, 1H), 8.50 (d, 1H, *J* = 8.52 Hz), 8.16 (s, 1H), 7.88 (d, 2H, *J* = 4.52 Hz), 7.62-7.59 (m, 1H), 3.08-3.06 (m, 2H), 2.88-2.83 (m, 2H), 2.71-2.67 (m, 1H), 2.21-2.19 (m, 1H).

LCMS: *m/z* calculated for $C_{14}H_{14}N_2O_2$: 242.27; Observed mass: 243.2 (M+1)

Anal. Calculated for $C_{14}H_{14}N_2O_2$: C, 69.41; H, 5.82; N, 11.56; Found C, 69.76; H, 5.86; N, 11.48.

9-amino-6-bromo-1,2,3,4-tetrahydroacridine-2-carboxylic acid (21b): Synthesised following the same protocol as 21a.Starting material is 19b

White solid; yield 0.8 g, 87 %.

^{1}H NMR (400 MHz, DMSO-*d6*): δ 8.12 (d, 1H, *J* = 9.0 Hz), 7.79 (s, 1H), 7.39 (dd, 1H, *J* = 8.92, 8.96 Hz), 6.58 (s, 2H), 2.87-2.81 (m, 2H), 2.66-2.60 (m, 2H), 2.13-2.10 (m, 1H), 1.89-1.81 (m, 1H).

LCMS: *m/z* calculated for $C_{14}H_{13}BrN_2O_2$: 321.17; Observed mass: 323.2 (M+2).

Anal. Calculated for $C_{14}H_{13}BrN_2O_2$: C, 52.36; H, 4.08; N, 8.72; Found:C, 52.32; H, 4.06; N, 8.68.

***9*-amino-6-(1-methyl-1H-pyrazol-4-yl)-1,2,3,4-tetrahydroacridine-2-carboxylic acid (21c):**Synthesised following the same protocol as 21a.Starting material is 19c

White solid; 0.6 g, 79%.

^{1}H NMR (400 MHz, MeOD): δ 8.09-8.05 (m, 1H), 7.94 (s, 1H), 7.74 (s, 1H), 7.59 (d, *J* = 8.0 Hz, 1H), 3.96 (s, 3H), 2.99 (m, 2H), 2.89-2.86 (m, 2H), 2.78-2.75 (m, 1H), 2.27 (m, 1H), 1.93 (m, 1H).

LCMS: *m/z* calculated for $C_{18}H_{18}N4O_2$: 322.36; Observed mass: 323.2 (M+1).

Anal. Calculated for $C_{18}H_{18}N4O_2$: C, 67.07; H, 5.63; N, 17.38; Found:C, 67.09; H, 5.64; N, 17.39.

9-Amino-1,2,3,4-tetrahydro-acridine-2-carboxylic acid benzylamide (22a): An oven dried RB was charged with compound **21a** (100 mg, 0.413 mmol) in dry DMF (5 ml) was added triethyl amine (0.13 ml, 1.03 mmol) and T3P, 50% wt in ethyl acetate (0.3 ml, 1.03 mmol). The reaction mixture was allowed to stir at RT for 15 min before the addition of benzylamine (0.06 ml, 0.495 mmol) and the reaction mixture was stirred for 12h at RT. The reaction mixture was diluted with water (50 ml) and extracted with ethyl acetate (3 x 50 ml). The organic layer was washed with saturated sodium bicarbonate solution and brine. The organic layer was dried over anhydrous sodium sulphate and concentrated under vacuum. The residue obtained was purified by silica gel column chromatography (230-400 mesh) using 50 % ethyl acetate in pet ether as eluent to obtain 22**a** (80 mg, 60%).

White solid, Yield 80 mg, 60%.

^{1}H NMR (400 MHz, MeOD): δ 8.17 (d, J = 8.0 Hz, 1H), 7.6-7.69 (m, 2H), 7.46 (d, J = 8.0 Hz, 1H), 7.38-7.30 (m, 4H), 7.29-7.25 (m, 2H), 4.45 (s, 2H), 3.08-3.03 (m, 2H), 2.87-2.82 (m, 3H), 2.23 (m, 1H), 2.03 (m, 2H).

LCMS: *m/z* calculated for $C_{21}H_{21}N_3O$: 321.17; Observed mass: 323.2 (M+2).

Anal. Calculated for $C_{12}H_{21}N_3O$: C, 76.11; H, 6.39; N, 12.68; Found: C, 76.14; H, 6.36; N, 12.72.

9-amino-N-phenethyl-1,2,3,4-tetrahydroacridine-2-carboxamide(22b): Synthesised following the same protocol as 22a

White solid, Yield 85 mg, 60%.

^{1}H NMR (400 MHz, MeOD): δ 8.10 (d, J = 8.0 Hz, 1H), 7.74 (d, J = 8.0 Hz, 1H), 7.64 (t, J = 7.2Hz, 1H), 7.42 (t, J = 7.2Hz, 1H), 7.31-7.22 (m, 5H), 3.57-3.45 (m, 2H), 3.00 (m, 2H), 2.89-2.85 (m, 2H), 2.75-2.72 (m, 3H), 2.10 (m, 1H), 1.93 (m, 1H).

LCMS: *m/z* calculated for $C_{22}H_{23}N_3O$: 345.17; Observed mass: 346.2 (M+2); Anal. Calculated for $C_{22}H_{23}N_3O$: C, 76.49; H, 6.71; N, 12.16; O, 4.63; Found: C, 76.50; H, 6.66; N, 12.18.

9-amino-N-(3-phenylpropyl)-1,2,3,4-tetrahydroacridine-2-carboxamide (22c): Synthesised following the same protocol as **22a**.

White solid; yield 100 mg, 67 %.

^{1}H NMR (400 MHz, MeOD): δ 8.09 (d, 1H, *J* = 8.4 Hz), 7.73 (d, 1H, *J* = 8.4 Hz), 7.64-7.60 (m, 1H), 7.43-7.39 (m, 1H), 7.30-7.16 (m, 5H), 3.29-3.26 (m, 2H), 3.09-3.00 (m, 2H), 2.83-2.77 (m, 2H), 2.76-2.68 (m, 3H), 2.18-2.14 (m, 1H), 2.01-1.97 (m, 1H), 1.96-1.85 (m, 2H).

LCMS: *m/z* calculated for $C_{23}H_{25}N_3O$: 359.46; Observed mass: 360/2 (M+1).

Anal. Calculated for $C_{23}H_{25}N_3O$: C, 76.85; H, 7.01; N, 11.69; Found: C, 76.82; H, 7.06; N, 11.72.

9-amino-6-bromo-N-phenethyl-1,2,3,4-tetrahydroacridine-2-carboxamide (22e): Synthesised following the same protocol as 22a.Starting material is 21b

White solid; yield 80 mg, 63 %.

^{1}H NMR (300 MHz, DMSO-*d6*): δ 8.13-8.05 (m, 2H), 7.79 (s, 1H), 7.41-7.18 (m, 6H), 6.56 (s, 2H), 3.39-3.24 (m, 1H), 2.84-2.73 (m, 5H), 2.68-2.57 (m, 3H), 1.98-1.94 (m, 1H), 1.83-1.74 (m, 1H).

LCMS: *m/z* calculated for $C_{22}H_{22}BrN_3O$: 423.33; Observed mass: 425.2 (M+2)

Anal. Calculated for $C_{22}H_{22}BrN_3O$: C, 62.27; H, 5.23; N, 9.90; Found: C, 62.24; H, 5.22; N, 9.94.

9-amino-6-bromo-N-(3-phenylpropyl)-1,2,3,4-tetrahydroacridine-2-carboxamide (22f): Synthesised following the same protocol as 22a. Starting material is 21b

Brown solid; yield 90 mg, 66 %.

^{1}H NMR (400 MHz, DMSO-*d6*): δ 8.11 (d, 1H, *J* = 8.8 Hz), 8.01 (s, 1H), 7.79 (s, 1H), 7.40 (dd, 1H, *J* = 8.8, 9.2 Hz), 7.31-7.17 (m, 6H), 6.57 (s, 2H), 3.16-3.08 (m, 2H), 2.88-2.84 (m, 2H), 2.75-2.68 (m, 1H), 2.63-2.59 (m, 4H), 2.02-1.98 (m, 1H), 1.80-1.66 (m, 3H).

LCMS: *m/z* calculated for $C_{23}H_{24}BrN_3O$: 338.36; Observed mass: 340.0 (M+2).

Anal. Calculated for $C_{23}H_{24}BrN_3O$: C, 63.02; H, 5.52; N, 9.59; Found: C, 63.08; H, 5.56; N, 9.60.

9-Amino-6-(1-methyl-1H-pyrazol-4-yl)-1,2,3,4-tetrahydro-acridine-2-carboxylic acid benzylamide (22g): Synthesised following the same protocol as ***22***a. Starting material is 21b

White solid; yield 80 mg, 63 %.

^{1}H NMR (400 MHz, MeOD): δ 8.30-8.26 (m, 2H), 8.03 (s, 1H), 7.80 (dd, J = 9.2 Hz, 2H), 7.46 (m, 1H), 7.36 (m, 3H), 7.28 (m, 1H), 4.45 (s, 2H), 4.00 (s, 3H), 3.10 (m, 2H), 2.87 (m, 1H), 2.84 (m, 2H), 2.24 (m, 1H), 2.10 (m, 1H).

LCMS: *m/z* calculated for $C_{25}H_{25}N_5O$: 411.21; Observed mass: 412.2 (M+1).

Anal. Calculated for $C_{25}H_{25}N_5O$: C, 72.97; H, 6.12; N, 17.02; Found: C, 73.00; H, 6.14; N, 17.08.

9-amino-6-(1-methyl-1H-pyrazol-4-yl)-N-phenethyl-1,2,3,4-tetrahydroacridine-2-carboxamide (22h): Synthesised following the same protocol as ***22***a. Starting material is 21c

White solid; yield 80 mg, 60 %.

^{1}H NMR (400 MHz, DMSO-*d6*): δ 8.16 (d, *J* = 8.4 Hz, 1H), 7.64 (d, *J* = 8.4 Hz, 1H), 7.50 (t, *J* = 7.2 Hz, 1H), 7.35-7.20 (m, 3H), 6.99 (d, *J* = 8.0 Hz, 2H), 6.90 (d, *J* = 7.6 Hz, 1H), 6.29 (bs, 1H), 4.00 (s, 3H), 3.50-3.38 (m, 2H), 3.30-3.10 (m, 2H), 3.00-3.85 (m, 3H), 3.80-3.72 (m, 1H), 3.70-3.60 (m, 1H), 2.05-1.95 (m, 1H), 1.90-1.78 (m, 1H).

LCMS: *m/z* calculated for $C_{26}H_{27}N_5O$: 425.53; Observed mass: 426.2 (M+1).

Anal. Calculated for $C_{26}H_{27}N_5O$: C, 73.39; H, 6.40; N, 16.46; Found: C, 73.38; H, 6.41; N, 16.48.

9-amino-6-(1-methyl-1H-pyrazol-4-yl)-N-(3-phenylpropyl)-1,2,3,4-tetrahydroacridine-2-carboxamide (22i): Synthesised following the same protocol as ***22***a.Starting material is 21c

White solid; yield 90 mg, 66 %.

^{1}H NMR (400 MHz, CD3OD): δ 8.11 (s, 1H), 8.05 (d, 1H, *J* = 8.76 Hz), 7.95 (s, 1H), 7.83 (s, 1H), 7.59 (d, 1H, *J* = 8.76 Hz), 7.28-7.17 (m, 4H), 7.16-7.12 (m, 1H), 3.97 (s, 3H), 3.29-3.26 (m, 2H), 3.05-3.00 (m, 2H), 2.82-2.68 (m, 5H), 2.18-2.15 (m, 1H), 1.92-1.90 (m, 1H), 1.89-1.87 (m, 2H).

LCMS: *m/z* calculated for $C_{27}H_{29}N_5O$: 439.55; Observed mass: 440.2 (M+1); Anal. Calculated for $C_{27}H_{29}N_5O$: C, 73.78; H, 6.65; N, 15.93; Found: C, 73.80; H, 6.64; N, 16.00.

9-amino-N-(3-phenylpropyl)-6-(pyrimidin-5-yl)-1,2,3,4-tetrahydroacridine-2-carboxamide (22j): Synthesised following the same protocol as ***22***a.Starting material is 21d

White solid; yield 80 mg, 59 %.

^{1}H NMR (400 MHz, CD_3OD): δ 9.18 (s, 3H), 8.22 (d, 1H, *J* = 8.8 Hz), 8.00 (s, 1H), 7.69 (d, 1H, *J* = 8.8 Hz), 7.29-7.21 (m, 4H), 7.18-7.15 (m, 1H), 3.31-3.24 (m, 2H), 3.07-3.00 (m, 2H), 2.86-2.82 (m, 2H), 2.80-2.75 (m, 1H), 2.73-2.67 (m, 2H), 2.18-2.15 (m, 1H), 2.00-1.95 (m, 1H), 1.92-1.84 (m, 2H).

LCMS: *m/z* calculated for $C_{27}H_{27}N_5O$: 437.54; Observed mass: 438.2 (M+1); Anal. Calculated for $C_{27}H_{27}N_5O$: C, 74.12; H, 6.22; N, 16.01; Found: C, 74.16; H, 6.20; N, 16.06.

9-amino-N-(1-methyl-1H-pyrazol-5-yl)-1,2,3,4-tetrahydroacridine-2-carboxamide (23a): Synthesised following the same protocol as ***22***a.Starting material is 21c

White solid; yield 20 mg, 63 %.

^{1}H NMR (400 MHz, DMSO-*d6*): δ 8.27 (s, 1H), 8.16 (d, *J* = 8.4 Hz, 1H), 7.99 (s, 1H), 7.95 (d, *J* = 4.4 Hz, 1H), 7.81 (s, 1H), 7.56 (d, *J* = 8.0 Hz, 1H), 3.89 (s, 3H), 2.89 (m, 2H), 2.68-2.64 (m, 2H), 2.15 (m, 1H), 1.99-1.91 (m, 1H), 1.81-1.78 (m, 1H).

LCMS: *m/z* calculated for $C_{18}H_{19}N_5O$: 321.38; Observed mass: 322.2 (M+1); Anal. Calculated for $C_{18}H_{19}N_5O$: C, 67.27; H, 5.96; N, 21.79; Found: C, 67.28; H, 5.97; N, 21.79.

9-amino-6-bromo-N-(1-methyl-1H-pyrazol-5-yl)-1,2,3,4-tetrahydroacridine-2-carboxamide (23b): Synthesised following the same protocol as ***22***a.Starting material is 21c

White solid; yield 33 mg, 71 %.

^{1}H NMR (400 MHz, MeOD): δ 8.19 (d, *J* = 8.8 Hz, 1H), 7.94 (s, 1H), 7.77-7.71 (m, 1H), 7.53-7.49 (m, 1H), 7.43 (d, *J* = 7.2 Hz, 1H), 4.00 (s, 3H), 3.02-3.06 (m, 2H), 2.97-2.92 (m, 2H), 2.88-2.80 (m, 1H), 2.38-2.30 (m, 1H), 2.07-1.97 (m, 1H).

LCMS: *m/z* calculated for $C_{18}H_{18}BrN_5O$: 399.38; Observed mass: 400.2, 402.2 (M+1, M+3); Anal. Calculated for $C_{18}H_{18}BrN_5O$: C, 54.01; H, 4.53; N, 17.50; Found: C, 54.00; H, 4.52; N, 17.51.

CHAPTER 5

SYNTHESIS OF IMIDAZOPYRIDINE[4,5-*c*]QUINOLINE - 6-ESTERS AND IMIDAZOPYRIDINE[4,5-*d*] AZEPINONES FROM MBH ACETATES AND BIOLOGICALSTUDIES AGAINST ACETYLCHOLIN- ESTERASE AS ITS INHIBITORS

5.1 Introduction

5.1.1 Introduction to Imidazopyridine

In the past few years, much attention has been drawn on the imidazopyridine scaffolds because of their wide range of biological activities. Among the various imidazopyridine derivatives, imidazo[1,2-*a*]pyridine moiety is the most important in the area of various biologically active molecules and pharmaceuticals. For example, antiviral, antimicrobial, antitumor, anti-inflammatory, antiparasitic, hypnotic, etc. Some marketed drugs like alpidem, zolpidem, saripidem, necopidem, zolimidine, etc., (Figure 5.1) contain this scaffold [George, P. G, et al, 1993; Monti, J. M, et al. 2009; George, P, et al. 1991; Hanson, et al, 2008; Enguehard-Gueiffier, C, et al, 2007; Kim, O, et al, 2011; Kamal, A, et al, 2010; Veron, J. B, et al, 2008; Scribner, A, et al. 2007].They also act as β-amyloid formation inhibitors, GABA and benzodiazepine receptor agonists and cardiotonic agents [Humphries A C, et al, 2006; Fuchs K, et al, 2002; Dvey D, et al, 1987; Fookes C J R, et al, 2008]. The Imidazo[1,2-*a*]pyridine scaffold broadly applied in organometallic chemistry and material science because of their structural characteristics[Stasyuk A J, et al, 2012; Shao N, et al, 2011]. Significant efforts have been made in the area of developing novel strategies for the construction of imidazo[1,2-a]pyridine scaffold. The metaal catalysed synthesis of imidazo[1,2-*a*]pyridine scaffold was developed by Hajra *et al* and anil kumar *et al* recently[Bagdi A K, et al, 2016;Hajra A, et al, 2015; Pericherla K, et al, 2015; Samanta S, et al, 2016; Mishra, S, et al, 2014; Monir, K, et al, 2014; Monir, K, et al. 2014, 356; Bagdi, A, et al, 2013; Santra, S, et al. 2013]. Meanwhile, a set of synthetic methods have been established for the functionalization of imidazo[1,2-*a*]pyridine derivatives. The C-3 position of the imidazo[1,2-*a*]pyridine moiety is electron rich, which enables it to be attacked by electrophiles or radicals. Thus, a series of metal-

catalysed C-H functionalization reactions on C-3 position to form C-C bonds, including regioselective arylation, alkenylation, formylation, and trifluoro methylation, were achieved. The methods for the formation of carbon-heteroatom bonds at the same position were also developed like halogenation, sulfenylation, hydrazination, glyoxalates and nitrosylation [Ghosh, M, et al, 2015; Yongyuan Gao, et al, 2016; Monir, K, et al, 2015; Bagdi, A. K, et al, 2015].Herewith, we reported the synthesis of imidazo[1,2-*a*]pyridine quinoline esters and imidazopyridine azepinones using copper and iron salts via imidazo[1,2-*a*]pyridine-3-glyoxalates.

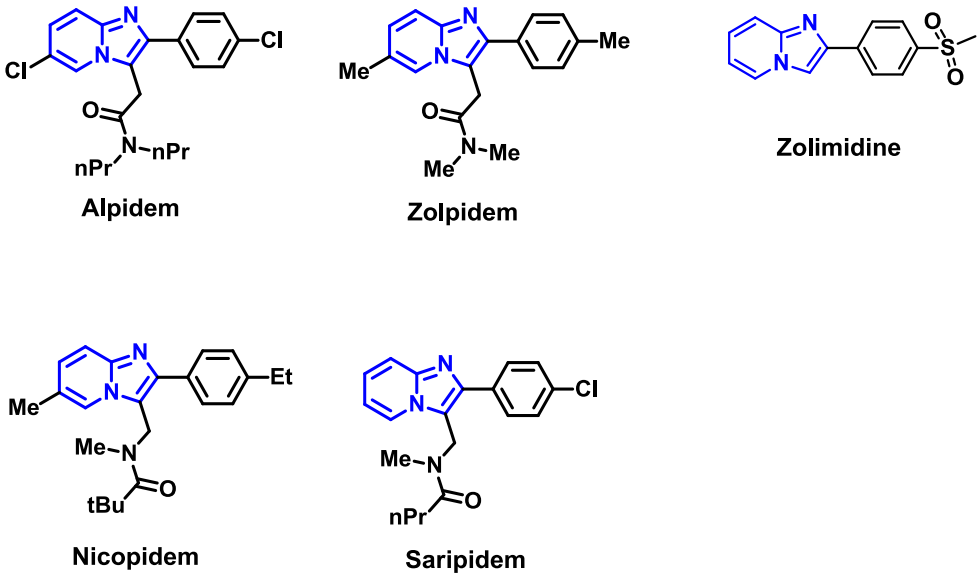

Figure 5.1: Biologically active imidazo[1,2-*a*]pyridine and azepinone

5.1.2 Introduction to Quinolines

Quinolines are important nitrogen containing heterocyclic compounds to be found in various natural products and biological active compounds [Joule J A, et al, 2010; Eicher T, et al, 2003; Stork G, et al, 2001; Balasubramanian, M, et al, 1996].Quinolines represent a major class of nitrogen-containing heterocyclic compounds which are found to be the key structural unit in many natural products (Fig. 5.2). Quinoline derivatives show a wide range of biological activities such as anti- malarial [Cagir A, 2004], anti-microbial, anti-bacterial [Bax B D, et al, 2010], anti-inflammatory [El-Gazzar, et al, 2009], anti-diabetic [Edmont, et al, 2000], anti-alzheimer [Camps P, et al, 2001], tyrosine kinase inhibitor [Maguire M P, et al, 1994], anti-platelet activity [Ko T C, et al, 2001], and anti-hypertensive [Bradbury R H, et al, 1993]. The core structure quinoline contains

in many of currently marketed drugs such as Singulair, Tafenoquine, and Hydroxychloroquine etc [Elslager E, et al, 1969; Halama A, et al, 2010].Because of wide range bioactivity of quinoline derivatives and imidazopyridine scaffold, several research groups are focusing on the synthesis of Imidazopyridine 6-aryl quinoline derivatives and naptho fused imidazo[1,2-a]pyridines using copper or palladium chemistry [Xue-Sen Fan, et al, 2015; Boganyi, et al, 2009; Anandkumar Pandey, et al, 2014]. Quinolines, in particular, constitute the core structure of many currently marketed drugs such as Singulair, Tafenoquine, and Hydroxychloroquine etc. In addition, quinoline based polymers have applications in the field of electronics, optoelectronics and nonlinear optics. Furthermore, quinoline derivatives have been used as organocatalysts and are well known as useful tools for asymmetric synthesis [Kim J I, et al, 2005].Among various quinoline derivatives, 2-arylquinoline scaffolds are associated with a wide range of biological properties, such as P-selectin antagonism, antimalarial, and antitumor activities [Kaila N, et al, 2007; Krishnamurthy, et al, 2004; Chaires J B, et al, 2003;Strekowski L, et al, 1996; Atwell G J, et al, 1989].Due to their wide range of bioactivities, synthesis of 2-arylquinoline derivatives has gained special attention. Established strategies for assembling quinoline rings are the classic annulation reactions like Friedlander Combes, Povarov1967, Doebnervon Miller and Skraupsyntheses etc.

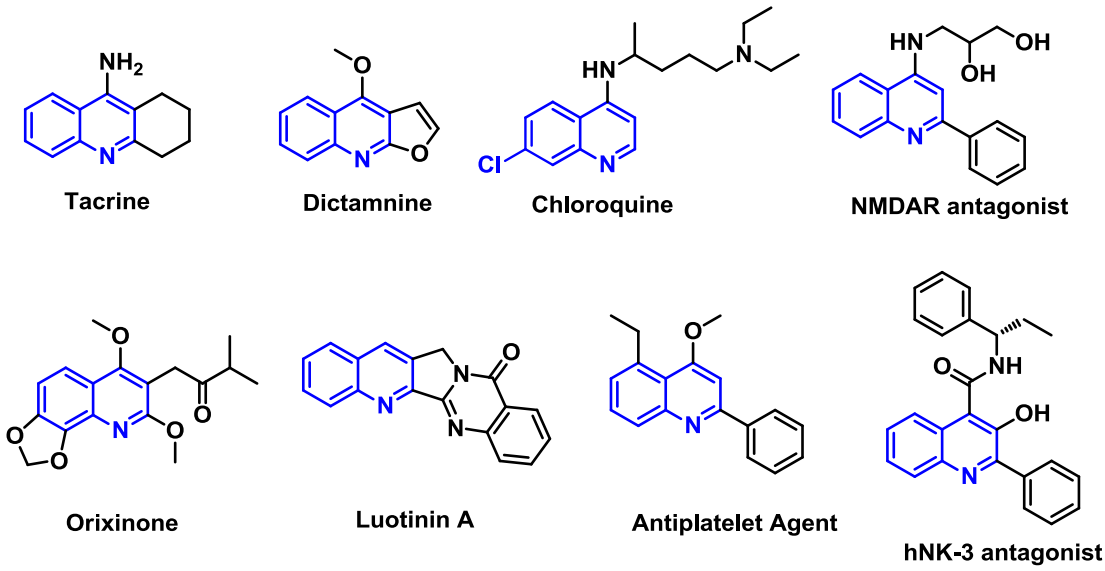

Figure 5.2: Biologically active Quinoline moiety.

5.1.3 Introduction to Azepinones

The synthesis of azepinone rings has been a challenging and fascinating endeavour in synthetic and medicinal chemistry. The importance of azepinone moiety have been described as potent, ATP-competitive inhibitors of the cell cycles regulating cyclin-dependent kinases (CDKs), glycogen-synthase kinases (GSKs), and mitochondrial malate dehydrogenase (mMDH) and have become a class of very useful agents for the treatment of neurodegenerative and proliferative disorders [Kunick C, et al, 2004; Gussio R, et al, 2000;Schultz C, et al, 1999]. The presence of azepinone moiety in Microtubule-Stabilizing Sponge alkaloids like Ceratamines A, B and Desbromoceratamine A represents a new class of anti-cancer drug discovery and development, especially for multidrug resistance cancer cells [Donovan, D, et al. 2008; Bhushan, S, et al. 2008]. We were interested in the development of the azepinone scaffold' as it shows interesting structural resemblance with the framework of the γ-secretase inhibitor LY411575, which was developed by Eli Lilly [Vasiliev, I. A. et al, 2007; Deomling, A, et al. 2002; Audia, J. E, et al. 2000]. Because of these biological importance of azepinones has been increasing interest in the development of easy and simple methodologies.

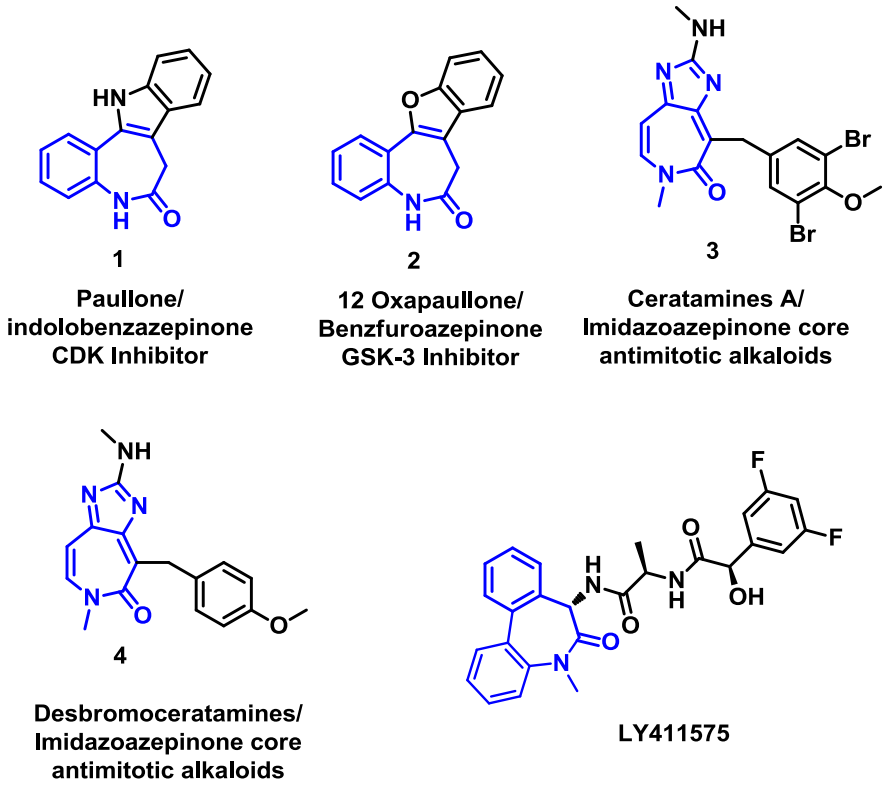

Figure 5.3: Biologically active azepinone containing molecules

The Morita-Baylis-Hillman (MBH) reaction has an attractive strategy for the synthesis of multifunctional heterocyclic molecules in recent years. The MBH reaction is a key step in the synthesis of bioactive molecules and designed molecules. Earlier, Baylis and Hillman reported the synthesis of α-hydroxyethyl nitroethylenes from MBH reaction. Later, Namboothiri and Chen made further investigation on this reaction and emphasized the use of electrophilic ethylglyoxylate. The MBH reaction of nitroalkenes have been utilised for the synthesis of several heterocycles and carbocycles. Further acetylation on hydroxyl group of these conjugated nitroalkene afforded MBH Acetates as excellent Michael acceptors containing four potential electrophilic sites (α, β, γ, δ). The MBH adducts, can act as dielecrophilic agents to undergo cascade reactions with various bifunctional nucleophiles. All four electrophilic sites are highly reactive and used as efficient synthons to synthesise the diversified molecules (Scheme-5.1) of fused furans(α-β), imidazopyridines(α-β), substituted imidazoles (α-β), benzimidazo[2,1-*b*]-1,3-thiazine (γ-α) and thiazolo[3,2-*a*]benzimidazole (γ-β), imidazo[1,2-*a*]pyridines(α-α), indolizines (α-β), pyrroles (α-γ), benzo[*b*][1,6]oxazocin-2-ones (α-δ)and functionalised dihydroazapyrimidine derivatives (γ-α). Herein, we reported that MBH adducts acts as a tri electrophilic agents for the synthesis of pyrido[2',1':2,3] imidazo[4,5-c]quinoline-6-carboxylate esters and Imidazopyridine[4,5-*d*]azepin-2-one from MBH adducts derived from 2-nirto Benzaldehyde by reacting with 2- amino pyridine derivatives in moderate to good yields by *α-β-γ* and *α-β-δ* cyclisation respectively. The reaction involves a cascade S_N2' reaction (*α*-attack) followed by intramolecular Michael addition (*β* -attack) then reductive cyclisation (*γ*/*δ*–attack) with the generation of three new carbon-Nitrogen bonds.

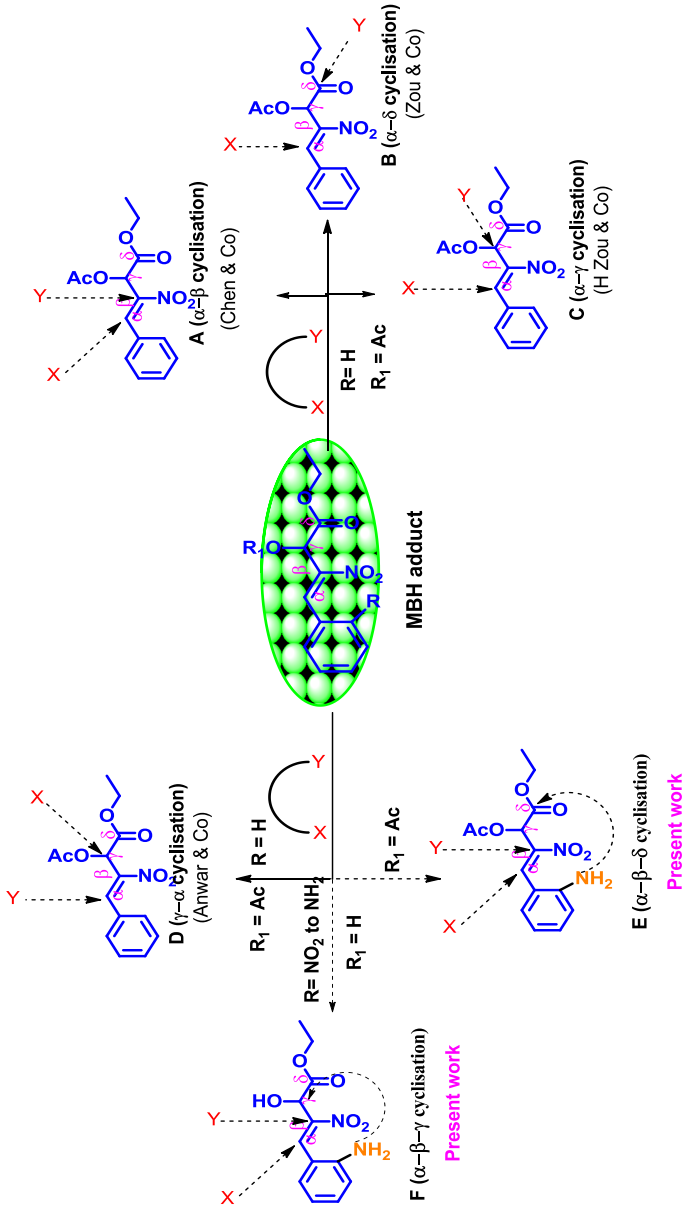

Scheme 5.1: Potential electrophilic sites of MBH Acetates

In continuation of our research in the synthesis of heterocyclic molecules as a cholinesterase inhibiors, we report a simple and efficient protocol for synthesis of pyrido[2',1':2,3]imidazo[4,5-c](dihydro)quinoline-6-carboxylate esters and imidazopyridine[4,5-*d*]azepin-2-one from MBH adducts derived from 2-nirto benzaldehyde by reacting with 2-aminopyridine derivatives by *α-β-γ* and *α-β-δ* cyclisation (scheme 5.2).

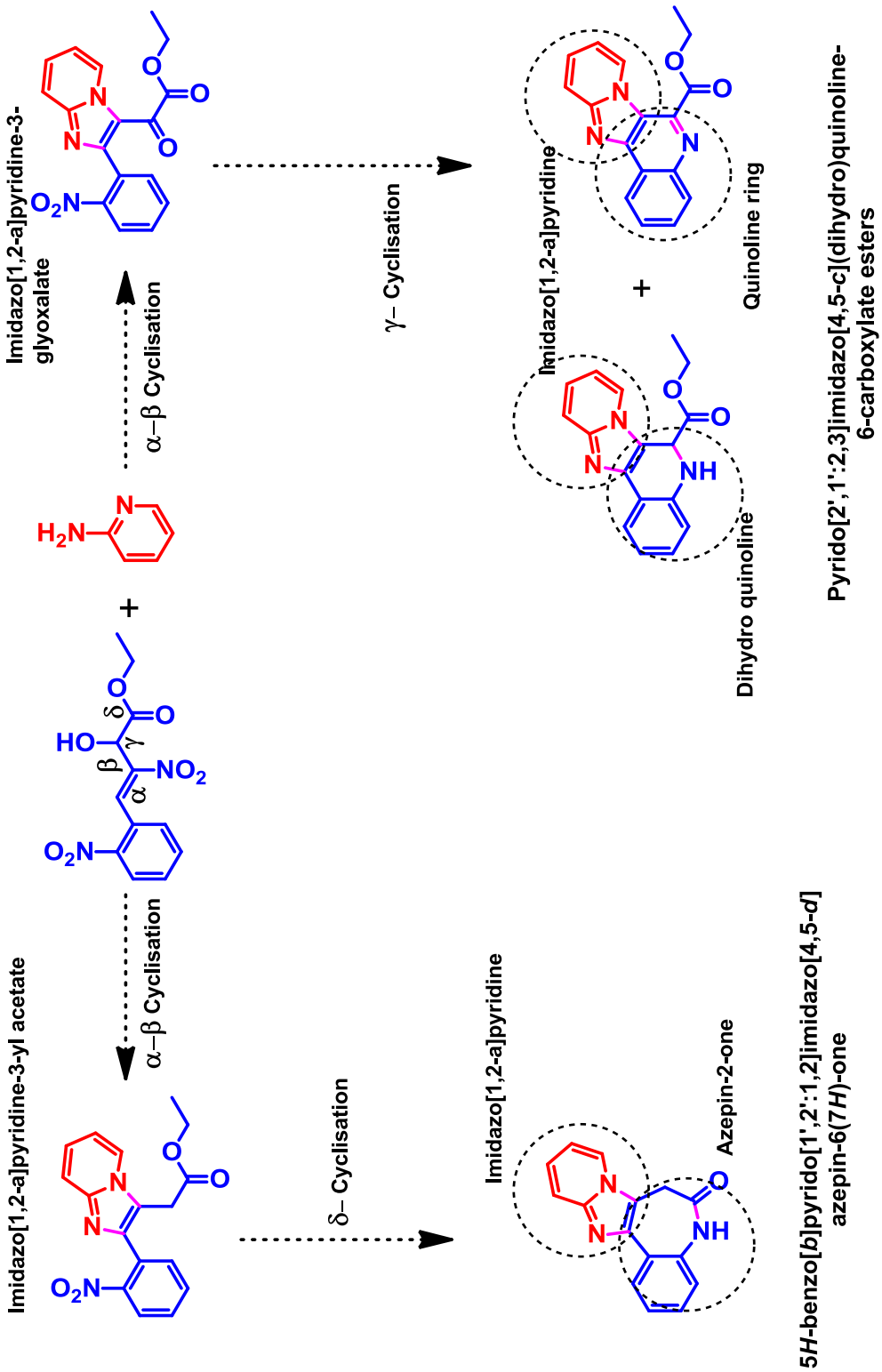

Scheme 5.2: Strategy towards the synthesis of imidazopyridine[4,5-*c*](dihydro)quinoline-6-carboxylate esters and Imidazopyridine[4,5-*d*]azepin-6(7H)-one

5.2 Results and discussion

The study was started by investigating the reaction between 2-nitro MBH adduct **24** was treated with acetyl chloride in presence of pyridine as a base and MDC as a solvent followed by the addition of 2-aminopyridine **25** in oxygen atmosphere. Interestingly, the product of imidazo[1,2-*a*]pyridine-3-glyoxate ester **26** (40%) was observed in scheme 5.3. The product was confirmed by LCMS, NMR and X-ray crystal. The nitro of the compound was reduced to amine using iron in acetic acid which was cyclised insitu and formed imidazopyridine[4,5-*c*]quinoline-6-carboxilic ester **27** at RT and the dihydro quinoline **28** derivative was observed when the reaction was refluxed to 100 ^{o}C for 4h.

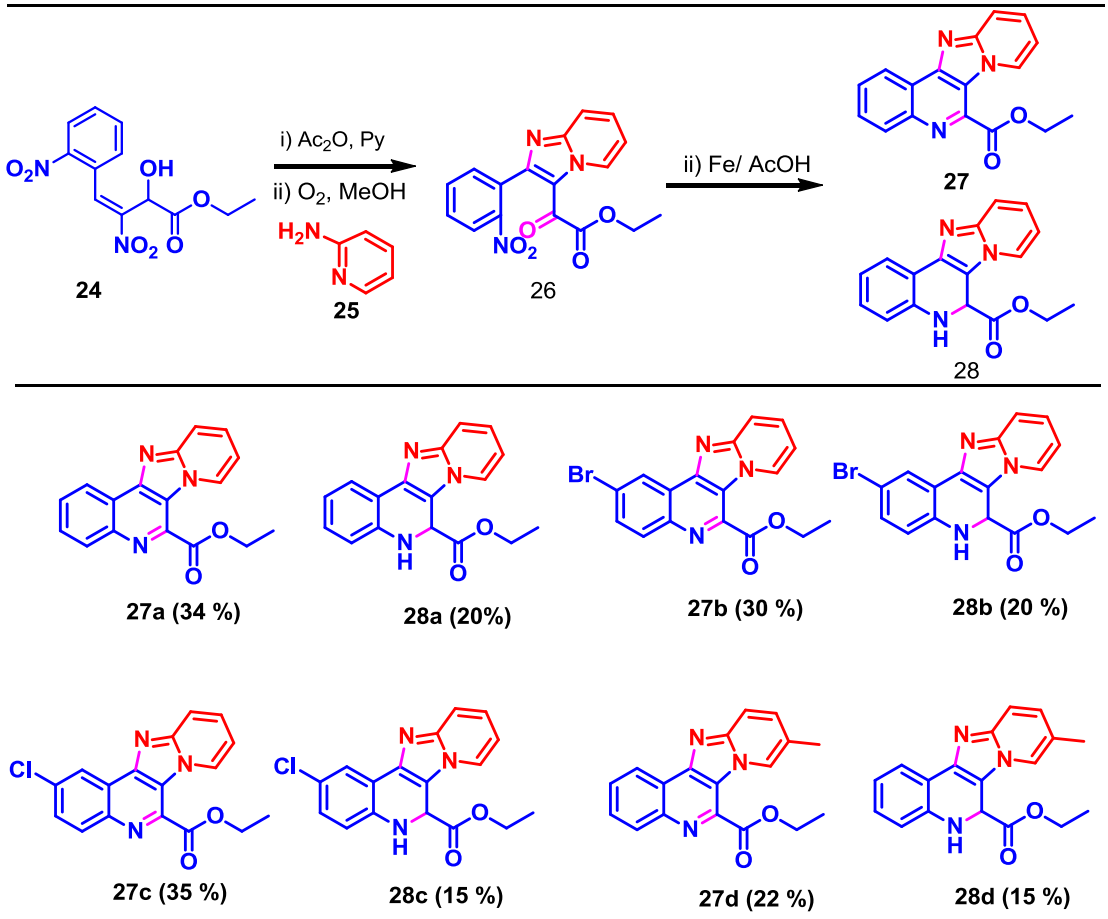

Scheme 5.3: synthetic scope of imidazopyridine[4,5-*c*]quinoline(dihydro) derivatives

Table 5.1: Crystal data and structure for compound **27a**

Table: Crystal data and structure refinement for **27a**.

Identification code	RED
Empirical formula	$C_{17}H_{12}N_3O_2$
Formula weight	290.30
Temperature/K	298(2)
Crystal system	orthorhombic
Space group	$P2_12_12_1$
a/Å	4.4573(10)
b/Å	17.680(5)
c/Å	17.847(4)
α/°	90
β/°	90
γ/°	90
Volume/Å^3	1406.5(6)
Z	4
ρ_{calc}g/cm^3	1.371
μ/mm^{-1}	0.093
F(000)	604.0
Crystal size/mm^3	0.25 × 0.24 × 0.23
Radiation	MoKα (λ = 0.71073)
2Θ range for data collection/°	5.114 to 50.046
Index ranges	$-5 \leq h \leq 4$, $-13 \leq k \leq 21$, $-21 \leq l \leq 17$
Reflections collected	6198
Independent reflections	2466 [R_{int} = 0.1525, R_{sigma} = 0.3042]
Data/restraints/parameters	2466/0/200
Goodness-of-fit on F^2	0.970
Final R indexes [I>=2σ (I)]	R_1 = 0.0983, wR_2 = 0.0973
Final R indexes [all data]	R_1 = 0.2888, wR_2 = 0.1475
Largest diff. peak/hole / e Å^{-3}	0.23/-0.18
Flack parameter	-6.1(10)

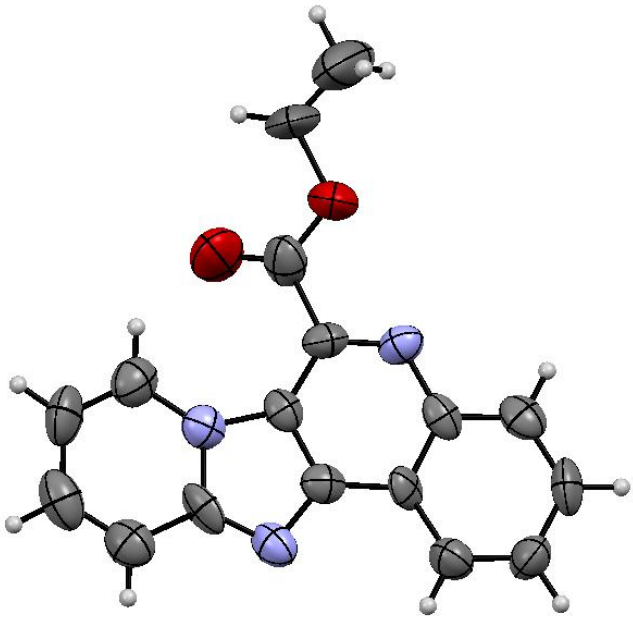

Figure 5.4: Single X-ray crystal structure of compound 27a

Based on optimised conditions, we next focused on the substrate of imidazo[1,2-*a*]pyridine azepinone **30** derivatives using different 2-nitro MBH acetates **29** and different 2-amino pyridines **25** in scheme 5.4. To our delight the best results were obtained when we treated 2-nitro MBH acetate with 2-amino pyridine in methanol solvent at room temperature for 1 hr followed by the treatment with Fe/AcOH at reflux for 4h providing 5H-benzo[b]pyrido[1',2':1,2] imidazo[4,5-*d*]azepin-6(7H)-one (**30**) in 75% yield after the usual workup followed by column chromatography. The structure of this molecule was confirmed by ^{1}H NMR, ^{13}C NMR and LCMS. To examine this strategy, different MBH acetates derived from 2-nitrobenzaldehydes were subjected to synthetic sequence to provide the desired imidazo pyridine[4,5-*d*]azepin-2-one in 50-80% isolated yields (scheme-5.4). The MBH acetates derived from nitro isonicotinaldehyde (**30f & 30g**) gave moderate yield towards the synthesis of corresponding azepinone derivatives about 60% yield. To examine the strategy of different 2-amino pyridine derivitatives with 2-nitro MBH acetates (**30h – 30o**), halo substituted amines gave good yields to synthesis of corresponding imidazopyridine[4,5-*d*]azepinones (75%).

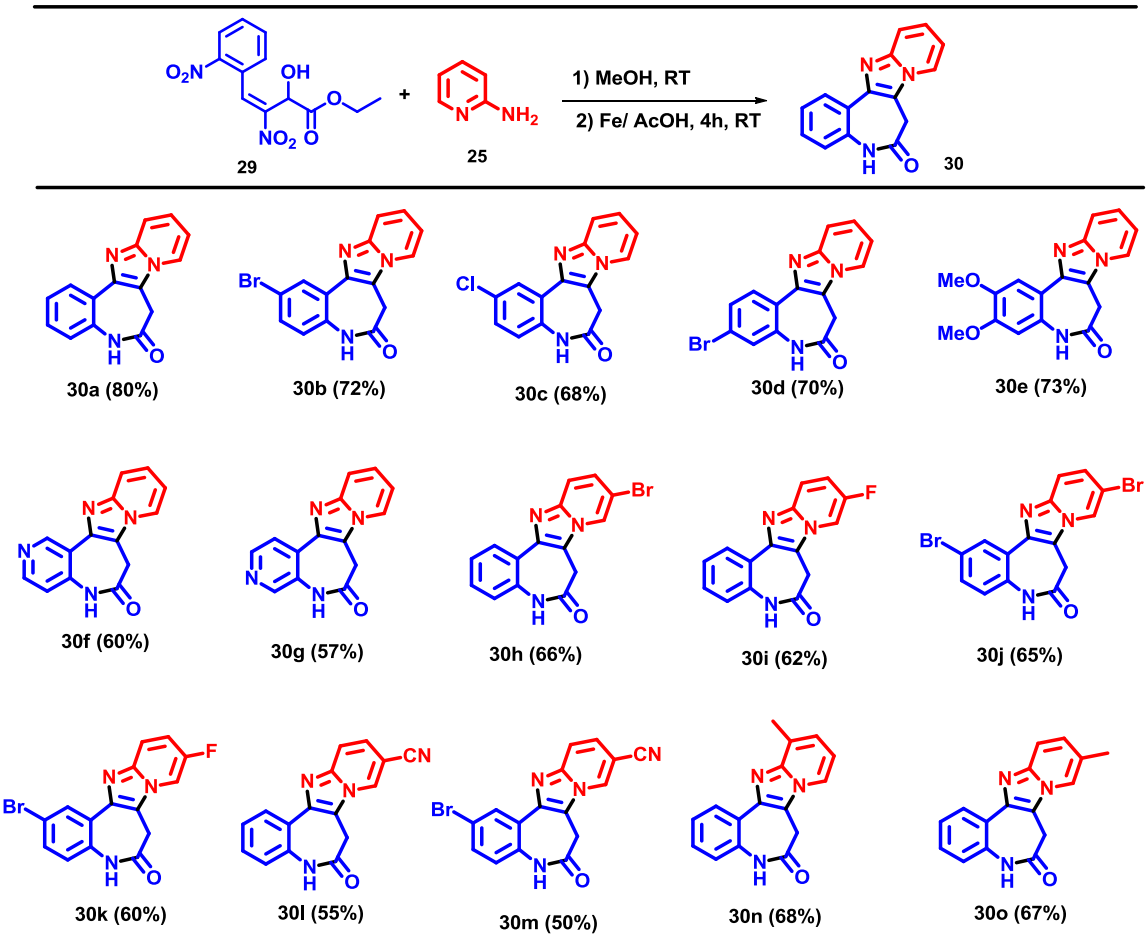

Scheme 5.4: synthetic scope of imidazopyridine[4,5-*d*]azepin-2-one derivatives

To understand the generality of this reaction we employed phenols and naphthols as a nucleophiles in scheme 5.5. Thus the reaction of 2-nitro MBH acetates (**29**) with phenol derivatives **31** in methanol was not shown promising results towards the formation of intermediate **32**. Then we treated the 2-nitro MBH acetates (**29**) with phenol in presence of cesium carbonate in different solvents like CH_2Cl_2, $CHCl_3$, THF, EtOH and 1,4-dioxane. The product was observed in good yield (78%) using $CHCl_3$ as a solvent in presence of cesium carbonate as a base at room temperature for 6 hrs followed by the treatment of resulting product (obtained after removal of THF) with Fe/AcOH at reflux for 4 hrs provide the resulting compound 5H-benzo[b]benzofuro[2,3-*d*]azepin-6(7H)-one (**33**). To examine the potentiality of this strategy we used a different phenol and napthaol derivatives as a nucleophiles and subjected them to this synthetic sequence to provide the desired benzofuro[2,3-*d*]azepin-6(7H)-one derivatives **(33)** (scheme 5.2.3) in 50-80% isolated yields. The 2-nitro MBH acetates bearing halo groups (**33b - 33d**) and without any substituents (**33a**) on their benzene ring gave good yields towards the corresponding

benzfuro[2,3-d]azepinones. Next, we studied the strategy of different phenol derivatives (33h–33i) towards the synthesis of corresponding benzfuroazepinones gave in moderate yields (~65%). The yields are pretty good (~80%) in napthaols as a nucleophiles to their corresponding azepinone derivatives.

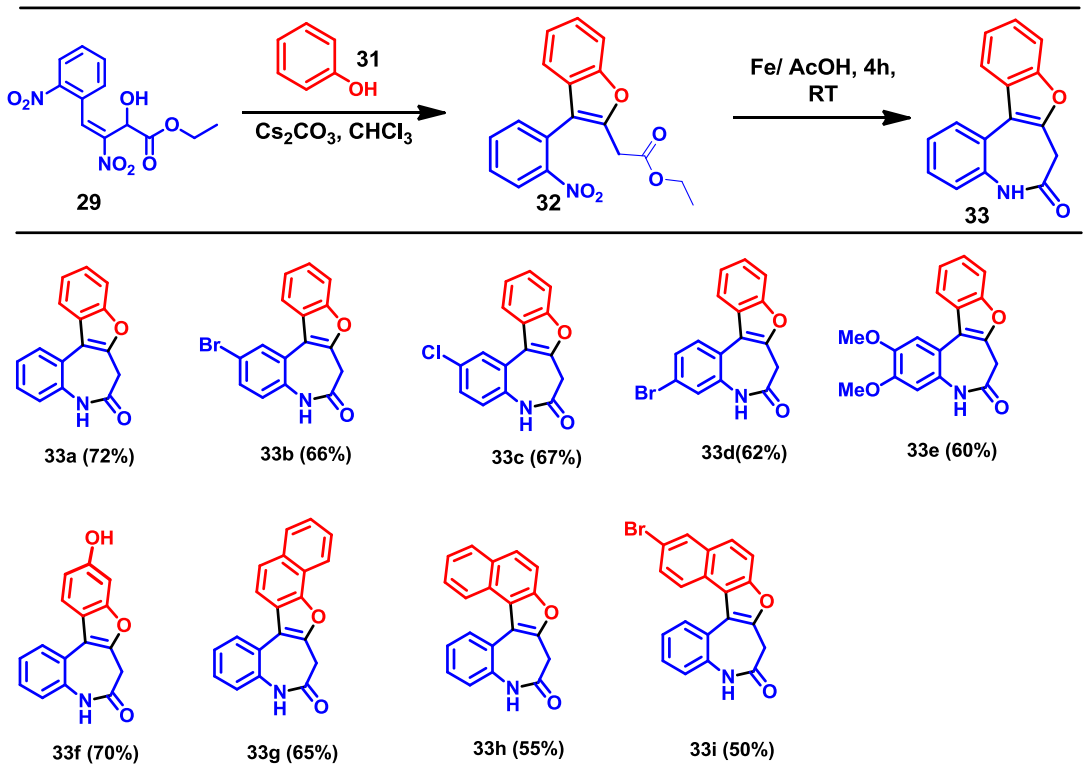

Scheme 5.5: synthetic scope of Benzfuro[2,3-*d*] azepin-2-one derivatives

5.3 Conclusions

In conclusion, we have developed an efficient method for the synthesis of functionalized imidazo[1,2-*a*]pyridine[4,5-*c*]quinoline-6-carboxylic esters from 2-nitro MBH acetates and 2-aminopyridines. The reaction involves a cascade Michael addition followed by aerobic oxidation forms glyoxalates and then intramolecular reductive cyclisation with iron metal generates three new carbon-Nitrogen bonds as α-β-δ cyclisation in good yields. Similarly, we reported the synthesis of imidazopyridine[4,5-*d*]azepinones and benzfuro[2,3-*d*]azepinones from MBH acetates by α-β-γ cyclisation in good yields. This reaction involves a cascade inter-intramolecular aza-Michael addition followed intramolecular reductive cyclisation.

5.4: Experimental procedure

ethyl pyrido[2',1':2,3]imidazo[4,5-c]quinoline-6-carboxylate (27a): To a solution of compound 24 (0.2 g, 0.5 mmol, 1.0 eqiv) in chloroform (10 mL) was added acetyl chloride (70 mg, 0.88 mmol, 1.5 eqiv) followed by the addition of pyridine (0.1 mL, 1.0 mmol, 2.0 eqiv) at 0 ^{o}C and the reaction mixture stirred for 12h at rt under oxygen balloon purging. The reaction mixture was quenched with water (20 mL) and extracted with chloroform (3 x 25 mL). The combined oraganic layers were dried over sodium sulphate and concentrated. The crude product was taken in methanol and acetic acid (1:1) (10 mL). To this reaction mixture was added iron (0.1 g) and the reaction mixture was stirred for 12 h at rt. The reaction mixture was quenched with saturated bicarbonate solution (20 mL) and extracted with ethyl acetate (3 x 25 mL). The combined organic layers were dried over sodium sulphate and concentrated. The crude product was purified by coloumn chromatography using 30% ethyl acetate in hexane gives compound 27a (50 mg, 34 %).

^{1}H NMR (300 MHz, DMSO-*d6*): δ 9.35 (d, 1H, *J*= 7.2 Hz), 8.69 (s, 1H), 8.28 (m, 1H), 8.02 (d, 1H, *J* = 9.0 Hz), 7.87 (m, 3H), 7.30 (d, *J* = 7.2 Hz, 1H), 4.61 (q, 2H, *J* = 7.2 Hz, 14.4 Hz), 1.47 (t, 3H, *J* = 7.2 Hz,).

LCMS: *m/z* calculated for $C_{17}H_{13}N_3O_2$: 291.12; Observed mass: 292.2 (M+1).

ethyl 9-bromopyrido[2',1':2,3]imidazo[4,5-c]quinoline-6-carboxylate (27b): yield: 40 mg; **^{1}H NMR** (400 MHz, $CDCl_3$): δ 9.72 (d, 1H, *J*= 7.2 Hz), 8.96 (d, 1H, *J*= 8.0 Hz) 8.43 (d, 1H, *J*= 8.0 Hz); 7.92 (m, 1H), 7.85 (m, 2H), 6.97(t, *J* = 7.2 Hz, 1H), 4.74 (q, 2H, *J* = 7.2 Hz, 14.4 Hz), 1.61 (t, 3H, *J* = 7.2 Hz).

LCMS: *m/z* calculated for $C_{17}H_{12}BrN_3O_2$: 368.1; Observed mass: 369.2, 371.2 (M+1, M+3).

5H-benzo[b]pyrido[1',2':1,2]imidazo[4,5-d]azepin-6(7H)-one (30a): To a solution of compound 29 (0.2 g, 0.59 mmol, 1.0 eqiv) in methanol was added 2-aminopyridine (65 mg, 0.71 mmol, 1.5 eqiv) and the reaction mixture stirred for 2h at rt under nitrogen. The reaction mixture was quenched with water (20 mL) and extracted with chloroform (3 x 25 mL). The combined oraganic layers were dried over sodium sulphate and concentrated. The crude product was taken in methanol and acetic acid (1:1) (10 mL). To this reaction mixture was added iron (0.1 g) and the reaction mixture was stirred for 12 h at rt. The reaction mixture was quenched with saturated bicarbonate solution (20 mL) and extracted with ethyl acetate (3 x 25 mL). The combined organic layers were dried over sodium sulphate and concentrated. The crude product was purified by coloumn chromatography using 50% ethyl acetate in hexane gives compound 30a (60 mg, 41 %).

^{1}H NMR (400 MHz, MeOD): δ 8.50 (d, 1H, *J*= 7.2 Hz), 8.04 (d, 1H, *J*= 8.0 Hz), 7.74 (d, 1H, *J*= 8.8 Hz), 7.40 (m, 4H), 7.28 (d, 1H, *J* = 8.0 Hz), 3.91 (s, 2H)

LCMS: *m/z* calculated for $C_{15}H_{11}N_3O$: 249.12; Observed mass: 250.2 (M+1).

REFERENCES

Akrami H, Mirjalili B F, Khoobi M, Nadri H, Moradi A, Sakhteman A, Emami S, Foroumadi A, Shafiee A, Indolinone-based acetylcholinesterase inhibitors: Synthesis, biologicalactivity and molecular modeling, Eur. J. Med.Chem. 84 (**2014**) 375-381.

Alavijeh, M. S.; Chishty, M.; Qaiser, M. Z. and Palmer, A. M. Drug metabolism and pharmacokinetics, the blood–brain barrier, and central nervous system drug discovery, NeuroRx,**2005**, 2, 554;

Albert, A.; Gledhill, W. Improved syntheses of aminoacridines. IV. Substituted 9-aminoacridines. J. Soc. Chem. Ind. **1945,** 64, 169.

Alipour M, Khoobi M, Moradi A, Nadri H, Moghadam F H, Emami S, Hasanpour Z, Foroumadi A, Shafiee A, Synthesis and anti-cholinesterase activity of new 7-hydroxycoumarin derivatives, Eur. J. Med. Chem. 82 (**2014**) 536-544.

Alp N J, Channon K M, Regulation of endothelial nitric oxide synthase by tetrahydrobiopterin in vascular disease, Arterioscler. Thromb. Vasc. Biol. 24 (**2004**) 413-420.

Alpan A. S., Parlar, S., Carlino, L., Tarikogullari, A. H., Alptuzun, V. And Gunes, H. S. Bioorg. Med. Chem., **2013**, 21, 4928.

Alzheimer A. Über einen eigenartigen schweren Erkrankungsprozeβ der Hirnrincle. Neurol Central.**1906**, 25, 1134.

Alzheimer's Association. 2015 Alzheimer's disease facts and figures. www.alz.org. Accessed on March 26th 2015.

Alzheimer's disease Education & Referral (ADEAR) Center. Alzheimer's disease Fact Sheet. Publication. National Institute on Aging, **2008.**

Alzheimer's disease International, World Alzheimer report 2011, p. 1.

Alzheimer's Association **2010**. Web. 01 Oct. 2010. <http://alz.org>.

Anand Kumar Pandey, Rashmi Sharma, Awantika Singh, Sanjeev Shukla, Kumkum Srivastava, Sunil K. Puri, Brijesh Kumar and Prem M. S. Chauhan; RSC Adv., **2014**, 4, 26757.

Anwar S., Huang, W.-Y.; Chen, C.-H.; Cheng, Y.-S. andChen, K. Chem. Eur. J., **2013**, 19, 4344.

APA Practice Guidelines. Treatment of patients with Alzheimer's disease and other dementias. **2007**.

Asadipour. A, Alipour. M, Jafari. M, Khoobi. M, Emami. S, Nadri. H, Sakhteman. A, Moradi. A, Sheibani. V, Moghadam. F. H, Novel coumarin-3-carboxamides bearing Nbenzylpiperidine moiety as potent acetylcholinesterase inhibitors, Eur. J. Med. Chem. 70 (**2013**) 623-630.

Atwell G J, Baguley B C and Denny W A, J. Med. Chem., **1989**, 32, 396.

Audia, J. E.; Hyslop, P. A.; Nissen, J. S.; Thompson, R. C.; Tung, J. S.; Tanner, L. I Patent WO 00/19210, 2000.

Bagdi A K and Hajra A, Chem. Rec, **2016**, 16, 4, 1868-1885

Bagdi, A. K.; Mitra, S.; Ghosh, M.; Hajra, A. Org. Biomol. Chem. **2015**, 13, 3314.

Bagdi, A. K.; Rahman, M.; Santra, S.; Majee, A.; Hajra, A. Adv. Synth. Catal. **2013**, 355, 1741.

Balasubramanian, M.; Keay, J. G. In Comprehensive Heterocyclic Chemistry II; Katritzky, A. R., Rees, C. W., Scriven, E. F. V., Eds.; Pergamon: Oxford, **1996**; Vol. 5, Chapter 5.06, p 245.

Barnham K J, Masters C L, Bush A I, Neurodegenerative diseases and oxidative stress, Nat. Rev. Drug Discov. 3 (**2004**) 205-214.

Bartzokis G, Lu P, Mintz J. Human brain myelination and amyloid beta deposition in Alzheimer's disease: A short report. Alzheimer's & dementia. **2007**, 3, 122.

Basavaiah, D.; Dharma Rao, P.; Suguna, H. R. Tetrahedron **1996**, 52, 8001.

Basha S J, Kumar P B, Mohan P, Kasi Viswanath K, Subba Rao D, Siddhartha E, Manidhar D M, Dinakara Rao A, Ramakrishna V, Damu A G; Eur. J. Med. Chem 107 (**2016**) 219-232.

Bax B D, Chan P F, Eggleston D S, Fosberry A, Gentry D R, Gorrec F, Giordano L, Hann M M, Hennessy A, Hibbs H, Huang J, Jones E, Jones J, Brown K K, Lewis C J, May E W, Saunders M R, Singh O, Spitzfaden C E, Shen C, Shillings A, Theobald A J, Wohlkonig A, Pearson N D and Gwynn M N, Nature, **2010**, 466, 935.

Baylis, A. B.; Hillman, M. E. D. German Patent 2155113, 1972; Chem. Abstr. **1972**, 77, 34174.

Bencharit B, Morton C L, Hyatt J L, Kuhn P, Danks, M K, Potter P M, Redinbo M R, Crystal structure of human carboxylesterase 1 complexed with the Alzheimer's

drug tacrine: from binding promiscuity to selective inhibition, Chem. Biol. 10 (**2003**) 341-349.

Bhushan, S.; Walko, C. M. Ixabepilone. Ann. Pharmacother. **2008**, 42, 1252–1261.

Biewenga G P, Haenen G R, Bast A, The pharmacology of the antioxidant lipoic acid, Gen. Pharmacol. 29 (**1997**) 315-331

Boganyi, Borbala and Kaman, Judit, J. Het. Chem, 46(1), 33-38; **2009**.

Bradbury R H, Allott C P, Dennis M, Girdwood J A, Kenny P W, Major J S, Oldham A A, Ratcliffe A H, Rivett J E, Roberts D A and Robins P J, J. Med. Chem., **1993**, 36, 1245.

Cagir A, Eisenhauer B M, Gao R, Thomas S J and Hecht S M, Bioorg. Med. Chem., **2004**, 12, 6287.

Camps P, Formosa X, Galdeano C, Gomez T, Munoz-Torrero D, Ramirez L, Viayna E, Gomez E, Isambert N, Lavilla R, Badia A, Clos M V, Bartolini M, Mancini F, Andrisano V, Bidon-Chanal A, Huertas O, Dafni T, Luque F J, Tacrine-based dual binding site acetylcholinesterase inhibitors as potential disease-modifying anti-Alzheimer drug candidates, Chem. Biol. Interact.187 (**2010**) 411-415.

Camps P, Gomez E, Munoz-Torrero, Badia A, Vivas N M, Barril X, Orozco M and Luque F J, J. Med. Chem., **2001**, 44, 4733.

Cao C. L., Zhou, Y. Y., Zhou, J., Sun, X. L., Tang, Y., Li, Y. X., Li, G. Y. and Sun, J. Chem. Eur. J., **2009**, 15, 11384.

Carey, F. A.; Sundberg, R. J. Advanced Organic Chemistry; Part A & B, 3rd ed.; Plenum: New York, **1990**.

Castro. A, Martinez. A, Peripheral and dual binding site acetylcholinesterase inhibitors: implications in treatment of Alzheimer's disease, Mini Rev. Med. Chem. 1 (**2001**) 267-272.

Chaires J B, Ren J, Henary M, Zegrocka O, Bishop G R and Strekowski L, J. Am. Chem. Soc., **2003**, 125, 7272.

Chao X, He X, Yang Y, Zhou X, Jin M, Liu S, Cheng Z, Liu P, Wang Y, Yu J, Design, synthesis and pharmacological evaluation of novel tacrine–caffeic acid hybrids as multitargeted compounds against Alzheimer's disease, Bioorg. Med. Chem. Lett. 22 (**2012**) 6498-6502.

Chazot PL. The NMDAR NR2B subunit: a valid therapeutic target for multiple CNS pathologies. Curr. Med. Chem. **2004**, 11, 389.

Ciganek, E. Organic Reactions; Paquette, L. A., Ed.; Wiley: New York, **1997**, 51, 201.

Clark D. E., Rapid calculation of polar molecular surface area and its application to the prediction of transport phenomena. 2. Prediction of blood–brain barrier penetration, J. Pharm. Sci., **1999**, 88, 815;

Clements-Jewery S.; Danswan, G.; Gardner, C. R.; Matharu, S. S.; Murdoch, R.; Tully, W. R. and Westwood, R. J. Med. Chem., **1988**, 31, 1220.

Comprehensive Asymmetric Catalysis; Jacobsen, E. N., Pfaltz, A., Yamamoto, H., Eds; Springer: Berlin, **1999**, Vols. 1-3.

Comprehensive Organic Synthesis; Trost, B. M., Fleming, I., Eds; Pergamon: New York, **1991**, Vols. 1-9.

Current Trends in Organic Synthesis; Scolastico, C., Nocotra, F., Eds; Plenum: New York, **1999**.

D€omling, A.; Hamon, L. PatentWO01/25212 A2, 2002.

da Costa J S, Lopes J P B, Russowsky D, Petzhold C L, de Amorim Borges A C, Ceschi M A, Konrath E, Batassini C, Lunardi P S, Gonçalves C A S, Synthesis of tacrine-lophine hybrids via one-pot four component reaction and biological evaluation as acetyl-and butyrylcholinesterase inhibitors, Eur. J. Med. Chem. 62 (**2013**) 556-563.

Davis, K. L.; Thal, L. J.; Gamzu, E. R.; Davis, C. S.; Woolson, R. F.; Gracon, S. I.; Drachman, D. A.; Schneider, L. S.; Whitehouse, P. J.; Hoover, T. M.; et al. A double-blind, placebo-controlled multicenter study of tacrine for Alzheimer's disease. The Tacrine Collaborative Study Group. N. Engl. J. Med. **1992,** 327, 1253.

de Aquino, R. A., Modolo, L. V., Alves, R. B., de Fatima, A., Curr. Drug Targets 14 (**2013**) 378-397.

Deb I., Shanbhag, P.; Mobin, S.M.; Namboothiri, I. N. N. Eur. J. Org. Chem. **2009**, 4091.

Deb, I,; Dadwal, M.; Mobin, S. M.; Namboothiri, I. N. N. Org. Lett. **2006**, 8, 1201.

Deli, M. A.; Abraham, C. S.; Kataoka, Y. and Niwa, M. Permeability studies on in vitro blood–brain barrier models: physiology, pathology, and pharmacology, Cell. Mol. Neurobiol., **2005**, 25, 59.

Desai, K. G. and Desai, K. R. Bioorg. Med. Chem., **2006**, 14, 8271;

Di Braccio M.; Grossi, G.; Signorello, M. G.; Leoncini, G.; Cichero, E.; Fossa, P.; Alfei, S. and Damonte, G. Eur. J. Med. Chem., **2013**, 62, 564.

Dominguez, J. L., Fernandez-Nieto, F., Castro, M., Catto, M., Paleo, M. R, Porto, S., Sardina, F. J., Brea, J. M., Carotti, A., Villaverde, M. C., Sussman, F., J. Chem. Inf. Model, 55 (**2015)** 135–148.

Dominic M. Walsh, Dennis J. Selkoe; Neuron, 44 (**2004**), 181-193.

Dong J, Atwood C S, Anderson V E, Siedlak S L, Smith M A, Perry G, Carey P R, Metal binding and oxidation of amyloid-β within isolated senile plaque cores: Raman microscopic evidence, Biochemistry 42 (**2003**) 2768-2773.

Donovan, D.; Vahdat, L. T. Oncology **2008**, 22, 408−416.

Drewes, S. E.; Roos, G. H. P. Tetrahedron **1988**, 44, 4653.

Dvey D, Erhardt P W, Lumma, Wiggins J, Sullivan M, Pang D and Cantor E, J. Med. Chem., **1987**, **30**, 1337.

Edmont D, Rocher R, Plisson C and Chenault J, Bioorg. Med. Chem. Lett., **2000**, 10, 1831.

Eicher T and Hauptmann S, The Chemistry of Heterocycles, Wiley-VCH, Weinheim, 2nd edn, **2003**, p. 316.

El-Gazzar A B A, Hafez H N and Nawwar G A M, Eur. J. Med. Chem., **2009**, 44, 1427;

Ellman, G. L., Courtney, K. D., Andres jr, V. and Featherstone, R. M. BiochemPharmacol, 7 (**1961**) 88.

Elslager E, Tendick F and Werbel L, J. Med. Chem., **1969**, 12, 600.

Enguehard-Gueiffier C. and Gueiffier, A. Mini-Rev. Med. Chem., **2007**, 7, 888.

Fang L, Appenroth D, Decker M, Kiehntopf M, Roegler C, Deufel T, Fleck C, Peng S, Zhang Y, Lehmann J, Synthesis and biological evaluation of NOdonor-tacrine hybrids as hepatoprotective anti-Alzheimer drug candidates, J. Med. Chem. 51 (**2008**) 713-716.

Feng R. M., Assessment of blood-brain barrier penetration: in silico, in vitro and in vivo, Curr. Drug Metab.,**2002**, 3, 647;

Fernández-Bachiller M I, Pérez C, Campillo N E, Páez J A, González-Muñoz G C, Usán P, García-Palomero E, López M G, Villarroya M, García A G, Tacrine–melatonin hybrids as multifunctional agents for Alzheimer's disease, with cholinergic, antioxidant, and neuroprotective properties, Chem. Med. Chem. 4 (**2009**) 828-841.

Fernández-Bachiller M I, Pérez C, Monjas L, Rademann J and Rodríguez-Franco M I, J. Med. Chem., **2012**, 55 (3), pp 1303–1317.

Fernández-Bachiller, Pérez C, González-Munoz G C, Conde S, López M G, Villarroya M, García A G, Rodríguez-Franco, Novel tacrine− 8-hydroxyquinoline hybrids as multifunctional agents for the treatment of Alzheimer's disease, with neuroprotective, cholinergic, antioxidant, and copper-complexing properties, J. Med. Chem. 53 (**2010**) 4927- 4937.

Fookes C J R, Pham T Q, Mattner F, Greguric I, Loch C, Liu X, Berghofer P, Shepherd R, Gregoire M C and Katsifis A, J. Med. Chem., **2008**, 51, 3700.

Forstl H, Kruz A. Clinical features of Alzheimer's disease. European Archives of Psychiatry and Clinical Neuroscience. **1999**, 249, 288.

Francis PT, Palmer AM, Snape M, Wilcock GK. The cholinergic hypothesis of Alzheimer's disease: A review of progress. Journal of Neurology, Neurosurgery and Psychiatry. **1999**, 66, 137.

Friedel-Crafts Chemistry; Olah, G. A., Ed; Wiley: New York, **1973**.

Fuchs K, Romig M, Mendla K, Briem H and Fechteler K, WO2002014313. Chem. Abstr., 2002, **136**, 183824r.

Furstner, A. Angew. Chem., Int. Ed. **2000**, 99, 3012.

Furstner, A. Synthesis **1989**, 571.

Fylaktakidou K C, Hadjipavlou-Litina D J, Litinas K E, Nicolaides D N, Natural andsynthetic coumarin derivatives with anti-inflammatory/antioxidant activities, Curr. Pharm. Des. 10 (**2004**) 3813-3833.

Gemma S, Gabellieri E, Huleatt P, Fattorusso C, Borriello M, Catalanotti B, Butini S, De Angelis M, Novellino E, Nacci V, Discovery of huperzine A-tacrine hybrids as potent inhibitors of human cholinesterases targeting their midgorge recognition sites, J. Med. Chem. 49 (**2006**) 3421-3425.

George, P. G.; Rossey, G.; Sevrin, M.; Arbilla, S.; Depoortere, H.; Wick, A. E. L. E. R. S. Monograph Ser. **1993**, 8, 49.

George, P.; Rossey, G.; Depoortere, H.; Allen, J.; Wick, A. Actual. Chim. Ther. **1991**, 18, 215.

Ghanei-Nasab S, Khoobi M, Hadizadeh D, Marjani, Moradi A, Nadri H, Emami S, Foroumadi A, Shafiee A, Synthesis and anticholinesterase activity of coumarin-3-carboxamidesbearing tryptamine moiety, Eur. J. Med. Chem.121 (**2016**) 40-46.

Ghose, A. K., Herbertz, T., Hudkins, R. L., Dorsey, B. D. and Mallamo, P. J. Knowledge-Based, Central Nervous System (CNS) Lead Selection and Lead Optimization for CNS Drug Discovery, ACS Chem. Neurosci., **2012**, 3, 50.

Ghosh, M.; Naskar, A.; Mitra, S.; Hajra, A. Eur. J. Org. Chem. **2015**, 715.

Giacobini, E., Neurochem. Int. 32 (**1998**) 413-419.

Gopi, E. and Namboothiri, I. N. N. J. Org. Chem., **2014**, 79, 7468.

Gopi, E., Kumar, T., Menna-Barreto, R. F. S., Valenca, W. O., Silva Junior, E. N. D. and Namboothiri, I. N. N. Org. Biomol. Chem., **2015**, 13, 9862.

Greig N H, Utsuki T, Ingram D K, Wang Y, Pepeu G, Scali C, Yu Q S, Mamczarz J, Holloway H W, Giordano Y, Selective butyrylcholinesterase inhibition elevates brain acetylcholine, augments learning and lowers Alzheimer β-amyloid peptide in rodent, Proc. Natl. Acad. Sci. U. S. A. 102 (**2005**) 17213-17218.

Grubbs, R. H.; Pine, S. H. Comprehensive Organic Synthesis; Trost, B. M., Ed.; Pergamon: New York, **1991**, 5, Chapter 9.3.

Gussio R, Zaharevitz D W, McGrath C F, Pattabiraman N, Kellogg G E, Schultz C, Link A, Kunick C, Leost M, Meijer L, Sausville E A, Anti-Cancer Drug Des. **2000**, 15, 53.

Hajra A, Bagdi A K, Santra S and Monir K, Chem. Commun., **2015**, 51, 1555-1575.

Halama A, Jirman J, Bouskova O, Gibala P and Jarrah K, Org. Process Res. Dev., **2010**, 14, 425.

Hansen, Richard A. et al. "Efficacy and Safety of Donepezil, Galantamine, and Rivastigmine for the Treatment of Alzheimer's disease: A Systematic Review and Meta-analysis." Clinical Interventions in Aging. **2008**, 3, 211.

Hanson, S. M.; Morlock, E. V.; Satyshur, K. A. and Czajkowski, C. J. Med. Chem., **2008**, 51, 7243;

Harrison, T. S. and G. M. Keating, CNS Drugs, **2005**, 19, 65.

Hassner, A.; Stumer, C. Organic Synthesis Based on Name Reactions and Unnamed Reactions; Tetrahedron Organic Chemistry Series; Baldwin, J. E., Magnus, P. D., Eds.; Pergamon: New York, **1998**; Vol. 11.

Heathcock, C. H. The Aldol Addition Reaction in Asymmetric Synthesis; Morrison, J. D., Ed.; Academic Press: New York, **1984**; Vol. 3, Part B, p 111.

Heilbronn, E. Inhibition of cholinesterases by tetrahydroaminacrin. Acta Chem. Scand. **1961,** 15, 1386.

Helmchen, G.; Karge, R.; Weetman, J. Modern Synthetic Methods; Scheffold, R., Ed.; Springer, Berlin, **1986**, 4, 261.

Holmes C, Boche D, Wilkinson D, Yadegarfar G, Hopkins V, Bayer A, et al. Long-term effects of Abeta42 immunisation in Alzheimer's disease: follow-up of a randomised, placebo-controlled phase I trial. The Lancet. **2008**, 372, 216.

Humphries A C, Gancia E, Gilligan M T, Goodacre S, Hallett D, Marchant K J and Thomas S R, Bioorg. Med. Chem. Lett., **2006**, 16, 1518.

Ismaili L, Refouvelet B, Benchekroun M, Brogi S, Brindisi M, Gemma S, Campiani G, Filipic S, Agbaba D, Esteban G, Unzeta M, Nikolic K, Butini S, Marco-Contelles J, Multitarget compounds bearing tacrine- and donepezil-like structural and functional motifs for the potential treatment of Alzheimer's disease, Prog. Neurobiol.

Jameel E, Meena P, Maqbool M, Kumar J, Ahmed W, Mumtazuddin S, Tiwari M, Hoda N, Jayaram B; European Journal of Medicinal Chemistry 136 (**2017**) 36-51.

Jansen M, Dannhardt G. Antagonists and agonists at the glycine site of the NMDAR for therapeutic interventions. Eur. J. Med. Chem. **2003**, 38, 661.

Jantzi M. Use of medications for management of Alzheimer's disease in Ontario's home care population. **2010**.

Jones E. D., Vandegraaff, N., Le, G., Choi, N., Issa, W., Macfarlane, K., Thienthong, N., Winfield, L. J., Coates, J. A. V., Lu, l., Li, X., Feng, X., Yu, C., Rhodes, D. I. and Deadman, J. J. Bioorg. Med. Chem. Lett., **2010**, 20, 5913.

Joule J A and Mills K, Heterocyclic Chemistry, Wiley, New York, 5th edn, 2010.

Kaila N, Janz K, DeBernardo S, Bedard P W, Camphausen R T, Tam S, Tsao D H H, Keith J C, Nickerson-Nutter, Shilling A,Young-Sciame and Wang Q, J. Med. Chem., **2007**, 50, 21.

Kamal, A.; Reddy, J .S.; Ramaiah, M. J.; Dastagiri, D.; Bharathi, E. V.; Sagar, M. V. P.; Pushpavalli, S. N. C. V. L; Ray, P.; Pal-Bhadra, M. Med. Chem. Commun. **2010**, 1, 355.

Karjala, G.; Chan, Q.; Manzo, E.; Andersen, R. J.; Roberge, M. Ceratamines, Cancer Res. **2005**, 65, 3040–3043.

Kazimierczuk Z., Andrzejewska, M.; Kaustova, J. and Klimesova, V. Eur. J.Med. Chem.,**2005**, 40, 203.

Kelder J., Grootenhuis, P. D. J.; Bayada, D. M.; Delbressine, L. P. C. and Ploemen, J.-P.; Polar molecular surface as a dominating determinant for oral absorption and brain penetration of drugs, Pharm. Res., **1999**, 16, 1514.

Kemp JA, McKernan RM. NMDAR pathways as drug targets. Nature Neurosci. **2002**, 5, 1039.

Khoobi M, Ghanoni F, Nadri H, Moradi A, Hamedani M P, Moghadam F H, Emami S, Vosooghi M, Zadmard R, Foroumadi A, New tetracyclic tacrine analogs containing pyrano [2, 3-c] pyrazole: efficient synthesis, biological assessment and docking simulation study, Eur. J. Med. Chem. 89 (**2015**) 296-303.

Kim J I, Shin I S, Kim H and Lee J K, J. Am. Chem. Soc., **2005**, 127, 1614.

Kim, O.; Jeong, Y.; Lee, H.; Hong, S.-S.; Hong, S. J. Med. Chem. **2011**, 54, 2455.

Ko T C, Hour M J, Lien J C, Teng C M, Lee K H, Kuo S C and Huang L J, Bioorg. Med. Chem. Lett., **2001**, 11, 279.

Kostova I, Synthetic and natural coumarins as cytotoxic agents, Curr. Med. Chem. Anticancer Agents 5 (**2005**) 29-46.

Krishnamurthy M, Gooch B D and Beal P A, Org. Lett., **2004**, 6, 63.

Kuan H., Reddy, R. J. and Chen, K. Tetrahedron, **2010**, 66, 9875.

Kuiper M A, Visser J J, Bergmans P L, Scheltens P, Wolters E C, Decreased cerebrospinal fluid nitrate levels in Parkinson's disease, Alzheimer's disease and multiple system atrophy patients, J. Neurol. Sci. 121 (**1994**) 46-49.

Kumar J, Meena P, Singh A, Jameel E, Maqbool M, Mobashir M, Shandilya A, Tiwari M, Hoda N, Jayaram B; European Journal of Medicinal Chemistry 119 (**2016**) 260-277.

Kumar T., S. M. Mobin and I. N. N. Namboothiri, Tetrahedron, **2013**, 69, 4964.

Kumar, T.; Verma, D.; Menna-Barreto, R. F. S.; Valenca, W. O.; da Silva Junior, E. N. and Namboothiri, I. N. N. Org. Biomol. Chem., **2015**, 13, 1996.

Kunick C, Lauenroth K, Wieking K, Xie X, Schultz C E, Gussio R, Zaharevitz D, Leost M, Meijer L, Weber A, Jorgensen F S, Lemcke T, J. Med. Chem. **2004**, 47, 22.

Kypta R. M., Expert Opin. Ther. Pat., **2005**, 15, 1315.

Lanctot, Krista L., Ryan D. Rajaram, and Nathan Herrmann. "Therapy for Alzheimer's disease: How Effective Are Current Treatments? Therapeutic Advances in Neurological Disorders **2009**, 2, 163.

Langer, P. Angew. Chem., Int. Ed.**2000**, 39, 3049.

Larock, R. C. Comprehensive Organic Transformations: a guide to functional group transformations; VCH: New York, **1989**.

Lee H P, Zhu X, Casadesus G, Castellani G J, Nunomura A, Smith M A, Lee H G, Perry G, Antioxidant approaches for the treatment of Alzheimer's disease, Expert Rev. Neurother. 10 (**2010**) 1201-1208.

Lenz G. R., Technical problems in getting results, in From data to drugs: strategies for bene□ting from the new drug discovery technologies, ed. Haberman, A. B., Lenz, G. R., and.Vaccaro, D. E. Scrip Reports, London, **1999**, 95.

Leong S W, Abas F, Lam K W, Shaari K, Lajis N H, Bioorg. Med. Chem. 24 (**2016**) 3742-3751

Lin M T, Beal M F, Mitochondrial dysfunction and oxidative stress in neurodegenerative diseases, Nature 443 (**2006**) 787-795.

Lipinski CA, Lombardo F, Dominy BW, Feeney PJ (2001) Experimental and computational approaches to estimate solubility and permeability in drug discovery and development settings. AdvaDrug Del Rev 46 (**2001**), 3–26.

Lippincott, Williams, and Wilkins. "Alzheimer Disease Drugs." Nursing 2010 Drug Handbook. Philadelphia: Wolters Kluwer Health, **2010**. 546.

Lowenthal, Birnbaum H, Vitamin K and coumarin anticoagulants: dependence of anticoagulant effect on inhibition of vitamin K transport, Science 164 (**1969**) 181-183.

Loy C and Schneider L. "Galantamine for Alzheimer's disease and mild cognitive impairment". Cochrane Database of Systematic Reviews**. 2006.**

Luo W, Wang T, Hong C, Yang YC, Chen Y, Cen J, Xie SQ, Wang CJ; European Journal of Medicinal Chemistry 122 (**2016**) 17-26.

Maguire M P, Sheets K R, Mc Vety K, Spada A P and Zilberstein, J. Med. Chem., **1994**, 37, 2129.

Mahdavi M, Saeedi M, Gholamnia L, Jeddi S A B, Sabourian R, Shafiee A, Foroumadi A, Akbarzadeh T, Synthesis of novel tacrine analogs as acetylcholinesterase inhibitors, J. Heterocyclic Chem. **2016**

Mahrwald, R. Chem. Rev. **1999**, 99, 1095.

Mane, V.; Kumar, T.; Pradhan, S.; Katiyar, S. and Namboothiri, I. N. N. RSC Adv.**2015**, 5, 69990.

March, J. Advanced Organic Chemistry, 4th ed.; Wiley: New York, **1992**.

Margiotta N., Ostuni, R.; Ranaldo, R.; Denora, N.; Laquintana, V.; Trapani, G.; Liso, G. and Natile, G. J. Med. Chem., **2007**, 50, 1019

Maryanoff, B. E.; Rietz, A. B. Chem. Rev. **1989**, 89, 863.

Masaki M., Yamakawa, T.; Nomura, Y. and Matsukura, H. US Pat., US5576341, **1996**;

McLachlan. D. C, Kruck. T, Kalow. W, Andrews. D, Dalton. A, Bell. M, Smith. W, Intramuscular desferrioxamine in patients with Alzheimer's disease, Lancet 337 (**1991**) 1304-1308.

Meijere, A. de; Meyer, F. Angew. Chem., Int. Ed. Engl. **1994**, 33, 2379.

Messer Jr, W. S.; Rajeswaran, W. G.; Cao, Y.; Zhang, H. J.; el-Assadi, A. A.; Dockery, C.; Liske, J.; O'Brien, J.; Williams, F. E.; Huang, X. P.; Wroblewski, M. E.; Nagy, P. I. and Peseckis, S. M. Pharm. Acta Helv, **2000**, 74, 135.

Minarini, A., Milelli, A., Simoni, E., Rosini, M., Bolognesi, M. L., Marchetti, C., Tumiatti, V. Curr. Top. Med. Chem. 13 (**2013**) 1771-1786.

Mishra, S.; Monir, K.; Mitra, S.; Hajra, A. Org. Lett. **2014**, 16, 6084.

Miyaura, N.; Suzuki, A. Chem. Rev. **1995**, 95, 2457.

Möller HJ. Graeber MB. The case described by Alois Alzheimer 1911. Eur. Arch Psychiatrry Clin Neurosci. **1998**, 248, 111.

Monir, K.; Bagdi, A. K.; Ghosh, M.; Hajra, A. J. Org. Chem. **2015**, 80, 1332.

Monir, K.; Bagdi, A. K.; Ghosh, M.; Hajra, A. Org. Lett. **2014**, 16, 4630.

Monir, K.; Bagdi, A. K.; Mishra, S.; Majee, A.; Hajra, A. Adv. Synth. Catal. **2014**, 356, 1105.

Monti J. M., Warren Spence, D.; Pandi-Perumal, S. R.; Langer, S. Z. and Hardeland, R. Clin. Med.: Ther.**2009**, 1, 123.

Monti, J. M.; Warren, S. D.; Pandi-Perumal, S. R.; Langer, S. Z.; Hardeland, R. Clin. Med.: Ther. **2009**, 1, 123.

Morita K.; Suzuki, K. and Hirose, H. Bull. Chem. Soc. Jpn., **1968**, 41, 2815;

Muñoz-Ruiz P, Rubio L, García-Palomero, Dorronsoro I, del Monte-Millán, Valenzuela R, Usán P, de Austria C, Bartolini M, Andrisano V, Bidon-Chanal, Orozco M, Luque F J, Medina M, Martínez A, Design, synthesis, and biological evaluation of dual binding site acetylcholinesterase inhibitors: new disease-modifying agents for Alzheimer's disease, J. Med. Chem. 48 (**2005**) 7223-7233.

Nair D. K., Mobin, S. M. and Namboothiri, I. N. N. Org. Lett., **2012**, 14, 4580.

Nair D. K., Mobin, S. M. and Namboothiri, I. N. N. Tetrahedron Lett, **2012**, 53, 3349.

Najafi Z, Saeedi M, Mahdavi M, Sabourian R, Khanavi M, Tehrani M B, Moghadam F H, Edraki N, Karimpor-Razkenari, Sharifzadeh M, Design and synthesis of novel anti-Alzheimer's agents: acridine-chromenone and quinoline-chromenone hybrids, Bioorg. Chem. 67 (**2016**) 84-94.

National Institute for Health and Clinical Excellence. Quick Reference Guide: Dementia. London, UK.

Nunomura, A., Castellani, R. J., Zhu, X., Moreira, P. I., Perry, G., Smith, A. M., J. Neuropathol. Exp. Neurol. 65 (**2006**) 631-641.

Olah, G. A.; Krishnmurti, R.; Prakash, G. K. S. Comprehensive Organic Synthesis; Trost, B. M., Fleming, I., Eds.; Pergamon: New York **1990**, 3, 293 and references cited therein.

Ong. E B B, Watanabe N, Saito A, Futamura Y, El Galil K H A, Koito A, Najimudin N, Osada. H, Vipirinin, a coumarin-based HIV-1 Vpr inhibitor, interacts with a hydrophobic region of Vpr, J. Biol. Chem. 286.14056-14049 (**2011**).

Oppolzer, W. Angew. Chem., Int. Ed. Engl. **1984**, 23, 876.

Packer L, Witt E H, Tritschler H J, Alpha-lipoic acid as a biological antioxidant, Free Radic. Biol. Med. 19 (**1995**) 227-250.

Pajouhesh H. and Lenz, G. R. Medicinal chemical properties of successful central nervous system drugs, NeuroRx, **2005**, 2, 541.

Pericherla K, Kaswan P, Pandey K and Kumar A, Synthesis **2015**, 47, 887–912.

Perry E K, Blessed G, Tomlinson B, Changes in brain cholinesterases insenile dementia of Alzheimer type, Neuropathol. Appl. Neurobiol. 4 (**1978**) 273-277.

Perry G, Moreira P I, Santos M S, Oliveira C R, Shenk J C, Nunomura A, Smith M A, Zhu X, Alzheimer disease and the role of free radicals in the pathogenesis of the disease, CNS Neurol. Disord. Drug Targets. 7 (**2008**) 3-10.

Piazzi, L., Rampa, A., Bisi, A., Gobbi, S., Belluti, F., Cavalli, A., Bartolini, M., Andrisano, V., Valenti, P., Recanatini, M., J. Med. Chem. 46 (**2003)** 2279-2282.

Pourshojaei Y, Gouranourimi A, Hekmat S, Asadipour A, Rahmani-Nezhad S, Moradi A, Nadri H, Moghadam F H, Emami S, Foroumadi A, Design, synthesis and anticholinesterase activity of novel benzylidenechroman-4-ones bearing cyclic amine side chain, Eur. J. Med. Chem. 97 (**2015**) 181-189.

Prince, M., Bryce, R., Albanese, E., Wimo, A., Ribeiro, W., Ferri, C. P. The global prevalence of dementia: A systematic review and metaanalysis. Alzheimer's Dementia,**(2013),** 9, 63–75.

Puttaraju K. B.; Shivashankar, K.; Mahendra, C. M.; Rasal, V. P.; Venkata Vivek, P. N.; Rai, K. and Chanu, M. B. Eur. J. Med. Chem. **2013**, 69, 316.

Raschetti R, Albanese E, Vanacore N, Maggini M. Cholinesterase inhibitors in mild cognitive impairment: a systematic review of randomised trials. PLoS Med. **2007,** 4, 338.

Rastogi N.; Namboothiri, I. N. N.; Cojocaru, M. Tetrahedron Lett. **2004**, 45, 4745.

Recanatini M, Cavalli A, Belluti F, Piazzi L, Rampa A, Bisi A, Gobbi S, Valenti P, Andrisano V, Bartolini M, SAR of 9-amino-1, 2, 3, 4-tetrahydroacridine-based acetylcholinesterase inhibitors: synthesis, enzyme inhibitory activity, QSAR, and structure-based CoMFA of tacrine analogues, J. Med. Chem. 43 (**2000**) 2007-2018.

Reddy, E. K., Remya, C., Sajith, A. M., Dileep, K. V., Sadasivan, C., Anwar, S. RSC Adv, 6 (**2016**) 77431-77439.

Reichel A., Begley, D. J. and Abbott, N. J. An overview of in vitro techniques for blood–brain barrier studies, Methods Mol. Med., **2003**, 89, 307.

Reisberg, Barry et al. "Memantine in Moderate-to-Severe Alzheimer's Disease." New England Journal of Medicine. **2003**, 348, 1333.

Relman, A. S. Tacrine as a treatment for Alzheimer's dementia. N. Engl. J. Med**. 1991,** 324, 349.

Remya, C., Dileep, K. V., Tintu, I., Variyar, E. J., Sadasivan, C. Frontiers in Life Science 6.3-4 (**2012**): 107-117.

Remya, C., Dileep, K. V., Tintu, I., Variyar, E. J., and Sadasivan, C. Med Chem Res 21 **(2012)** 2779–2787.

Remya, C., Dileep, K. V., Tintu, I., Variyar, E. J., and Sadasivan, C. J Mol Model 19**(2013)** 1179–1194.

Riedel, G., B. Platt, and J. Micheau. "Glutamate Receptor Function in Learning and Memory." Behavioral Brain Research. **2003**, 140, 1.

Rivkin A., Ahearn, S. P., Chichetti, S. M., Kim, Y. R., Li, C. M., Rosenau, A., Kattar, S. D., Jung, J., Shah, S., Hughes, B. L., Crispino, J. L., Middleton, R. E.,

Szewczak, A. A., Munoz, B. and Shearman, M. S. Bioorg. Med. Chem. Lett., **2010**, 20, 1269.

Rosini M, Andrisano V, Bartolini M, Bolognesi M L, Hrelia P, Minarini A, Tarozzi A, Melchiorre C, Rational approach to discover multipotent anti-Alzheimer drugs, J. Med. Chem. 48 (**2005**) 360-363.

Sajith A. M., Abdul Khader, K. K., Joshi, N., Nageswar Reddy, M., Syed Ali Padusha, M., Nagaswarupa, H. P., Nibin Joy, M., Bodke, Y. D., Karuvalam, R. P., Banerjee, R., Muralidharan, A. and Rajendra, P. Eur. J. Med. Chem., **2015**, 89, 21.

Sakaeda T.; Okamura, N.; Nagata, S.; Yagami, T.; Horinouchi, M.; Okumura, K.; Yamashita, F. and Hashida, M. Molecular and pharmacokinetic properties of 222 commercially available oral drugs in humans, Biol. Pharm. Bull., **2001**, 24, 935.

Saltiel, Emmanuel. "Memantine (Namenda)." Medicine Net. 2 Nov. 2003. Web. 12 Nov. 2010.

Samanta S, Jana S, Mondal S, Monir K, Chandra S K and Hajra A, Org. Biomol. Chem., **2016**, 14, 5073.

Santra, S.; Bagdi, A. K., Majee, A.; Hajra, A. Adv. Synth. Catal. **2013**, 355, 1065.

Sassa, S., Sugita, O., Galbraith, R. A., &Kappas, A. **(1987).** Drug metabolism by the human hepatoma cell, Hep G2. Biochemical and biophysical research communications, 143(1), 52-57.

Scarpini, E., Scheltens, P., Feldman, H., Lancet Neurol. 2 (**2003**) 539-547.

Schneider, L. S., Mangialasche, F., Andreasen, N., Feldman, H., Giacobini, E., Jones, R., Mantua, V., Mecocci, P., Pani, L., Winblad, B., Kivipelto, M., Clinical trials and latestage drug development for Alzheimer's disease: an appraisal from 1984 to 2014. J. Intern. Med. 275 (**2014**) 251–283.

Schultz C, Link A, Leost M, Zaharevitz D W, Gussio R, Sausville E A, Meijer L, Kunick C, J. Med. Chem. **1999**, 42, 2909.

Scribner, A.; Dennis, R.; Hong, J.; Lee, S.; McIntyre, D.; Perrey, D.; Feng, D.; Fisher, M.; Wyvratt, M.; Leavitt, P.; Liberator, P.; Gurnett, A.; Brown, C.; Mathew, J.; Thompson, D.; Schmatz, D.; Biftu, T. Eur. J. Med. Chem. **2007**, 42, 1334.

Selkoe, D., J. Alzheimer's disease: genes, proteins, and therapy.Physiol. Rev. 81 (2001) 741−766.

Shao N, Pang G X, Yan C X, Shi and Cheng Y, J. Org. Chem., 2011, **76**, 7458.

Shao N.; Chen, T.; Zhang, T.; Zhu, H.; Zheng, Q. and Zou, H. Tetrahedron, **2014**, 70, 795.

Shaw, F. H.; Bentley, G. A. The pharmacology of some new anticholinesterases. Aust. J. Exp. Biol. Med. Sci. **1953,** 31, 573.

Shimmyo Y, Kihara T, Akaike A, Niidome T, Sugimoto H, Flavonols and flavones as BACE-1 inhibitors: structure–activity relationship in cell-free, cell-based and in silico studies reveal novel pharmacophore features, Biochim. Biophys. Acta 1780 (**2008**) 819-825.

Shutske, G. M.; Pierrat, F. A.; Cornfeldt, M. L.; Szewczak, M. R.; Huger, F. P.; Bores, G. M.; Haroutunian, V.; Davis, K. L. (+/-)-9-Amino-1,2,3,4-Tetrahydroacridin-1-ol - A Potential Alzheimer's-Disease Therapeutic of Low Toxicity. J. Med. Chem. **1988,** 31, 1278.

Shutske, G. M.; Pierrat, F. A.; Kapples, K. J.; Cornfeldt, M. L.; Szewczak, M. R.; Huger, F. P.; Bores, G. M.; Haroutunian, V.; Davis, K. L. 9-Amino-1,2,3,4-Tetrahydroacridin-1-ols - Synthesis and Evaluation as Potential Alzheimers-Disease Therapeutics. J. Med. Chem. **1989,** 32, 1805.

Special Issue on Catalytic Asymmetric Synthesis. Acc. Chem. Res. **2000**, 33, 323.

Spencer J P, Beyond antioxidants: the cellular and molecular interactions of flavonoids and how these underpin their actions on the brain, Proc. Nutr. Soc. 69 (**2010**) 244-260.

Squitti R, Rossini P, Cassetta E, Moffa F, Pasqualetti P, Cortesi M, Colloca A, Rossi L, d-penicillamine reduces serum oxidative stress in Alzheimer's disease patients, Eur. J. Med. Chem. 32 (**2002**) 51-59.

Stasyuk A J, Banasiewicz M, Cyranski M K and Gryko D T, J. Org. Chem., **2012**, **77**, 5552.

Stork G, Niu D, Fujimoto A, Koft, Balkovec J M,. Tata J R and Dake G R, J. Am. Chem. Soc., **2001**, 123, 3239.

Strekowski L, Gulevich Y, Baranowski T C, Parker A N, Kiselyov A S, Lin S Y, Tanious F A and Wilson W D, J. Med. Chem., **1996**, 39, 3980.

Suh, Y. H. and Checler, F. Pharmacol. Rev., **2002**, 54, 469.

Suh, Y. H., Checler, F. Amyloid precursor protein, presenilins, and alpha-synuclein: molecular pathogenesis and pharmacological applications in Alzheimer's disease. Pharmacol. Rev. 54 (**2002)** 469−525.

Summers, W. K.; Kaufman, K. R.; Altman, F.; Fischer, J. M. THA - A Review of the Literature and its Use in Treatment of Five Overdose Patients. Clin. Toxicol. **1980,** 16, 269.

Summers, W. K.; Majovski, L. V.; Marsh, G. M.; Tachiki, K.; Kling, A. Oral. tetrahydroaminoacridine in long-term treatment of senile dementia, Alzheimer type. N. Engl. J. Med. **1986,** 315, 1241.

Sussman J L, Harel M, Frolow F, Oefner C, Goldman A, Toker L, Silman I, Atomic structure of acetylcholinesterase from Torpedo californica: a prototypic acetylcholine-binding protein, Science 253 (**1991**) 872-879.

Tachibana Y, Kikuzaki H, Lajis N H, Nakatani N, Antioxidative activity of carbazoles from Murraya koenigii leaves, J. Agric. Food Chem. 49 (**2001**), 5589-5594.

Tang, H., Zhao, H. T., Zhong, S. M., Wang, Z. Y., Chen, Z. F., Liang, H. Bioorg. Med. Chem. Lett. 22 (**2012**) 2257-2261.

Thabrew M, Robin D. Hughes G. MCFARLANE Screening of hepatoprotective plant components using a HepG2 cell cytotoxicity assay. J Pharm Pharmacol **1997**, 11: 1132-1135.

Thiratmatrakul S, Yenjai C, Waiwut P, Vajragupta O, Reubroycharoen P, Tohda M, Boonyarat C, Synthesis, biological evaluation and molecular modeling study of novel tacrineecarbazole hybrids as potential multifunctional agents for the treatment of Alzheimer's disease, Eur. J. Med. Chem. 75 (**2014**), 21-30.

Touaibia M, Jean-Francois J, Doiron J, Caffeic acid, a versatile pharmacophore: an overview, Mini Rev. Med. Chem. 11 (**2011**) 695-713.

Trost, B. M. Science **1991**, 254, 1471.

Tully W. R.; Gardner, C. R.; Gillespie, R. J. and Westwood, R. J. Med. Chem., **1991**, 34, 2060.

Tumiatti, V., Minarini, A., Bolognesi, M. L., Milelli, A., Rosini, M., Melchiorre, C. Tacrine derivatives and Alzheimer's disease. Curr. Med. Chem. 17 (**2010**) 1825−1838.

Valasani, K. R.; Chaney, M. O.; Day, V. W. and Yan, S. S. D. Pharmacophore, **2013**, 53, 2033.

Vasiliev, I. A. et al. Patent WO 2007/117180 A1, **2007**.

Veron J. B., Allouchi, H.; Gueiffier, C. E.; Snoeck, R.; Andrei, G.; De Clercq, E. and Gueiffier, A. Bioorg. Med. Chem., **2008**, 16, 9536;

Walborsky, H. M. Acc. Chem. Res. **1990**, 23, 286.

Walsh D. M. and Selkoe, D. J., Neuron, **2004**, 44, 181.

Wang X Q, Xia C L, Chen S B, Tan J H, Ou J M,Li Huang, D Li, L-Q Gu, Z-S Huang; Eur. J. Med. Chem 89 (**2015**) 349-361.

Watkins, P. B.; Zimmerman, H. J.; Knapp, M. J.; Gracon, S. I.; Lewis, K. W. Hepatotoxic effects of tacrine administration in patients with Alzheimer's disease. JAMA, J. Am. Med. Assoc. **1994,** 271, 992.

Wen Luo, Yan-Ping Li, Yan He, Shi-Liang Huang, Ding Li, Lian-Quan Gu, Zhi-Shu Huang, European Journal of Medicinal Chemistry 46 (**2011**) 2609-2616.

Williams College Neuroscience, 1998 Betty Zimmerberg et al Multimedia Neuroscience ducation Project. Synaptic Transmission: A Four Step Process

Xue-Sen Fan, Ju Zhang, Bin Li, and Xin-Ying Zhang, Chemistry - An Asian Journal, **2015**, 10(6), 1281-1285.

Yeh L. F.; Anwar, S.; and Chen, K. Tetrahedron, **2012**, 68, 7317.

Yongyuan Gao, Weiye Lu, Ping Liu and Peipei Sun, J. Org. Chem. **2016**, 8, 2482-2487.

Yoon, Y. K.; Ali, M. A.; Wei, A. C.; Choon, T. S.; Khaw, K.-Y.; Murugaiyah, V.; Osman, H. and Masand, V. H. Bioorg. Chem., **2013**, 49, 33.

Zhang J. Q., Liu, J.-J.; Gu, C.-L.; Wang, D. and Liu, L. Eur. J. Org. Chem., **2014**, 5885.

Zhang L, qaing Xing G, Barker J L, Chang Y, Maric D, Ma W, Li B S, Rubinow D R, a-Lipoic acid protects rat cortical neurons against cell death induced by amyloid and hydrogen peroxide through the Akt signalling pathway, Neurosci. Lett. 312 (**2001**) 125-128.

Zhi H., Chen, L. M.; Zhang, L. L.; Liu, S. J.; Wan, D. C. C.; Lin, H. Q. and Hu, C. Chem. Res. Chin. Univ., **2009**, 25, 332;

Zhi H., Chen, L. M.; Zhang, L. L.; Liu, S. J.; Wan, D. C. C.; Lin, H. Q. and Hu, C. ARKIVOC, **2008**, 266.

Zhu H., Shao, N.; Chen, T and Zou, H. Chem. Commun., **2013**, 49, 7738.

Zhu, J.; Wu, C. F.; Li, X.; Wu, G. S.; Xie, S.; Hu, Q. N.; Deng, Z.; Zhu, M. X.; Luo, H. R.; and Hong, X. Bioorg. Med. Chem**., 2013**, 21, 4218.

Ziegler, F. E. Chem. Rev. **1988**, 88, 1423.

APPENDIX

Spectrum 1: ^{1}H NMR for compound 14a

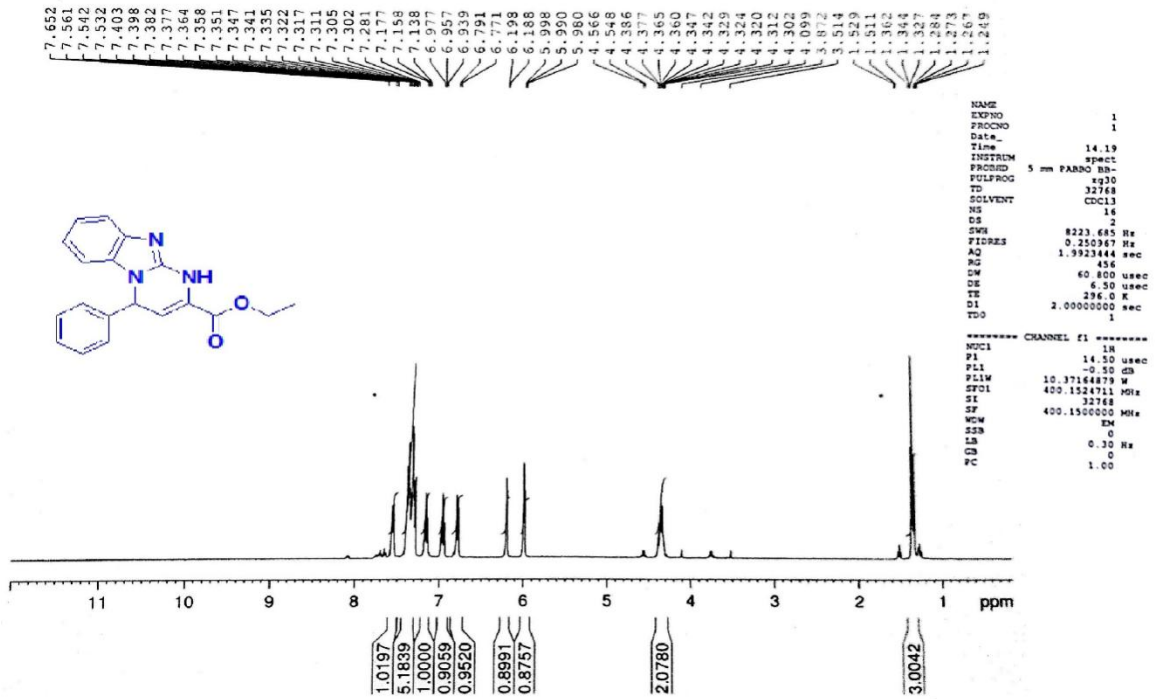

Spectrum 2: ^{13}C NMR for compound 14a

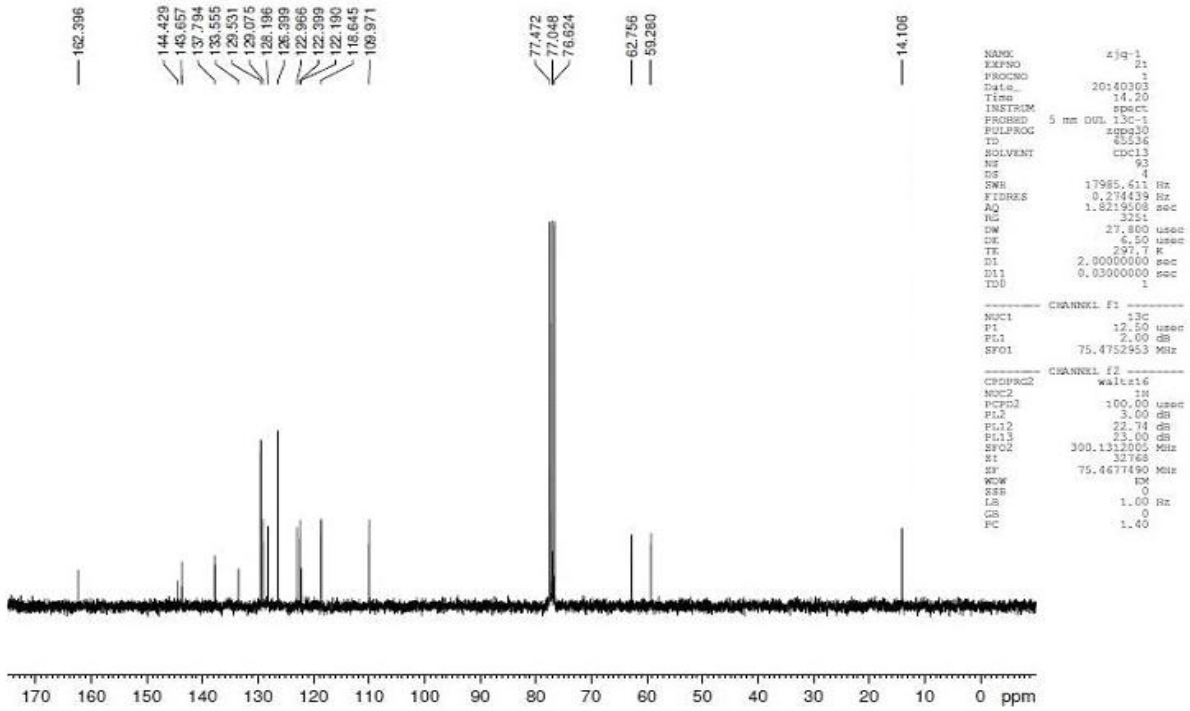

Spectrum 3: ^{1}H NMR for compound 14b

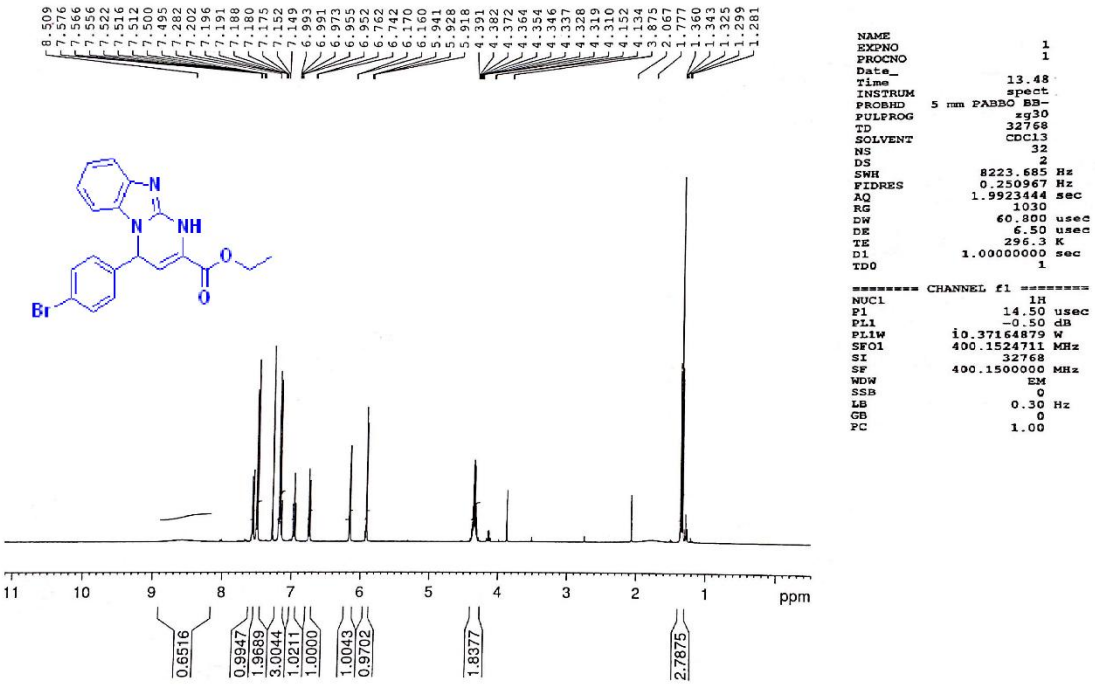

Spectrum 4: ^{13}C NMR for compound 14b

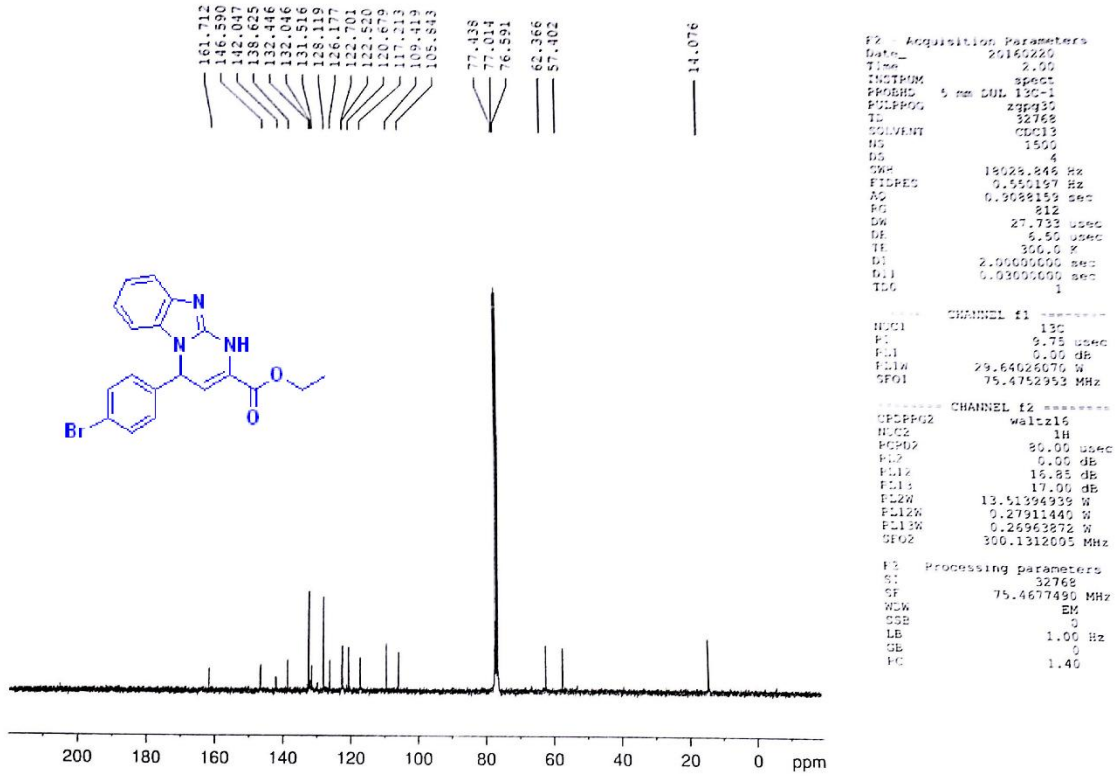

Spectrum 5: ^{1}H NMR for compound 14c (DMSO-d6, 400 MHz)

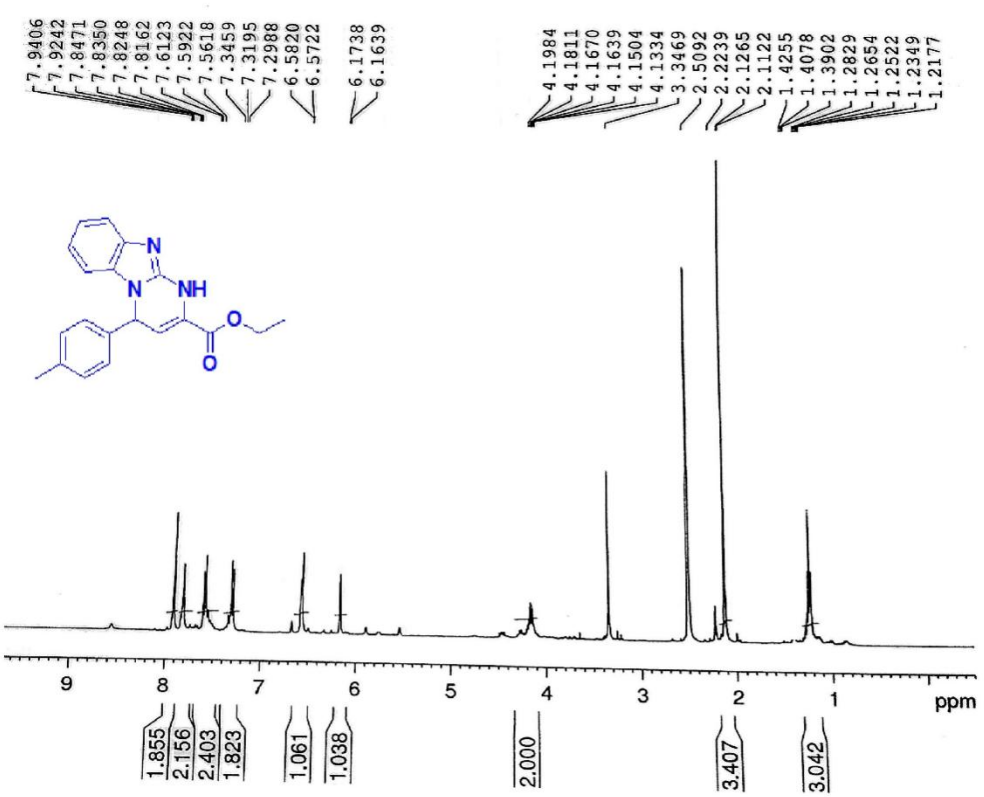

Spectrum 6: ^{13}C NMR for compound 14c

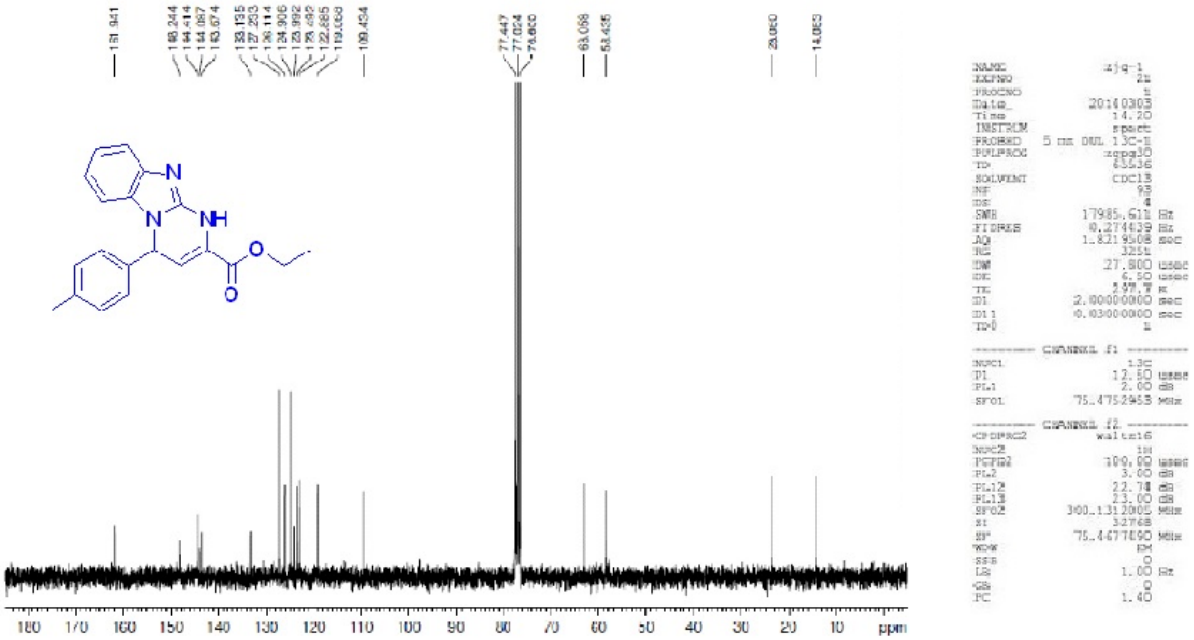

Spectrum 7: ^{1}H NMR for compound 14d (DMSO-d6, 300 MHz)

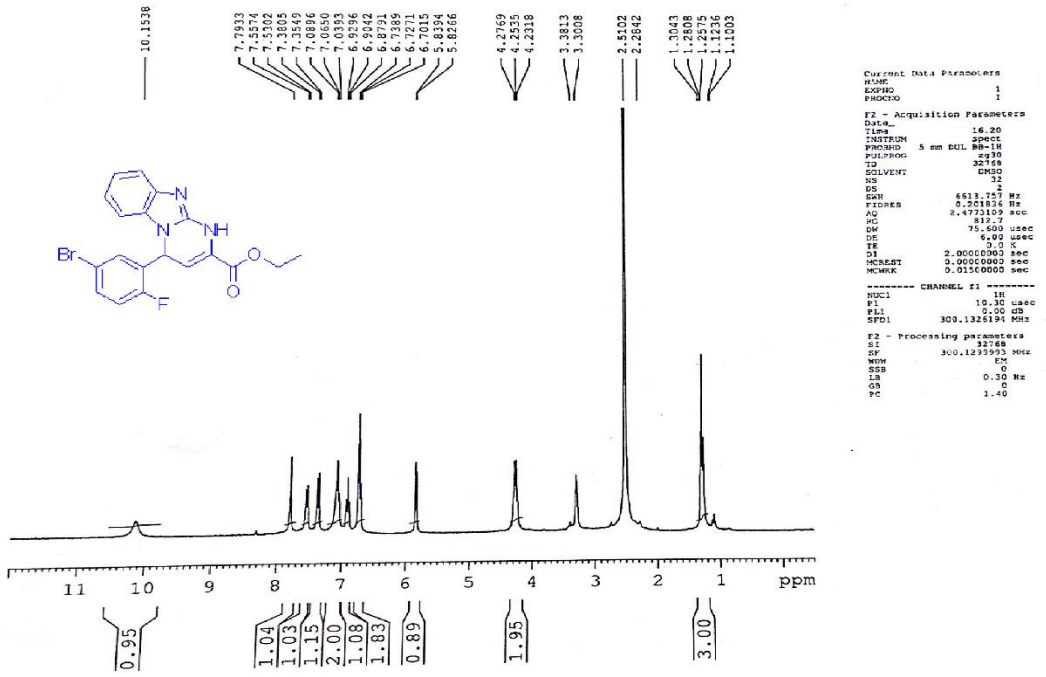

Spectrum 8: ^{13}C NMR for compound 14d

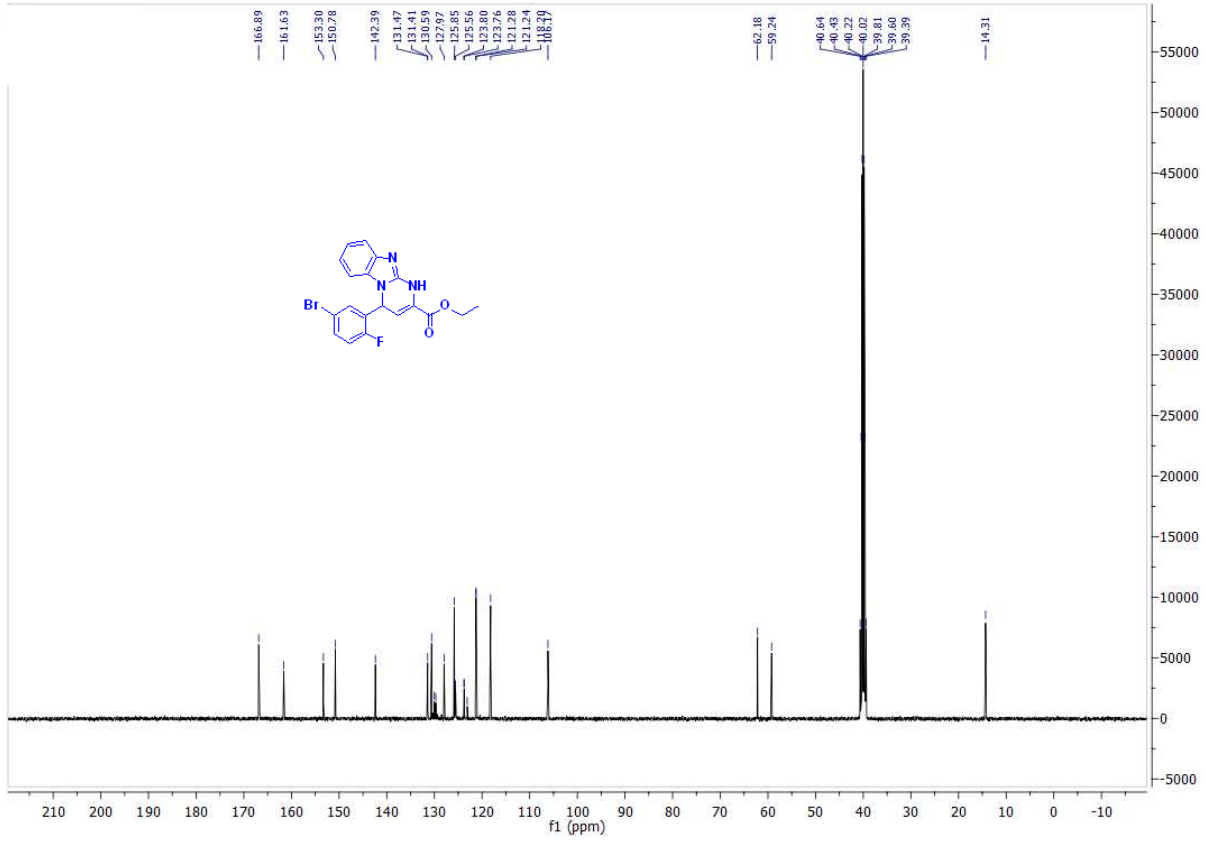

Spectrum 9: ^{1}H NMR for compound 14e

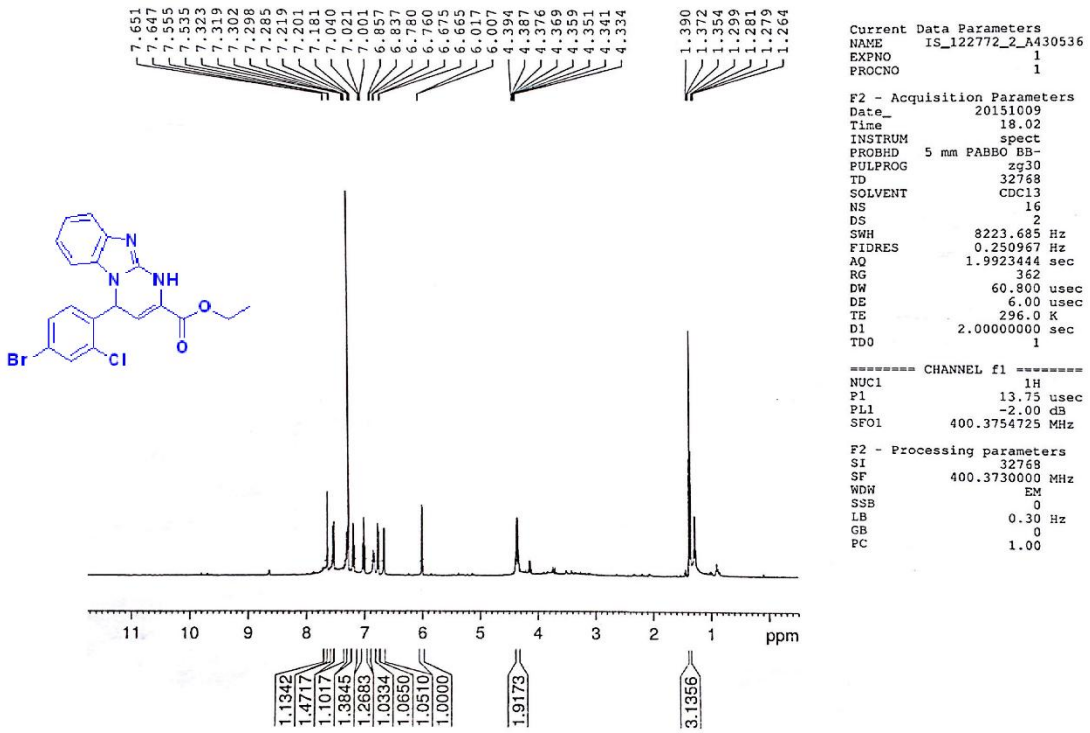

Spectrum 10: ^{13}C NMR for compound 14e

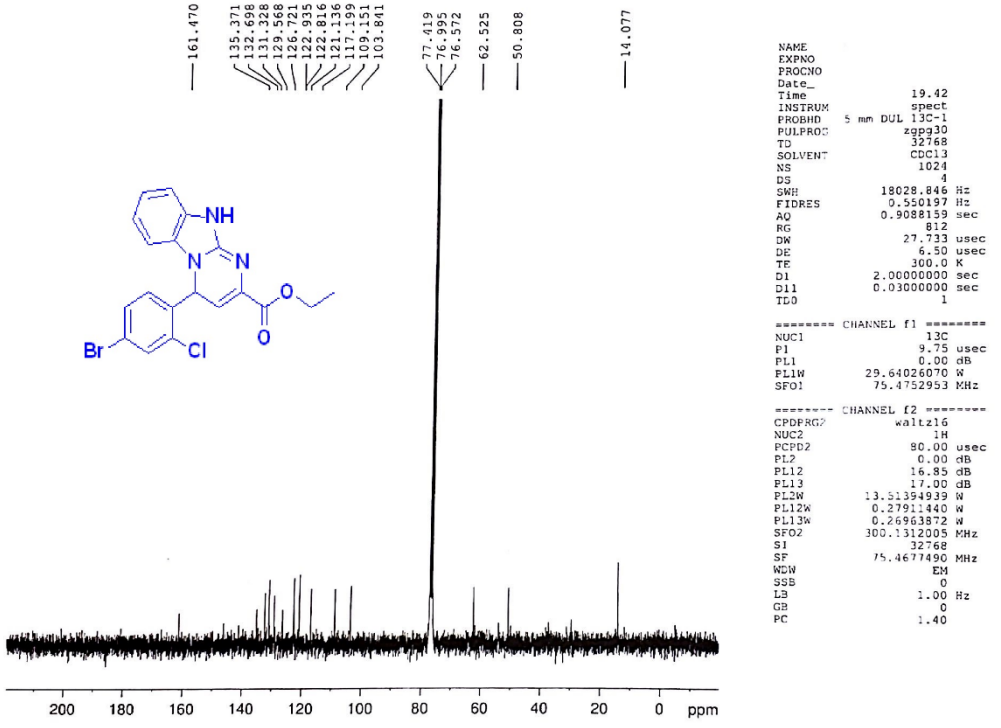

Spectrum 11: ^{1}H NMR compound 14f

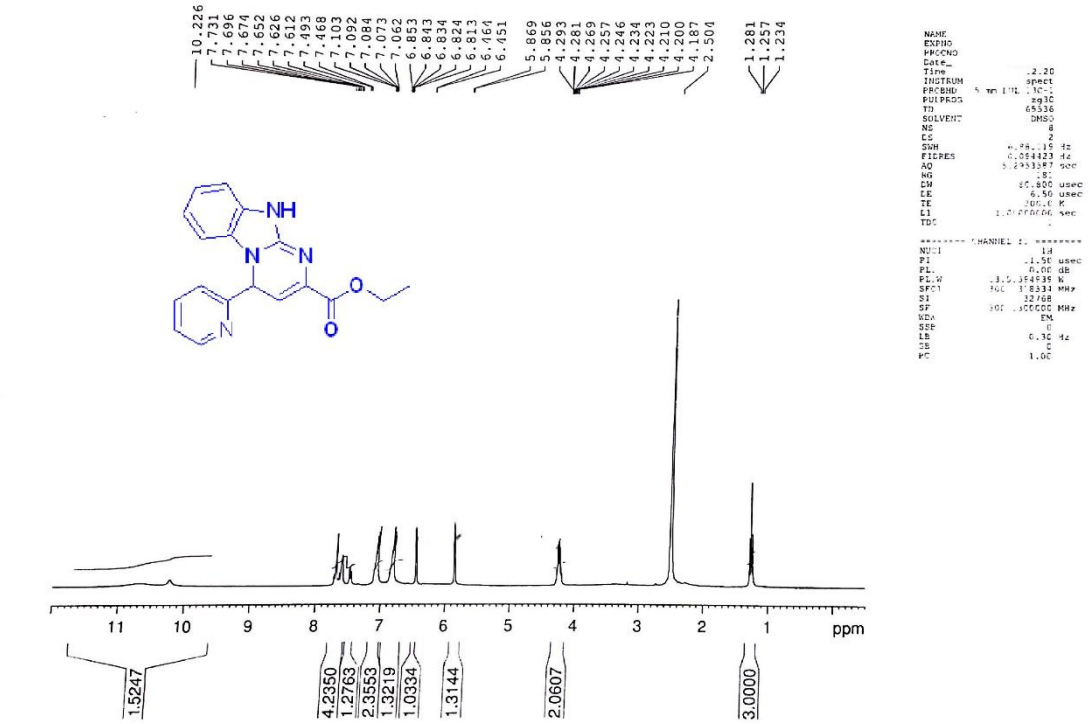

Spectrum 12: ^{13}C NMR for compound 14f

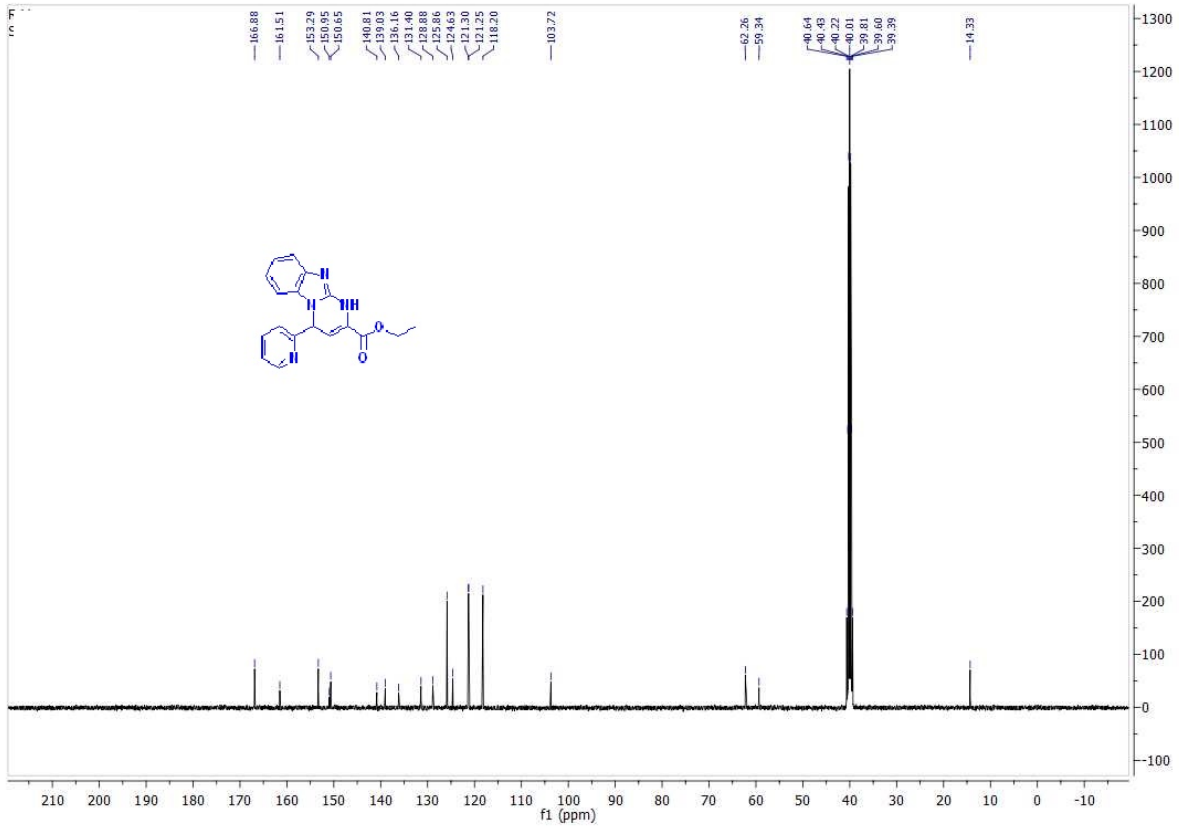

Spectrum 13: ^{1}H NMR for compound 14g

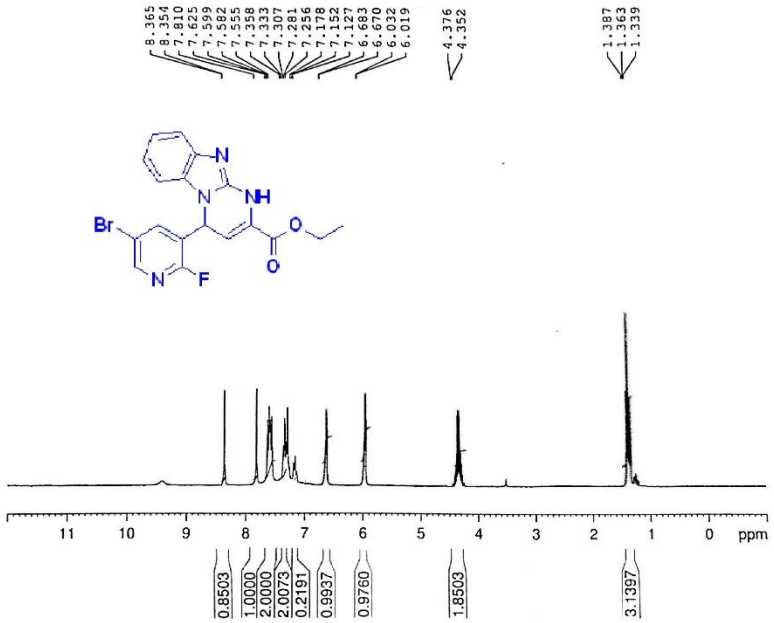


```
NAME
EXPNO
PROCNO
Date_
Time                  12.42
INSTRUM               spect
PROBHD     5 mm DUL 13C-1
PULPROG               zg30
TD                   65536
SOLVENT              CDCl3
NS                       8
DS                       2
SWH                6188.119 Hz
FIDRES            0.094423 Hz
AQ                5.2953587 sec
RG                     181
DW                  80.800 usec
DE                   6.50 usec
TE                  300.0 K
D1                1.00000000 sec
TD0                      1

======== CHANNEL f1 ========
NUC1                   1H
P1                  11.50 usec
PL1                  0.00 dB
PL1W          13.51394939 W
SFO1          300.1318534 MHz
SI                   32768
SF            300.1300000 MHz
WDW                    EM
SSB                     0
LB                   0.30 Hz
GB                      0
PC                   1.00
```

Spectrum 14: ^{13}C NMR for compound 14g

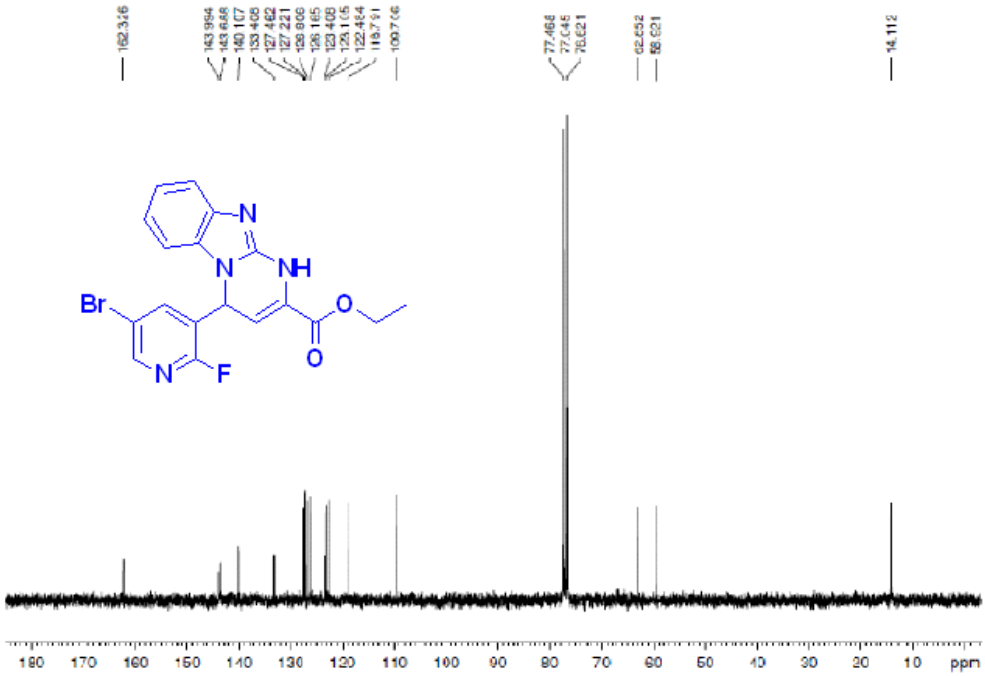


```
NAME
EXPNO
PROCNO
Date_
Time                  16.26
INSTRUM               spect
PROBHD     5 mm DUL 13C-1
PULPROG               zgpg30
TD                   65536
SOLVENT              CDCl3
NS                     144
DS                       4
SWH                17986.631 Hz
FIDRES             0.274439 Hz
AQ                1.8279508 sec
RG                    1290.2
DW                   27.800 usec
DE                    6.50 usec
TE                   297.4 K
D1                2.00000000 sec
D11               0.03000000 sec
TD0                      1

======== CHANNEL f1 ========
NUC1                   13C
P1                   12.50 usec
PL1                   2.00 dB
SFO1          75.4752953 MHz

======== CHANNEL f2 ========
CPDPRG2              waltz16
NUC2                   1H
PCPD2               100.00 usec
PL2                   2.00 dB
PL12                 22.74 dB
PL13                 23.00 dB
SFO2          300.1312005 MHz
SI                   32768
SF            75.4677490 MHz
WDW                    EM
SSB                     0
LB                   1.00 Hz
GB                      0
PC                   1.40
```

Spectrum 15: ^{1}H NMR for compound 14h (CDCl3, 400 MHz)

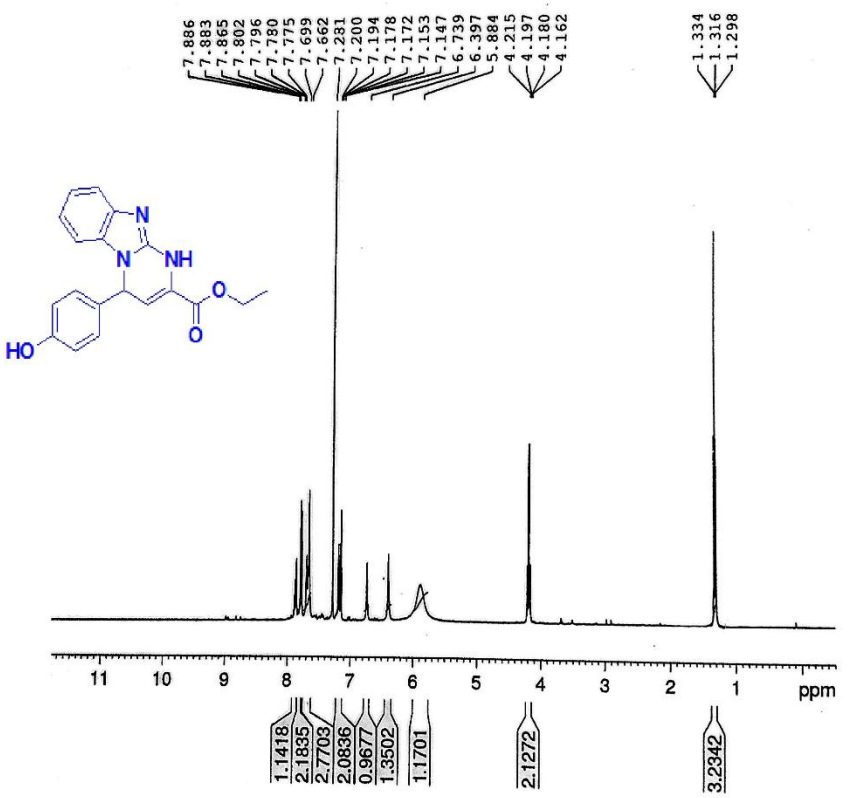

Spectrum 16: ^{13}C NMR for compound 14h

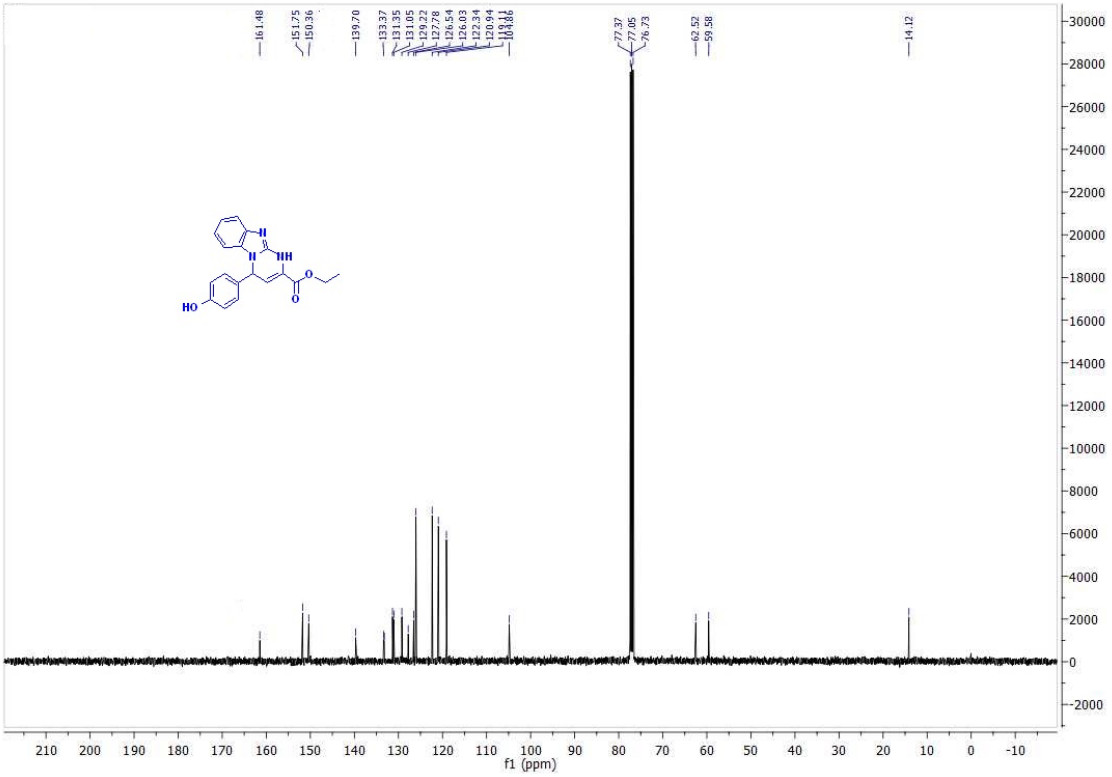

Spectrum 17: ^{1}H NMR for compound 14i

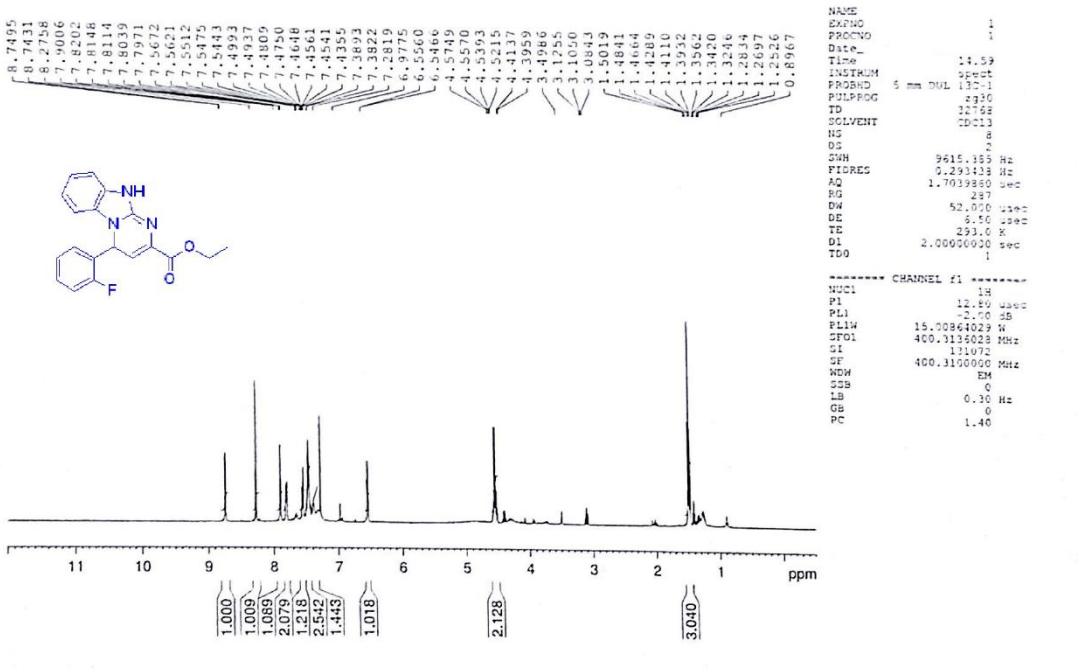

Spectrum 18: ^{13}C NMR for compound 14i

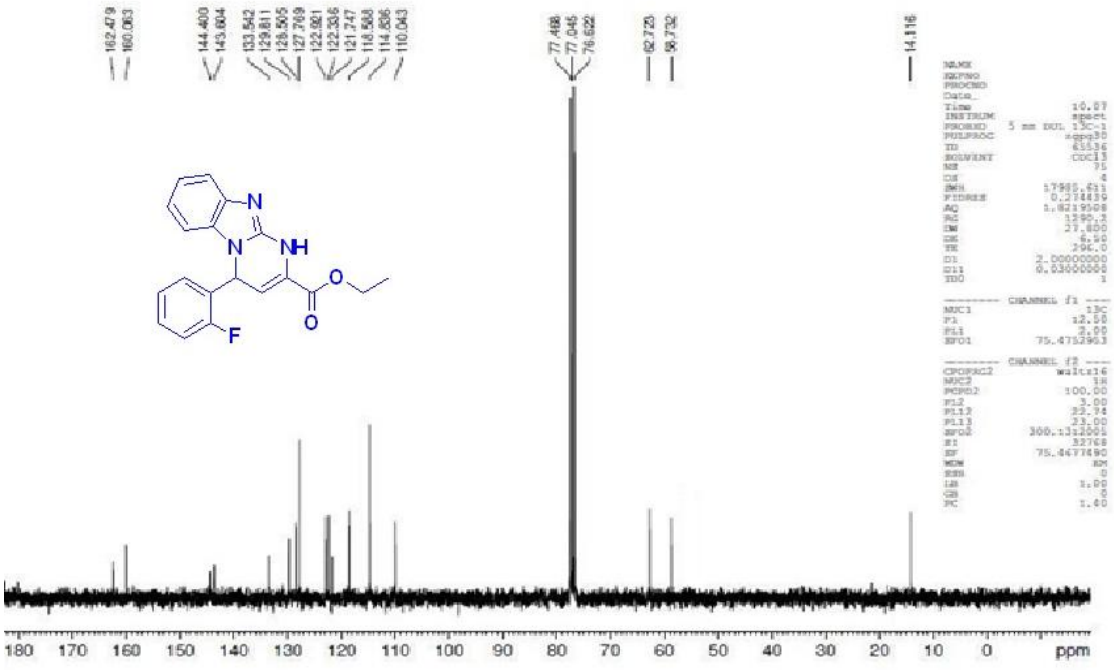

Spectrum 19: ^{1}H NMR for compound 14j

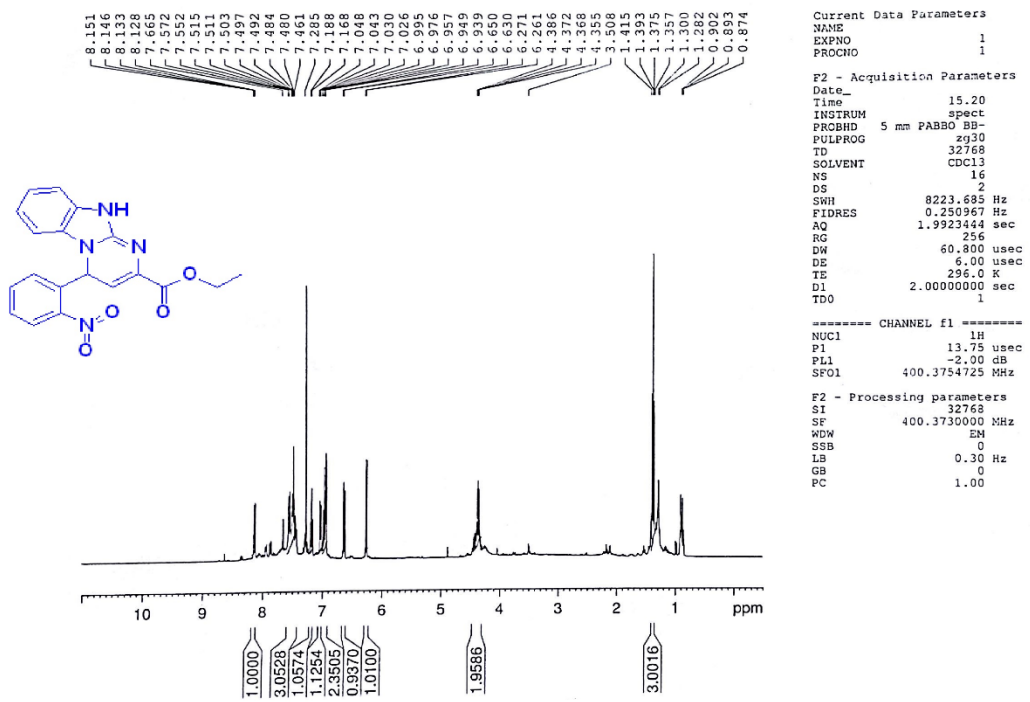

Spectrum 20: ^{13}C NMR for compound 14j

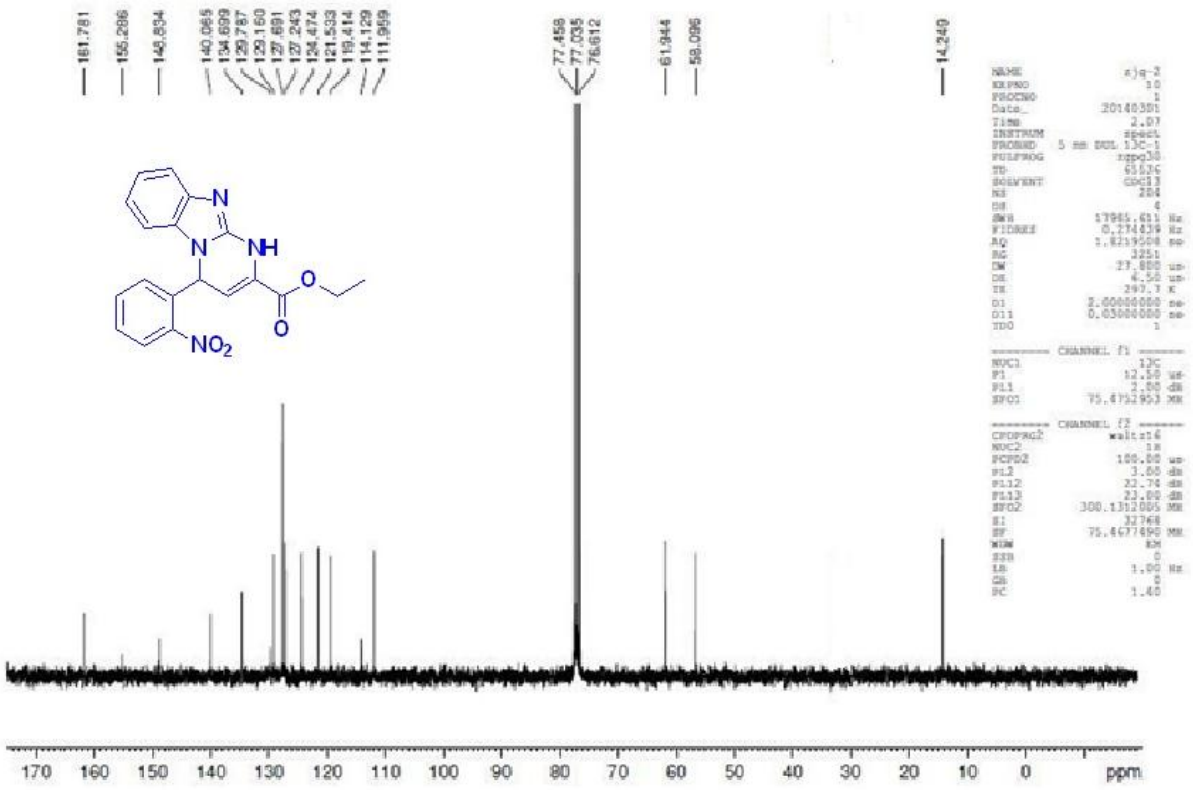

Spectrum 21: ^{1}H NMR for compound 14k

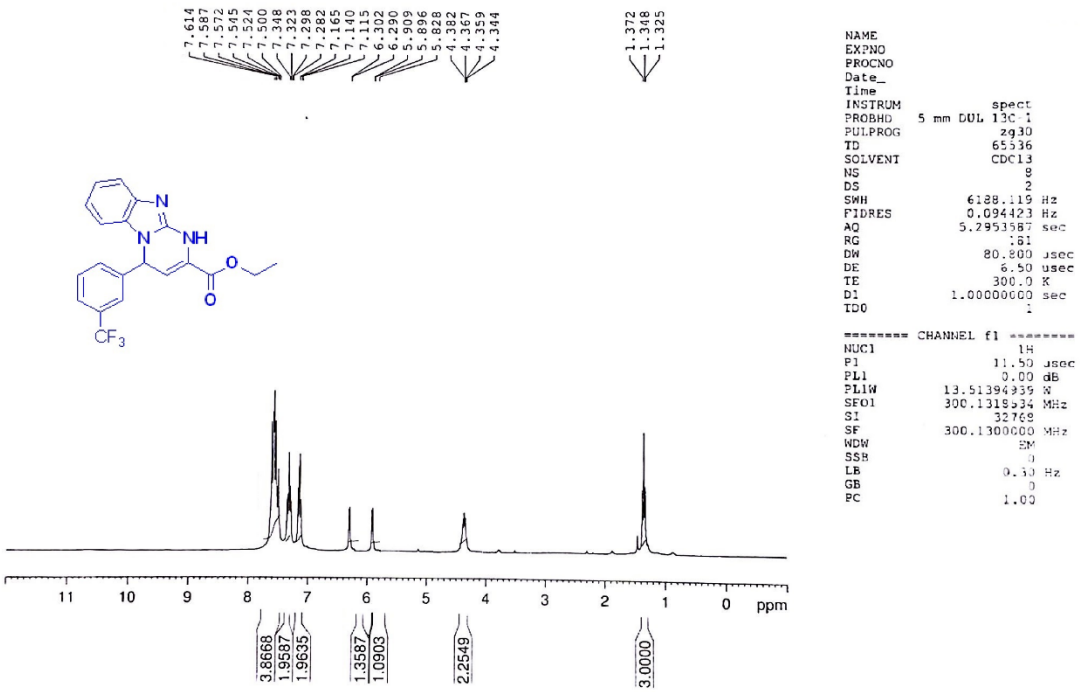

Spectrum 22: ^{13}C NMR for compound 14k

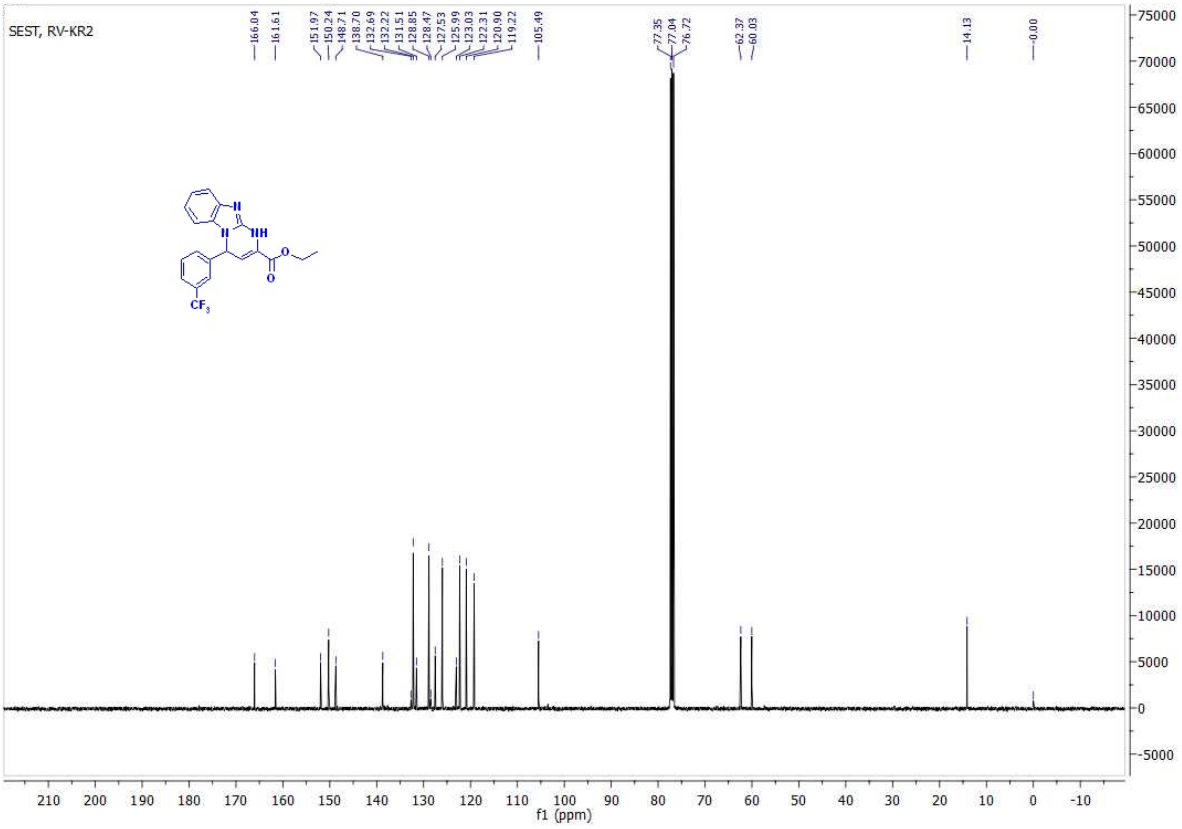

Spectrum 23: ^{1}H NMR for compound 14l

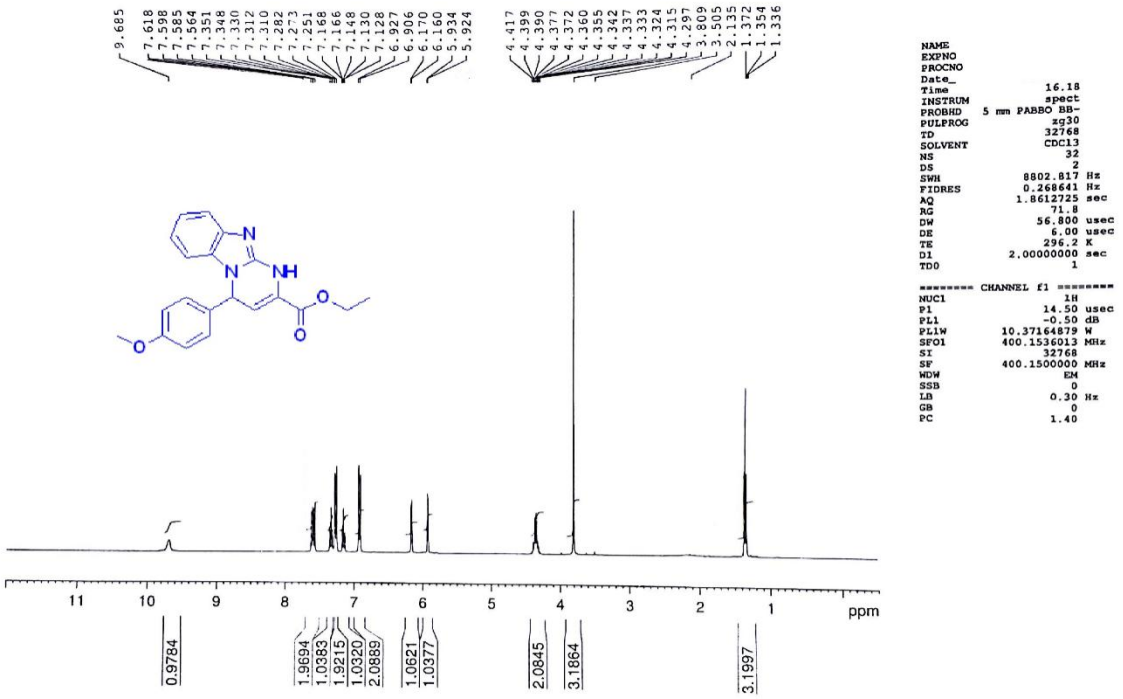

Spectrum 24: ^{13}C NMR for compound 14l

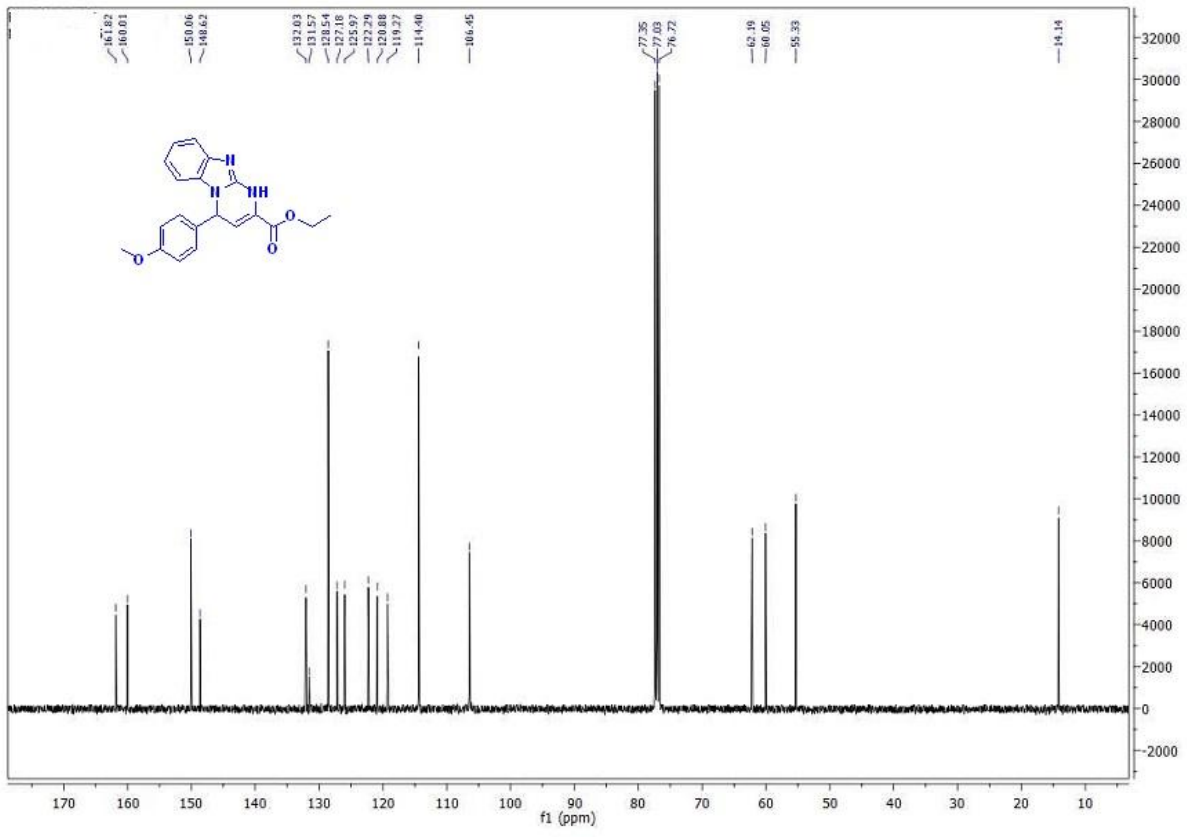

Spectrum 25: ^{1}H NMR for compound 14m

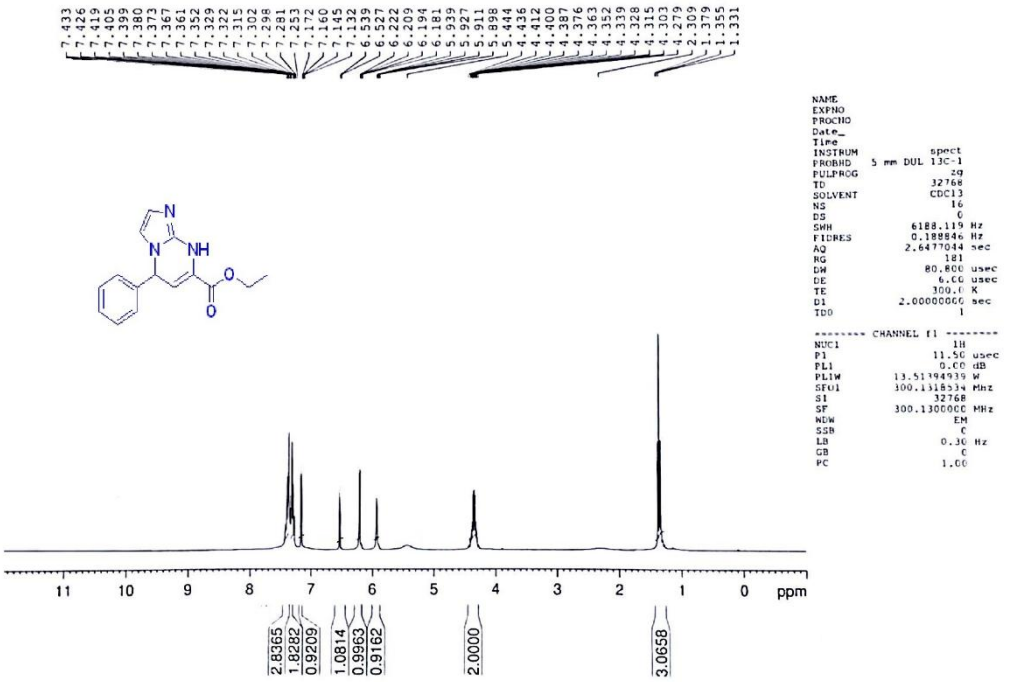

Spectrum 26: ^{13}C NMR for compound 14m

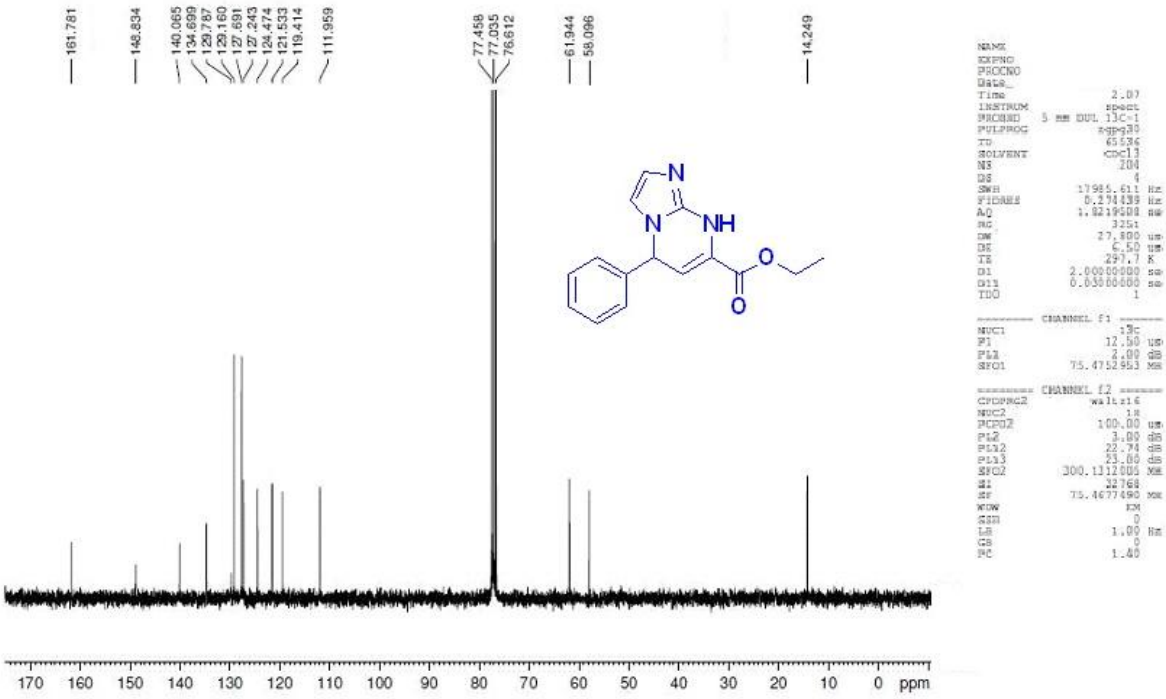

Spectrum 27: ^{1}H NMR for compound 14n

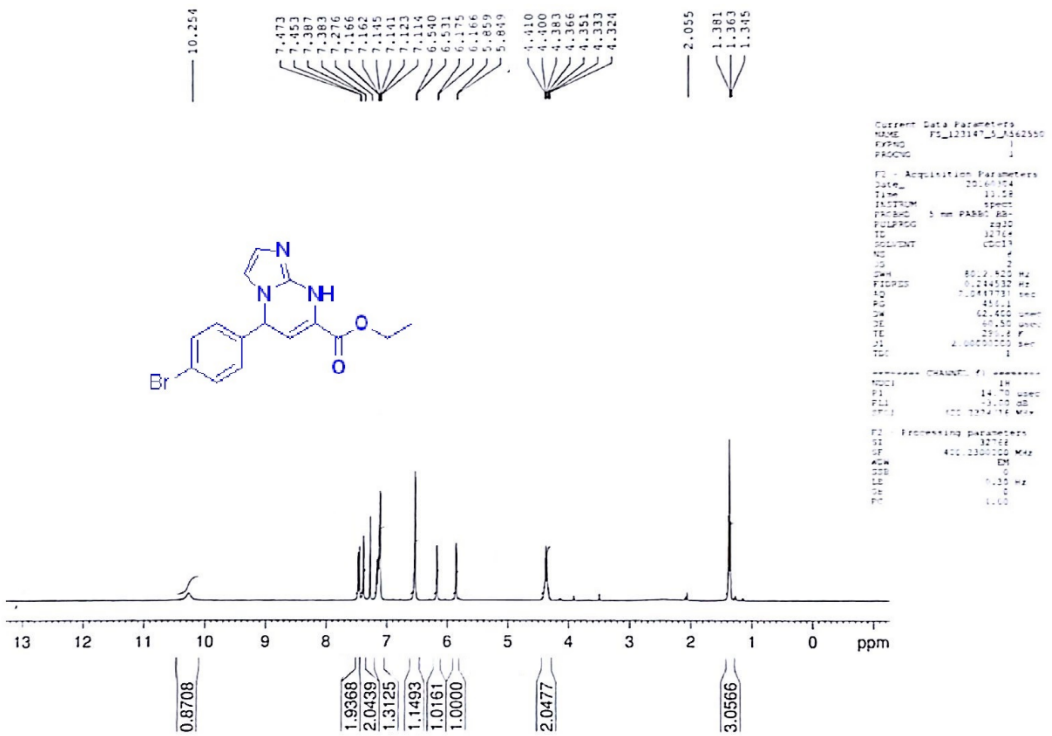

Spectrum 28: ^{13}C NMR for compound 14n

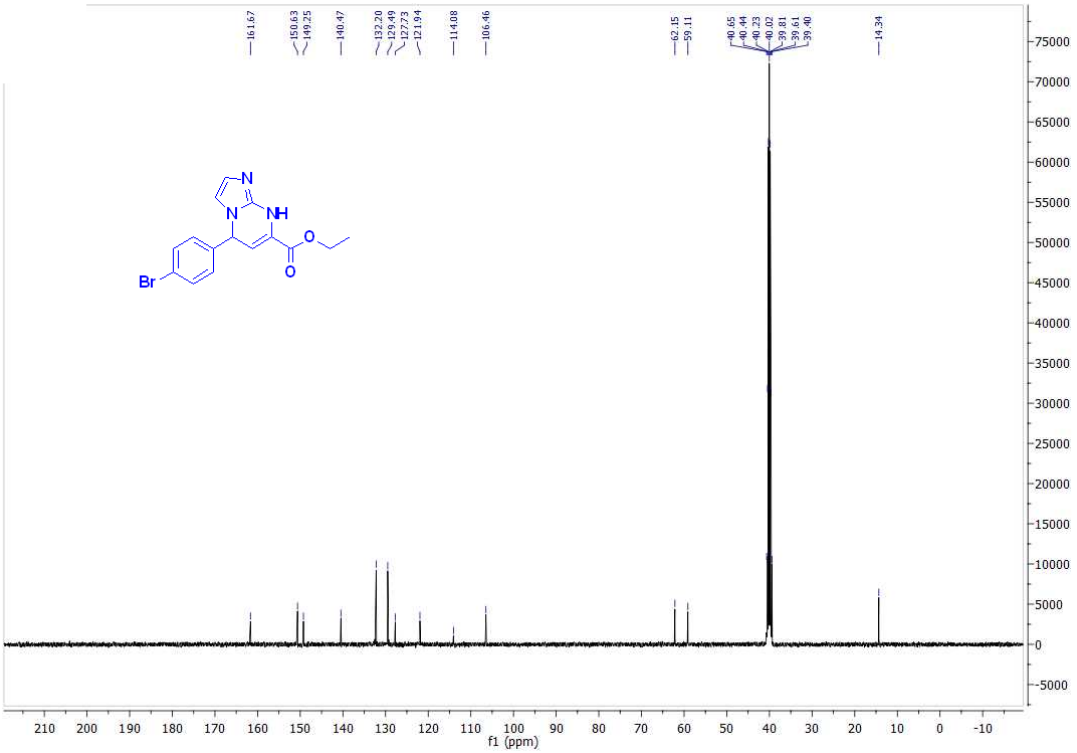

Spectrum 29: ^{1}H NMR for compound 14o

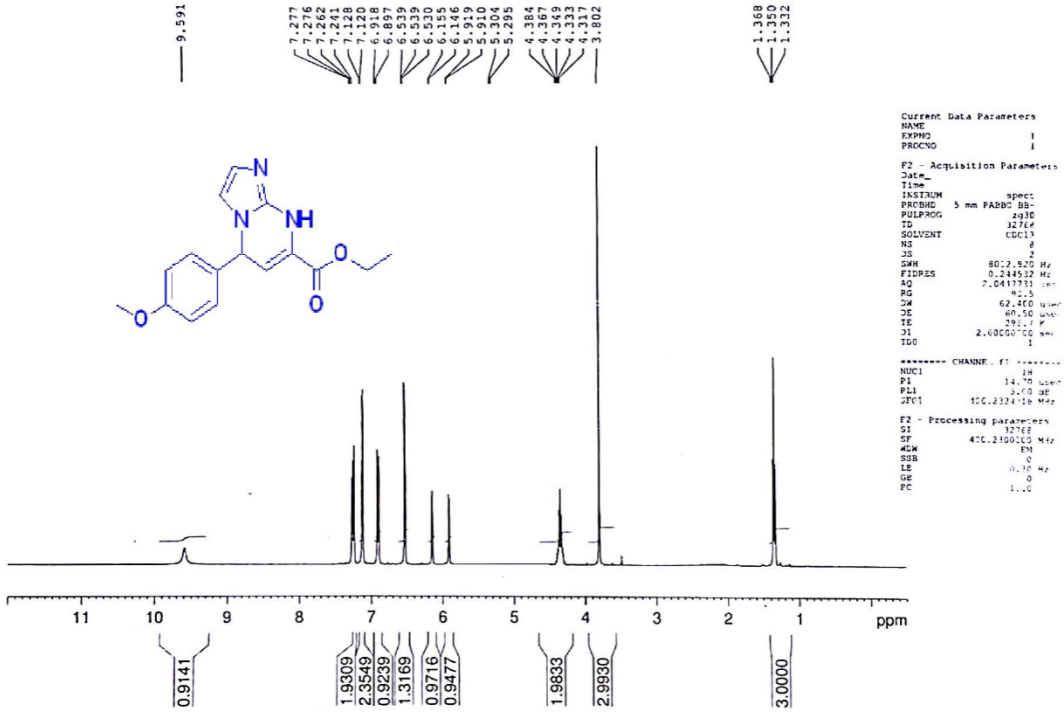

Spectrum 30: ^{13}C NMR for compound 14o

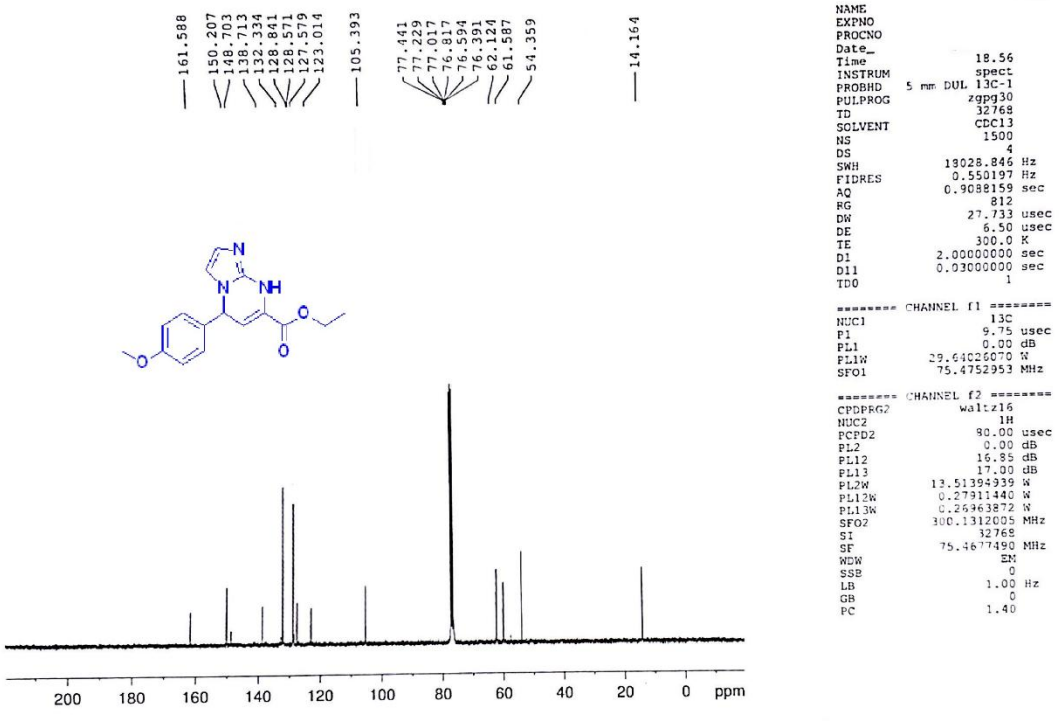

Spectrum 31: ^{1}H NMR for compound 14p

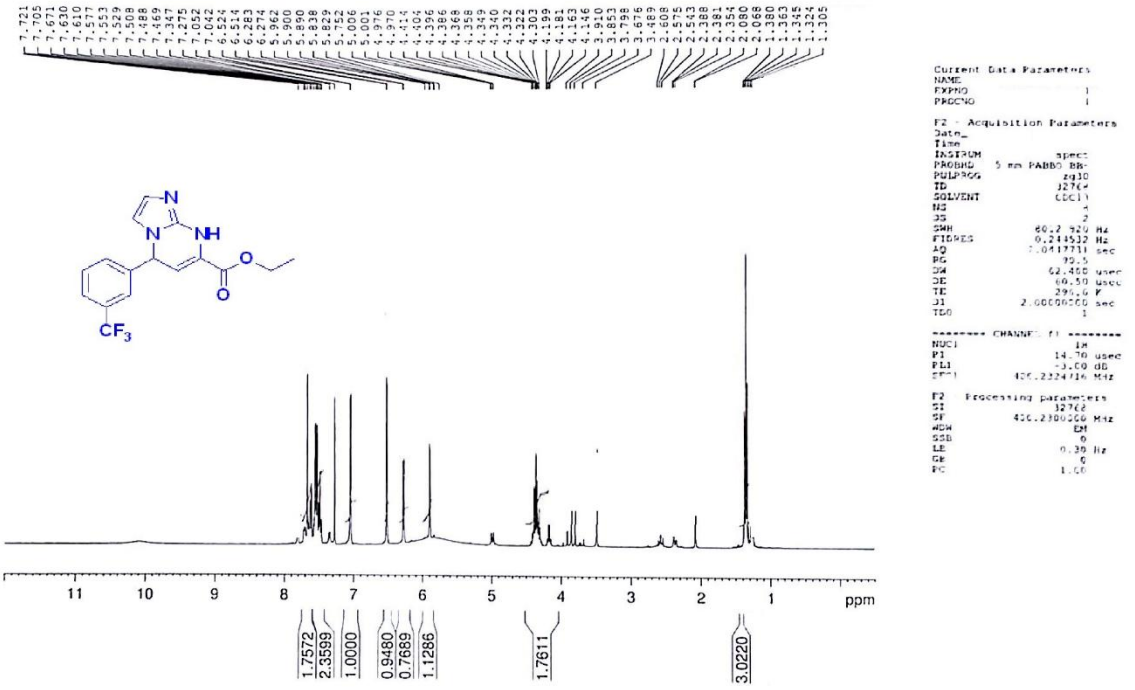

Spectrum 32: ^{13}C NMR for compound 14p

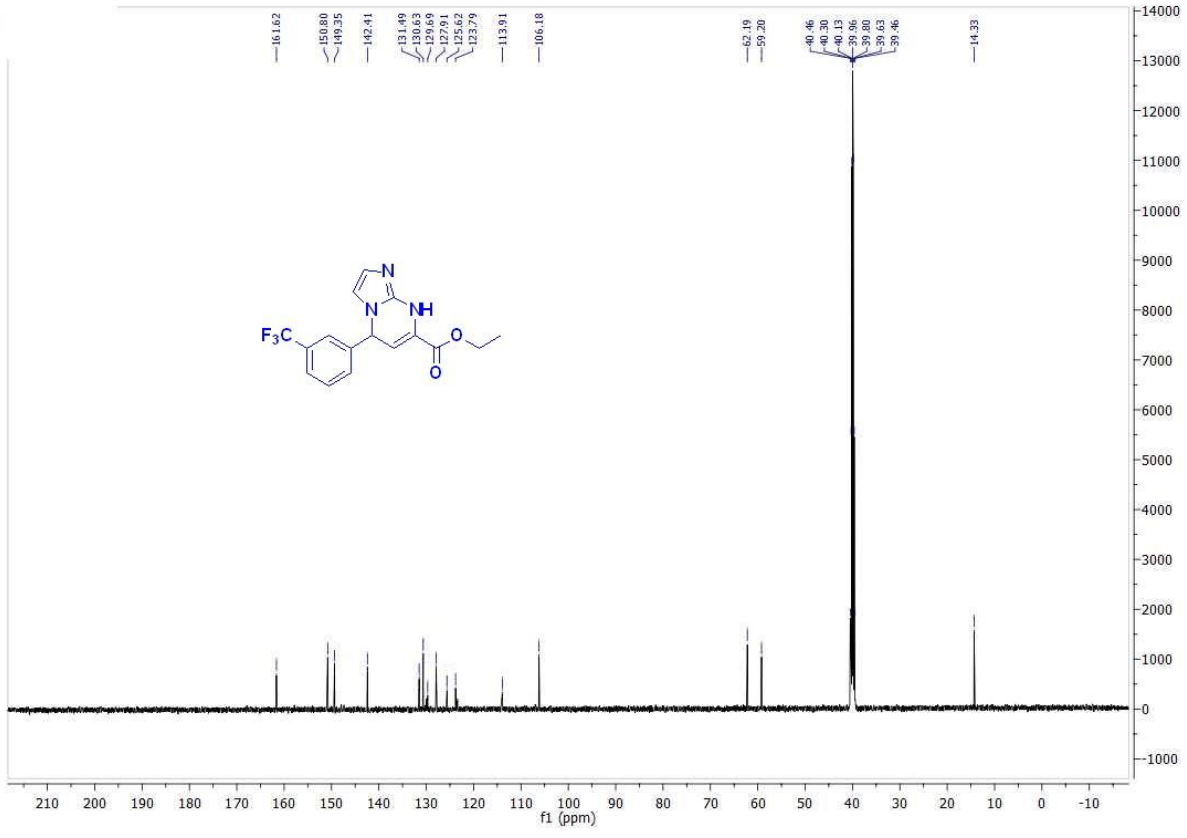

Spectrum 33: ^{1}H NMR for compound 14q

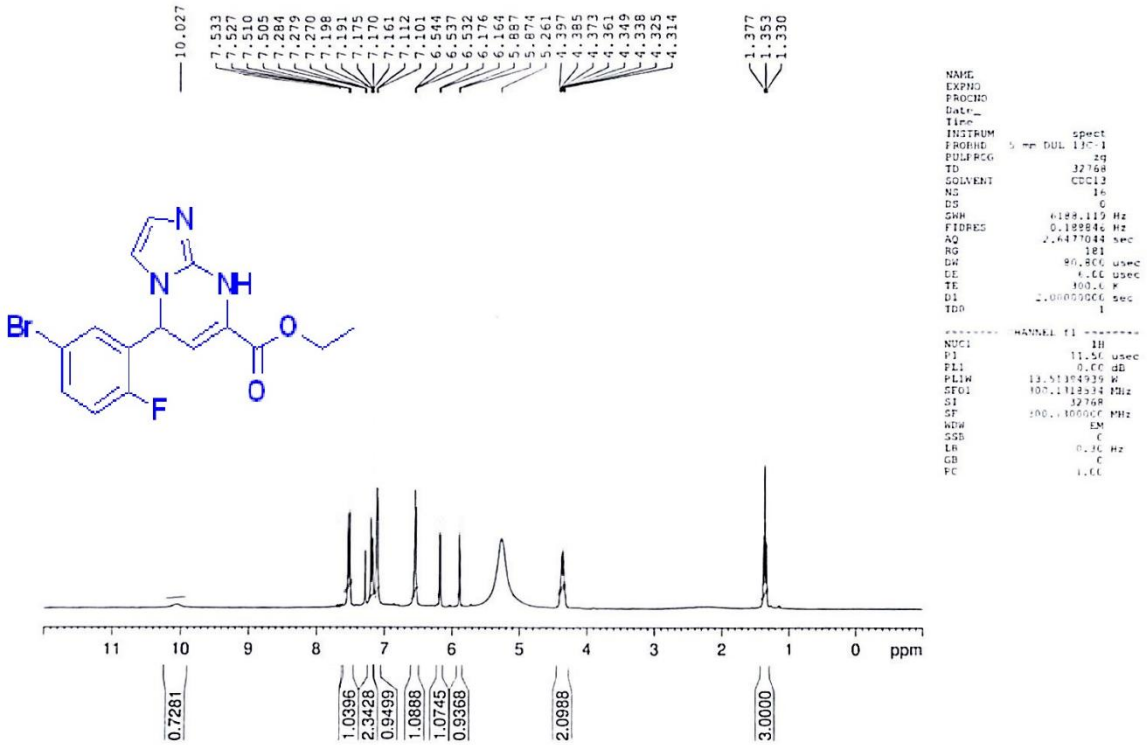

Spectrum 34: ^{13}C NMR for compound 14q

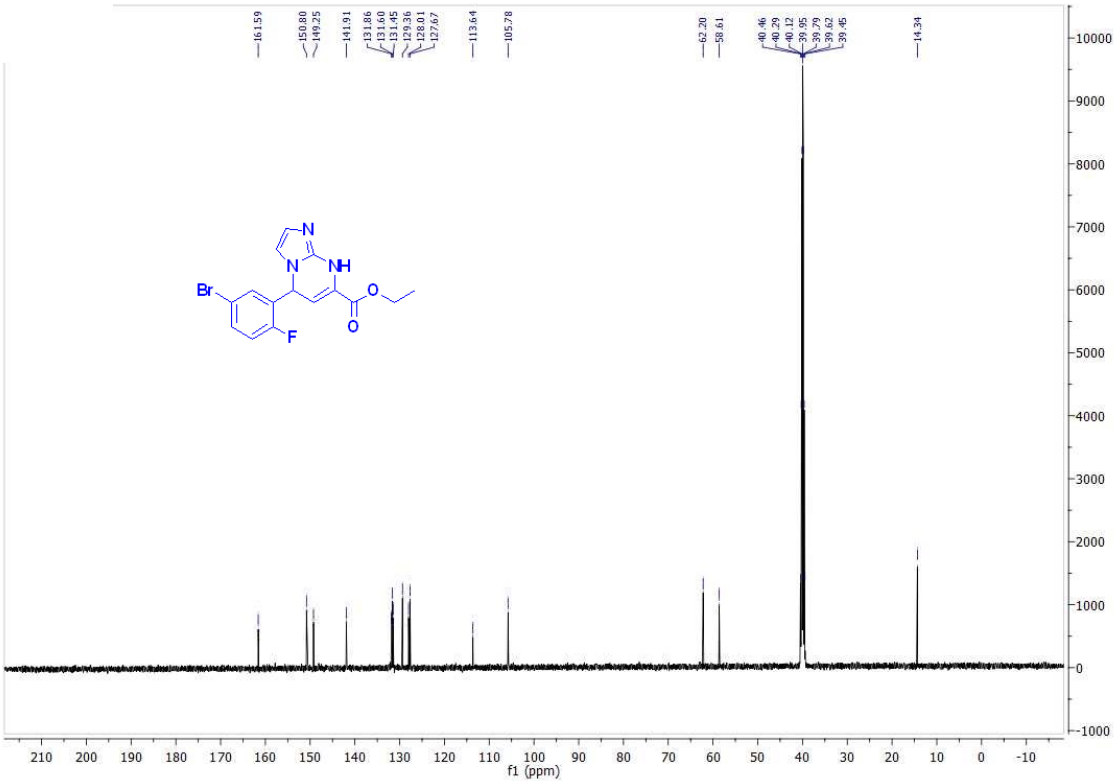

Spectrum 35: ^{1}H NMR for compound 14r

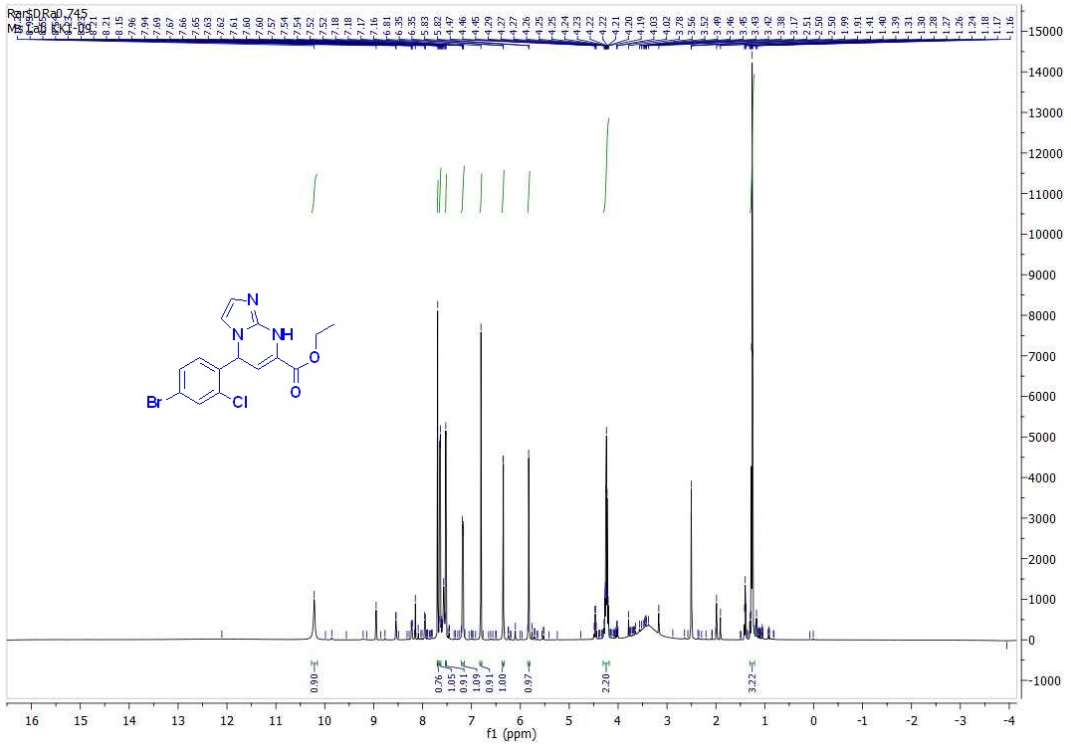

Spectrum 36: ^{13}C NMR for compound 14r

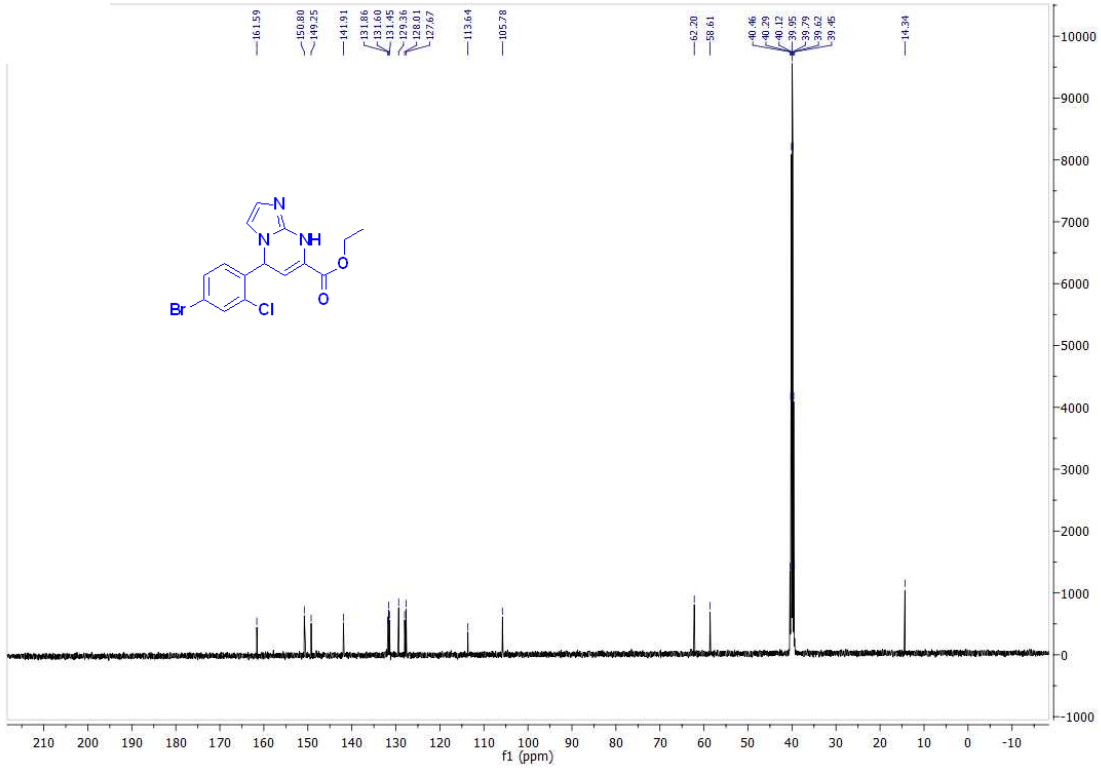

Spectrum 37: ^{1}H NMR for compound 15a

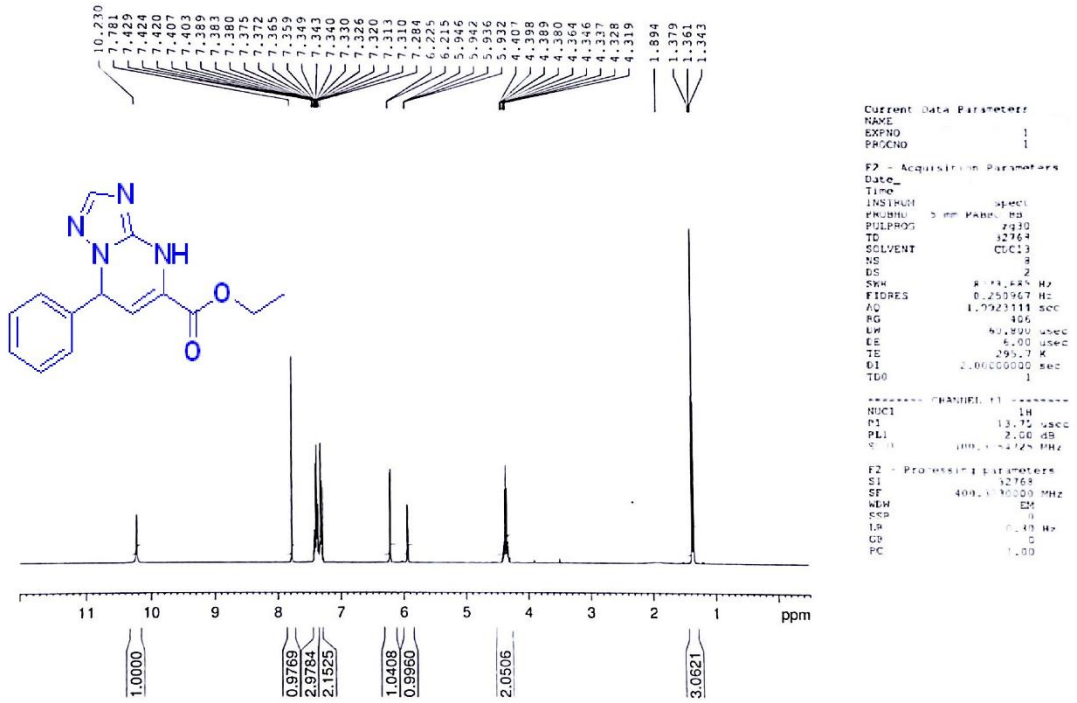

Spectrum 38: ^{13}C NMR for compound 15a

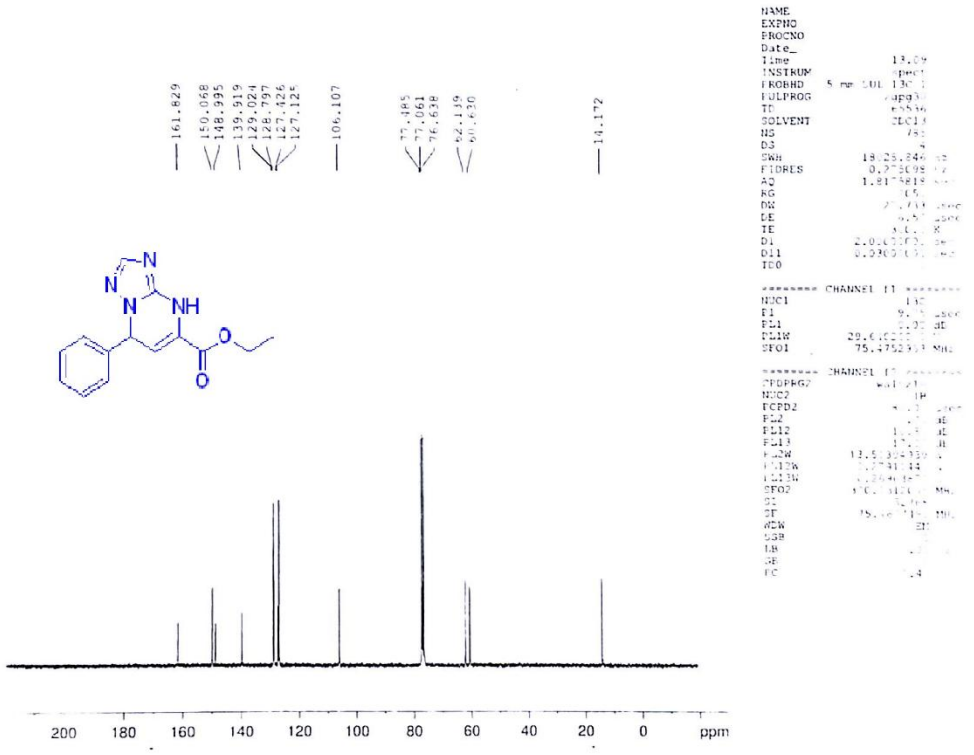

Spectrum 39: ^{1}H NMR for compound 15b

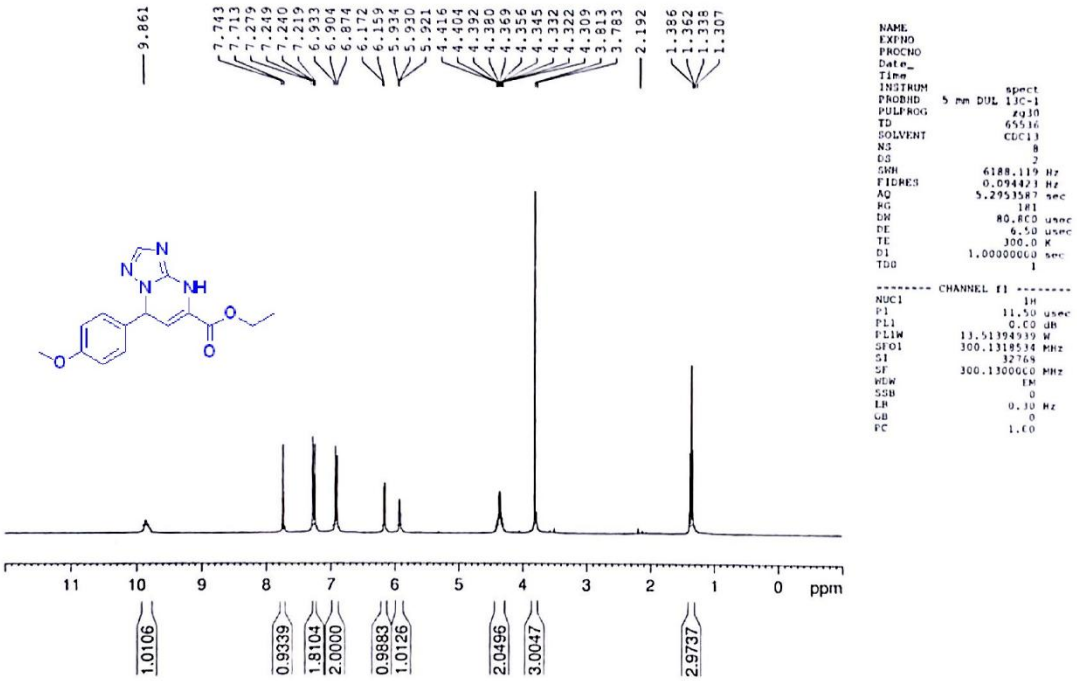

Spectrum 40: ^{13}C for compound 15b

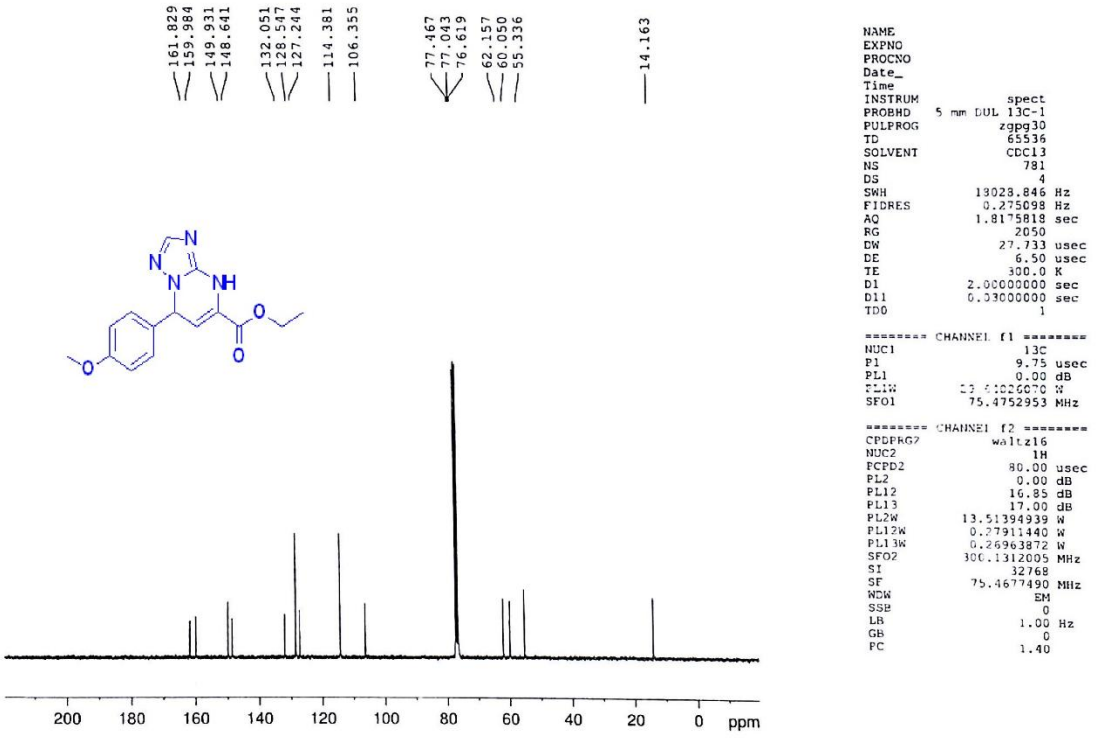

Spectrum 41: ^{1}H NMR compound 15c

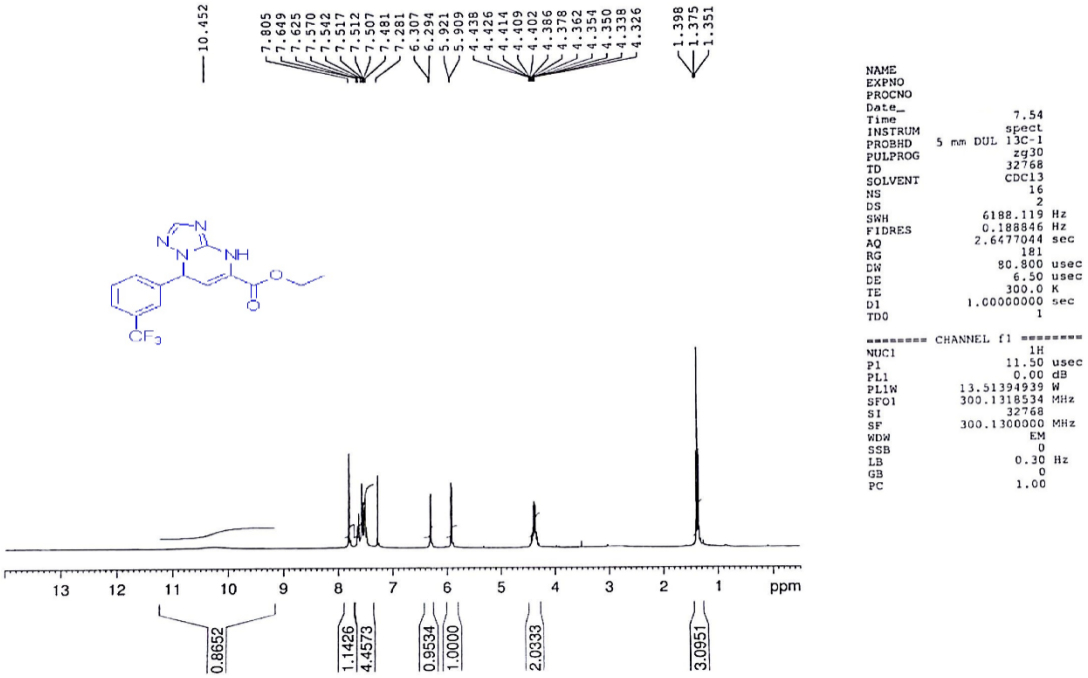

Spectrum 42: ^{13}C NMR for compound 15c

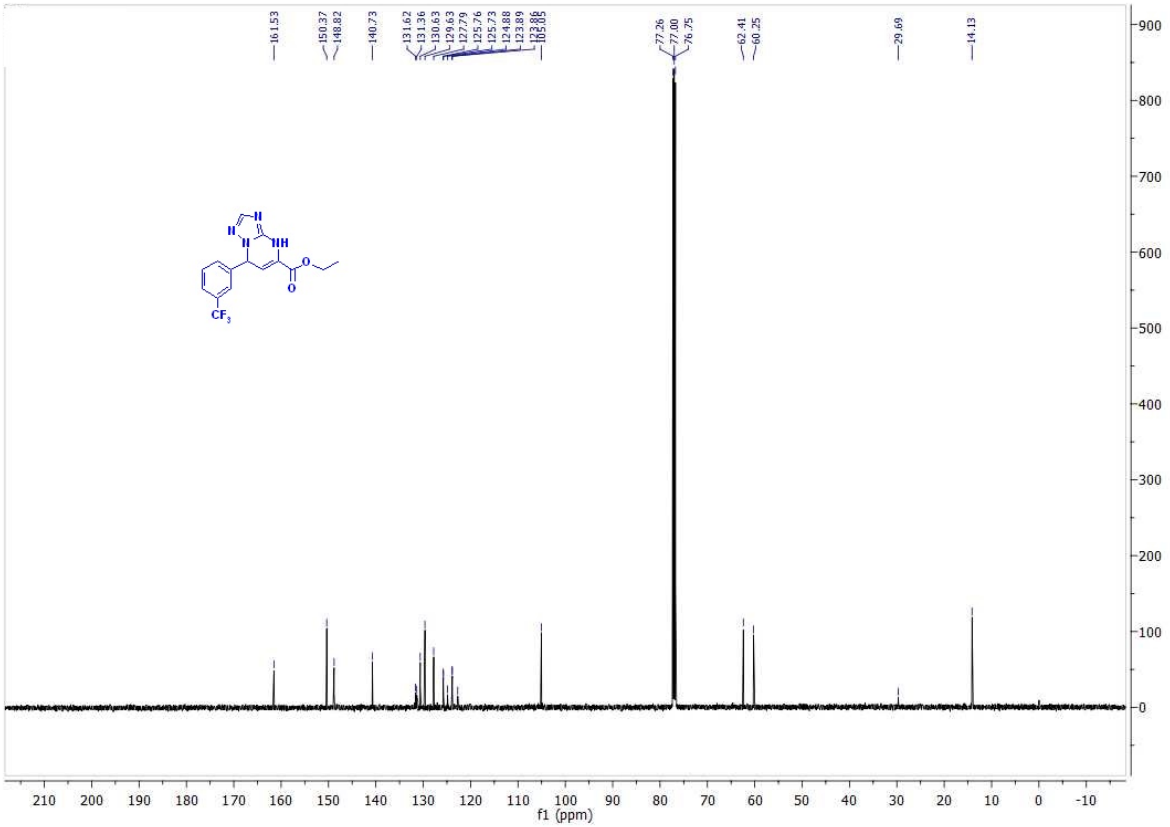

Spectrum 43: ^{1}H NMR for compound 15d

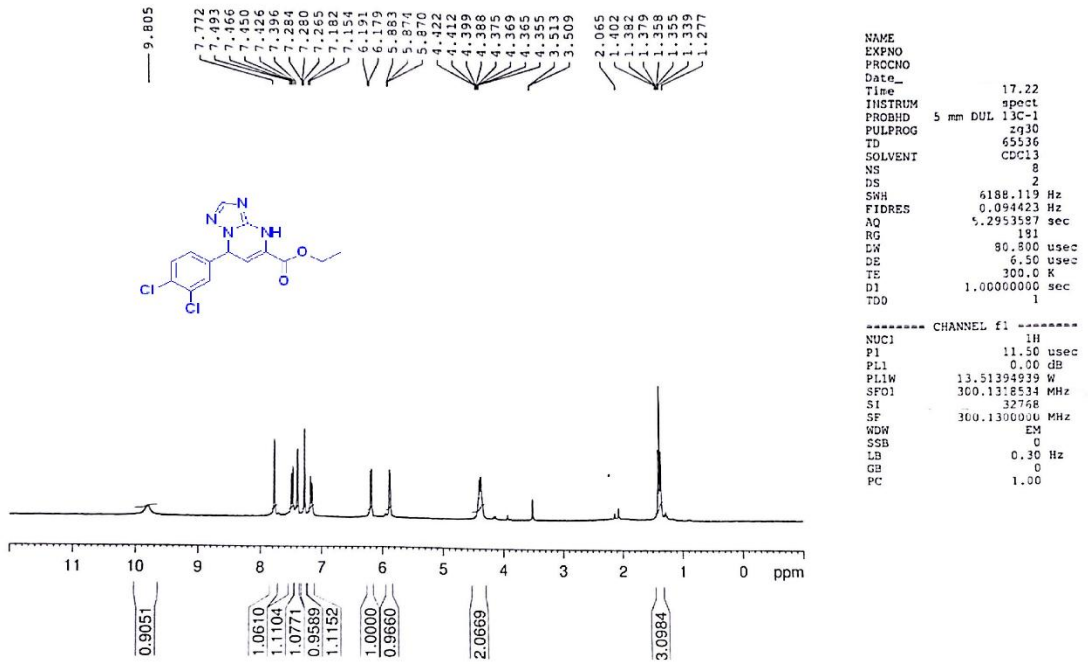

Spectrum 44: ^{13}C NMR for compound 15d

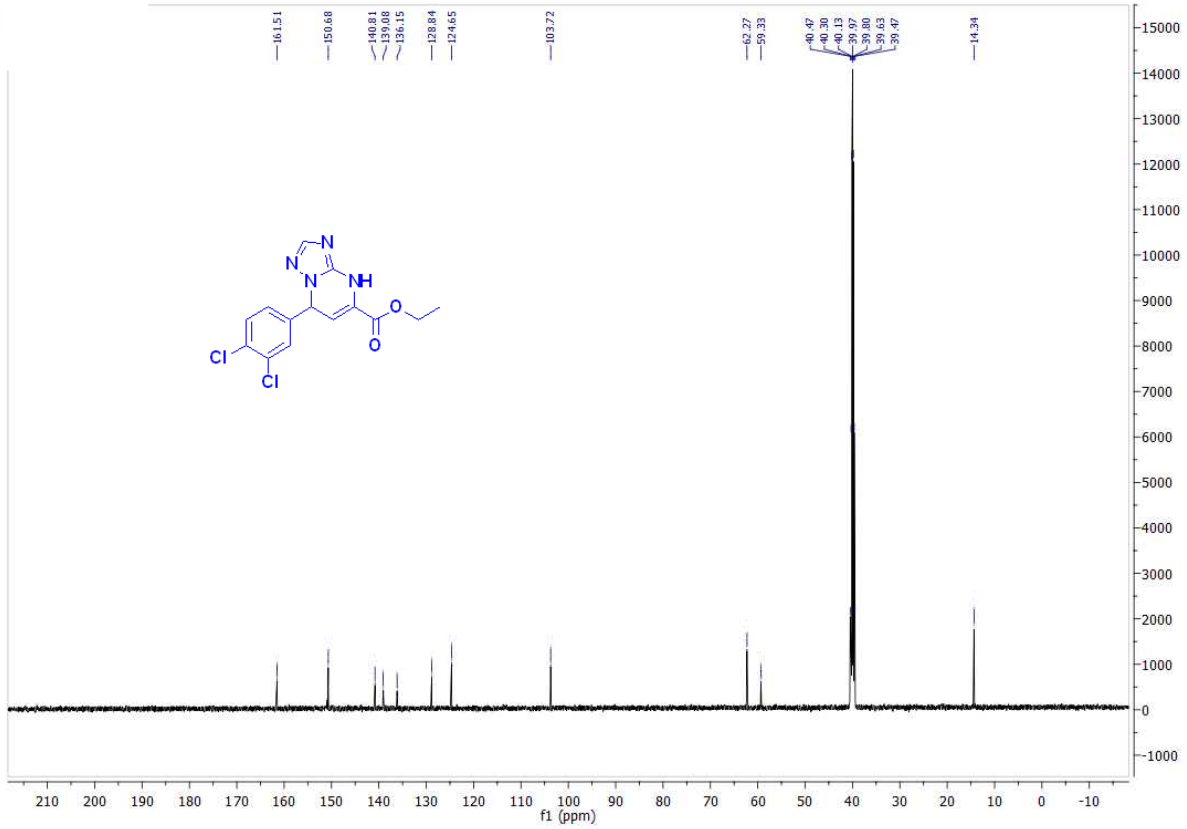

Spectrum 4: ^{1}H NMR for compound 15e

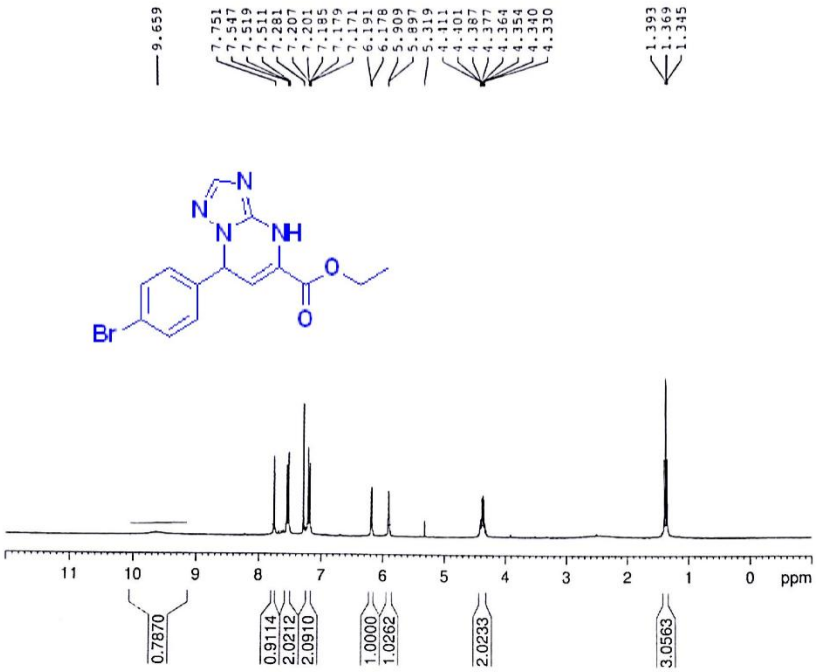


```
NAME
EXPNO
PROCNO
Date_
Time                    15.14
INSTRUM                 spect
PROBHD     5 mm DUL 13C-1
PULPROG                 zg30
TD                      65536
SOLVENT                 CDCl3
NS                          8
DS                          2
SWH                6188.119 Hz
FIDRES             0.094423 Hz
AQ                 5.2953587 sec
RG                        181
DW                   80.800 usec
DE                    6.50 usec
TE                   300.0 K
D1                 1.00000000 sec
TD0                         1

======== CHANNEL f1 ========
NUC1                      1H
P1                     11.50 usec
PL1                     0.00 dB
PL1W               13.51394939 W
SFO1              300.1318534 MHz
SI                      32768
SF                300.1300000 MHz
WDW                        EM
SSB                         0
LB                     0.30 Hz
GB                          0
PC                      1.00
```

Spectrum 46: ^{13}C NMR for compound 15e

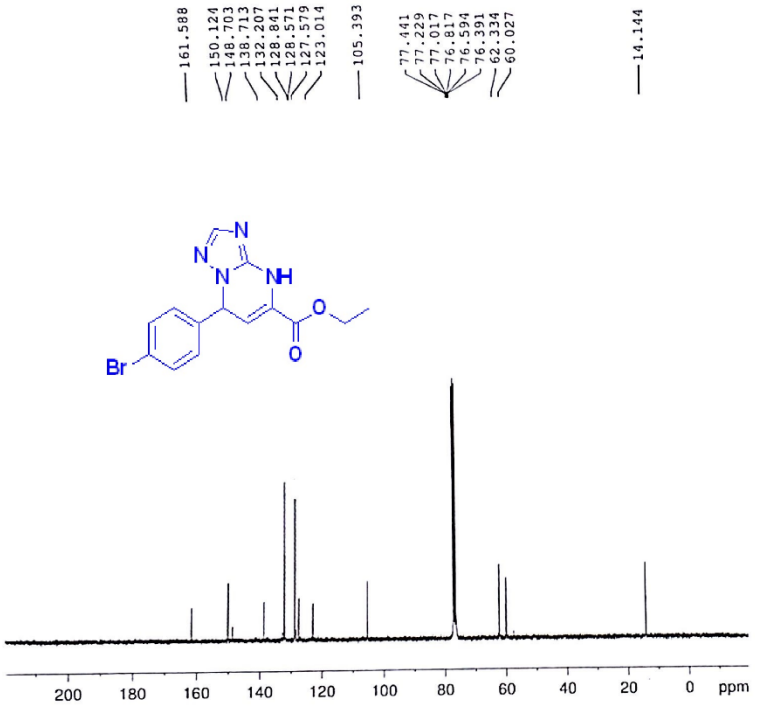


```
NAME
EXPNO
PROCNO
Date_
Time                    18.56
INSTRUM                 spect
PROBHD     5 mm DUL 13C-1
PULPROG                 zgpg30
TD                      32768
SOLVENT                 CDCl3
NS                       1500
DS                          4
SWH               18028.846 Hz
FIDRES             0.550197 Hz
AQ                 0.9088159 sec
RG                        812
DW                   27.733 usec
DE                    6.50 usec
TE                   300.0 K
D1                 2.00000000 sec
D11                0.03000000 sec
TD0                         1

======== CHANNEL f1 ========
NUC1                      13C
P1                      9.75 usec
PL1                     0.00 dB
PL1W               29.64026070 W
SFO1               75.4752953 MHz

======== CHANNEL f2 ========
CPDPRG2                 waltz16
NUC2                      1H
PCPD2                  80.00 usec
PL2                     0.00 dB
PL12                   16.85 dB
PL13                   17.00 dB
PL2W               13.51394939 W
PL12W              0.27911440 W
PL13W              0.26963872 W
SFO2              300.1312005 MHz
SI                      32768
SF                 75.4677490 MHz
WDW                        EM
SSB                         0
LB                     1.00 Hz
GB                          0
PC                      1.40
```

Spectrum 47: ^{1}H NMR for compound 15f

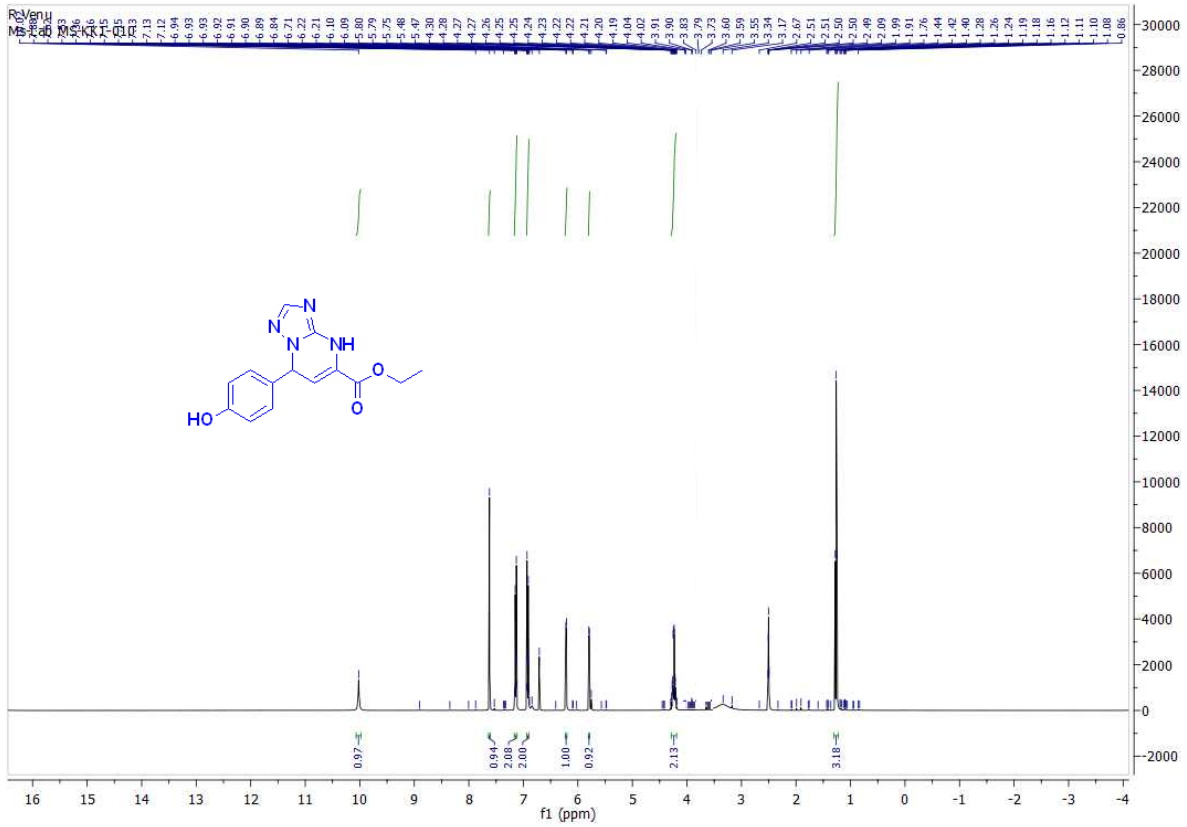

Spectrum 48: ^{13}C NMR for compound 15f

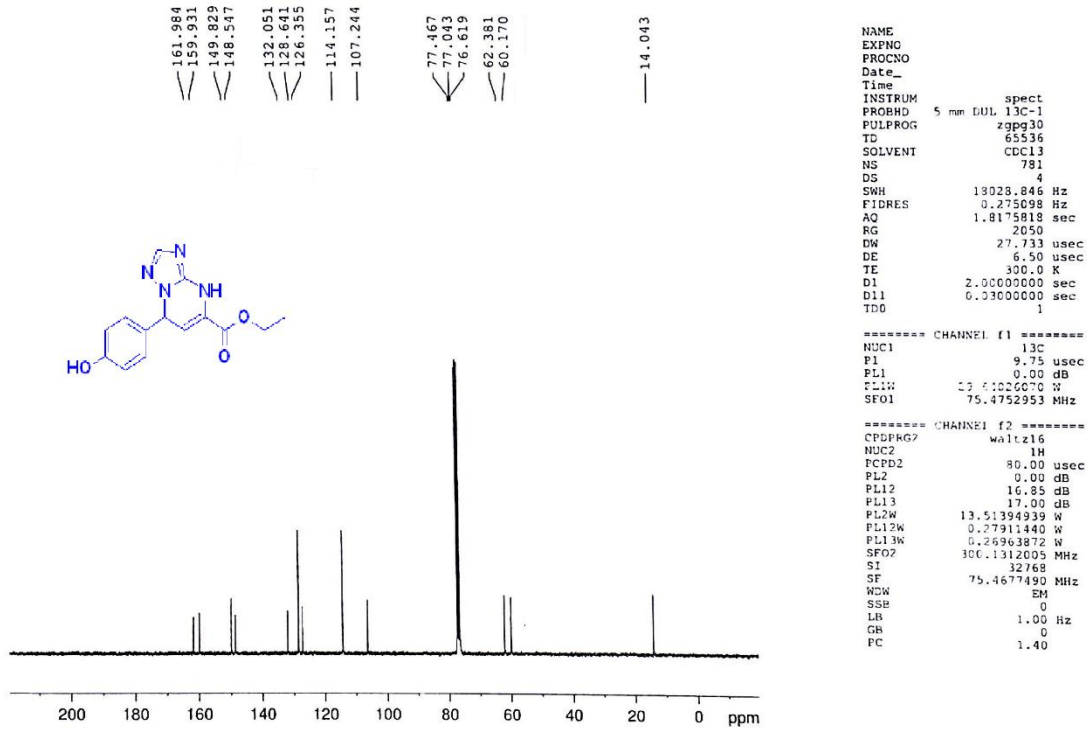

NAME	
EXPNO	
PROCNO	
Date_	
Time	
INSTRUM	spect
PROBHD	5 mm DUL 13C-1
PULPROG	zgpg30
TD	65536
SOLVENT	CDCl3
NS	781
DS	4
SWH	18028.846 Hz
FIDRES	0.275098 Hz
AQ	1.8175818 sec
RG	2050
DW	27.733 usec
DE	6.50 usec
TE	300.0 K
D1	2.00000000 sec
D11	0.03000000 sec
TD0	1
======== CHANNEL f1 ========	
NUC1	13C
P1	9.75 usec
PL1	0.00 dB
PLIW	53.61026070 W
SFO1	75.4752953 MHz
======== CHANNEL f2 ========	
CPDPRG2	waltz16
NUC2	1H
PCPD2	80.00 usec
PL2	0.00 dB
PL12	16.85 dB
PL13	17.00 dB
PL2W	13.51394939 W
PL12W	0.27911440 W
PL13W	0.26963872 W
SFO2	300.1312005 MHz
SI	32768
SF	75.4677490 MHz
WDW	EM
SSB	0
LB	1.00 Hz
GB	0
PC	1.40

Spectrum 49: ^{1}H NMR for compound 15g

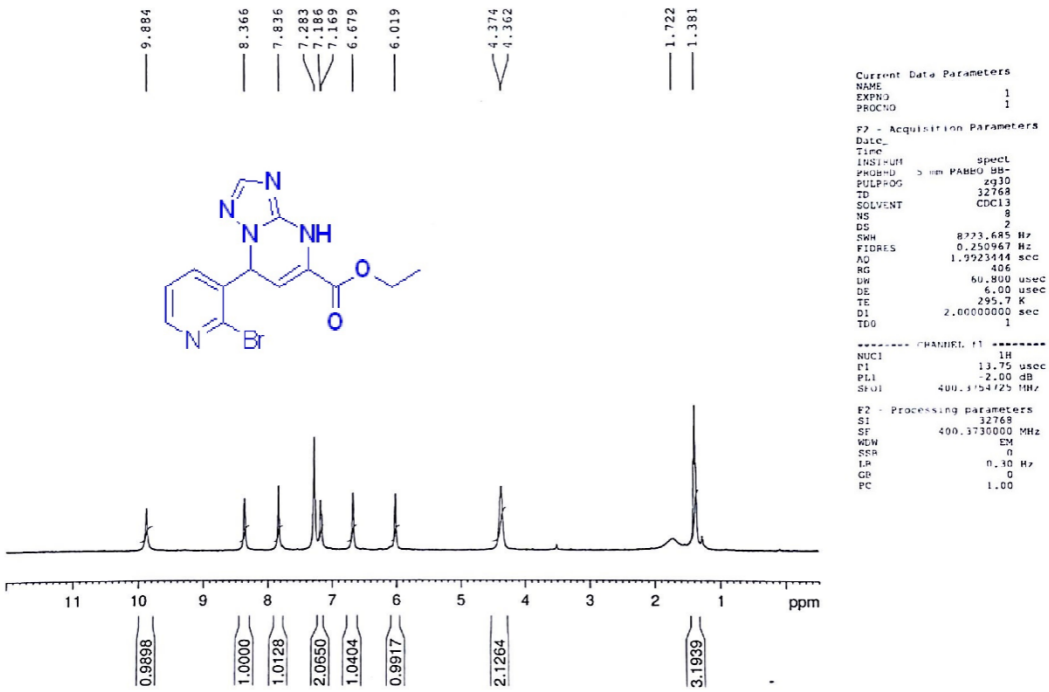

Spectrum 50: ^{13}C NMR for compound 15g

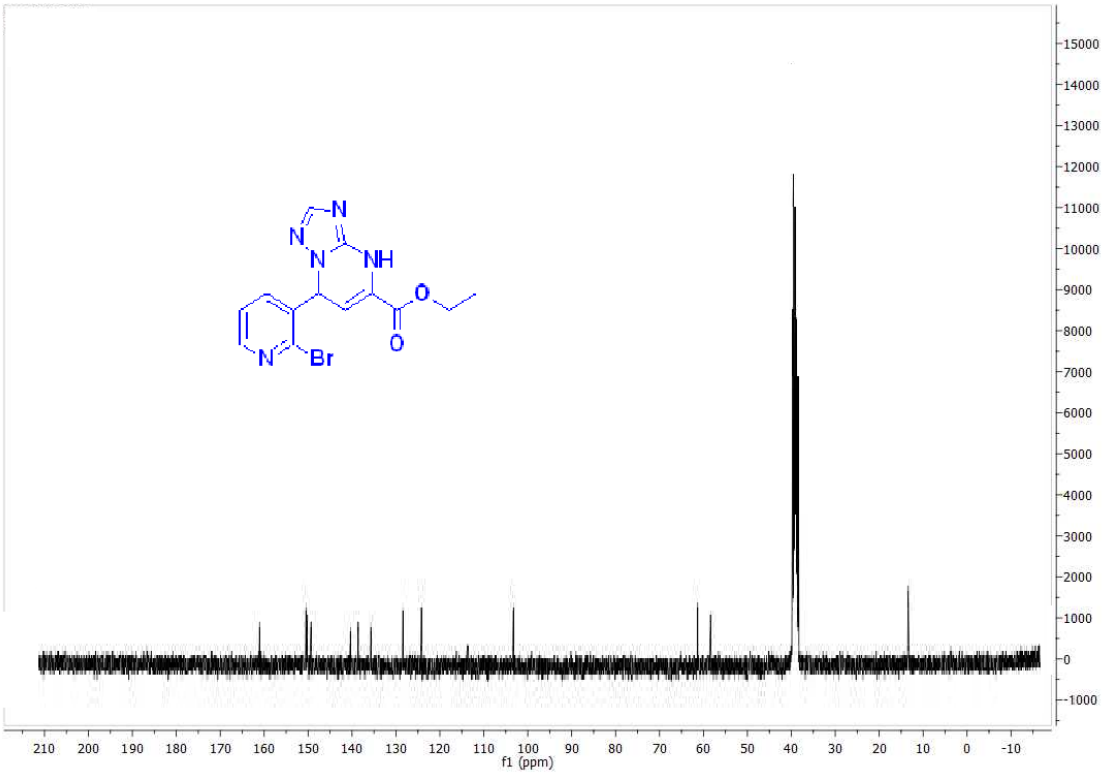

Spectrum 51: ^{1}H NMR for compound 15h

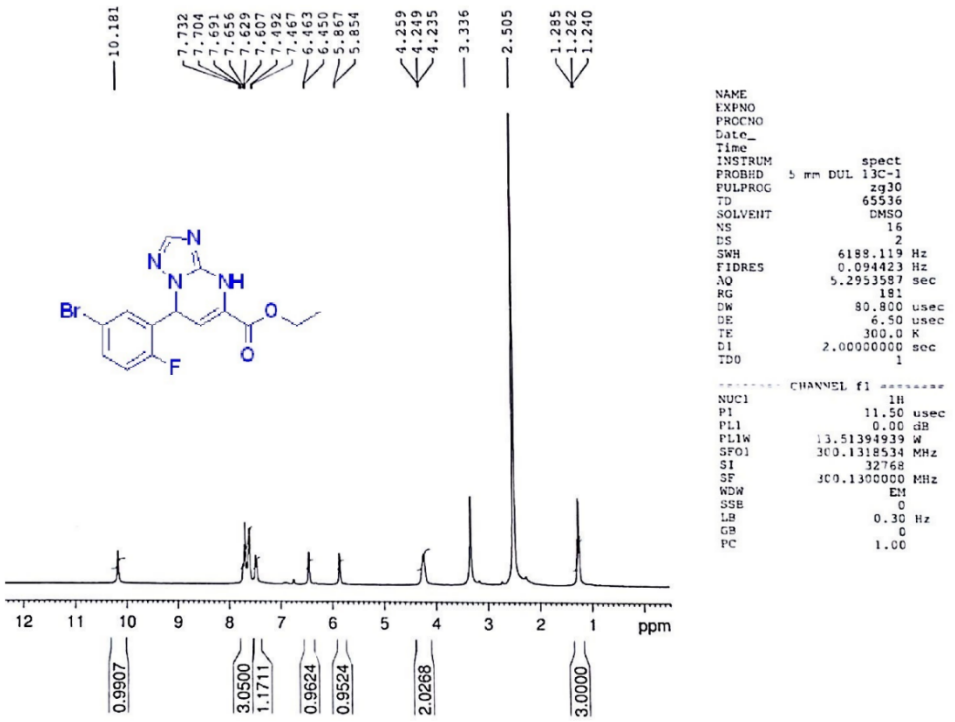

Spectrum 52: ^{13}C NMR for compound 15h (DMSO-*d6*)

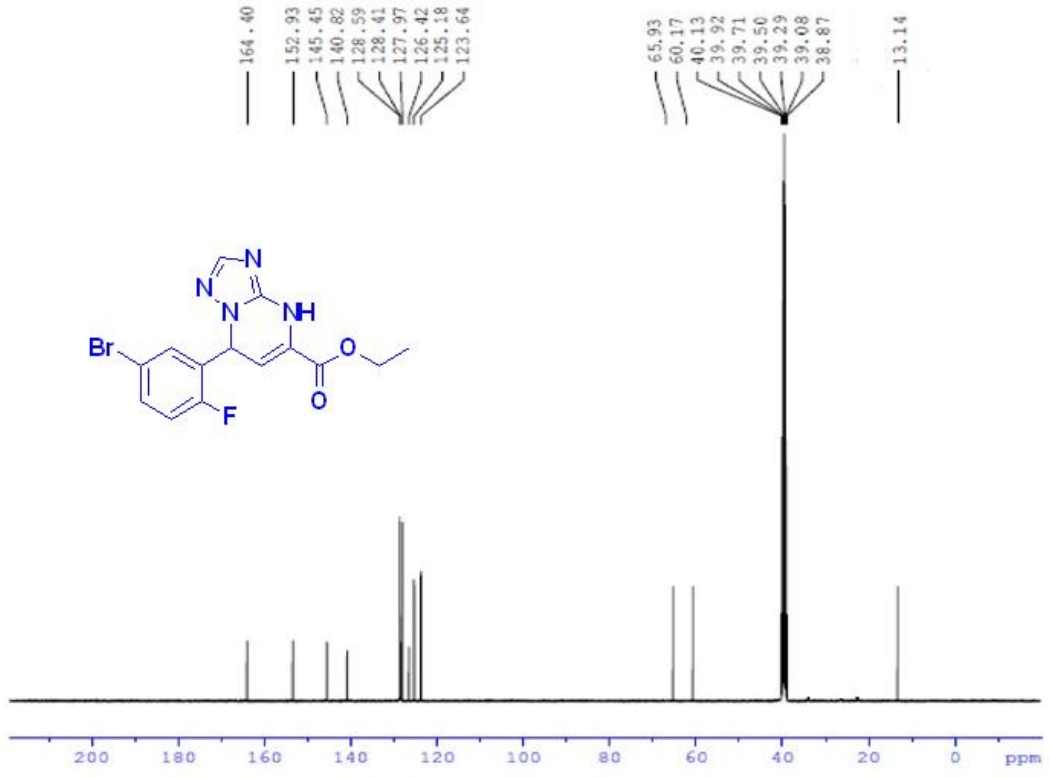

Spectrum 53: ^{1}H NMR for compound 16a

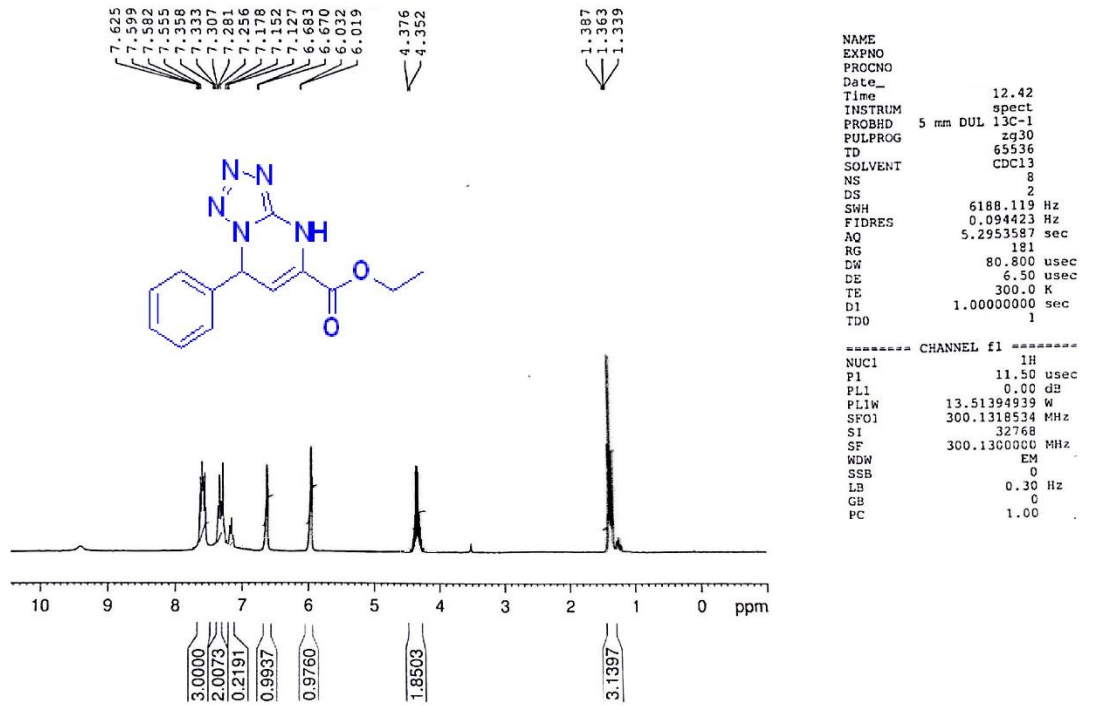

Spectrum 54: ^{1}H NMR for compound 16b

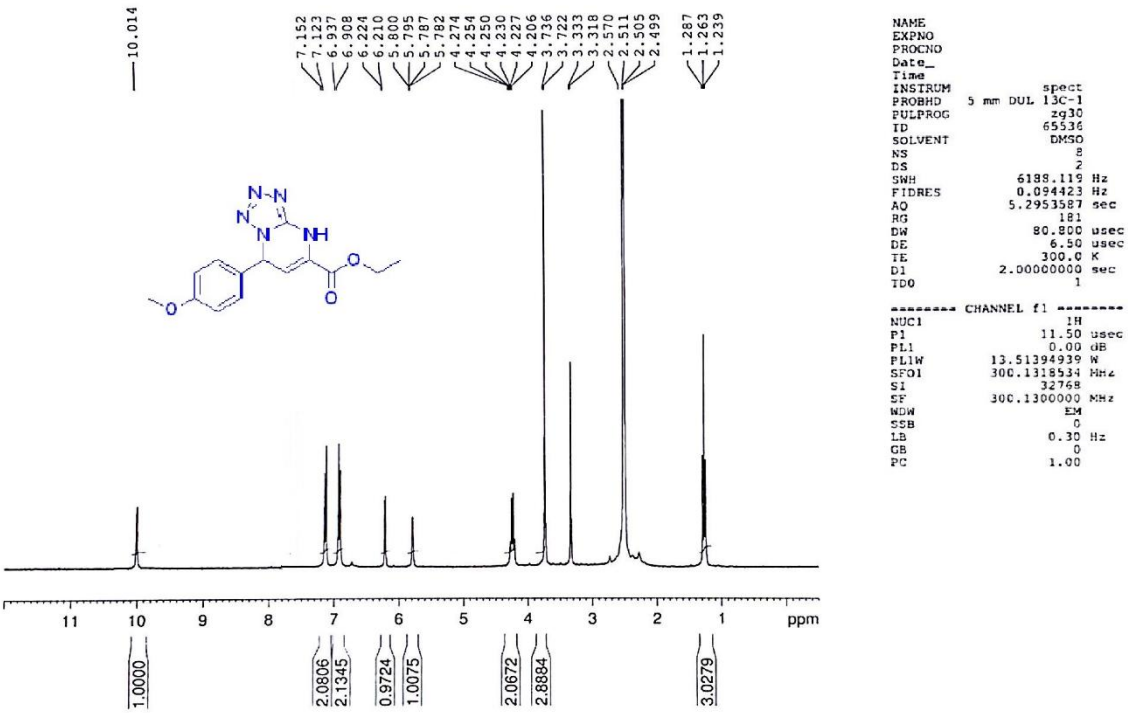

Spectrum 55: ^{1}H NMR of Compound 19a

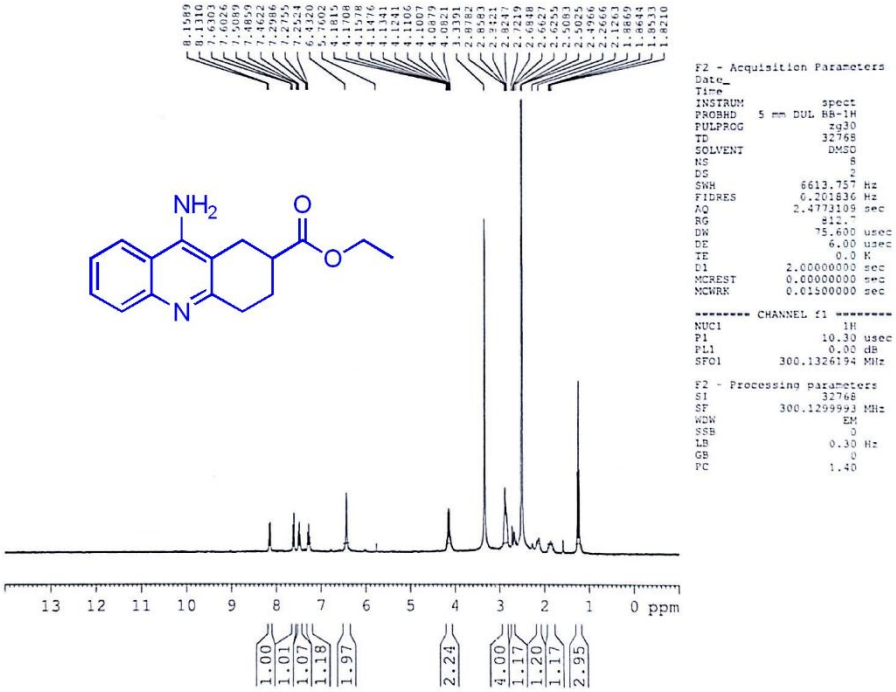

F2 - Acquisition Parameters
Date_
Time
INSTRUM spect
PROBHD 5 mm DUL BB-1H
PULPROG zg30
TD 32768
SOLVENT DMSO
NS 8
DS 2
SWH 6613.757 Hz
FIDRES 0.201836 Hz
AQ 2.4773109 sec
RG 812.7
DW 75.600 usec
DE 6.00 usec
TE 0.0 K
D1 2.00000000 sec
MCREST 0.00000000 sec
MCWRK 0.01500000 sec

-------- CHANNEL f1 --------
NUC1 1H
P1 10.30 usec
PL1 0.00 dB
SFO1 300.1326194 MHz

F2 - Processing parameters
SI 32768
SF 300.1299991 MHz
WDW EM
SSB 0
LB 0.30 Hz
GB 0
PC 1.40

Spectrum 56:LCMS of compound 19a

Method info :

A: 95% Water: 5% Acetonitrile;10mM NH4OAC
B: 5% Water:95% Acetonitrile;10mM NH4OAC
Flow: 1.1 ml/min
Temp :50°C
Column: Ascentis Express C18 (50x2.1)mm ,2.7µm
Time (min) : 0---3
%B : 0---100

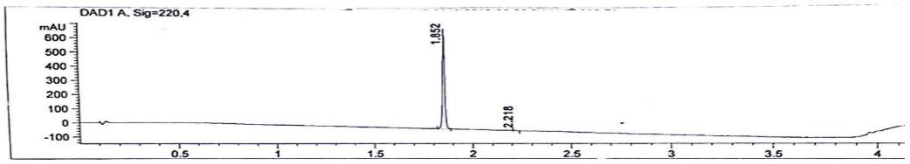

#	Meas. R	Area	Area %
1	1.852	543.249	97.844
2	2.218	11.969	2.156

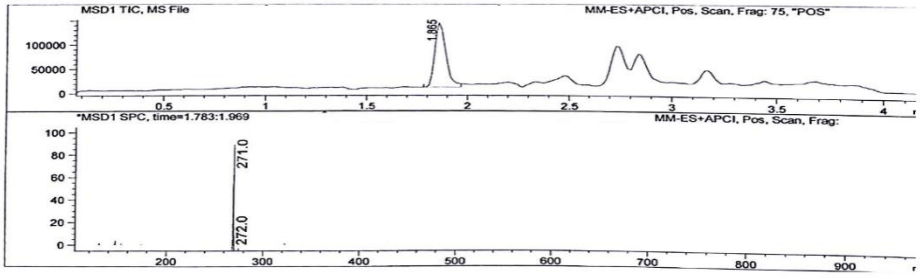

Spectrum 57: ^{1}H NMR of compound 19b

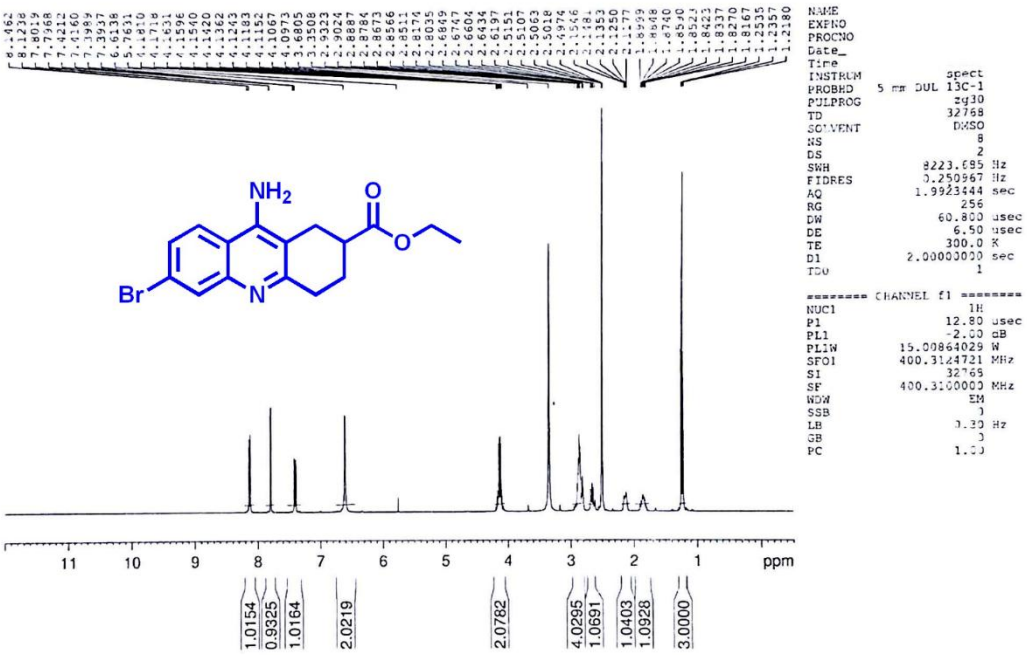

Spectrum 58: ^{1}H NMR of compound 19c

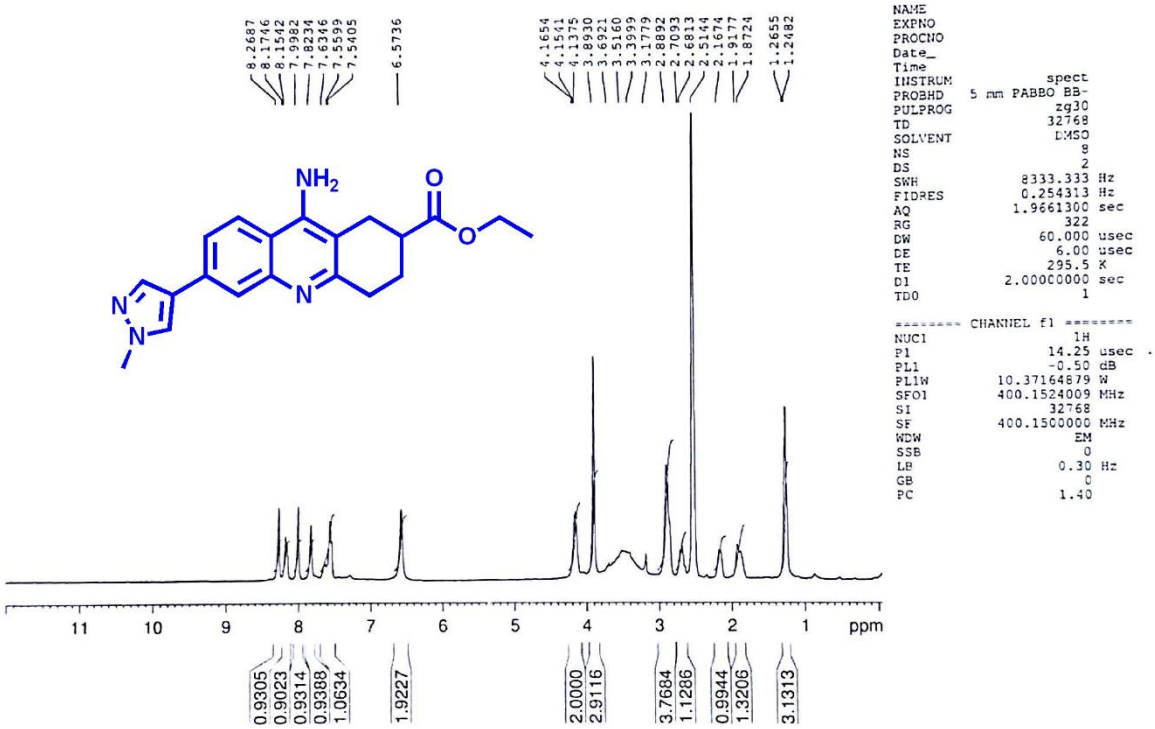

Spectrum 59: ^{1}H NMR of compound 20a

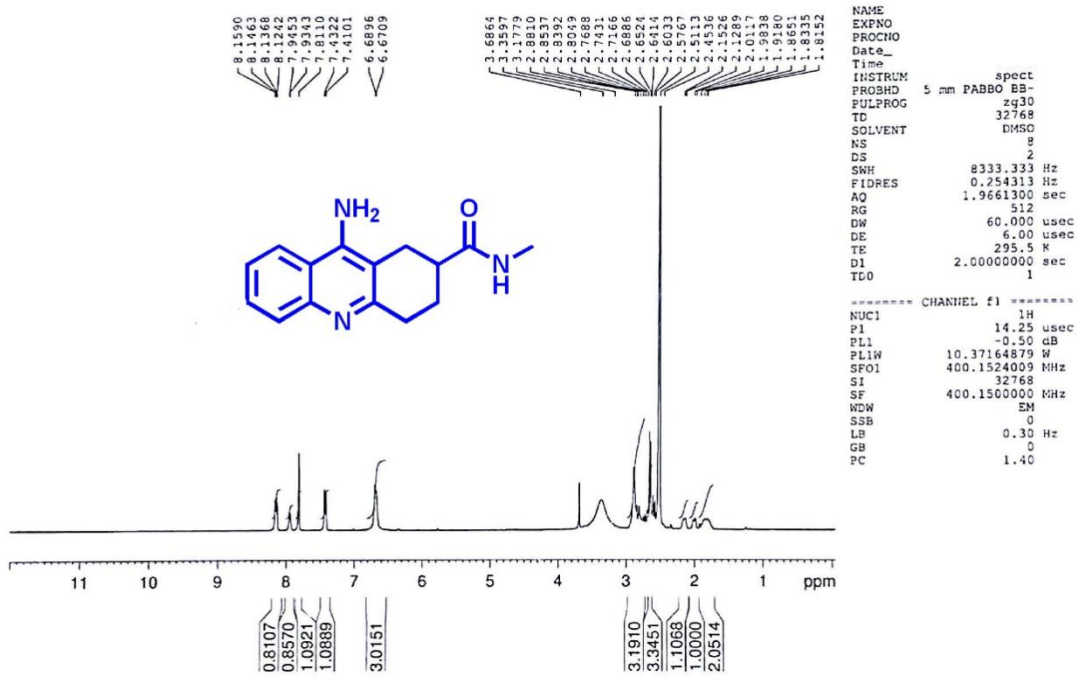

Spectrum 60: LCMS of compound 20a

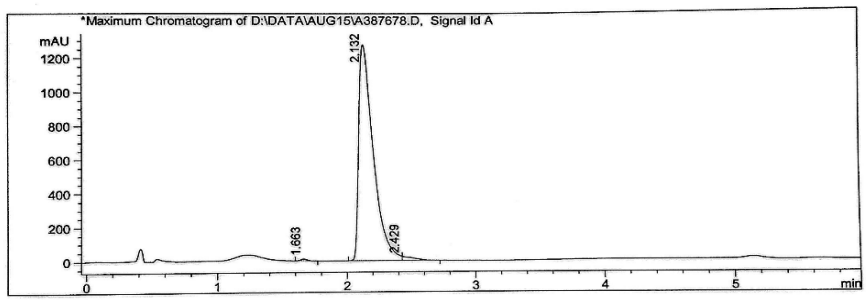

Peak No	RT min	Area	Area %
1	1.663	4.552e+001	0.442
2	2.132	1.010e+004	98.073
3	2.429	1.529e+002	1.485

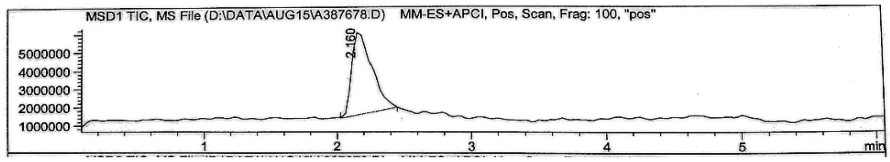

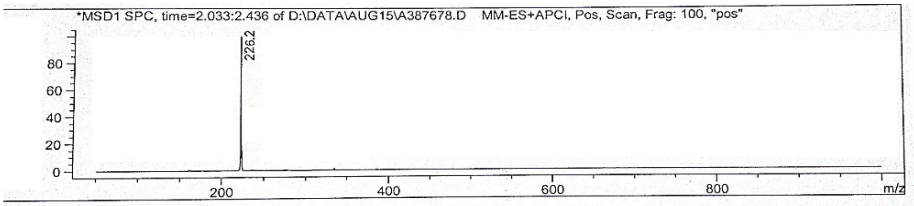

Spectrum 61: ^{1}H NMR of compound 20c

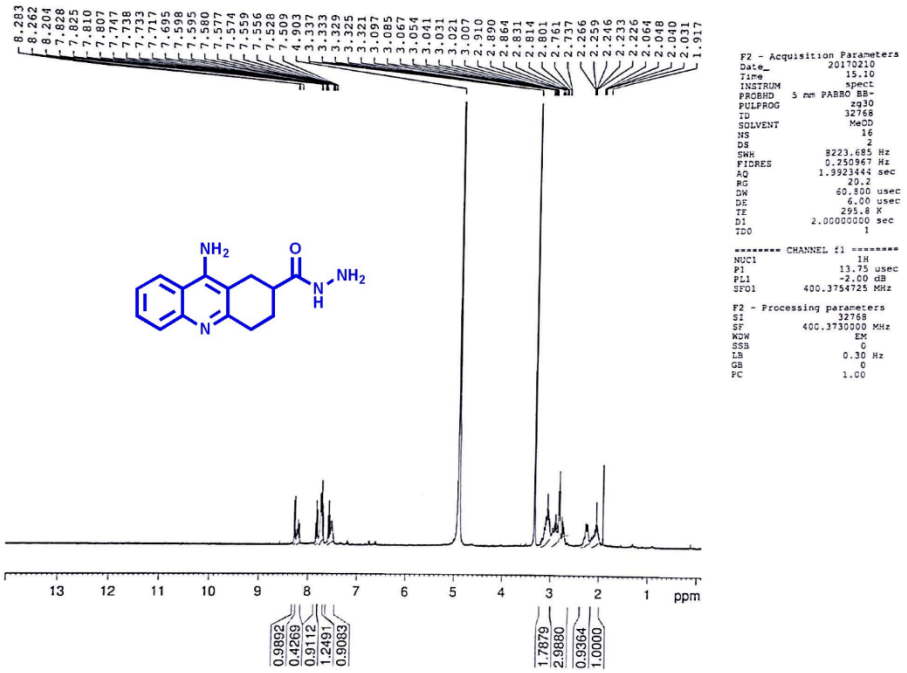

Spectrum 62: ^{1}H NMR of compound 20d

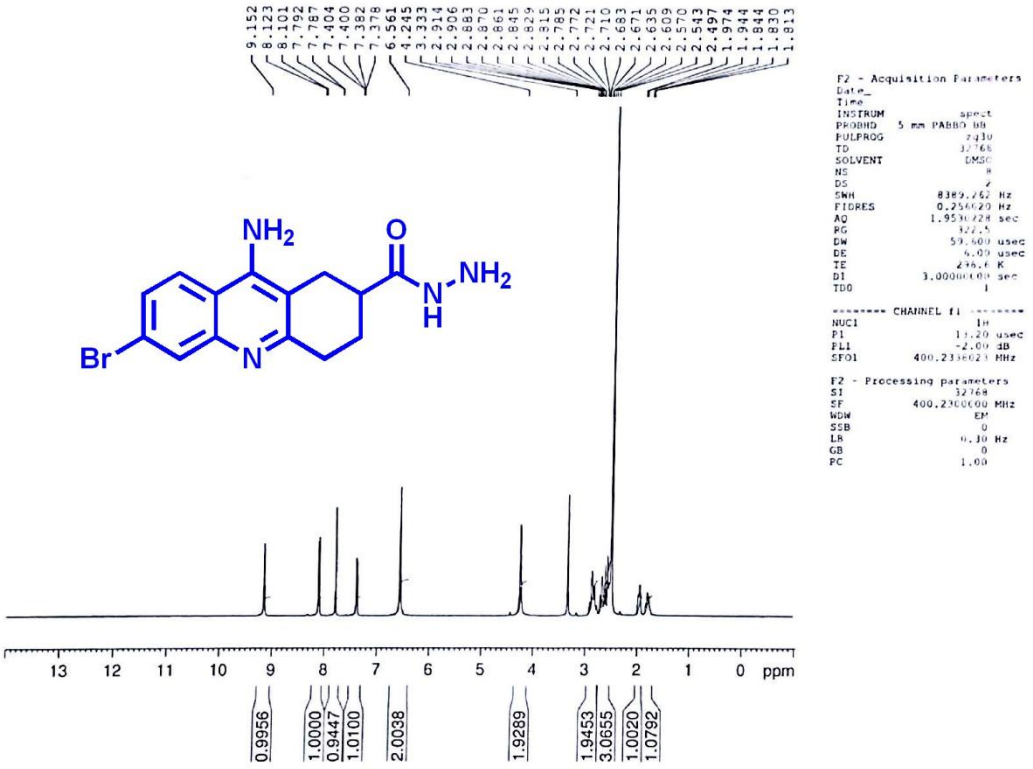

Spectrum 63: ^{1}H NMR of compound 21a

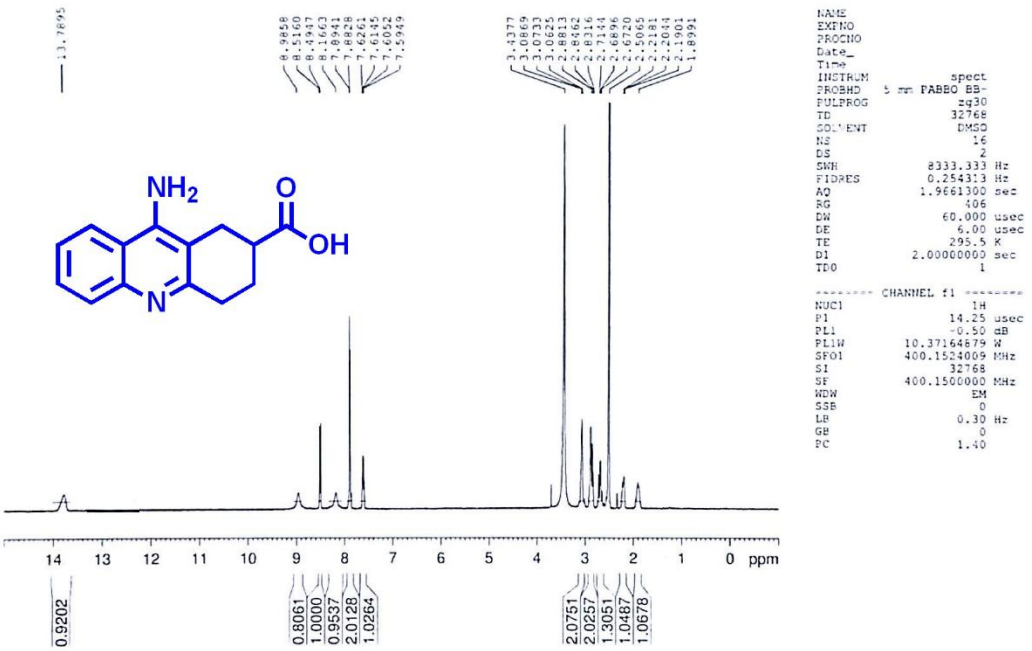

Spectrum 64: ^{1}H NMR of compound 21b

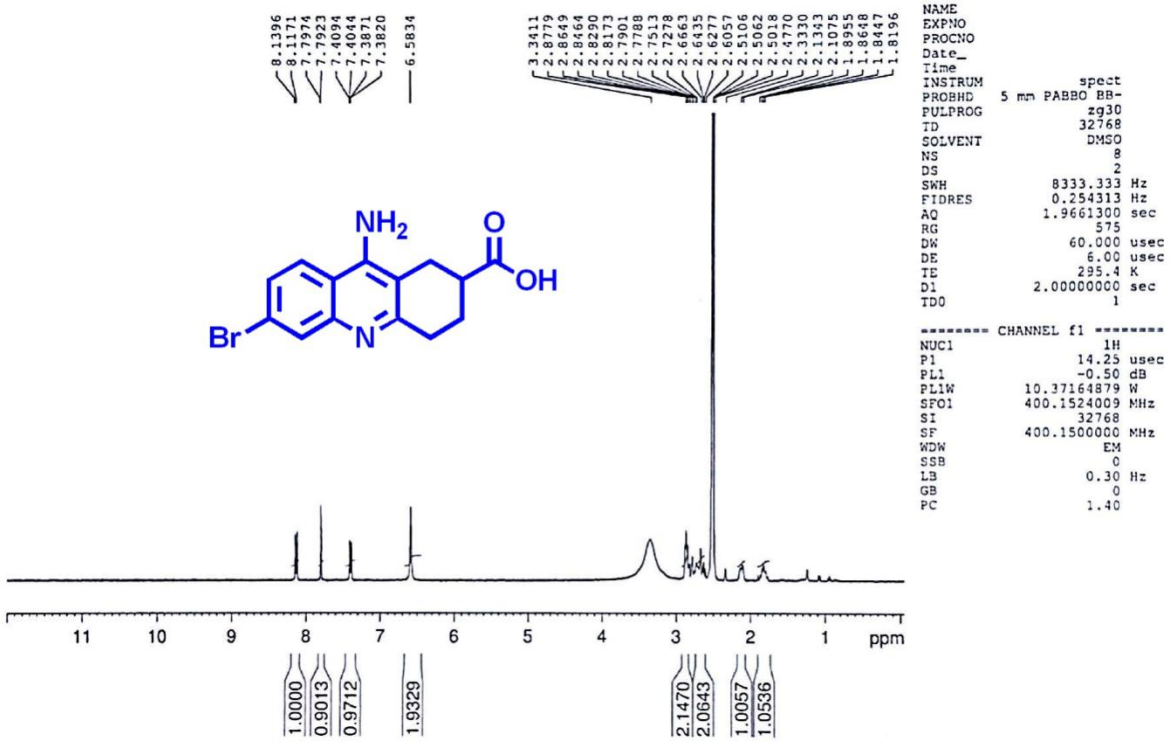

Spectrum 65: ^{1}H NMR of compound 21c

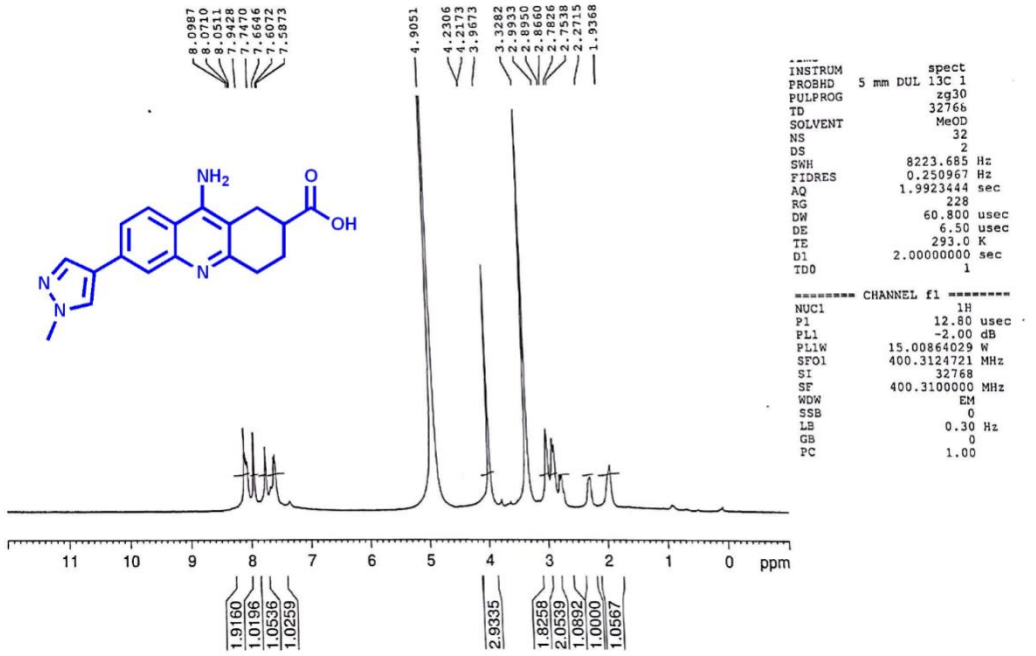

Spectrum 66: ^{1}H NMR of compound 22a

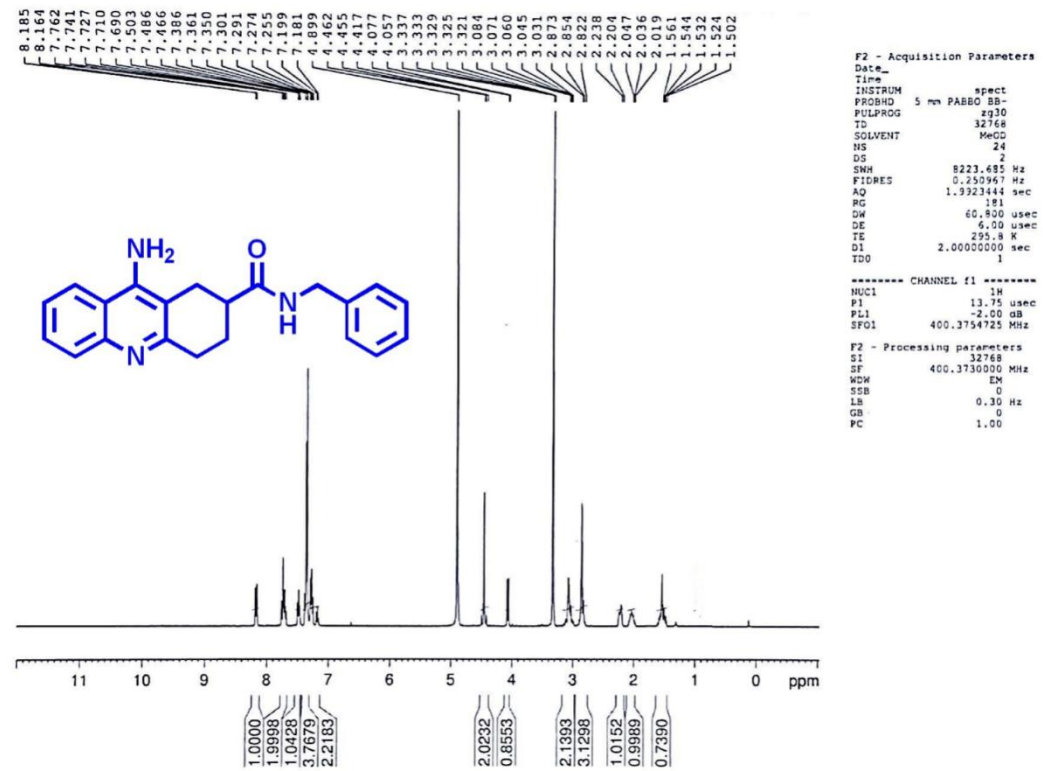

Spectrum 67: ^{1}H NMR of compound 22b

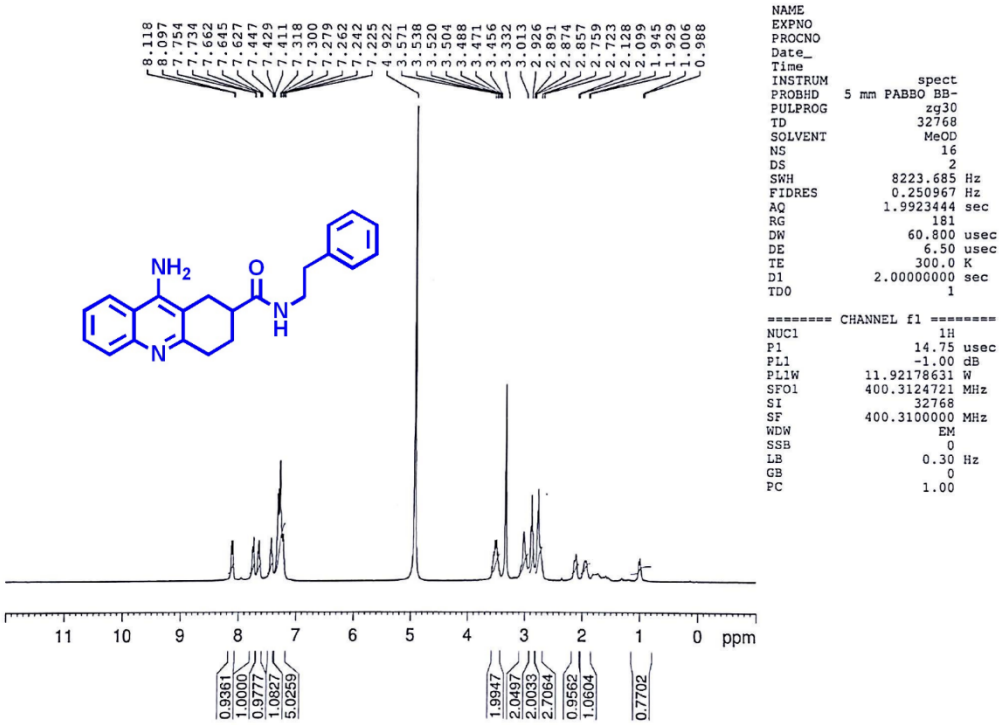

Spectrum 68: ^{1}H NMR of compound 22c

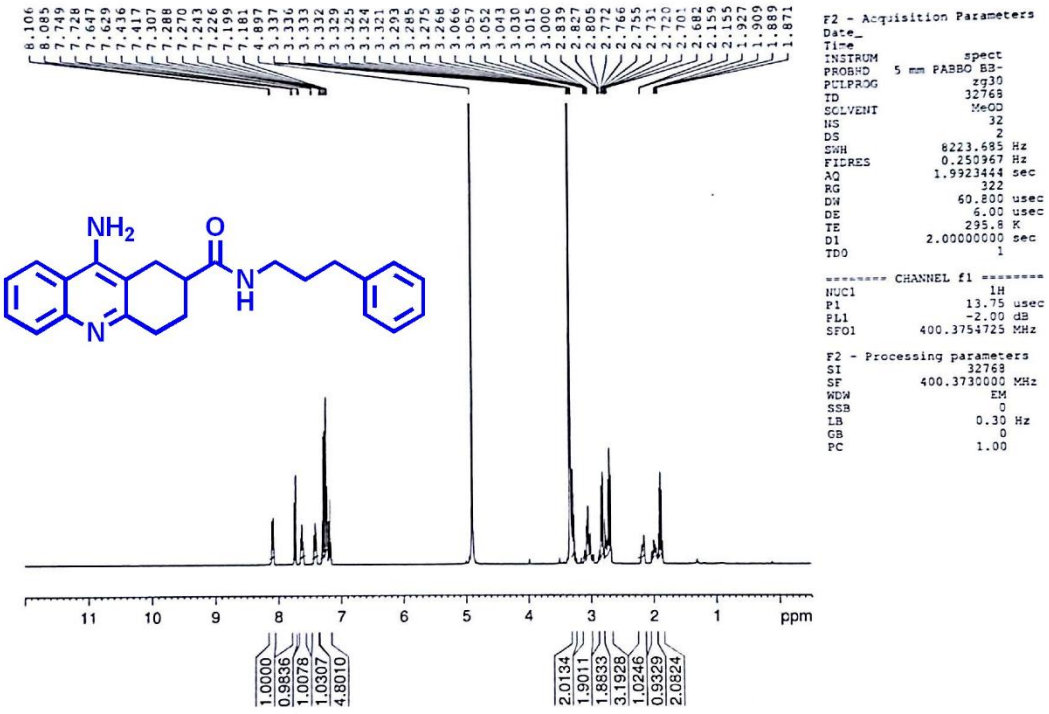

Spectrum 69: ^{1}H NMR of compound 22e

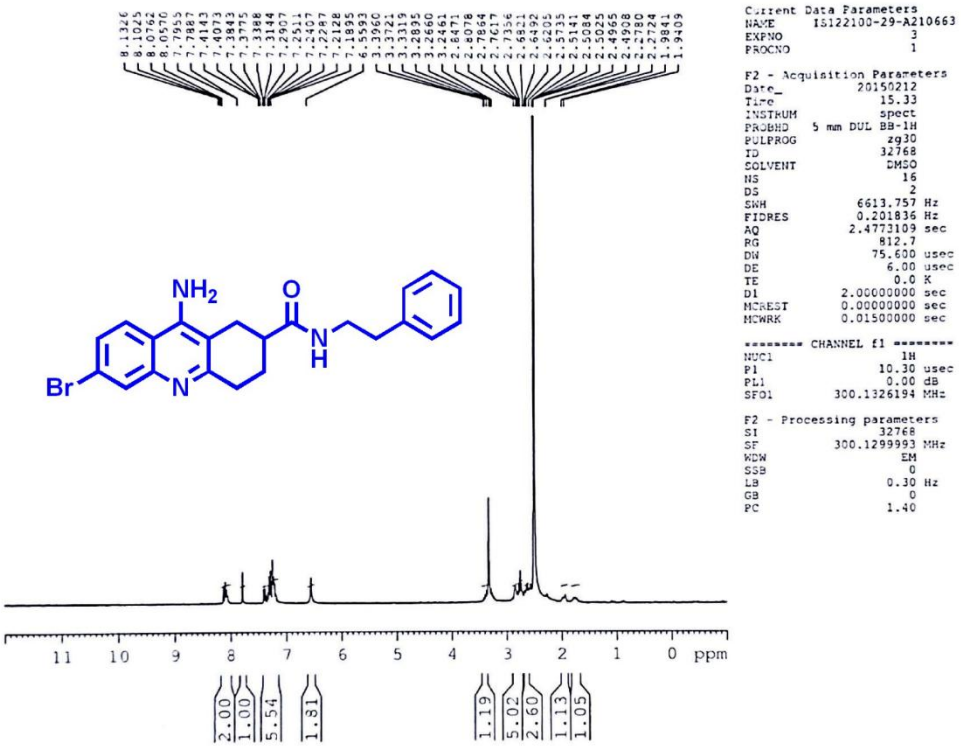

Spectrum 70: ^{1}H NMR of compound 22f

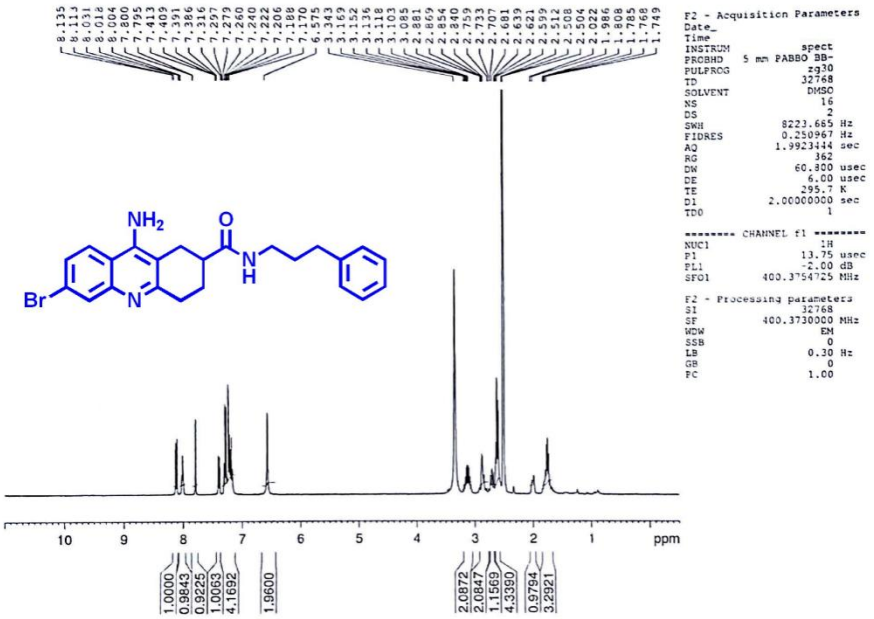

Spectrum 71: ^{1}H NMR of compound 22g

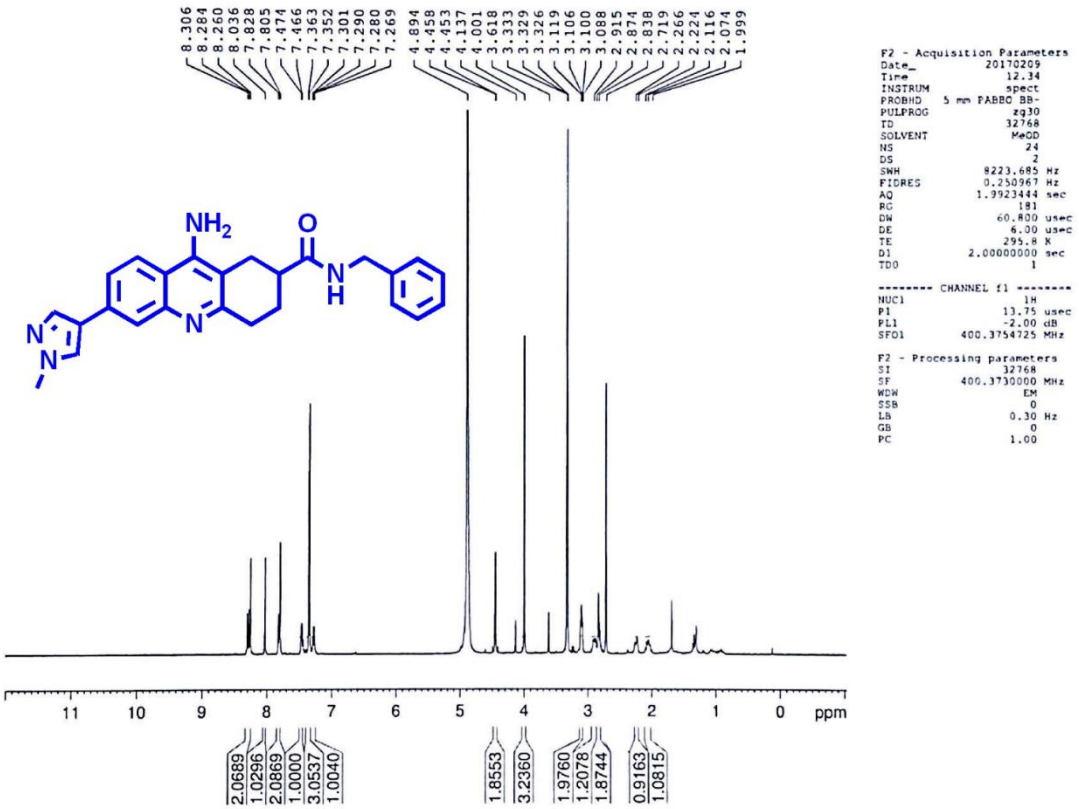

Spectrum 72: ^{1}H NMR of compound 22h

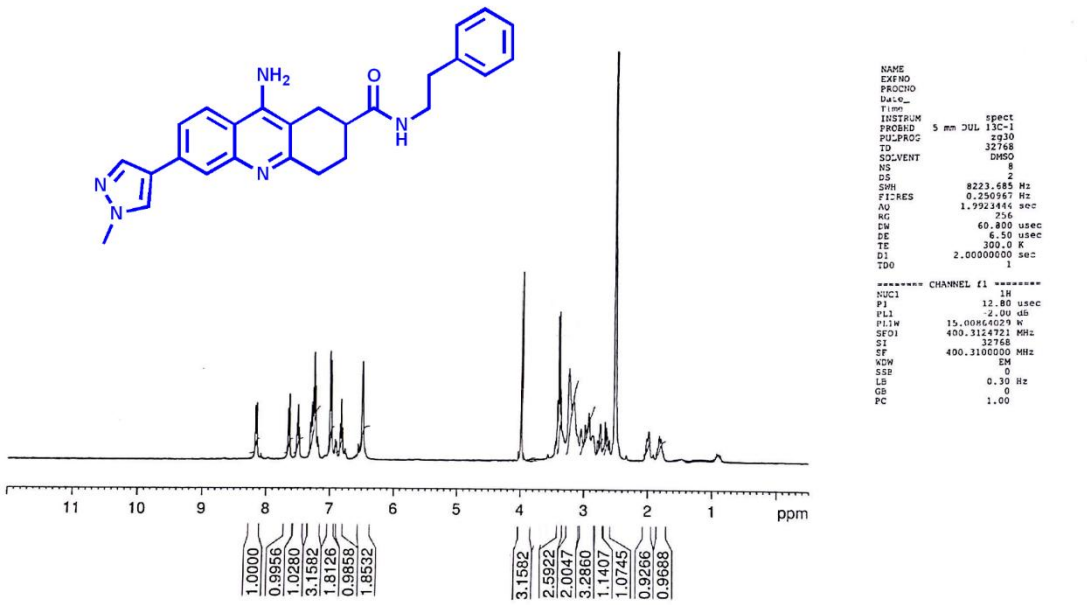

Spectrum 73: ^{1}H NMR of compound 22i

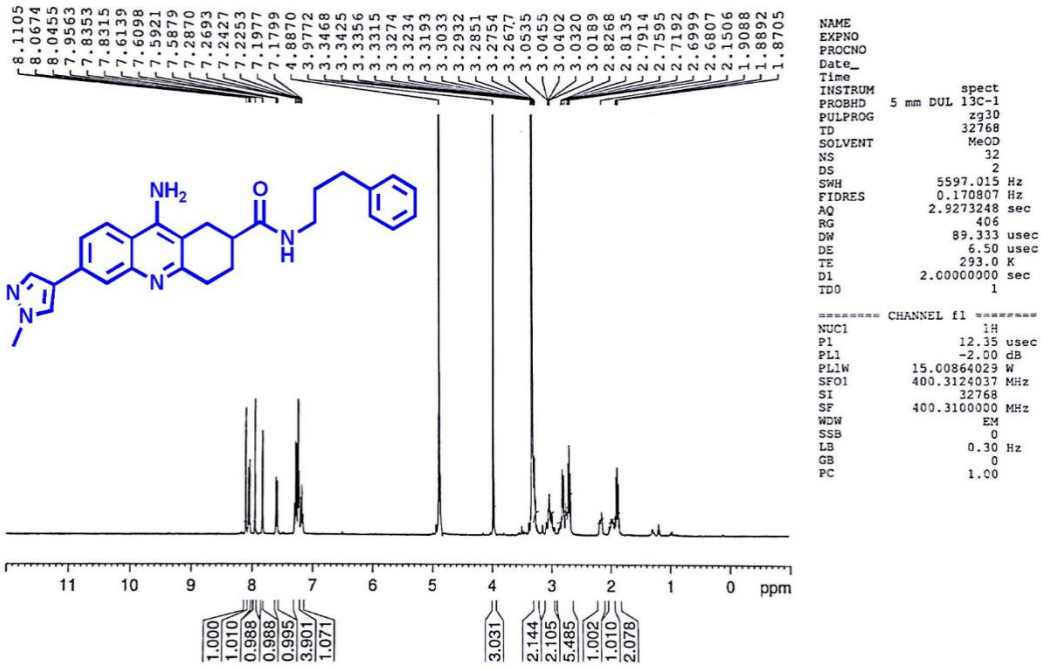

Spectrum 74: ^{1}H NMR of compound 22j

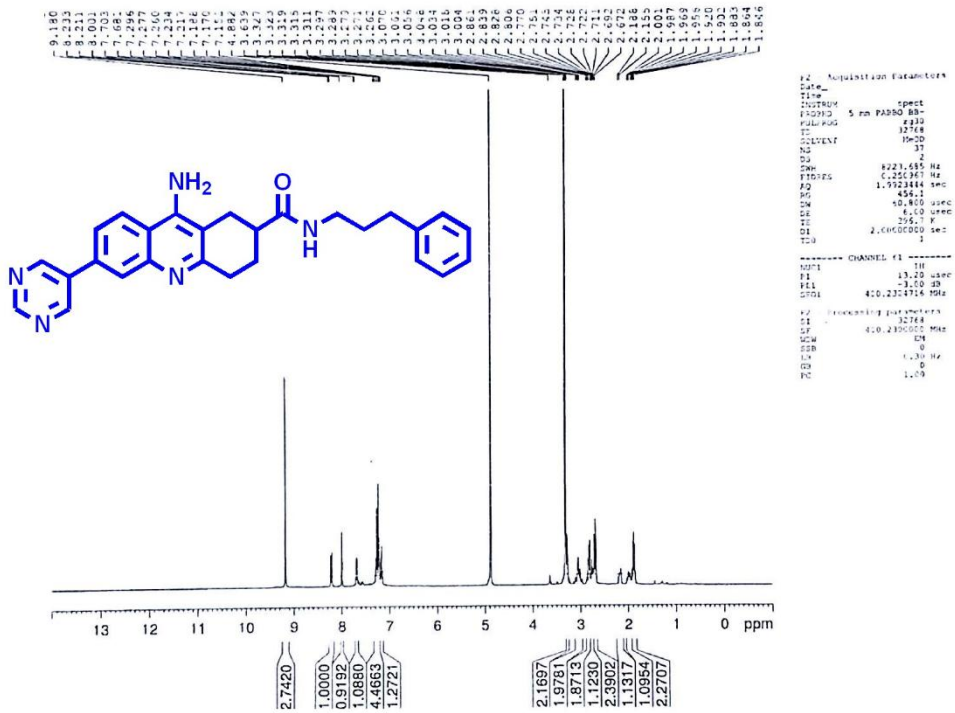

Spectrum 75: ^{1}H NMR of compound 23a

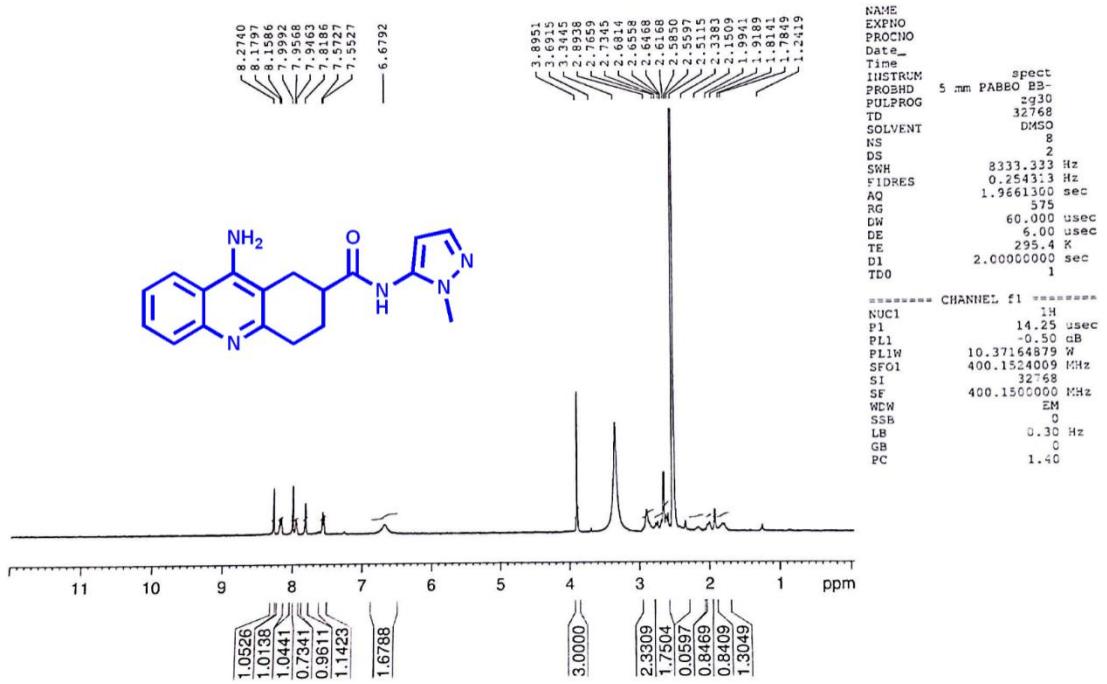

Spectrum 76: ^{1}H NMR of compound 23b

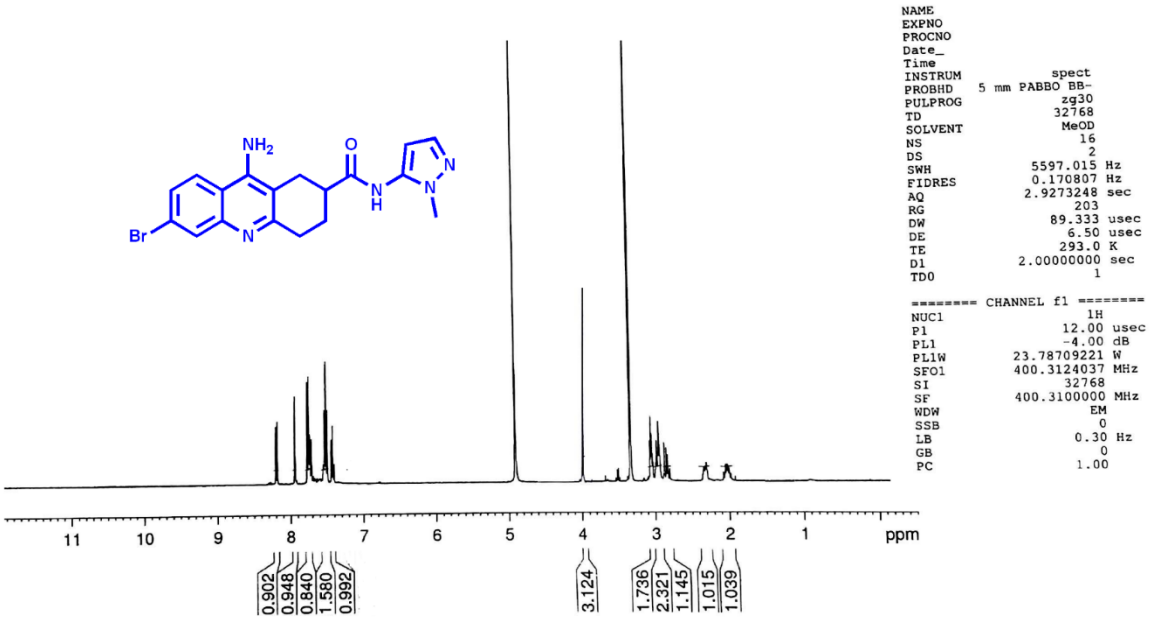

LIST OF PUBLICATIONS

- Novel tacrine derivatives exhibiting improved acetylcholinesterase inhibition: Design, synthesis and biological evaluation; **Eeda Koti Reddy**, Chandran Remya, Kumar Mantosh, Ayyiliath M. Sajith, R.V. Omkumar, C. Sadasivan, Shaik Anwar;***Eur. J. Med. Chem*** **139 (2017) 367-377;** DOI: 10.1016/j.ejmech.2017.08.013; ***Impact Factor 4.519.***

- **Eeda Koti Reddy**, Remya C., Ayyiliath M. Sajith, Dileep K. V., Sadasivan C, and **Shaik Anwar***, Functionalised dihydroazo pyrimidine derivatives from Morita–Baylis–Hillman acetates: synthesis and studies against acetylcholinesterase as its inhibitors; ***RSC Adv., 2016, 6, 77431;*** ISSN 2046-2069***; Impact Factor 3.289*.**

- Bhaskaran Savitha, Ayyiliath M. Sajith, **Eeda Koti Reddy**, C. S. Ananda Kumar, and M. Syed Ali Padusha; Suzuki-Miyaura cross–coupling reaction in water: facile synthesis of (hetero) aryl uracil bases using potassiumorganotrifluoroborates under microwave irradiation.***ChemistrySelect (Wiley) 2016, 1, 4721 – 4725;*** ISSN 2365-6549.

Curriculum Vitae

Koti Reddy Eeda

Syngene International Ltd,
A Biocon company,
Bangalore, India.

Phone: +91-8884300505
E-mail: ekr.chem@gmail.com
koti.reddy@syngeneintl.com

PROFESSIONAL EXPERIENCE

- Working as Senior Associate Scientist for **Syngene International Ltd (A Biocon Company)** in Discovery Chemistry, Bangalore, India from Nov- 2008 to till date.
- Worked as a Research Chemist for **Actimus Biosciences Pvt Ltd,** Hyderabad, India from June 2007 to Oct 2008.

EDUCATION

2013 - 2017	**Doctor of Philosophy (Synthetic and Medicinal Chemistry)** Vignan University, Andhra Pradesh, India **Thesis title:**Design, Synthesis and Biological Studies of Novel Molecules Derived from MBH Acetates and Tacrine Derivatives as Acetylcholinesterase Inhibitors to treat Alzheimer`s disease. **Supervisor:** Dr. Shaik Anwar
2005- 2007	**M. Sc. (Organic Chemistry)** School of Chemistry, Acharya Nagarjuna University, AP, India
2002 - 2005	School of Chemistry, Acharya Nagarjuna University, AP, India

RESEARCH EXPERIENCE

- Design, synthesis of novel tacrine molecules as acetylcholinesterase inhibitors and NMDA receptors to treat Alzheimer`s disease.
- Synthesis of novel ligands as acetylcholine inhibitors to treat Alzheimer`s disease.
- Synthesis of novel 2-amino-1,3-oxazine ligands and 2-amino-1,3-thiazine ligands as BACE inhibitors
- Synthetic methodologies, C-C coupling (Suzuki, shonagashira, etc), C-N coupling (Buchwald) and C-H activation.
- Synthetic chemistry and medicinal chemistry.

LIST OF PUBLICATIONS

1. Novel tacrine derivatives exhibiting improved acetylcholinesterase inhibition: Design, synthesis and biological evaluation; **Eeda Koti Reddy**, Chandran Remya, Kumar Mantosh, Ayyiliath M. Sajith, R.V. Omkumar, C. Sadasivan, Shaik Anwar;***Eur. J. Med. Chem*** **139 (2017) 367-377;** DOI: 10.1016/j.ejmech.2017.08.013.
2. Functionalised dihydroazo pyrimidine derivatives from Morita–Baylis–Hillman acetates: synthesis and studies against acetylcholinesterase as its inhibitors. **Eeda Koti Reddy,** Remya C., Ayyiliath M. Sajith, Dileep K. V., Sadasivan C, Shaik Anwar, ***RSCAdv.*****, 2016, 6, 77431;** DOI:10.1039/c6ra12507g.
3. Suzuki-Miyaura cross–coupling reaction in water: facile synthesis of (hetero) aryl uracil bases using potassiumorganotrifluoroborates under microwave irradiation. Bhaskaran Savitha, Ayyiliath M. Sajith, **Eeda Koti Reddy**, C. S. Ananda Kumar, M. Syed Ali Padusha; ***ChemistrySelect,*** **2016, 1, 4721 – 4725;** DOI: 10.1002/slct.201600943.
4. NMI/MsCl-Mediated Amide Bond Formation of Aminopyrazines and Aryl/Heteroaryl Carboxylic Acids: Synthesis of Biologically Relevant Pyrazine Carboxamides; Nagaraja Reddy G., **Eeda Koti Reddy,** Ayyiliath M Sajith, Shivaraj Y, Chandra Sekhar KB; ***ChemistrySelect,*** **2017, 2, 7706-7710**
5. XtalFluor-E, an Efficient Reagent for Synthesis of Oxazolines from Carboxylic Acids and O-Silylated Amino alcohols; **Eeda Koti Reddy**, Gudise Veerababu, Vadiga Shanthi Kumar, Shaik Anwar; (***Under review)***
6. Design, Synthesis and Biological Evalution of Triazole Substituted Oxadiazole derivatives as Anti-cancer and Anti-bacterial agents; T. Nagendra Prasad, **Eeda Koti Reddy**, Firoz Basha, Shaik Anwar; ***(Manuscript under preparation***).
7. Design, Synthesis and biological evolution of tacrine - propargyl amide derivatives as acetylcholinesterase inhibitors; Remya C., **Eeda Koti Reddy**, Shaik Anwar, Sadasivan C. ***(Manuscript under preparation***).

PATENTS

1. Tacrine Derivatives as Potent NMDA Receptor Antagonists with neuroprotective properties; Synthesis, *invitro* and *invivo* studies. Remya Chandran, Mantosh

Kumar, **Eeda Koti Reddy**, Lakshmi K, Shaik Anwar, Variyar EJ, Mayadevi M, Sadasivan C, Omkumar RV; ***(Patent under preparation***).

SENIOR RESEARCH ASSOCIATE (Syngene International Ltd)

- Working as a discovery chemist for medicinal chemistry projects.
- Involved in the multi-step synthesis upto 25 steps like patented drug molecule.
- Academic Knowledge of most modern analytical instrumentation and good Knowledge in characterization of organic molecules using NMR, IR, MS and LCMS.
- Guiding the trainees, planning of reactions, making project reports and handling team with five chemists.
- Involved in process development of various discovery molecules.
- Continuous updating on literature, Information seeking, mining and processing.
- Execution of experiments in the laboratory.
- Recording of experiments, observations and relevant data in Laboratory books.
- Writing of Research Reports with inputs from respective scientists.
- Generating reports and presentations on Method development.
- Dexterous deal with product complain and in investigating reasons for failure.
- Giving new routes, minimizing the cost and reducing the steps for synthesizing molecules.

REACTIONS HANDLED

- Accountable for performing reactions involving various organolithium, magnesium and tin reagents.
- Handled different Oxidations & Reductions.
- Involved in protection & deprotection of different functional groups.
- Possess expertise in Catalytic Hydrogenation.
- Have sufficient experience in performing various coupling reactions using modern Palladium chemistry on different moieties. (Buchwald, Suzuki, Stile and Sonogashira coupling).
- Have sufficient experience on Grignard, Acid-Amine couplings and Reductive aminations.
- Have sufficient experience on cyanation reactions and Nucleophilic substitution of alkyl halides with KCN or NaCN.

- Have sufficient experience in performing dry reactions by using LDA, n-BuLi, KHMDS, LiHMDS, DIBAL-H, etc.
- Have sufficient experience on reduction reactions using NaBH4, Na(CN)BH3, Na(OAc)3 and LAH.

TECHNICAL COMPETENCIES

- Expertise in column purification over silica and neutral alumina.
- Purification of liquid compounds in vacuum distillation, purification by using Isolera and Gilson instruments.
- Capable of performing various air and moisture sensitive reactions.

ACHIEVEMENTS AND AWARDS

- Certificate of Excellence from Syngene Internnational Ltd, for enthusiasm, productivity and ability to execute ideas were appreciated by the client in 2012.
- Certificate of excellence from syngene International Ltd, for excellence work for one of main client in 2013.
- Certificate of appreciation from client for outstanding efforts and valuable contributions to support the discovery partnership in 2015.
- Certificate of recognition from Syngene for challenging high priority targets and delivery of compounds in April 2017.
- Certificate of recognition for outstanding contribution as a member of chemistry team, in delivering crucial targets successfully from client in July 2017.

IT SKILLS

- Chem. Software: ISIS draw, chemdraw, Scifinder search and reaxys etc.
- MS Office, Internet Searching, and Literature collection.

Date of Birth:13 June 1985